

https://dspace.org/

Epidemiological, morphological, and physiological studies of selected plant diseases at Nylsvley

Rey, Marie Emma Christine

2015
http://hdl.handle.net/10539/19201

Downloaded from a DSpace repository. https://dspace.org/

EPIDEMIOLOGICAL, MORPHOLOGICAL, AND PHYSIOLOGICAL STUDIES OF SELECTED PLANT DISEASES AT NYLSVLEY

Marie Emma Christine Rey

Volume I

A THESIS SUBMITTED TO THE FACULTY OF SCIENCE, UNIVERSITY OF THE WITWATERSRAND, JOHANNESBURG, IN FULFILMENT OF THE REQUIREMENTS FOR THE DEGREE OF DOCTOR OF PHILOSOPHY.

July, 1982

DECLARATION BY CANDIDATE

I hereby declare that this thesis is my own work and it has not been submitted to any other university.

Christine Ley

25th day of July, 1982.

ACKNOWLEDGEMENTS

I wish to thank Professor H.M Garnett, Head of the Department of Microbiology, University of the Witwatersrand, for her supervision of this work, and the Council for Scientific and Industrial Research who funded the project. I would also like to acknowledge Dr. M.L. Frean for her invaluable encouragement, B. Cnoops for his photographic advice and Dr. A. Wight for his assistance in the sugar analyses. Thanks are also due to my fellow worker A. Amory for his advice on photosynthetic aspects and to Linda Godfrey, Mary Smith and Paulette Maingard for their typing. I am also indebted to Ruth Chomse for her help on the computer statistical programming, and to Julie and Jonty Frean for their hours of help and encouragement.

Volume I

PART I OF TWO VOLUMES

This thesis is presented in two volumes.
Volume I contains Chapters one, two, three and four; Tables 1-9; Figures 1-50 and A-J

Volume II contains Chapters five, six and seven; the references; Tables 10-25; Figures 51-114

Volume I

PART I OF TWO VOLUMES

This thesis is presented in two volumes.
Volume I contains Chapters one, two, three and four; Tables 1-9; Figures 1-50 and A-J

Volume II contains Chapters five, six and seven; the references; Tables 10-25; Figures 51-114

FRONTISPIECE



Burkea africana - *Eragrostis pallens* - savanna

TABLE OF CONTENTS

	PAGE
ABSTRACT	
CHAPTER ONE GENERAL INTRODUCTION	1
1.1 General literature review	1
1.2 Symptomatology..	1
1.3 Pathogens	2
1.4 Ecological concepts in plant pathology	3
1.5 Evolutionary concepts	4
1.6 Background to Nylsvley	5
1.7 Field descriptions of diseases	9
7.1 *B. afrizana*	9
7.2 *D. eriantha* and *P. maximum*	13
1.8 General aims and motivations	13
CHAPTER TWO IDENTIFICATION AND DESCRIPTIONS OF THE PATHOGENS	17
2.1 General irtroduction and objectives	17
2.2 METHODS...	18
2.1 Indexing for viral infection	18
2.2 Grafting	19
2.3 Isolation of bacteria	19
2.4 Light Microscopy	19
2.5 Scanning Electron Microscopy	19
2.6 Transmission Electron Microscopy	20
2.3 RESULTS	20
3.1 *B. afrizana*	20
3.1.1 Isolation attempts	20
3.1.2 Microscopical examination	20
3.2 *D. eriantha*	21
3.3 *P. maximum*	21
2.4 DISCUSSION	29
CHAPTER THREE EPIDEMIOLOGY	31
3.1 LITERATURE REVIEW	31
1.1 Ecological concepts and definitions	31
1.2 Monocyclic and polycyclic processes	32

PAGE

1.2.1 Monocyclic processes 32
1.2.2 Polycyclic processes 32
1.3 Epidemic, endemic and related concepts 33
1.4 Structure or anatomy of epidemics 35
1.5 Patterns of epidemics 35
1.6 Pathometry (disease measurements) 37
1.6.1 Background 37
1.6.2 Disease assessment keys or scales 38
1.7 Dynamics of epidemics 40
1.8 Elements of an epidemic 42
1.8.1 Host factors 42
1.8.2 Pathogens 44
1.8.3 Environment 45
1.9 Macro- and micro-climatic influences 45

49

3.2 AIMS 49
3.3 MATERIALS AND METHODS 49
3.1 Field methods 49
3.2 Disease assessment keys 50
3.3 Curve fitting 51

3.4 RESULTS 55
4.1 *B. africana* 55
4.2 *D. eriant* 60
4.3 *P. maximum* 61

3.5 DISCUSSION 77

CHAPTER FOUR DEVELOPMENTAL, MORPHOLOGICAL AND ULTRASTRUCTURAL STUDIES 89

4.1 LITERATURE REVIEW 89
1.1 The host-pathogen interface 89
1.2 Ultrastructural changes 93
1.3 Senescence and plant disease 96
1.4 Uredospore development 97

PAGE

4.2 AIMS 98
4.3 METHODS 99
3.1 Light microscopy 99
3.1.1 Freezing microtome sections 99
3.1.2 Wax sections 99
3.2 Fluorescence microscopy and histochemistry 100
3.2.1 Aniline-blue for callose detection 100
3.2.2 Phloroglucinol for lignin 100
3.3 Transmission electron microscopy 100

4.4 RESULTS 101
4.1 *B. africana* 101
4.1.1 TEM 101
4.1.2 Fluorescence microscopy and histochemistry 105
4.2 *D. eriantha* 105
4.3 *P. maximum* 124

4.5 DISCUSSION 129

FIGURE INDEX

Fig. 1 Nylsvley Nature Reserve, Northern Transvaal. 6

Fig. 2 The vegetation of Nylsvley Nature Reserve. 7

Fig. 3 External appearance of the necrotic lesions (L) on *B. africana* leaves. 10

Fig. 4 Local lesions (L) and chlorotic areas on rust-infected *D. eriantha*. 11

Fig. 5 External appearance of clypei and chlorosis on *P. maximum* leaves. 12

Fig. 6 Flow diagram illustrating the factors involved in host plants and their pathogens at Nylsvley. 16

Fig. 7 Transverse section (LM) through leaf tissue of *B. africana*. 23

PAGE

Fig. 8 A. SEM of the surface of healthy turgid epidermal cells of *B. africana*. B. Surface view of collapsed epidermal cells. C. Cross-section (SEM) through necrotic leaf tissue revealing collapse of the palisade cells. D. Section through non-necrotic tissue illustrating intact turgid palisade cells. 24

Fig. 9 A. TEM of a cross-section through a crystalline inclusion (spherosome) in semi-necrotic mesophyll cells of *B. africana*. B. 'Virogenic stroma' with virus-like particles in necrotic and semi-necrotic mesophyll. 25

Fig. 10 A-F Surface SEM of *D. eriantha* leaves. 26

Fig. 11 A. LM of the uredospores of *P. digitariae* on *D. eriantha*. B. Cross-section through a mature pustule. C. Clypei of tarspot fungi. D. An immature perithecium. 27

Fig. 12 A. Light micrograph of asci of *P. paspalicola* on *P. maximum*. B. L/S through a perithecium and clypeus. C. Intracellular hyphae in the epidermal and D. mesophyll cells. 28

Fig. 13 Disease assessment key for *D. eriantha* and *P. maximum*. 53

Fig. 14 Elements of a disease progress curve. 54

Fig. A Caterpillars defoliating *B. africana* trees. 56

Fig. B Rainfall data from 1978 to 1981. 57

Fig. C Relative humidities and saturation vapour pressure deficits. 58

Fig. D Number of rain days. 58

Fig. E Number of dew days. 58

Fig. F Dew (mm) 58

Fig. G Wind measurements. 58

Fig. H Lowest recorded saturation vapour pressure deficits. 59

Fig. I Mean MAX and MIN temperatures. 59

Fig. J Maximum relative humidities recorded in the morning and afternoon. 59

		PAGE
Fig. 15	Incidence and severity of necrotic lesions on *B. africana* (1978/79).	70
Fig. 16	Incidence and severity of necrotic lesions on *B. africana* (1979/80).	71
Fig. 17	Incidence and severity of rust on *D. eriantha* (1978/79).	72
Fig. 18	Incidence and severity of rust in the 1979/80 season.	72
Fig. 19	Incidence and severity of tarspot on *P. maximum* in the 1978/79 season.	73
Fig. 20	Incidence and severity of tarspot on *P. maximum* in the 1979/80 season.	73
Fig. 21	Relationship between incidence and severity in necrotic *B. africana* leaves (1978/79).	74
Fig. 22	Relationship between incidence and severity in the 1979/80 season.	74
Fig. 23	Relationship between incidence and severity in rust-infected *D. eriantha* leaves (1978/79).	75
Fig. 24	Relationship between incidence and severity in rust-infected *D. eriantha* leaves (1979/80).	75
Fig. 25	Relationship between incidence and severity in tarspot-infected *P. maximum* leaves (1978/79).	76
Fig. 26	Relationship between incidence and severity in tarspot-infected *P. maximum* leaves (1979/80).	76
Fig. 27 A.	TEM micrograph of a transverse section through a healthy mesophyll cell. B. A necrotic mesophyll cell.	103
Fig. 28 A-D	TEM micrographs of high power sections through *B. africana* leaf tissue. A. Electron-dense deposition along the cell wall. B. Boundary formation. C. Plasmalemmasome. D. Myelinic body.	104
Fig. 29 A-D	TEM micrographs of transverse sections through *B. africana* chloroplasts A. Young healthy chloroplast. B. Young chloroplast from semi-necrotic mesophyll cell. D. Degenerated chloroplast from necrotic lesion cell.	106
Fig. 30	Unstained cross-section through non-necrotic *B. africana* leaf tissue (UV).	107

PAGE

...ined section through ...y *B. africana* leaf tissue (+UV). 107

...ine-blue stained cross-section through ...ecrotic and semi-necrotic zones (+UV). 108

...unstained section through necrotic leaf tissue (-UV). 108

...n through necrotic tissue of *...africana* (-UV: unstained). 109

...ction taken through necrotic and semi-necrotic ...issue (+UV: unstained). 109

...ross-section (LM) through necrotic leaf tissue ...f *B. africana* (unstained). 110

...ross-section through necrotic *B. africana* ...issue stained with phloroglucinol. 110

Non-necrotic *B. africana* leaf tissue stained with phloroglucinol. 111

Fig. 38 A. TEM micrograph of an intracellular haustorium of *P. digitariae* infecting *D. eriantha*. B. Intercellular hyphae. C. Healthy mesophyll cell. 113

Fig. 39 A-D Toluidine-blue semi-thin transverse sections through *D. eriantha* leaf tissue. A. Mature pustule. B. Immature uredosorus. C. Healthy leaf tissue. D. Disruption of mesophyll ...sue by the rust f...gus. 114

Fig. 40 A. TEM section through a healthy *D. eriantha* mesophyll cell. B. Rust-infected mesophyll cells. 115

Fig. 41 A-F TEM of mitochondria from *D. eriantha* leaves. A. Mitochondria (mt_0) from healthy bundle sheath cells. B. Swollen mitochondria (mt_1) in infected bundle sheath cell. C. Mitochondria in healthy mesophyll cell. D. Rounded-off degenerating mitochondrion (mt_3). E. Elongated mitochondrion (mt_2). F. Haustorial mitochondrion. 116

Fig. 42 A-D TEM micrographs of rust-infected *D. eriantha*. A. Mesophyll cells below the B. basal cells in the fertile layer from which C. sporophores/spores are formed. D Mature released uredospores. 119

PAGE

Fig. 43 A-E TEM of developing rust pustules on *P. virgatum*. A. Uredospores and collars formed around old sporophores. B. High power of remnant collars. C. Inner folds of the old sporophore wall. D. Remainder of old sporophore and uredinial initial below. E. High power of collars and sporophore. 121

Fig. 44 A-D Uredospore ontogeny of *P. digitariae*. A. Basal cell. B. and D. New wall growth occurring from further down the inner sporogenous cell wall. C. Laterally displaced septa.

Fig. 45 A. Uredospore of *P. digitariae* exhibiting dense cytoplasm and lipid droplets. B. Spine formation.

Fig. 46 A-D Toluidine-blue stained semitnin transverse sections through *P. maximum* leaf tissue. A. Healthy leaf tissue. B. Disintegration of mesophyll. C. Bundle sheath cells in tarspot-infected tissue. 123

Fig. 47 A-D TEM micrographs of healthy and tarspot-infected *P. maximum* leaf tissue. A. High power of healthy bundle sheath cells. B. Bundle sheath cells with displaced chloroplasts. C. Intracellular hyhae in mesophyll cells. D. High power of chloroplasts in infected bundle sheath cells.

Fig. 48 A. Chloroplasts in healthy bundle sheath cell and C. mesophyll cell. B. and D. Chloroplasts from tarspot-infected tissue.

Fig. 49 A. High power TEM micrograph of bundle sheath cells from tarspot-infected tissue. B. Bundle sheath cell (high power) from healthy tissue. C. Intracellular hyphal penetration. D. Intercellular hyphae appressed to host cell wall

Fig. 50 A. TEM of densely packed hyphae forming the clypeus. B. The host-pathogen interface *P. maximum* and *P. paspalodes*.

LIST OF TABLES

		PAGE
1.	Basal cover and frequency of *D. eriantha* and *P.maximum* and frequency and biomass of *B. africana*.	8
2.	Incidence and severity data of *B.africana* (1978-1980).	62
3.	Incidence and severity data and curve fitting analysis of rust-infected *D. eriantha*.	63
4.	Incidence and severity data and curve fitting analysis of *P. maximum*.	64
5 A.	Linear regression analysis of the progressive legs of disease progress curves.	65
5 B.	The relationships between incidence and severity for *B. africana*, *D. eriantha* and *P. maximum* (1978/79 and 1979/80 seasons)	66
6.	Rainfall data from the main weather station at Nylsvley (1978-1982)	67
7.	Average monthly climatic data from October 1978 to April 1980	68
8.	Selected climatic data from the Nylsvley weather station 2 (1978-1980)	69
9.	Distribution of different types of mitochondria in healthy and rust-infected *D. eriantha*	117

LIST OF ABBREVIATIONS

ADP - adenosine 5' - diphosphate
ATP - adenosine 5' - triphosphate
BSA - Bovin Serum Albumin
C - carbon
chl - chlorophyll
CO_2 - carbon dioxide
DTT - dithiothrietol
EDTA - ethylenediaminotetraacetic acid
g - gram
h - hour
H_2O - water
IRGA - Infra Red Gas Analyser
kPa - kiloPascals
l - litre
LM - light microscopy
m - metre
M - molar
MAX - maximum
mb - millibars
MIN - minimum
min - minute
mCi - milliCurie
ME - malic enzyme
mE m^{-2} s^{-1} - micro-Einsteins metre^{-2} sec^{-1}
mg - milligram
$MgCl_2$ - magnesium chloride
ml - millilitre
mM - millimolar
$MnCl_2$ - manganese chloride
N - nitrogen
NAD - nicotinamide adenine dinucleotide
NADH - reduced nicotinamide adenine dinucleotide
NAD-MΔ - NAD-malic dehydrogenase

NADP - nicotinamide adenine dinucleotide phosphate
NADPH - reduced nicotinamide adenine dinucleotide phosphate
NH_4^+ - ammonium
nm - nanometre
NO_2^- - nitrite
NO_3^- - nitrate
O - oxygen
OAA - oxaloacetic acid
PCK - PEP caryboxykinase
PEP - phosphoenolpyruvate
PEPC - PEP carboxylase
PPO - 2,5-Diphenyloxazole
POPOP - 1,4-bis-2-(-5-phenyloxazdyl)-benzene
3-PGA - 3-phosphoglyceric acid
ppm - parts per million
RH - relative humidity
RuBP - ribulose-1-5-biphosphate
RuBPC - RuBP carboxylase
SEM - scanning electron microscopy
SVPD - saturation vapour pressure deficit
Tricine - N-tris (hydroxymethyl)methyl-glycine
T^o - temperature
TEM - transmission electron microscopy
Tris - Tris (hydroxymethyl)aminomethane
µCi - microCuries
µ - micro
µl - microlitres
µm - micrometre
v/w - volume per weight
x g - revolutions per minute

KEY FOR GRAPHS AND HISTOGRAMS

GENERAL

Graphs

Healthy

Infected

Histograms

HEALTHY

INFECTED

EPIDEMIOLOGY

Incidence

1. Smoothed untransformed

2. Linear regressions

Severity

1.

2.

SPECIFIC

Graphs

Healthy
Infected

1 – 5%

10%

25%

50–75%

50%

75%

Histograms

HEALTHY

Infected

1 – 5%

10%

25%

50–75%

f – flecking

s – sporulation

ps – post– sporulation

ABSTRACT

This study describes the epidemiological, morphological and physiological aspects of selected diseases at Nylsvley Nature Reserve. The plant species chosen were the grasses *D. eriantha* ssp *pentati* and *Panicum maximum* Jacq. and the tree species *B. africana* Hook.. The obligate parasites were identified as a rust (*Puccinia digitariae* Pole Evans) on *D. eriantha* and tarspot (*Phyllachora paspalicola*)on *P. maximum*. The nature of the necrotic lesions on *B. africana* is suspected to be of a viral nature introduced by a insect vector. However, until transmission is achieved, the question of the presence of a virus must remain.

Epidemiological studies show an increase in the incidence and severity of lesions on *B. africana* and of rust and tarspot on *D. eriantha* and *P. maximum* respectively throughout the season. The patterns and growth rates of the progress curves appear to be governed primarily by rain and moisture patterns.

Ultrastructural research (LM, SEM, and TEM) describes the'virus-like' particles in necrotic *B. africana* mesophyll cells, the uredosori of *P. digitariae* and the clypei or perithecia of *P. paspalicola* for the first time. Histochemical tests and fluorescence microscopy reveal the accumulation of lignin in the lesion areas of *B. africana*. Degradation of chloroplasts and mitochondria occur after sporogenesis.

Uredospore ontogeny of *P. digitariae* exhibits an unusual development, described for the first time, in this study. Collars form laterally as a result of new growth from the inner sporophore wall pushing the old walls aside as new uredospores are formed at the apex.

Physiological changes in the necrotic *B. africana* leaves are negligible. Photosynthesis, C_4 enzymes, nitrates, total nitrogen and sugars increase in the early stages of infection in *D. eriantha*

and *P. maximum* leaves but decline after sporogenesis. Chlorophyll content also decreases in content during post-sporulation. Dark respiration was stimulated at flecking and onset of sporolution in rust-infected *D. eriantha*.

Autoradiographic studies show the accumulation of ^{3}H-glucose in the mesophyll cells in the regions of fungal penetration in *D. eriantha* leaves. Incorporation of labelled glucose was observed for the first time in rust infections to be absorbed by the penetration peg, sub-stomatal vesicle and primary infection hyphae at the initial stage of disease.

The effect of pathogens on primary production in a natural ecosystem must be studied in association with the multitude of complex ecological factors operating . Host-pathogen systems can be regarded as discrete energy units within the framework of the ecosystem and play a regulatory role in natural populations.

1. CHAPTER ONE GENERAL INTRODUCTION

1.1 General literature review

Three phases can be outlined in forming the concepts of plant disease namely the descriptive phase, the dynamic-quantitative phase, and the theoretical-synthetic phase (Cowling and Horsfall,. 1978). The descriptive phase consists of three interacting components: the pathogen, the host and the environment. A pathogen must become established in an area before it can cause disease in established hosts (Roberts and Boothroyd, 1972). To persist in the region the disease agent must also have the ability to survive between growing seasons. A susceptible host must be present, and climatic and other environmental parameters must be favourable for the establishment and perpetuation of the agent. The dynamic-quantitative aspects of plant disease include concepts of inoculum arrival, inoculum potential and dose, disease gradients and disease progress curves describing the course of an epidemic. In establishing the progress of disease it is necessary to assess the extent and severity of infection over a time period (Van der Plank, 1975). Comparative epidemiology is useful in predicting rates and structures of epidemics in the field, and is used widely in plant pathology (Kranz, 1974b). However plant pathology is not merely a pure science, and the theoretical-synthetic phase includes aspects dealing with practical solutions to the problems. Horsfall and Cowling (1978) point out the importance of establishing models for developing integrated management for crops, as well as predictive models which could have a beneficial outcome on the economics of agriculture.

1.2 Symptomatology

The first stage in disease management is to identify the disease to be managed. Zadoks (1971,1973) proposes three useful definitions for describing the dynamics of crop destruction: Injury- any deviation from the normal crop, damage- any decrease in quality or quantity of a crop, and loss - any decline in economic returns, as a result from reduced yields or damage. The first step in the

diagnosis of a disease is to recognize the primary disease factors and this follows the procedures below:

a. Macroscopic observation of host symptoms and signs of the pathogen.

b. Microscopic examination of diseased tissue.

c. Isolation and purification of the pathogen.

d. Inoculation of host indicator plants to observe symptoms.

Pathogens usually produce characteristic symptoms on the host, and diagnosis of plant disease in the field is largely dependent upon recognition of these symptoms. However a diversity of factors may cause similar and therefore confusing symptoms. For instance wilts, cankers, soft rots, chloroses, necroses and lesions each are caused by more than one group of organisms or various abiotic factors (Tuite, 1969). The diagnostician narrows the field of causal factors by knowing common diseases of the host, the use of a host index and also by knowing diseases at a particular growth stage under certain environmental conditions. Symptoms and causal agents can also be detected by microbiological examination of the diseased tissue once field discriptions have been made (Butler and Jones,1979). Classification of symptoms is arbitary to some extent but is usually based on the plant functions or plant parts affected. Rusts for example cause chlorosis and affect photosynthesis and respiration processes(Dickinson and Lucas, 1977). The morphological symptoms found can be classified generally as necroses/chloroses; hypoplasias; and hyperplasias (Dickinson and Lucas, 1977). Necroses are characterised by death of the cells, tissues or organs of plants. This involves localised necrosis on leaf tissue, but necroses can also be manifested as yellowing, rot or wilting. Sub-normal size and pale coloration are the most common hypoplastic symptoms. Mosaics and chlorosis can result in partial repression of colour. Hyperplastic symptoms are the result of uncontrolled cell division or cell enlargement such as galls or scab.

1.3 Pathogens

Viruses, bacteria, fungi and mycoplasmas are by far the most numerous and important infective agents of plant disease. Plant pathogenic fungi are in turn the most widely spread organisms, almost all spending part of their life on their hosts and part in the

soil or plant debris, whilst others spend all of their vegetative life on their host (Agrios, 1976). Some fungi, such as the rusts are obligate parasites or biotrophs and send out haustoria penetrating the cell protoplast. Identification of fungi involves studies of morphological features and reproductive structures. Tsao (1970) points out that sometimes it may be necessary to isolate the fungus in pure culture using selective media. Almost all plant pathogenic bacteria are rod-shaped, the only exception being *Streptomyces*. Identification for bacterial diseases usually involves a number of physiological and biological tests, used in conjunction with morphological studies. Isolation on selective media is also practised (Lelliot, 1974). Many methods of virus identification have been developed and are reviewed by Ball(1974) and Matthews(1970). They include methods such as symptomatology; vector transmission; mechanical transmission or grafting; local lesion assays; physical properties; host range; antigenic nature; and electron microscopical examination of morphological characteristics. Mycoplasmas cause similar symptoms as some viruses and usually result in yellowing, stunting, or witches-broom growth of auxiliary shoots.

1.4 Ecological concepts in plant pathology

Epidemiology employs concepts, techniques and methodology of ecology in the study of plant disease phenomena. Disease is commonplace in most agricultural crops. In natural communities disease is just one of the many factors which regulate populations and hence determines the spectrum of species which are successful in any habitat. Disease may also accelerate change within established plant communities. For example forest trees may be killed, thereby opening the canopy and allowing regeneration to proceed (Schmidt, 1978). Not much attention has been focused on the extent of diseases occuring in natural ecosystems i.e. most disease outbreaks occur in homogeneous fields of agriculturally important crops. Therefore several new problems emerge in dealing with unknown pathogens in a natural population. The mere heterogeneity of natural ecosystems presents problems in determining the overall effect of disease on an entire system as opposed to a homogeneous field crop. Crop vegetations differ from natural vegetations in genetic diversity,

dersity, aggregation, conditions of growth and patterns of development (Zadoks and Schein, 1979). Biological populations have several spatial attributes, and this three-dimensional-attribute-structure becomes sign ficant to epidemiology in dense uniform stands such as wheat or bananas. However in a more heterogeneous system the degree of random dispersion is greater than agro-systems and this can influence the patterns and growth rates of epidemics. Every population consists of a variety of phenotypes, and the diversity of phenotypes reflects an even larger diversity of genotypes. In ecology the measurement of diversity in relation to ecosystem stability is an important aspect, and diversity is measured between species (interspecific). The fact that ecosystems have such diversity, carrying many genes at low frequency, enables them to adapt and cope with disease to a greater extent than in agricultural systems.

Disease in natural host populations usually exists in the endemic state; it becomes epidemic in uniform pioneer vegetations. Each population in a community plays a role in the flow of energy or materials through the system. The producers (green plants) bring in new energy and the heterotrophs or consumers depend on this energy. Pathogenic organisms may be considered as primary consumers and therefore have a place in an ecological food chain.

1.5 Evolutionary concepts

How did fungi become parasites? The answer is not known but it is postulated that in the long-term evolution of pathogenicity of fungi to plants (meso-evolution), some of the decomposing fungi developed the capability of utilizing living plant substances as food, enhancing their survival capacity. There are degrees of parasitism ranging from facultative to obligate parasites. In the natural field situation the biotrophs require living host tissue to live on e.g. rusts which are obligate parasites. They have created for themselves what Mode(1958) has called ' the problem of the pathogen existence without eliminating its host '. The co-evolution of host and parasite, in so far as they influence each other in their population genetics and evolution, has led to the concept of a pathological system at the community level, termed a 'pathosystem' (Robinson, 1976). Pathogen populations can adapt (forming new

physiological races) to changes in a host population (development of resistant cultivars). Most parasitic interactions must therefore be very old so that host and pathogen have co-evolved, each affecting selection of the other, and each responding to the other's genetic changes. Some of the most explosive epidemics result from introducing a pathog into a host population with which it has not co-evolved. No matter what their trophic mode is, fungi are natural, functional, interdependent members of ecosytems. It appears that natural interactions between pathogen and host and interdependencies, engender a homeostasis or dynamic stability.

1.2 Background to Nylsvley

The scope of topics involved in plant pathology is wide, and because of this only certain aspects have been chosen in this study as a preliminary investigation upon which further work may be based. This study took place at Nylsvley Provincial Nature Reserve in the Northern Transvaal, South Africa (Fig. 1). The Savanna Ecosystems Project being carried out at Nylsvley is one of several national scientific programmes administered by the CSIR (Council for Scientific and Industrial Research) under the National Programme for Environmental Sciences. For logistic reasons the major studies have been conducted within an intensive study site approximately 1 hectare situated in a 75 ha study area (Fig. 1). The vegetation of the study area comprises a mosaic of broad-leaf communities and grass patches of sweet thorn savanna (Fig. 2). The broad-leaf communities include *Eragrostis pallens- Burkea africana* tree savanna, the most dominant woody species being *Burkea africana* Hook. which has the highest density hectare^{-1} and frequency figures. This is followed by *Ochna pulchra*, *Grewia flavescens* and *Terminalia sericea* (Lubke, 1977). The herbaceous layer of *B. africana* savanna comprises a predominance of graminoid species, with *Digitaria eriantha* Steud. ssp *pentzii* (Stent) Kok and *E. pallens* each contributing 27 % of the basal cover of 5,96 % (van Rooyen and Theron, 1977) - see Table 1.

A preliminary investigation in 1977 at Nylsvley revealed the presence of several leaf pathogens occurring on both woody and herbaceous components. However only three plant species* were chosen

* Specimens are lodged in the herbarium at Nylsvley.

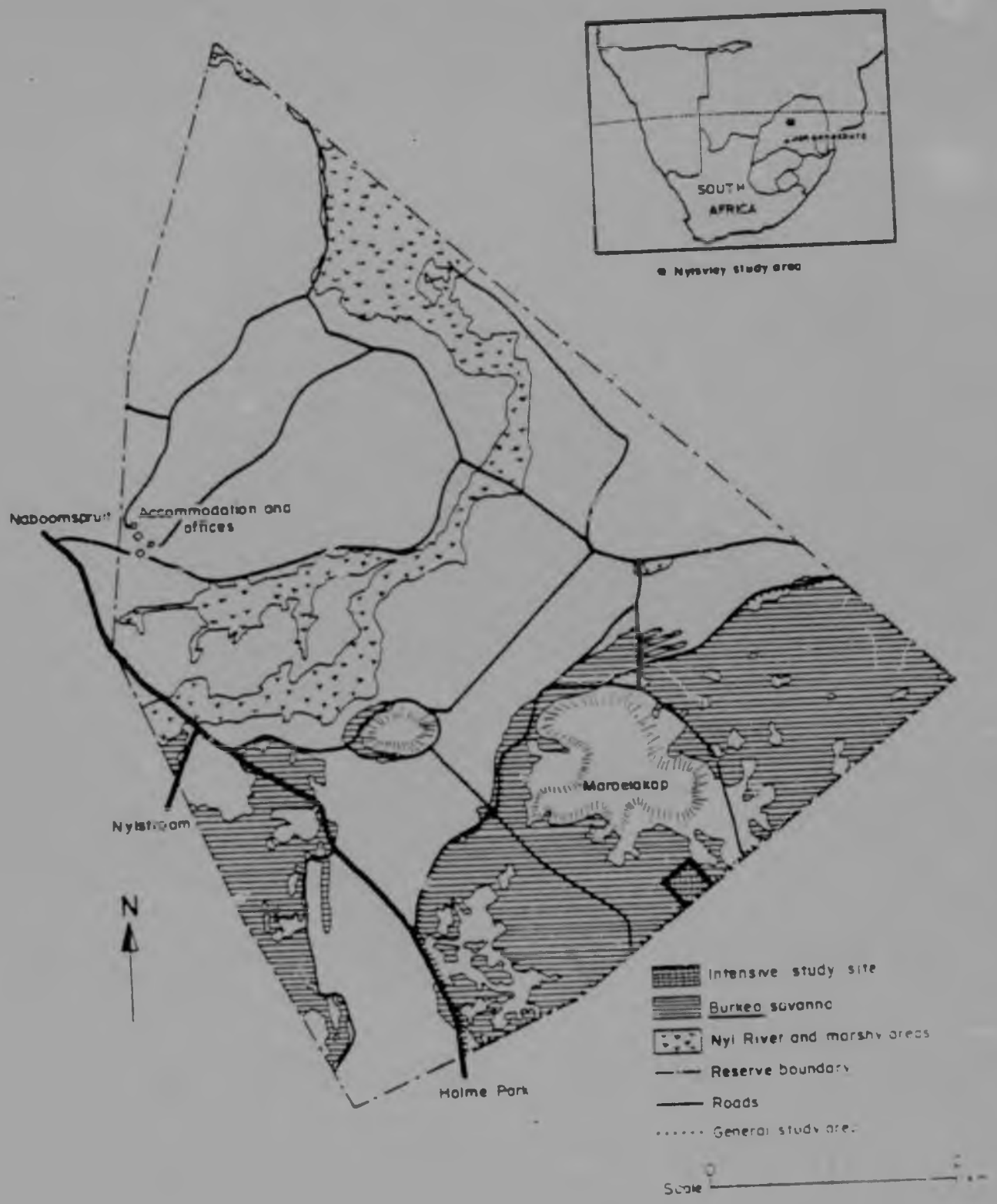


Fig.1 Nylsvley Nature Reserve, Northern Transvaal. The Savanna Ecosystem Project Study Area occupies approximately 745 ha of the south-eastern sector of the reserve.

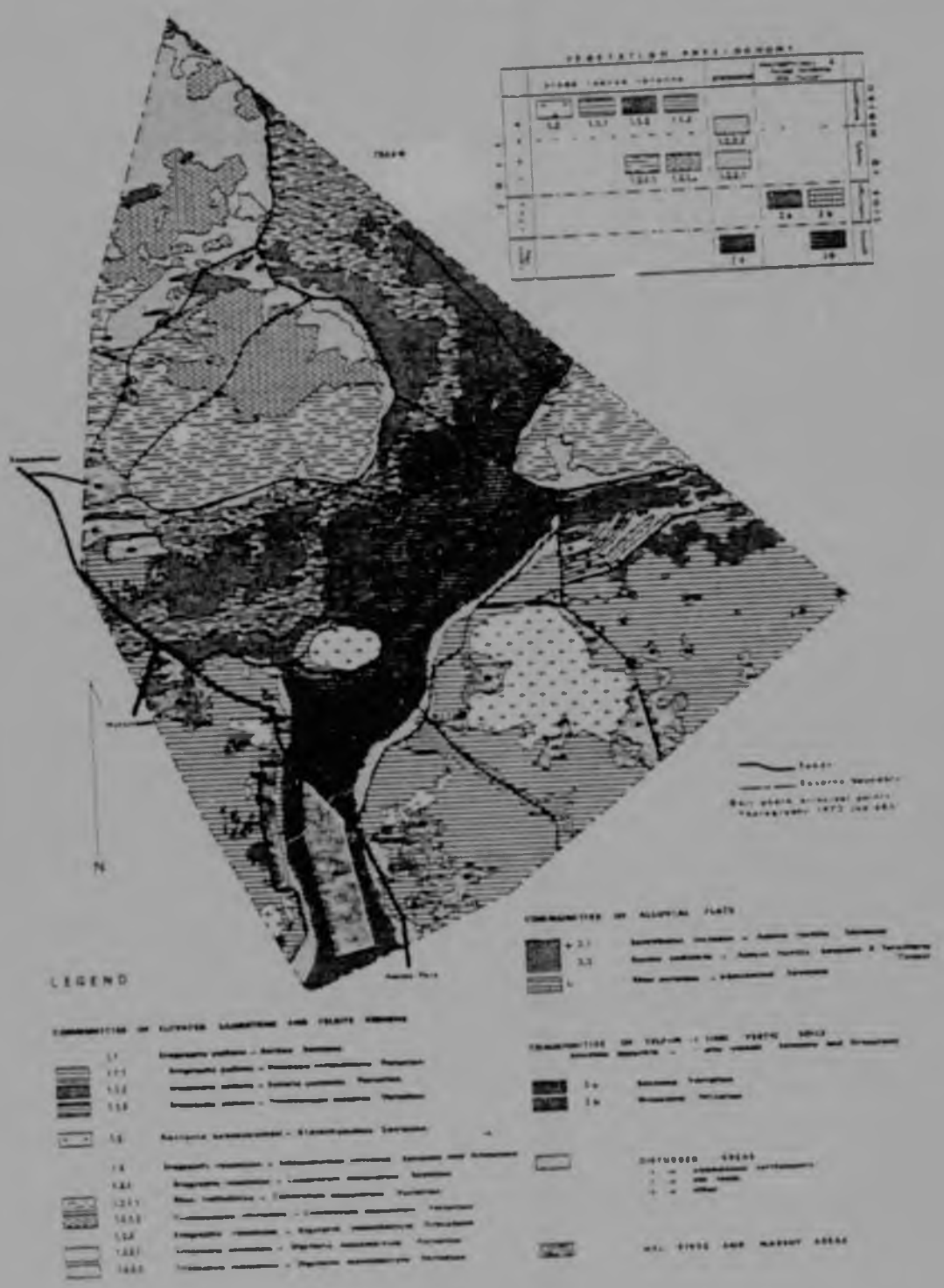


Fig.2 The vegetation of Nylsvley Nature Reserve. From Coetzee et al. (1977)

Table 1. Basal cover and frequency of *Digitaria eriantha* and *Panicum maximum* (van Rooyen and Theron,1977) and frequency and biomass of *Burkea africana* (Rutherford,1977)

SPECIES	% BASAL COVER	% FREQUENCY	BIOMASS (kg ha^{-1})
Burkea africana	-	50-63	8684
Digitaria eriantha	1.64	27.51	-
Panicum maximum	0.1	1.68	-

for this study for several reasons. *B. africana* was chosen for two reasons: Firstly for three consecutive years small necrotic lesions had been detected on the leaves. It was uncertain whether these lesions were a result of insect feeding, since the nature, size and frequency of the lesions did not appear to fit in conclusively with the type of insects identified on *B. africana*. Consequently it was decided to establish the nature of the lesions. Secondly *B. africana* contributes a major part to the biomass of the system and therefore ia an ecologically important woody species. Thus the presence of any factor, be it disease or not, that results in destruction of foliar tissue, may lead to physiological and morphological changes which in turn may have an adverse affect on biomass production. *Panicum maximum* Jacq. and *D. eriantha* were found to exhibit foliar fungal diseases. *D. eriantha* is an ecologically significant grass, having the highest frequency along with *E. pallens* (27%) (Van Rooyen and Theron. 1977) and was therefore chosen for this study. The pathogen identified on *D. eriantha* proved to be a rust, and since virtually no work has been done on rusts in a natural ecosystem, the study would prove both informative and interesting. *P. maximum* on the other hand occurs at a much lower frequency (1.68%), but is grazed widely at Nylsvley since it is soft in texture and extremely palatable. The pathogen was identified as an Ascomycete, *Phyllachora paspalicola*, a minor infection of grasses worldwide (Parbery, 1967). No evidence ofphysiological or ultrastructural studies on this fungus could be found in the literature and therefore work on this pathogen would add to our knowledge of parasite-host relationships.

1.7 Field description of diseases

7.1 *B. africana*

Symptoms on this species are manifested as small, dark brown lesions scattered randomly over the leaf surface, ranging in size from 0.5 to 3mm in diameter, usually increasing radially as the season progresses. In some cases areas of chlorosis developed in a halo around the lesions. It appeared as if these lesions could be attributed to insect feeding or alternatively a combination of insect probe and introduced virus. See Fig.3.



Fig.3 External appearance of the necrotic lesions (L) on *B. africana* leaves



Fig.4 Local lesions (L) and chlorotic areas (arrow) on rust-infected *D. eriantha*

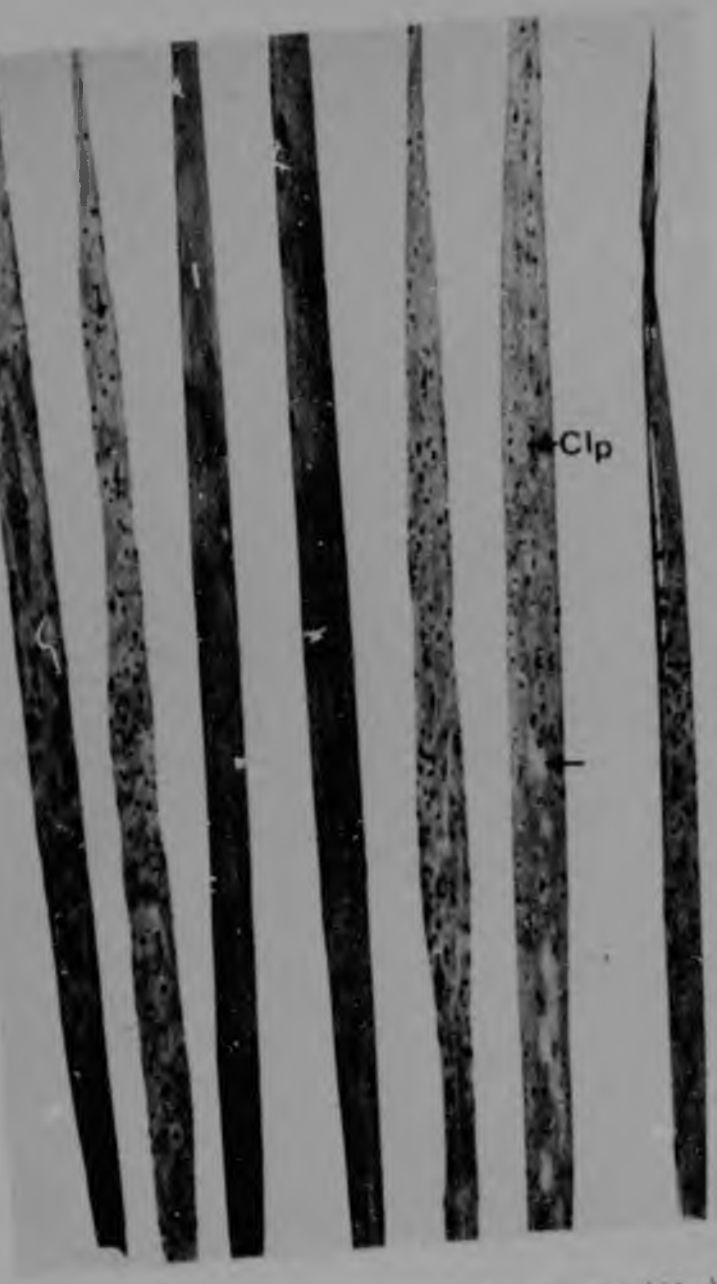


Fig.5 External appearance of clypei (Clp) and chlorosis (arrow) on tarspot-infected *P. maximum* leaves

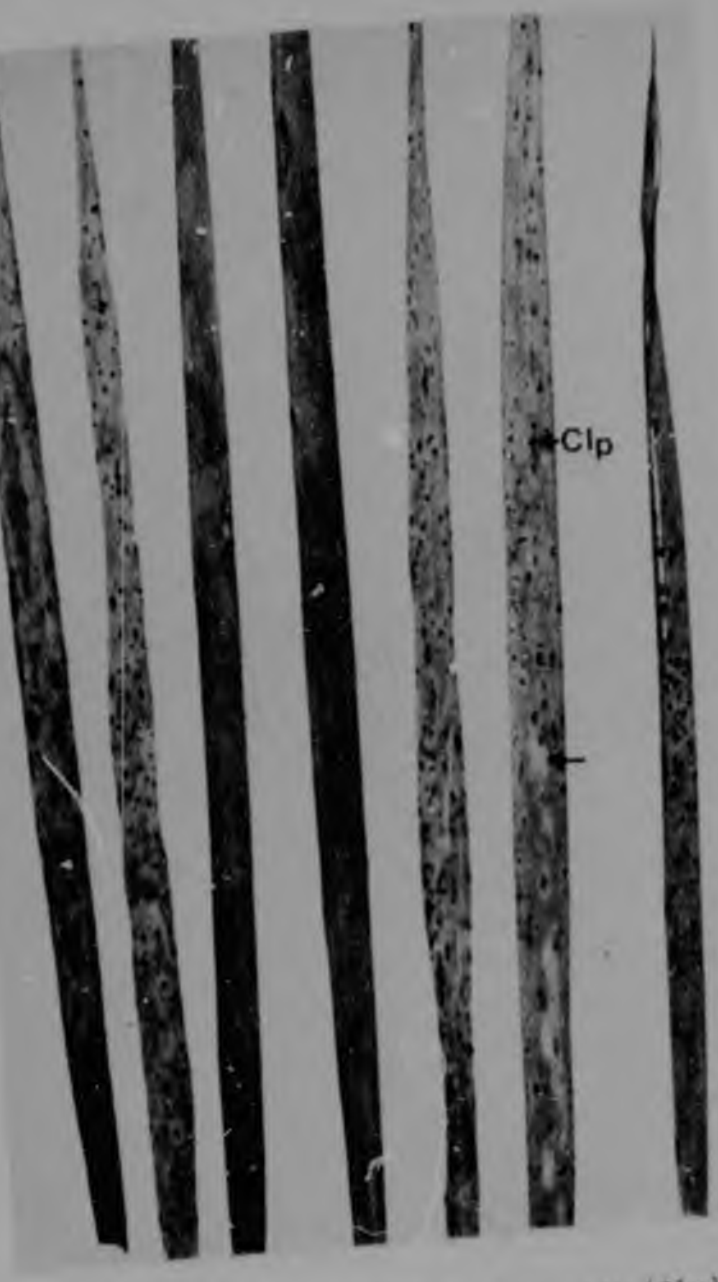


Fig.5 External appearance of clypei (Clp) and chlorosis (arrow) on tarspot-infected *P. maximum* leaves

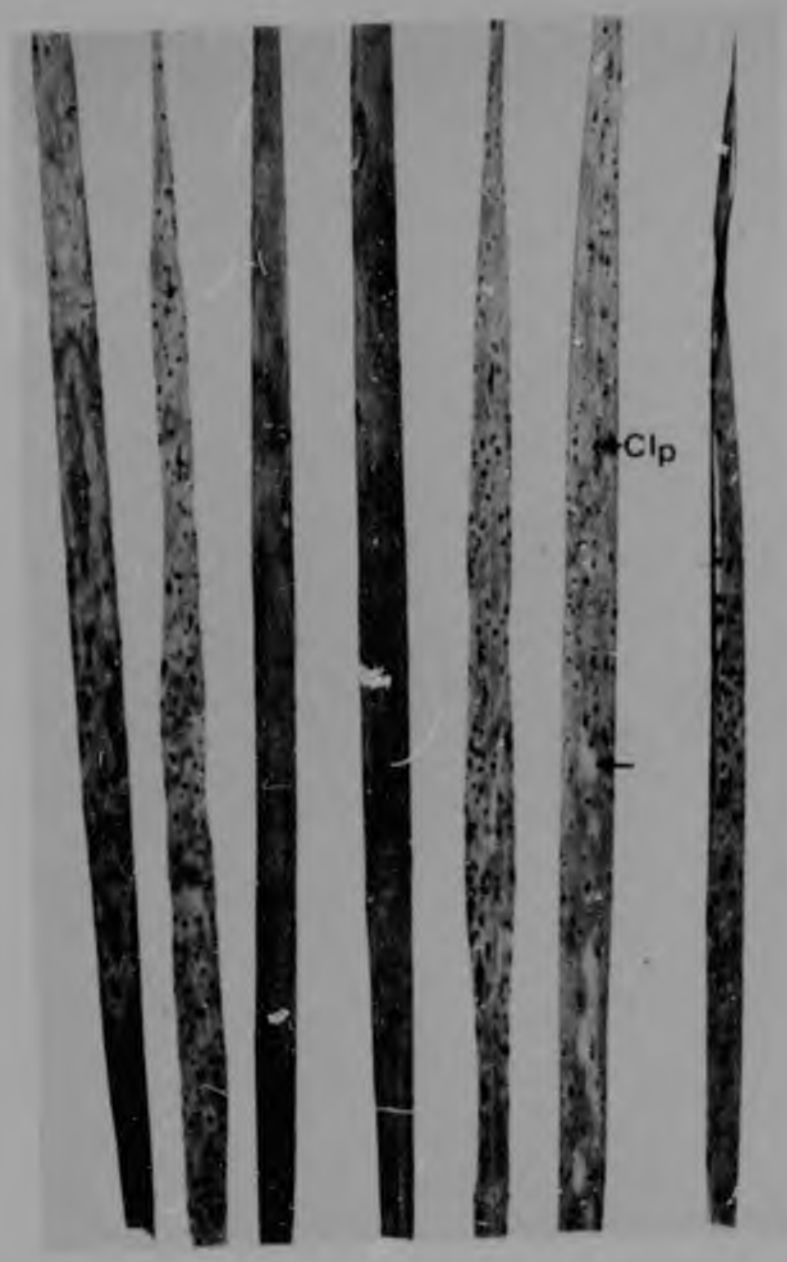


Fig.5 External appearance of clypei (Clp) and chlorosis (arrow) on tarspot-infected *P. maximum* leaves

7.2 *D. eriantha* and *P. maximum*.

Two types of fungal diseases were detected on these two grasses:

I. Rust Rusts are obligate, biotrophic parasites belonging to the Basidiomycetes and are manifested as foliar lesions. The symptoms on *D. eriantha* appear as slightly raised pustules, which develop from the localized yellow flecks, mostly on the abaxial surface. These uredosori are yellowish-brown in colour and contain light-brown uredospores. See Fig.4.

2. Tarspot This foliar disease on *P. maximum* commences in the form of small amber blisters which eventually darken as the clypei (fruiting bodies) mature, until the leaf blades are covered with small black spots resembling tar splashed capriciously over the surface of the blades. Occacionally colonies were noted on the leaf sheaths. Spots were also noted on both the abaxial and adaxial sides of the leaves and increased in size up to 1mm in diameter. Mature colonies sometimes had a chlorotic area but mostly lacked this feature. Tarspot fungi belong to the Ascomycetes. See Fig.5.

1.8 General aims and motivations

The aims of this study incorporate two important features: one, to study the morphological and physiological affects of pathogens on plants; and two, to view the status of these diseases within the framework of the ecosystem.

In order to achieve a better understanding of the ecosystem as a whole, a study of the potential primary productivity is necessary and requires inclusion of all the limiting factors. Parasites may be regarded as 'energy robbers', basically competing with the plant for nutrients and influencing the pathways involved in energy production or utilization. This host-parasite relationship can be regarded as a discrete energy unit within the broader energy flow concept of the ecosystem. A study of the specific problems in this energy unit may act as a 'barometer' to gauge the actual role of parasites in a natural environment where disease is kept to a lower level. This research aims to provide some answers on specific pathological questions and also to contribute to the broad objectives of the national co-operative project. The latter is concerned with the overall affect of limiting factors such as environmental parameters and pathogens on productivity. However as

natural ecosystems are heterogeneous there are problems in determining the affects on overall growth due to the influence of specific plant diseases. The current study, performed over a limited time period, although providing specific data during that period , can thus predict changes in physiological and ecological parameters on a greater time scale. Due to the wide nature of plant pathology and the inherent problems in working in a natural ecosystem only certain aspects were chosen for this study. These factors influencing plant disease are outlined in Fig.6. Each chapter is concerned with a specific problem or investigation which will reveal a picture of the processes occurring within an infected grass leaf and create a perspective of this study within the entire ecosystem taking into account the many other factors involved in productivity. Chapter two commences with the identification and description of the pathogens and is followed by the study of disease throughout the growing season in Chapter three. This is important with respect to the stage of host development at which infection occurs, for this along with incidence and severity will influence productivity. Chapters four and five describe the mophological and physiological changes within the discrete host-parasite system, whilst Chapter six develops further the concept of plant-pathogen competition for nutrients even at the early stage of pathogen growth. In Chapter seven the implications of energy flow and interference by parasites are viewed within the wider ecosystem concept and the definition of parasites in a natural population reviewed. Can an obligate parasite, despite influencing its hosts metabolism to a considerable extent, be regarded more as a 'co-exister' in a natural environment, whilst at the same time be viewed as a true parasite in an agricultural system?

This study commenced in February 1978 and was completed in March 1982. Data was collected for three growing seasons, whilst the initial research (February - May 1978) was devoted to developing suitable field and laboratory methods to meet the objectives below:

A. Description and identification of the plant diseases on the two grasses *Digitaria eriantha* ssp *pentzii* and *Panicum maximum* Jacq..

B. Attempt to establish the presence (or absence) of a virus in *Burkea africana* Hook. by transmission to indicator plants and utilising microscopical techniques.

C. Study of the epidemiology of disease i.e. the structure and growth rates of the epidemics by assessment of the extent and intensity of disease throughout the growing season.

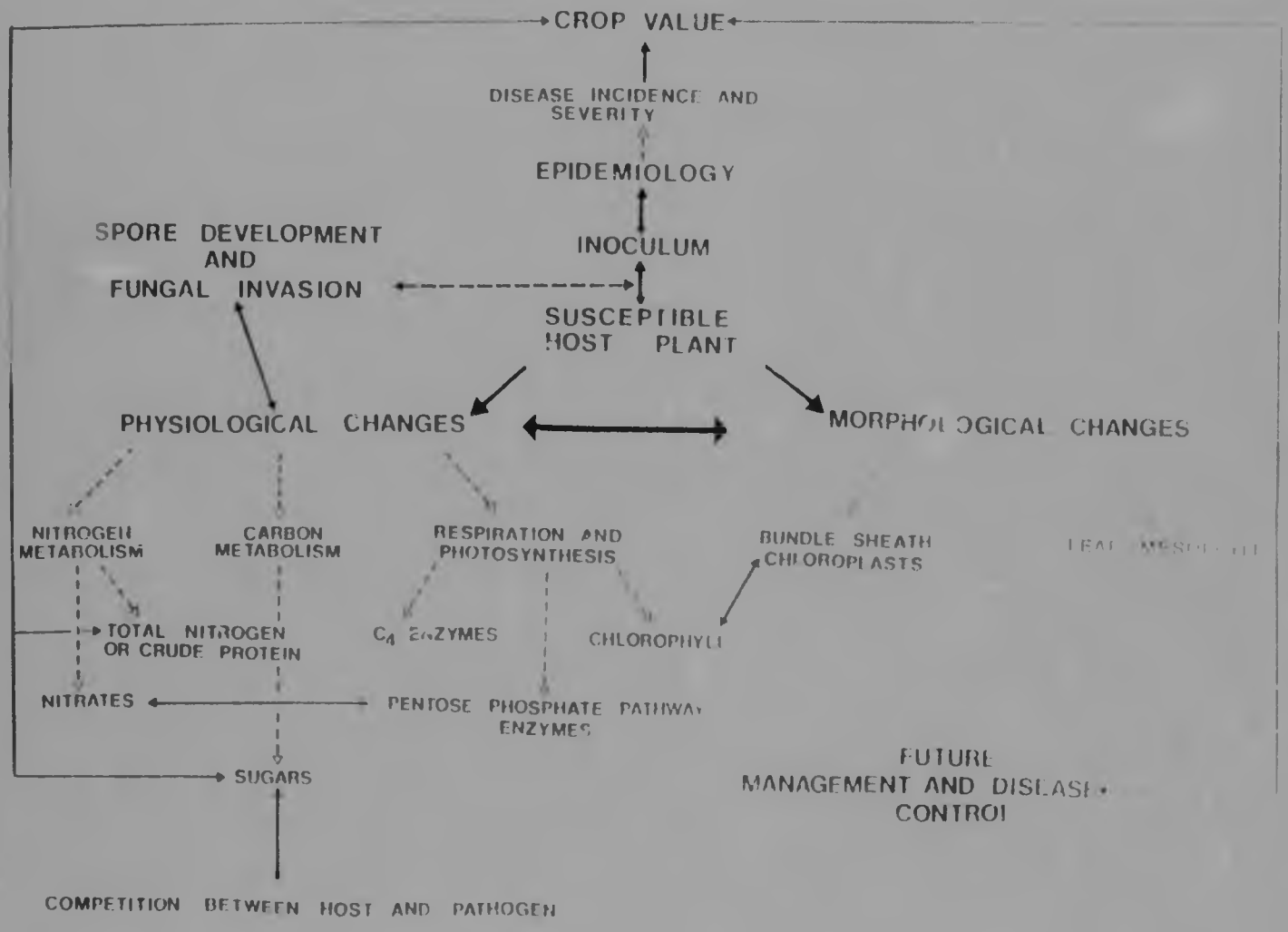
D. Study of the morphological and ultrastructural changes in leaf tissue caused by pathogens, using histochemical methods and light and electron microscopy.

E. Physiological responses of the host to infection.

F. Estimation of overall effect of pathogens on productivity of the grass layer.

G. Perspective of plant disease in natural ecosystems.

FIG.6 FLOW DIAGRAM ILLUSTRATING THE FACTORS INVOLVED IN HOST PLANTS AND THEIR PATHOGENS AT NYLSVLEY



CHAPTER TWO IDENTIFICATION AND DESCRIPTION OF THE PATHOGENS

2.1 General introduction and objectives

In the identification of any suspected plant disease it must be decided whether the symptoms are caused by an infective agent or environmental factors. Pathogens usually produce characteristic symptoms on the plant and diagnosis of a plant disease in the field is largely dependent upon recognition of these symptoms. Usually examination of an area of vegetation for pathogens involves visual detection of morphological symptoms exhibited by the plants. However in some cases, the external symptoms are similar to those caused by environmental factors such as nutrient deficiencies or insect damage, and therefore microscopical examination of the tissue has to be carried out.

One method of indexing for viral infection is by mechanical transmission of the virus to a range of indicator plants and examining the inoculated plants for symptoms. Several artificial methods for transmitting viruses can be employed. One technique is by the introduction of sap from suspected infected leaves into the tissues of susceptible indicator plants. However not all viruses are sap-transmissible and some depend on specific insect vectors for their spread. Another method of transmission is by grafting twigs of infected plants onto indicator plants (Garnsey and Whidden, 1970). Standard procedures for isolating plant pathogenic bacteria from diseased material are facilitated by the use of selective and diagnostic media. Five selective plating media (designated as the D-series media) have been developed by Kado and Heskett (1970). These were designed principally on the basis of altering surface components and membranes of bacterial cells, using specific inhibitors or anti-biotics, so that the growth of one bacterial genus was permitted whilst others were restricted.

Light microscopy is the easiest method for the identification of fungal pathogens. Often pathogens produce various structures

on the surface or interior of leaves such as spores, mycelia or fruiting bodies, and light microscopy, especially phase contrast, provides an adequate vehicle for studying these structures and using them for identification purposes. Scanning electron microscopy provides a rapid and useful technique in studying the surfaces of biological material. Many recent studies have employed scanning electron microscopy (SEM) in viewing the development of fungi on leaf surfaces (Hassan and Littlefield, 1979; Gold and Littlefield, 1979). Stobbs et al. (1977) have utilized this technique to study necrotic lesions on infected leaves and structural modifications of the epidermis. In contrast to the three-dimensional viewing advantage of SEM, transmission electron microscopy(TEM) only offers a two-dimensional image but on the other hand provides greater resolution and clarity at high magnifications. Ultra-thin sections of leaf material are useful not only in identification but also in studying pathogens 'in situ'.

The objectives of this research were to establish the nature of the lesions on *B. africana*, and to identify the fungal pathogens on the grasses *D. eriantha* and *P. maximum*. The study also included a description of the infective agents and their vegetative and reproductive structures.

2.2 METHODS

2.1 Indexing for viral infections

Mechanical inoculation was performed using the sap of *B. africana*. The indicator plants employed were *Nicotiana glutinosa*; *N. tabacum*; *Chenopodium quinoa* Willd; *Gomphrena globosa* L.; cauliflower 'snowball'; cabbage 'Early Jersey'; petunia; bean 'Canadian Wonder'; pea 'greenfast'; cucumber 'Marketer' and squash 'long white bush'. The leaves of *B. africana* were homogenized in a 1% solution of K_2HPO_4 in distilled water with a pestle and mortar. The sap from the homogenized leaves was passed through a muslin cloth and kept in the dark at $4^{o}C$ since a period of darkness at low temperatures has been found to increase the success of mechanical transmissions (Sill and Walker, 1952). The surfaces of the indicator plant leaves were dusted with carborundum and the sap rubbed gently over the

surface using a cheesecloth pad. After three minutes the leaves were washed with distilled water. Observations were made after 24h and every day to ascertain whether any symptoms appeared on the leaves.

2.2 Grafting

Wedge-grafting (Garnsey and Whidden, 1970) was carried out with *B. africana* twigs being grafted onto periwinkle (*Vinca*) species.

2.3 Isolation of bacteria

Almost all plant pathogenic bacteria are rod-shaped, the only exception being *Streptomyces*. The five genera are *Pseudomonas*, *Xanthomonas*, *Erwinia*, *Corynebacterium*, and *Agrobacterium*. *Xanthomonas* causes leaf-spot in several plant species. *B. africana* leaves were tested for the presence of a leaf-spot bacterium employing the selective D-5 medium of Kado and Heskett (1970). The leaves were surface-sterilized in 50% ethanol, rinsed in sterile distilled water, and homogenized in a pestle and mortar. The crude extract was centrifuged at 5000X g for 10 min to remove the debris and the extract streaked onto the D-5 medium in petri-dishes at 25°C. The D-5 medium consisted of the following: 10g cellobiose, 3g K_2HPO_4, 1g NaH_2PO_4, 1g NH_4Cl, 0.3g $MgSO_4.7H_2O$ and 7g agar. *Xanthomonas* colonies are yellow, circular pulvinate and mucoid on the medium.

2.4 Light microscopy (LM)

Frozen sections (10-15 µm) were cut on a freezing microtome (Photax Model 2) using glycerine jelly to support the leaf tissue during sectioning. Semi-thin resin sections (1µm) were cut on an ultra-microtome and stained with toluidine-blue before viewing.

2.5 Scanning electron microscopy (SEM)

Leaf segments ($2mm^2$) were fixed in 1% glutaraldehyde (in 0.1M sodium cacodylate buffer, pH 7.2) for 2h followed by 2% glutar-aldehyde overnight. The samples were rinsed in buffer, dehydrated in a graded alcohol series from 10-100% for 5min each and then critical-point dried. The leaf samples were then mounted on

aluminium stubs, coated with a film of gold-palladium and viewed under a JEOL JSM T-20 scanning electron microscope.

2.6 Transmission electron microscopy (TEM)

Leaf sections were fixed at 4°C in 4% glutaraldehyde (in 0.1M sodium cacodylate buffer) for 24h and rinsed in buffer several times. Post-fixation was carried out in 1% osmium tetroxide for 2h at 4°C, and the sections were dehydrated in a graded alcohol series. The samples were infiltrated with an Epon-Araldite mixture and polymerized at 60°C for 72h. Sectioning was performed on a Reichert 'OM 03' ultramicrotome. The specimens were stained in 2% uranyl acetate for 1h followed by lead citrate for 10min and viewed under the JEOL 100C electron microscope.

2.3 RESULTS

3.1 *B. africana*

3.1.1 Isolation attempts

Attempts to transmit a virus to the indicator plants failed, as did the grafting experiment. A further attempt to demonstrate the presence of a virus from *B. africana* was undertaken by an Honours student (Annalise Williamson, 1979) using leafhoppers (superfamily Jassoidea) and planthoppers (superfamily Fulgoroiclea) isolated from *B. africana* trees and allowing them to feed on bean leaves (*Phaseolus vulgaris*). However these insect feeding experiments also proved negative.

3.1.2 Microscopical examination

Light microscope studies of the cross-section through a *B. africana* leaf illustrated three distinct regions, namely the necrotic tissue (A), the yellow semi-necrotic area adjacent to necrosis (B) and the healthy tissue (C) (Fig. 7). The healthy tissue possessed normal cuboidal epidermal cells, well organized and distended palisade parenchyma and a spongy mesophyll with numerous air spaces. The necrotic area, however, lacked a distinct epidermal layer, whilst the palisade and spongy mesophyll cells were collapsed and disrupted. The collapse of the epidermal cells can also be seen in Fig. 8 B as compared to the non-necrotic, turgid

cells (Fig. 8 A). SEM of the cross-section through non-necrotic tissue revealed intact turgid palisade cells (Fig. 8 D), whilst sections through necrotic tissue disclosed necrotic collapse of the palisade cells (Fig. 8 C).

Transmission electron microscopy revealed the presence of apparent 'virogenic stroma' composed of long flexuous virus-like rods (0.13µmx0.01µm) with transverse banding (Fig. 9 B). These particles were detected in necrotic and semi-necrotic mesophyll cells, and were not observed in non-affected cells. Membrane-bound crystalline inclusions (Fig. 9 A) were also noted in semi-necrotic mesophyll cells.

3.2 *D. eriantha*

Using the keys and descriptions obtained from Cummins (1971) and Doidge (1929) the fungus was identified as *Puccinia digitariae* Pole Evans. The uredosori are mostly hypophyllous (Fig. 10 C , light-brown in colour and become erumpant at maturity (Fig. 10 D). The mature uredia lack a covering peridium, and few paraphyses were detected (Fig. 11 B). The uredospores are one celled, pedicellate, echinulate and ellipsoid/ovate in shape (Fig. 11 A). They vary from 23-33x19-24µm (Fig. 10 E). The uredospores germinate producing germ tubes and usually form appressoria over stomata and penetrate through into the intercellular space below (Fig. 10 F). In a few cases however the uredospore germ tubes were seen to directly penetrate through the epidermis (Fig. 107 and 109, Chapter 6).

Occasionally tarspot (*Phyllachora digitariae*) was noted on *D. eriantha*. This fungus was first identified on *D. smutsii* Stent in South Africa and the ascospores are similar to those of *P. paspalicola*. The ascospores are ellipsoid and vary from 8-13x4-10µm (Fig. 10 A).

3.3 *P. maximum*

Using the key described by Parbery (1967) an Ascomycete was identified, this being *Phyllachora paspalicola* which occurs on

LEGENDS

A - ascus
ap - appressorium
As - ascospores
Clp - clypeus
E - epidermis
er - endoplasmic reticulum
h - surface hyphae
ir - intracellular hyphae
L - lesion
m - mesophyll
P - pustule
Pe - perithecium
pl - palisade
vlp - virus-like particle
py - spermatogonium
sa - stomata
Ss - spherosome
u - uredospore
ui - uredinial initial
Vb - vascular bundle

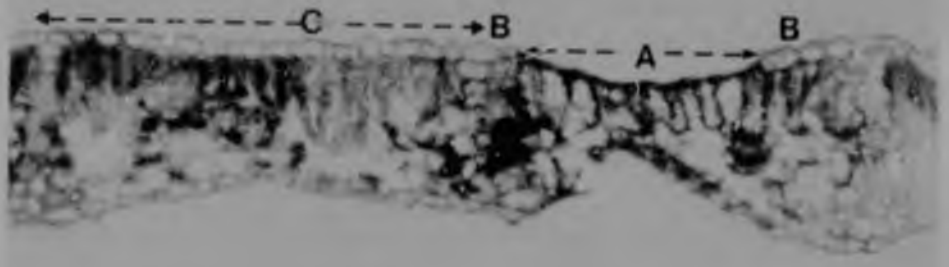


Fig.7 Transverse section (LM) through leaf tissue of *B. africana*. The necrotic lesion area (A), semi-necrotic tissue adjacent (B) and healthy tissue (C) can be distinguished.

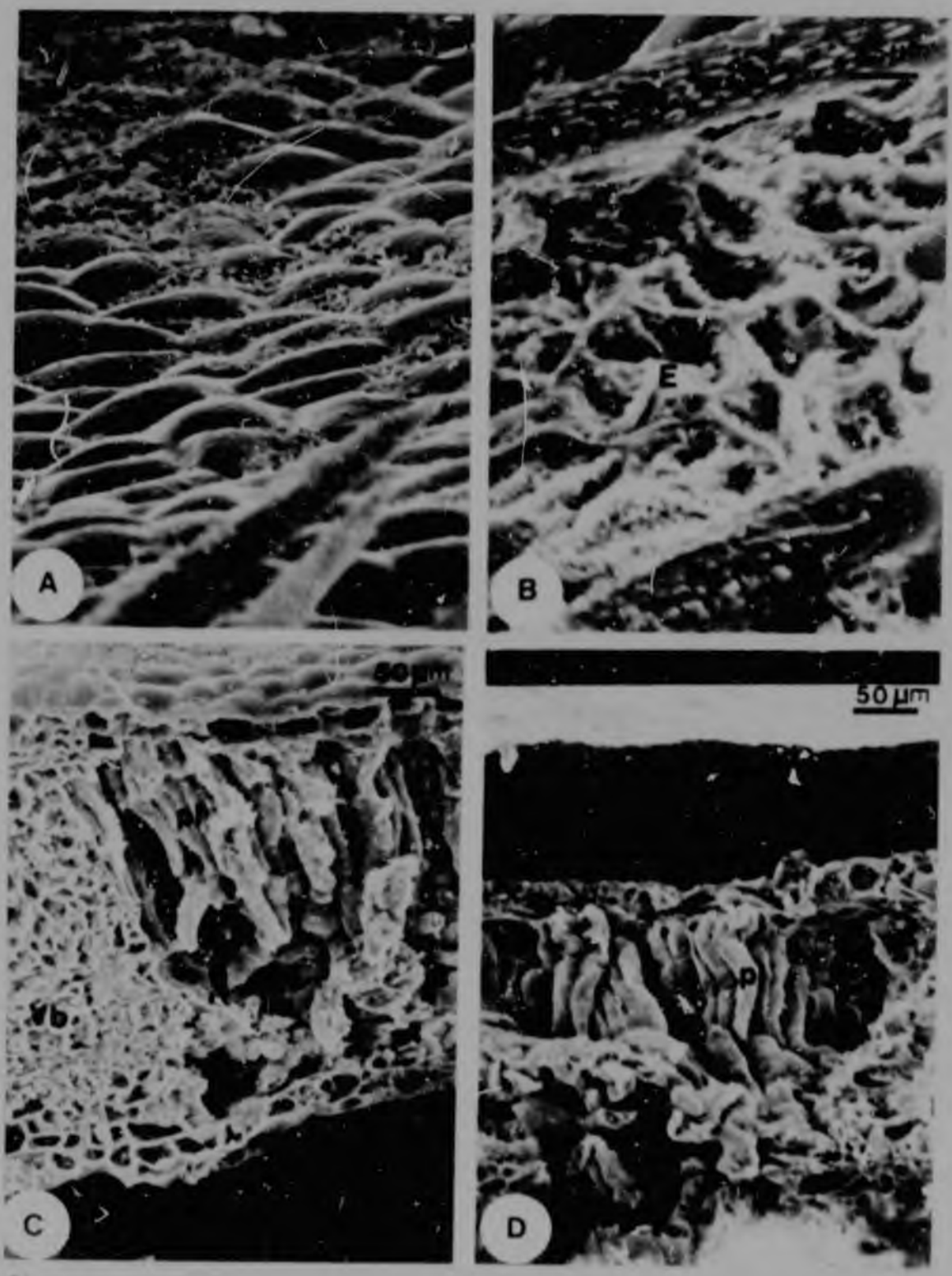


Fig.8 A. SEM of the surface of healthy turgid epidermal cells of [illegible]. B. Surface view of collapsed epidermal cells in the necrotic lesion area. C. Cross-section (SEM) through necrotic leaf tissue revealing collapse of the palisade cells. D. Section through non-necrotic tissue illustrating intact turgid palisade cells.



Fig.9 A. TEM micrograph of a cross-section through a crystalline inclusion (spherosome) in semi-necrotic mesophyll cells of *S. xylosma*. B. 'Virogenic stroma' with virus-like particles in necrotic and semi-necrotic mesophyll cells. Note the transverse bandings on the virus-like rods.

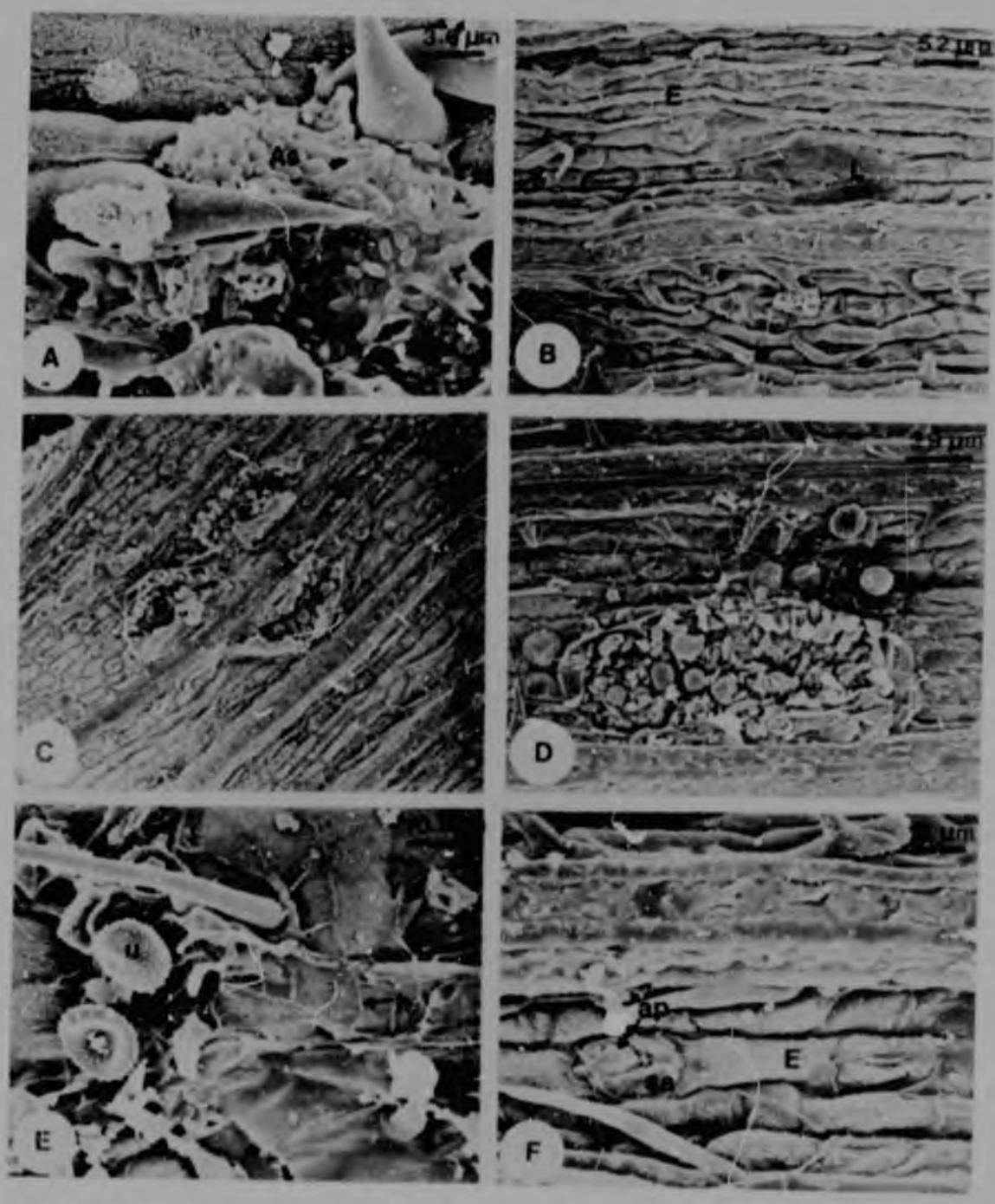
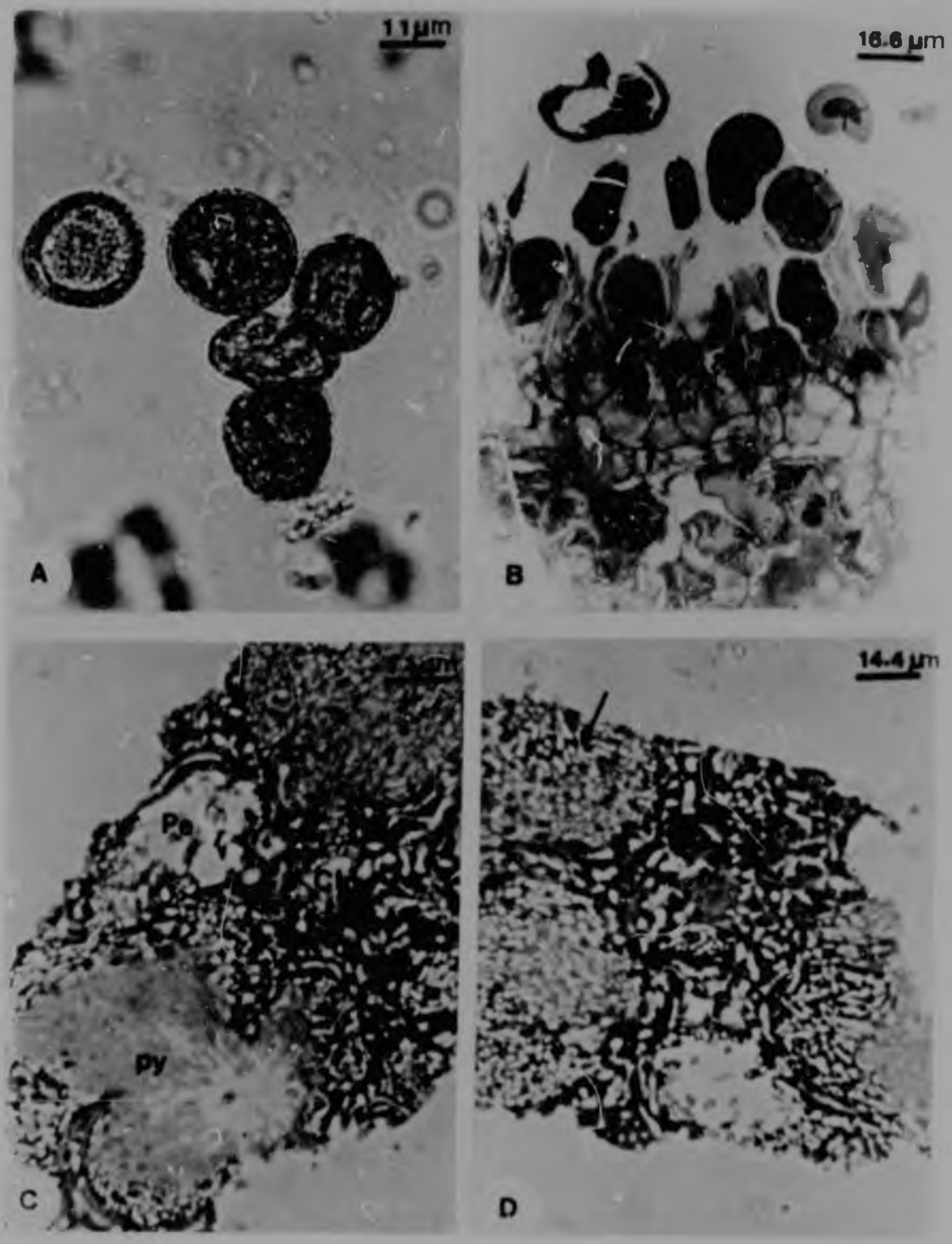


Fig.10 A-F Surface SEM of *D. eriantha* leaves. A. Ellipsoid ascospores of tarspot fungus (*Phyllachora digitariae*). B. Immature lesion before pustule erupts. C. Hypophyllous pustules. D. Erumpant pustules releasing uredospores of *D. eriantha*. E. Highpower of uredospores varying from 23-33 X 19-24 m. F. Appressorium formation over stomata.



A. LM of the uredospores of the rust fungus (*Puccinia digitatae*) exhibiting the echinulate surface. B. Cross-section (LM) through a mature pustule. Note the lack of paraphyses and the fertile layer giving rise to uredinial initials. C. Hypei of tarspot fungi and perithecia embedded in the mesophyll. Note the stromatagonium. D. Arrow points to an immature perithecium.

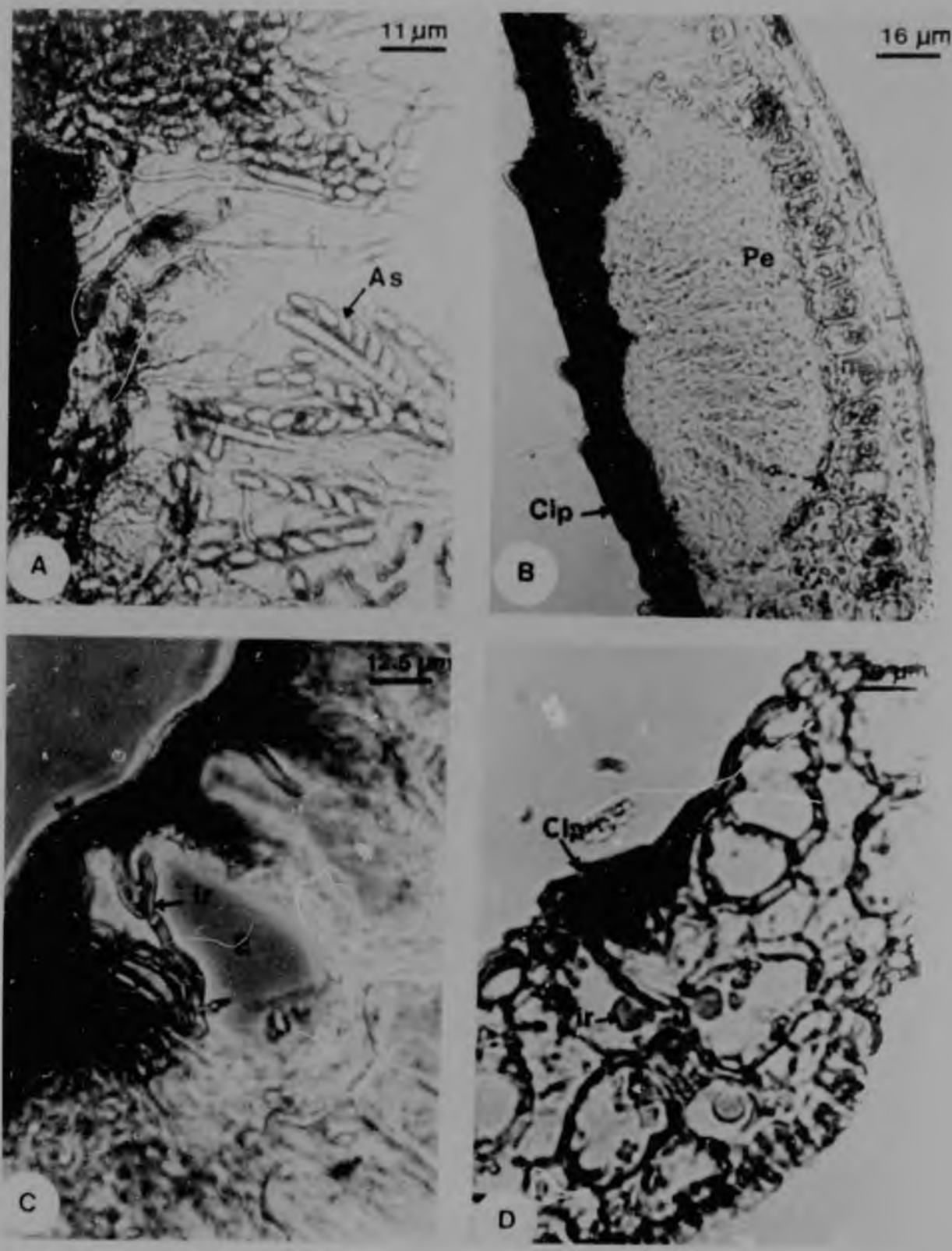


Fig.12 A. Light micrograph [illegible]
The ascospores are oval/ellipsoid in shape, [illegible]
B. L/S through a perithecium and clypeus. [illegible]
of the [illegible]spot fungus in epiderma and [illegible]

the genera *Panicum* and *Digitaria*. The symptoms are first visible as amber blisters which eventually darken as the clypei (perithecia or fruiting bodies) mature (Fig. 11 C and Fig. 12 B). The perithecia are embedded in the mesophyll (arrow, Fig. 11 D points to a young perithecium). The asci are cylindrical and the ascospores are ellipsoid to oval in shape, varying between 9-14 by 5-9µm (Fig. 12 A). Spermatagonia exist (Fig. 11 C) and the spermatia are filiform 8-20x0.5-1µm. This fungus is a biotroph, producing intercellular and intracellular hyphae which penetrate the epidermal (Fig. 12 C) and mesophyll cells (Fig. 12 D).

2.4 DISCUSSION

The nature of the lesions of *B. africana* remains uncertain. Until transmission of the infective agent is achieved, Koch's postulate cannot be fulfilled and, even though evidence suggests a viral infection, the nature of these 'virus-like' particles and the association of the crystalline bodies with viral inclusions must remain in doubt. Virus transmission in woody species is usually problemmatic, and in some cases it may take one year for transmission to be manifested. Difficulty in transmission in *B. africana* may therefore be attributed to the fact that it is a woody species, or alternatively to the lack of a suitable indicator plant. The particles appear to be flexuous rods and exhibit distinct bands similar to those observed in the closterovirus group (1250x13nm). The crystalline inclusions observed in semi-necrotic cells resemble those described by Bar Joseph et al. (1977) in carnation yellow fleck virus infections. Similar membrane-bound bodies have been observed by other workers studying viral inclusions (Martelli and Russo, 1977; Moline. 1974 and Wilcoxin et al., 1975), and hence the structures observed in the current study might only be due to the reaction of the cells to necrosis or wounding as a result of insect feeding. Crystalline inclusions consist of protein crystals, but these may not necessarily be viral proteins. However these inclusions were not detected in non-necrotic *B. africana* leaves. Nevertheless it remains uncertain whether or not these bodies are associated with a virus infection.

Both fungi infecting the grasses *D. eriantha* and *P.maximum* are obligate parasites. Since *Phyllachora graminis*(Pers. ex Fries) Nke. in Fckl. was described by Nitschke in Fuckel's "Symbolae Mycologicae" (1869), two hundred and seventy eight species have been recorded on hosts in the Gramineae (Parbery, 1967). Many species have wide host ranges and are widely distributed geographically so that many species' names have many synonyms eg. *Phyllachora paspalicola (digitariae)*. Another reason for the multiplicity of names is that several unstable and variable characteristics have been relied on previously for delimiting species (Parbery, 1963). *Phyllachora* species differ from other biotrophic fungal parasites in that their mycelia are intracellular instead of intercellular in the manner of downy mildew or rusts. Generally it is thought that *Phyllachora* species do not cause marked damage to their hosts so that they are rarely of economic importance. The host tissue does not usually die until after maturation of the fungal fructifications (Parbery, 1967). During the early and sometimes later stages of infection a chlorotic zone usually appears. As in the case of many obligate parasites, this fungus penetrates its host by means of a appressorium and infection peg, but usually penetrates directly through the cuticle and epidermis and not through stomata. The rust fungi belong to the class Basidiomycetes, and have a complex life cycle that may produce up to five spore stages. *Puccinia* species are macrocyclic rusts which usually possess all five spore stages and are heteroecious rusts, having some of their spore stages on two different host species. Rust fungi also infect a wide range of host plants and occur worldwide. They infect many important cash crops and are therefore of great ecomonic importance. Even though much work has been carried out on rusts occurring on economically significant plants, little research has been initiated concerning the graminicolous species. The following chapter aims at studying the epidemiology of these fungal diseases throughout the growing season of this savanna-type vegetation.

3. CHAPTER THREE EPIDEMIOLOGY

3.1 LITERATURE REVIEW

3.1.1 Ecological concepts and definitions

Epidemiology involves several concepts and methodology of ecology in the study of plant diseases (Zadoks and Schien, 1979). The term epidemiology has come to have a broad meaning within plant pathology. Van der Plank (1963) stated "Epidemiology is the science of disease in populations", which implies populations of hosts. However the study of diseases deals with other populations such as carriers of the pathogen (Zadoks and Schein, 1979). A useful definition is that epidemiology is the study of rates of change in the amount of disease in a host population in space and time (Kranz, 1974b). In epidemiology interactions of populations of hosts and of pathogens with each other and their environment ar observed, which leads to an extremely complex situation. Development of disease symptoms and rate of disease increase are dependent to a large extent on pathogen infection ability and susceptibility of the host (Populer, 1978).

Biological populations have several spatial attributes. The three-dimensional attribute structure becomes relevant to epidemiology in dense uniform stands, but is not as important when a population shares an area with other populations. Populations vary in dispersion (random, regular or aggregated) types, degrees and patterns (Zadoks and Schein, 1979). In epidemiology one is concerned about the area occupied by disease, the patterns of disease occurrence and the effect of crop aggregation on the occurrence of disease. Intensity characterizes the population at a given area and some attributes of intensity are density, disease prevalence and severity. A population's genetic attributes are important for adaptation to change in environmental conditions. Each population consists of a variety of phenotypes and genotypes. Lessening of genetic diversity can have effects on the occurrence of plant disease. Populations of crop plants are different from natural plant populations in ways that effect the occurrence of disease (Zadoks and Schein, 1979). Crop vegetations differ from natural vegetations in many ways, and the growing of crops brings

about changes in density, aggregation, genetic diversity conditions of growth and patterns of growth and development.

3.1.2 Moncyclic and polycyclic processes

1.2.1 Monocyclic processes

Epidemics are complex biological process, usually composed of a number of sub-processes-the infection cycles. One infection cycle leads from one dispersal unit through growth and multiplication to the next generation of dispersal units (Gaeumann, 1964). The monocyclic process is therefore one which takes place within the time span of a single infection cycle. Infection cycles are recurrent and epidemics, consisting of a sequence of infection cycles, are polycyclic processes which develop over several successive infection cycles.

When a dispersal unit such as a spore, comes into contact with a suitable plant part, the unit changes into an infection unit or mycelial structure, which may in turn give rise to many dispersal units. In time the infection unit induces on the infected plant an initial symptom that sometimes develops into a localized lesion or may become systemic. In epidemiology the interest centers on populations of infection units on populations of host plants. Spores in a population of spores are not perfectly synchronized. The epidemiologist is interested in the rate of change, rather than the instantaneous state of the development of a population of infection units. The ratio of the number of pustules formed to the number of spores applied is known as the infection efficiency, which may depend on pathogen virulence, host susceptibility and environmental conditions.

1.2.2 Polycyclic processes

Epidemiology concerns the study of the build up of an epidemic, this being a polycyclic process. An infection chain may be homogeneous or heterogeneous, branched or unbranched. A homogeneous infection chain consists of an endless succession of identical infection cycles as in yellow stripe rust (*Puccinia striiformis*). In a heterogeneous infection chain, different spore forms with

infection cycles of a different nature may be linked together. An infection chain is branched when two spore forms exist, but alternation of spore forms is not obligatory, as with the sexual and asexual spores of *Mycosphaerella musicola*, which causes Sigatoka disease on bananas (parallel arrangement of infection cycles). Epidemics starting at a low initial inoculum level will show a typical focal pattern, where the foci spread radially from a local source ie. focal epidemics. General epidemics start at high levels of well dispersed initial inoculum.

3.1.3 Epidemic, endemic and related concepts

Disease does exist in natural host populations but usually in the endemic form; it becomes epidemic in uniform pioneer vegetation. Crops are like the latter and favour epidemics (Zadoks and Schein, 1979). Natural ecosystems have evolved to produce a balanced interaction of component species. Various vegetation types are intermixed and co-exist in an interrelated, dynamic system of species dispersion and density. Large intraspecific variation exists. Against a background of low species density and genetic diversity parasites have co-evolved using diverse variability mechanisms to maintain themselves against changing mechanisms of resistance of their hosts. The resistances themselves have evolved in response to the parasites. For these reasons, in natural ecosystems explosive epidemics are rare and restricted in time and space. Therefore in a natural ecosystem disease is always present, but the hosts genetic make-up, the population's genetic diversity and the dispersion of genotypes combine to prevent extreme disease growth rates. In artificial agro-ecosystems, host plants with simple genetics of resistance are densely aggregated and the fungus soon develops a virulence capability that the host cannot withstand (Zadoks and Schein, 1979). Agrosystems are so young in relation to natural ecosystems that there has been insufficient time to attain stability. Because natural ecosystems are more stable, and the host and parasite have had a long, interdependent association, disease levels may be expected to be low and to vary little over time. The term polyetic epidemic is limited to epidemics whose increase in intensity takes many years (Zadoks and Schein, 1979). Sometimes they are not easily recognizable

if the amplitude of the annual cycle of x (proportion of disease) due to host and weather conditions is so large that it obscures the gradually increasing annual mean severity.

As mentioned previously, disease in natural populations, where the period of interaction between host and parasite has been sufficently long for these two components to evolve together, is the most natural form of disease, and the most truly endemic. However this does not necessarily mean that an endemic disease is never eruptive showing a sigmoid progress ie. endemic diseases may not cease to be epidemic (Gaeumann, 1950). The severity of disease may cycle with a small or large amplitude and wavelength. Epidemic refers to an increase in intensity and extensity. However only when the fungus increases its area of activity to a large extent, is it called a progressive epidemic. An endemic disease may become progressive whenever a new physiological race appears eg. yellow rust on wheat in the Netherlands (Zadoks and Schein, 1979). If an epidemic flares up and dies down annually for instance it is termed a cyclic epidemic. Therefore the terminology endemic and cyclic epidemic can mean the same thing providing the epidemic does not become progressive. There remains the question however of whether the several kinds of disease progress such as compound interest, simple interest and cycle occurrence also apply to endemics. In perennial crops disease on deciduous parts (such as leaves) would follow the rule of constant cycling. Diseases on twigs or trunks may actually be polyetic in development. Van der Plank (1975) viewed an endemic disease as one in which the product iR_c (i = the infectious period; R = the effective daily multiplication factor) tends to oscillate a little about 1. This however only fits an endemic disease in a large diverse population of perennial hosts and may not fit an endemic disease of annuals such as grasses or other crops. Disease from an introduced pathogen, after its initial explosive phase, will settle down to an annual cycle. The level of the endemic disease may be low or high and local eruptions are possible as a result of microscale factors.

3.1.4 Structure or anatomy of epidemics

Structural elements of an epidemic system stem from pathogen - host interactions, or from those of their populations. Environmental or human interference becomes part of the system by triggering or inhibiting the actior of these elements. To the epidemiologist, host, pathogen and disease can be termed as subsystems, and in turn subsystems are designated elements (eg. lesion growth, pathogenesis) which are usually measurable as state variables g(x) (Patten. 1971). Each variable in turn has a variable quantitative impact, and the structure of a whole epidemic is known by the sum of all the variables or functions involved as $Y = f(x_1 \ldots\ldots x_n)$. Robinson (1976) terms an *esodemic* infection one where each infection cycle results in one or more lesions on the same plant, whereas in an *exodemic* infection the lesions form on a previously non-infected host. Monocyclic diseases are ones where the pathogen produces one generation during the vegetative period of the host, and in polycyclic diseases more than one cycle occurs. Diseases caused by different etiological agents usually have different epidemiological structures e.g. an abiotic disorder will differ radically from that of a vector-borne virus such as tomato spotted wilt, and that for a fungal disease such as blue mould (in Kranz, 1978). Three closely related species can have different epidemiological structures and different structural elements such as survival mechanisms or infection processes.

3.1.5 Patterns of epidemics

Interactions of structural elements can result in different epidemiological patterns or rates. Epidemic patterns can be expressed in curves that show the progress of a disease as it spreads over time (in Kranz, 1978). The point of origin and shape of disease progress curves may reveal changes in host susceptibility during the growing period, the availibility of inoculum, recurrent climatic conditions or age distribution of lesions (Kranz, 1978). Nearly all progress curves are S-shaped e.g. stem rust of wheat, but deviations do sometimes occur in many virus diseases (Thresh, 1974). Disease progress is commonly plotted in cumulative curves

over time, while gradients are plotted in hyperbolic curves over distance. The derivative of the cumulative progress curve indicates the rate of growth of an epidemic and these rate curves identify at least three major classes of epidemiological patterns:- symmetrical; asymmetrical with positive skewness; or asymmetrical with negative skewness. All of these curves depict more or less continuous development of disease until harvest or death of the host population and in this sense they are incomplete. A complete undisturbed curve however is often bilateral ie. it has both progressive and degressive legs (Kranz, 1974a). Progress curves can also be bimodal, multimodel or oscillating (Kranz, 1975 and van der Plank, 1975). Baker (1971) suggested four consecutive phases which represent the biological facets of an epidemic (Fig 14):-

1) the true logarithmic phase
2) the synergistic (exponential) phase
3) the transitional and
4) the plateau phase

If one identifies each phase of the curves as a definable parameter, then these parameters can be used as a basis for quantitative comparisons, providing that their inherent variability is adequately understood.

Untransformed but smoothed progress curves are epidemiologically most meaningful (Kranz, 1978) but linear curves are a prerequisite for statistical or mathematical analysis. For comparisons of patterns over short intervals most disease progress curves can be considered linear even when not transformed. Wavelike annual and perennial progress curves cannot be described by straight line transformations (van der Plank, 1975), but need Fourier analysis (Kranz, 1974a). All smoothed unilateral curves can be compared by the following criteria: starting point; initial disease intensity (yo); slope of curves after various periods of time; maximum disease intensity (Y_{max}) (Kranz, 1974a).

Sigmoidal curves describe diseases where the initial development is slow, but then accelerates as host susceptibility increases late in the epidemic e.g. slow rusting of wheat (Kranz, 1968a, in Kranz, 1978). Straight line curves are typical of epidemics in

which disease progress is determined mainly by rate of multiplication of the pathogen which is not inhibited by host resistance or climate. Bi-modal and oscillating progress curves typically occur in diseases conditioned by a regular sequence of weather conditions and/or regular sequence of growth flushes eg. blister blight of tea (Visser et al., 1961). For effective comparisons of epidemics both the patterns and correlations between changes in patterns and essential components, need to be known. Different rates of disease epidemics need not necessarily alter the pattern of disease development.

3.1.6 Pathometry (disease measurement)

1.6.1 Background

Our ignorance of plant disease intensity and loss is profound because research has most extensively taken place in most other aspects of disease (Horsfall and Cowling, 1978). According to Chester (1950), W.D. Moore wrote, "It is too bad that so many have contributed so little to this very important subject." A few like Lyman and Chester in the United States, W.C. Moore and Grainer in Great Britain, James in Canada, and Chiarappa of the Food and Agriculture Organization (FAO) have struggled for research support, but by and large the results have not matched the need however, and most of our ignorance remains (Horsfall and Cowling, 1978). The FAO of the United Nations has more recently taken a greater interest in assessing disease losses. They publish a Plant Protection Bulletin and have prepared a manual in an effort to standardize methods of estimating crop losses (James, 1971). Large (1966) reviewed many of the methods used for measuring disease that have appeared as isolated examples in literature.

Large (1953) introduced the term pathometry for disease measurement. The main reason for measuring plant diseases is to obtain quantitative data on the occurrence and development of diseases. These measurements are also used in conjunction with yield or quality data to determine the relationship between disease intensity and crop loss so that economic losses can be calculated from surveys conducted to assess the importance of disease (James, 1971). To develop rational and economical control measures whether by breeding

resistant cultivars or using fungicides, it is not sufficient to state loss; the magnitude of the loss must be evaluated. Only by disease loss appraisal is it possible to determine the economic loss due to different amounts of disease (James, 1974). Disease measurement may involve two stages : the development of assessment keys or scales and secondly development of a reliable method for estimating yield loss for any given amount of disease (Large and Doling, 1962 ; James et al., 1968) or given progress curve (Burleigh et al., 1972).

1.6.2 Disease assessment keys or scales

Disease assessment keys illustrate or describe the appearance of a plant organ or whole plant when infected by different amounts of disease (James, 1974) e.g. James (1971) describes an illustrated series of assessment keys for foliar diseases based on growth stage and area of leaf tissue affected. Disease is assessed regularly throughout the season and disease progress curves are generated. Disease offers three parameters for measurement : incidence, intensity (or severity) and yield (reverse of loss) (Horsfall and Cowling, 1978). Disease incidence can be defined as the number of plant units infected, expressed as a percentage of the total number of units assessed e.g. percentage of diseased plants, twigs or leaves. Severity is defined as the area of plant tissue affected by disease expressed as a percentage of the total area (James, 1974). Yield is the amount of crop harvested and loss is the diminution of the crop (Horsfall and Cowling, 1978). The only disease-assessment methods that have been applied with adequate uniformity in practice are those that estimate incidence. Incidence is easy and quick to measure and one can transform the percentage incidence figures into logs, probits or logits. These methods are usually used for systemic infections e.g. virus or fungal wilts, or when diseased plants are total losses (Carr and Large, 1963). Intensity can be measured by counting individual lesions, but this is time consuming and therefore visual methods are usually employed. Intensity is related to loss and once conversion factors are established, loss can be measured more easily by intensity than yield (Horsfall and Cowling, 1978). The relationship

between incidence and severity is only tenuous at best with self-limiting lesions such as leaf spots and foliage rusts (Horsfall and Cowling, 1978).

The simpliest disease-assessment methods are ones least prone to error eg. assessing disease on individual leaves (James, 1971). In cereals the individual leaves and growth stages are easy to designate, but in other diseases, such as late blight of potato, this is not so easy since growth tends to lack any distinct growth stages except flowering (James, 1971), and therefore epidemics cannot be typified by a standard pattern. Therefore, although many arbitary indices and rating systems have been used (Chester, 1950) to measure disease, their use should be discouraged in favour of percentage scales of disease intensity and severity. Possibly the first historic example of a standard diagram in assessing disease visually, was that of Cobb (1892) for leaf rust of wheat in Australia. He drew sketches of infected leaves showing various degrees of rusting ranging from one to fifty percent of leaf area covered by pustules. By comparing the sketches with real leaves, he could derive a measure of the intensity of the rust. The idea of the Cobb scale has been extended to many other diseases. These grades he chose were clearly distinguishable by eye and therefore of great advantage. Modification of the Cobb scale (Melchers and Parker, 1922) labels the maximum possible amount of rust as one hundred percent, but the actual area occupied by the pustules is only thirty seven percent. James (1971) developed a series of standard area diagrams where the percentage of infection recorded always represents the actual area covered. All disease assessments are subjective to some extent because they are the results of visual judgements. However some years ago Horsfall and Barratt (1945) pointed out that the grades detected by the human eye are approximately equal divisions on a log scale, and therefore follow the Webber - Fechner law which states that response to stimuli depends on the logarithm of the intensity of the stimulus. From the epidemidogical point of view this is interesting because most pathogens multiply at a logarithmic rate whereas assessments are at a linear rate. Once the leaves have been graded the disease index is obtained by multiplying

the number of leaves in each category by the mean percentage of that category, adding the products and dividing by the total number of leaves. This is the arithmetical mean (Large, 1966). In the Horsfall and Barratt (1945) grading system the categories are numbered (0 - 3 percent = 1, and 3 to 6 = 2 etc.) and the mean score for the sample is obtained by adding these scores and dividing by the number of leaves. The mean score is thus a logarithm of the geometric mean of the percentage assessments, and is better than the arithmetical mean in that it is less distorted by extreme individual scores. From these severity scores, disease progress curves can be made, and consequently the epidemic can be studied.

3.1.7 Dynamics of epidemics

Both rates and patterns are essential characteristics of the dynamics of a system (Horsfall and Cowling, 1978). Patten (1971) points out that states give a transient picture of their variables and rates express the response of a system to a stimulus e.g. disease intensity. Rates can be intepreted as a discrete or continuous sequence of state changes in time (Patten, 1971). If a disease shows a very low porportionality in rates it eventually becomes an endemic disease due to a co-existing host and pathoger population (van der Plank, 1975). Factors influencing rates can be found in genetic and phenotypic variability of host and pathogen populations in space and time and also due to environmental parameters that influence processes of infection, dispersal and survival of spores. Van der Plank (1963) reports that in few cases does an epidemic wipe out a host population, and he relates this to a more or less transient stability; a balance achieved between new infections and new growths. The relationship between injury and resulting damage is seldom linear (Zadoks, 1970). Assessment models are usually based upon successive measurements in time. The simplest method of counting the number of infected plants so obtaining percentage infection is not adequate and usually levels of disease severity or intensity are measured using descriptive field keys. Once this has been obtained the progress of disease can be studied from the disease progress curves plotted. In recent years there have been several attempts to fit data of this

type to various mathematical equations. The equation thus becomes a model of the epidemic. Some of the more useful models are those of van der Plank (1963). The simplest situation is where disease is related linearly to one parameter, and the relationship is generally expressed by the equation $y = a + bx$ where y = the amount of disease, x the measured parameter and a and b are constants. Usually however, the disease progress curves follow a sigmoid - shape, where initial development is slow and then accelerates and finally slows down again as there is little healthy tissue left for the pathogen to colonize. Van der Plank (1963) suggests that at least in its early stages an epidemic can be described by the equation $x = x_0 e^{rt}$ where x = the proportion of disease at any one time; x_0 = amount of initial inoculum; r = average infection rate and t = the time during which infection has occurred. The overall rate at which an epidemic is progressing (r) is derived by taking logarithms through the equation $x = x_0 e^{rt}$ and transposing :

$$\log_e x = \log_e x_0 + rt$$

$$rt = \log_e x - \log_e x_0$$

$$r = \frac{1}{t} \log_e \frac{x}{x_0}$$

Average infection rate or logarithmic infection rate (r_1) is then calculated :

x_1 - first measurement of disease assessed at time t_1

$$r_1 = \frac{1}{t_2 - t_1} \log_e \frac{x_2}{x_1}$$

x_2 = second measurements taken at time t_2

Here we assume there is plenty of susceptible tissue. With higher disease levels, the factor $(1-x)$ is introduced when calculating r :

$$r = \frac{1}{t_2 - t_1} \log_e \frac{x_2(1-x)}{x_1(1-x_2)}$$

where r is the apparent infection rate.

Such S-shaped curves can be reduced to straight lines by transformation of the percentage figures to a probit scale. This transformation is based on the fact that as the epidemic progresses the rate of increase is determined not only by the amount of disease present (x), but by the proportion of susceptible tissue left (1-x). (Van der Plank, 1963). The stage at which this point is reached probably varies with the pathogen - host combination. Here, where there are several disease assessments, $\log_e x$ is plotted against time (if x remains low throughout) or $\log_e (x/(1-x))$ if the disease levels go beyond about five percent. The slopes of the lines directly measure r_1 or r respectively. Since rates can vary during an epidemic, transformation of whole progress curves into straight lines should be handled with care (Kranz, 1975; Berger, 1975). The researcher must keep in mind that such transformations may disguise variations in rates, and that in using transformed curves, comparisons can only be made with distinct sections. In some cases untransformed curves may in fact be better for comparing epidemics (Kranz, 1975).

3.1.8 Elements of an epidemic

Rate determinants of epidemics involve three elements - the host, pathogen and environment (Kranz, 1978).

1.8.1 Host factors

Type of crop

Rate of development of an epidemic varies with the crop type. For example van der Plank reports highest rates for vegetatively propogated crops. In woody plants the rate at which viruses spread is usually relatively slow (Thresh, 1974). Fungal and viral spread on annuals can however be comparable and usually fast.

Stand density

Although more foliage provides more sites for infection, leaf area as such rarely appears to be a limiting factor in continuously growing host (Zadoks, 1961). In virus diseases increased plant size facilitates rapid spread by increasing the changes of direct contact between infected and non-infected plant parts and by increasing amounts of infected and susceptible host tissue that are accessible to vectors. (Thresh, 1974). Epidemics of systemic diseases that receive their inoculum from outside the field, may on the other hand even be slowed down by a dense crop (van der Plank, 1960).

Geretic resistance

Rates are affected by the horizontal or race - nonspecific resistance in cultivars, whereas vertical resistance primarily affects the initial inoculum (y_0) (Robinson, 1976). The greater the horizontal resistance is, the lower the infection rate (r) becomes. This is most predominant in long lasting epidemics. Norse (1971) also reports that at different times rates may vary considerably.

Predisposition

Environmentally conditioned predisposition of host plants to increased susceptibility usually is not race - specific, and therefore infection rate r, is most likely greater with increased predisposition. Kato (1974) reports that predisposition causes an increase in infection rate of rice blast (*Pyricularia oryzae*) by about forty percent.

1.8.2 Pathogens

Changes in structural elements of pathogen populations can be either qualitative (eg. new races) or quantitative (eg. amount of inoculum). There is no evidence for important differences between rates of epidemics caused by viruses, fungi or bacteria, but different rates have been reported between certain taxa (Kranz, 1968b). Wheat leaf rust is usually slower in developing and less explosive than wheat stem rust. Overall damage however may be greater with leaf rust since there is less fluctuation from year to year (van der Plank, 1960). Mechanisms of pathogen survival often determine the primary inoculum availability early in cropping season. Seed-borne pathogens often develop at more rapid rates due to random distribution of inoculum and because the number infection cycles required to cover a given crop is less with seed-borne diseases than those that develop from more localized but equally strong primary foci. Larger amounts of primary inoculum seem to be correlated with earlier disease incidence and higher initial disease intensity (van der Plank, 1963). Earliness of start is highly correlated with greater final severity of disease (y_{max}), larger areas under progress curves and a greater frequency of killed plants, in many fungal diseases studied (Kranz, 1968b). Hamilton and Stakman (1967), show this to be the case with wheat stem rust (*Puccinia graminis ters.*) in the Mississippi basin. Also for virus diseases the date on which first infection appears is of crucial significance in their epidemiology (Thresh, 1974). Rates of epidemics are also affected by proximity of older or overwintering crops with abundant inoculum. The delay between emergence of host and onset of epidemics is a major factor affecting growth functions. The amount and time of availability of initial inoculum are major determinants of the speed at which the threshold is reached. Kato (1974) reports that during the first phase of rice blast epidemics the disease intensity gradually reaches the five percent level of y, and then the infection rate increases steeply. For linearized progress curves, an initial rapid infection rate tends to remain rapid (- or a slow one slow). Such a rapid rate brings about a low average age of the population of lesions, and this tends to favor further development of the epidemic (van der Plank, 1975). This relationship may be consistent for linearized progress curves, but may not be so

for nontransformed epidemics. Duration of latent periods can determine the maximum rate of infection. In simulated progress curves the most rapid increase in abundance of stipe rust on wheat occurred where the latent period was short (Zadoks, 1971), whereas in endemic diseases of trees, the latent period is the longest and therefore the infection rate becomes small (van der Plank, 1975,.
Spatial aspects of the environment call for a sub-division into macro, meso and micro-environment in order to identify specific areas of interest (Zakoks and Schein, 1979). The micro-environment is the space in which the epidemiological processes at cell and organ level occur. The meso-environment is formed by the crop. The macro-environment is the air layer from the crop surface to the troposphere.

1.8.3 Environment

Very often environmental influences have a relative rather than absolute effect on epidemics. Thus a favorable level of one or more factors may compensate for a certain deficiency in another factor e.g. infection rate of late blight on tomatoes increases with larger amounts of inoculum, but if inoculum and leaf wetness are constant, then temperature becomes the dominant determinant (Rotem et al., 1971)

1.9 Macro- and Micro- climatic influnces

Climate describes the average patterns of atmospheric conditions (temperature, precipitation, etc.) typical for a given location, whereas weather represents the actual atmospheric conditions prevailing at a given site and time (Rotem, 1978). Atmospheric factors affect an epidemic through their effects on pathogens and individual host plants. In the soil environment an epidemic results from a relatively slow and prolonged buildup of the inoculum and therefore is little influenced by short-term weather fluctuations. By contrast, the habitat of pathogens, which invade aerial parts of plants, is immediately and profoundly influenced by weather (Rotem, 1978).
The resulting epidemics are often sporadic, and their frequency is determined by the occurrence of suitable weather rather than climatic conditions. Atmospheric parameters are usually expressed as daily,

monthly, or seasonal means, but disease development actually depends upon the frequency of occurrence of favorable and unfavorable conditions (Schröder, 1963). There are other complicating effects in that disease is also affected by the microclimatic values.

Influence of weather on airborne pathogens

Survival of pathogens is important not only from one season to the next, but also over the relatively short time of sporulation until the time of infection. Spores of fungi survive better at low temperatures and usually at low relative humidity although there are notable exceptions e.g. basidiospores of rust fungi which are mainly dispersed at night (Cohen and Rotem, 1971). The ability to survive is adversely affected by solar radiation (Hsieh and Buddenhagen, 1975). Survivability is basically a genetic feature of any given species, and ra[illegible] from minutes to years (Rotem, 1968). From the epidemiological point of view, survival is most important when adverse conditions exist between two growing seasons or between the time of sporulation and infection.

Temperature, radiation and light effects

Unfavorable temperatures in the field often inhibit an epidemic temporarily, but do not eradicate the pathogen, unless they last for prolonged periods (Rotem, 1978). In cool seasons low night temperatures reduce the rate of infection and sporulation processes, rather than having an effect on the pathogen already present in infected tissue. In hot zones, inhibition of epidemics is due to high daytime temperatures which endanger spore viability, speed up lesion development (optimum temperature for which is usually higher than that for colonization) and thus decrease the sporulating potential of obligate parasites. Since evapotranspiration is increased in general during hot daytime temperatures, and in infected leaves in particular, high temperatures can speed up the destruction of infected leaves in spite of inhibited development of the pathogen. Extreme solar radiation can in some cases inhibit epidemics e.g. as with late blight on potatoes (Rotem et al. 1970).

The indirect effect of light intensity and photoperiod, acting via

host's susceptibility, has been proved on several occasions (Colhoun, 1973), in growth chamber experiments, but in field studies researchers were not able to separate the effects of varying conditions of light from other factors such as temperature and humidity. Through its effects on photosynthesis by the host, light stimulates sporulation of all obligate parasites (Cohen and Rotem 1970), but under most environmental conditons light intensity in the field is not the factor limiting sporulation. Light in conjunction with high (but not low) temperatures inhibits most species in the final stage of sporogenesis (Bashi and Rotem, 1976).

Moisture effects

Except for powdery mildews and some 'wound' pathogens, a film of free moisture on the surface of leaves is essential for infection by most pathogens e.g. some pathogens like *Phytophthora palmivora* on papaya, penetrate after a wetting period as brief as 15 min (Hunter and Kunimoto 1974). Although sporulation of some species occurs at a relative humidity close to 100 percent (except for rusts, powdery mildews and some minor pathogens), the most abundant sporulation usually is induced by free water on the leaf surface. In general sporulation requires longer wet periods than infection, but some fungi sporulate after several short wet periods interrupted by dry intervals (Rotem et al., 1976).

The three major sources of moisture for plant disease epidemics are rain, dew and overhead irrigation. Rain is a macroclimatic factor in contrast to sprinking and affects larger areas. Most literature mentions epidemics associated with the total amount of rainfall but few indicate the effect of intensity of seasonal distribution of rain on epidemics (Rotem, 1978). In dewless areas, for example, foliage epidemics are expected to be affected by frequent and evenly distributed rains rather than occasional heavy but short periods of rain. Pathogens not adapted to wind dispersal may benefit more from heavy showers. Specific preferences for a type of rain regime therefore depends apon characteristics of the host or pathogen e.g. in the case of sunflower downy mildew, rain is critical in the first fortnight of growth because only then are the seedlings susceptible to

systemic infection (Zimmer, 1975). Dew is a microclimatic factor. Causal relationships between dewfall and epidemics have been established (Wallin, 1967) despite limitations in recording. Dew, which largely coincides with darkness, will usually promote sporulation. The duration of dew periods is more important than the amount of water deposited (Rotem, 1978). The effect of dew may be more pronounced in hot and rainless areas (Rotem et al., 1970). The importance of dew in these areas stems from relatively high night temperatures which accompany dewfall. The influence of dew continues until the drops of films of water evaporate from the leaf surface, and this depends on the density of foliage as well as weather conditions. The hotter, drier or windier it is, the quicker the drying process will be.

Phases of infection, sporulation, and dispersal are all affected by microclimatic conditions ir the phyllosphere. The microclimate of a plant tissue is affected by the ambient climate through an exchange of energy, radiation flux and air temperature. Wind speed, relative humidity and transpiration all influence the final balance (Rotem, 1978). These microclimatic phenomena are also influenced by topography. Plant density also plays a role in determining the degree to which the microclimate within a plant canopy differs from that of the surrounding air. In less dense stands, sunlight reaches most parts of the plant. The field is also well aerated because wind movement is not hampered, and this results in more rapid drying of rain or dew. Radiation energy also penetrates the ground and raises the temperature of the upper soil (Geiger, 1957), thereby creating less favorable conditions for foliage pathogens. In dense stands radiation acts primarily on the outer leaves (Rotem, 1978). Because of shading, and less radiation, the inner leaves remain in a more humid surrounding and at night retain more heat, thereby allowing more favorable sites for infection than the outer leaves. However the macroclimate does influence the conditions of the microclimate ultimately. The density of plant canopy also affects the pattern of spore dispersal. Spores in denser stands are longer protected from macroclimatic conditions (Rotem, 1978). Thus interactions between several physical and biotic factors in the micro-environment of the pathogens will result in the

development of amounts of disease in a certain season or habitat.

3.2 AIMS

The general aim of this study is to attain a better understanding of naturally occurring diseases. Rust diseases on economically important agricultural crops have been studied extensively but little is known about graminaceous species in a natural population. *Phyllachora* species are widely distributed geographically, and are found on hosts in the Gramineae and on hosts in mary other plant families. The taxonomy and morphology of this fungus has been studied in the past (Parbery, 1963, 1967) but no work has been done on the extent or occurrence of this fungus in a natural savanna ecosystem. The specific aims incorporate aspects as follows:

1) The measurement of the amount of infection present throughout the season using the parameters incidence and severity. Incidence is the proportion of infected plants, and severity is the extent to which each leaf is infected. Consequently, in order to measure severity, an assessment key based on field assessment, had to be devised.

2) Description of the epidemics and comparisons of the relative growth rates and patterns of the disease progress curves between seasons and between infections within a growing season.

3) Relationship between intensity and severity.

3.3 MATERIALS AND METHODS

3.1 Field methods

Studies were carried out in camp three of the study area. For sampling. 10m line transects were taken randomly throughout the research area. For the grasses, tufts falling on the line and 0.5m on either side were sampled. Whole tufts were analysed to overcome sampling bias as spores tend to land on the more accessible outer leaf blades. Only living blades were sampled, since the dead blades would have been included in the previous assessment. Sampling was carried out twice a month, and the leaf blades assessed individually. For *B. africana* similar transects were laid down, and the trees falling within one metre either side of the transect were sampled. Since the distribution of the necrotic spots on the leaves proved to be uniform over the entire tree, only the lower branches within reach

were sampled. Several branches were picked around the tree and all the leaves assessed. Only whole intact leaves were used.

3.2 Disease assessment keys

Disease was measured using the parameters, incidence and severity. Disease incidence was calculated as the percentage of plant units (leaves) infected. Severity was estimated as the percentage of leaf area affected by lesions. Leaves were categorized into several infection classes (0-6) based on the key of percentage leaf area infected The classes were based on a logarithmic scale since pathogens tend to multiply geometrically whereas time progresses arithmetically. Such a logarithmic scale attaches equal importance to both pathogen and time increases. Also the human eye can more readily detect differences on a logarithmic scale. Preliminary leaf samples were collected and keys devised for diseases at Nylsvley using James (1971) as a guideline (Fig. 13).

The average values for incidence and severity for each transect and for all transects at a given sampling time were calculated. From these figures, the disease severity index was calculated using a formula devised by McKinney (1923):

$$S.I. = \frac{\text{sum of all disease ratings}}{\text{total no. ratings x max. disease grade}} \times 100$$

Maximum disease grade = 6 on a 0-6 scale. Provided the above determinations are made at frequent intervals the values can be plotted on a time basis, the resulting disease progress curves defining the course of the diseases. Curves for the progress of incidence and severity were plotted for the two grass species and *T. africana* for two consecutive growing seasons October 1978 - April 1979 and October 1979 - April 1980. The incease of a foliage disease is usually the result of two simultaneous processes: an increase in incidence and severity. In characterizing the relationship between incidence(I) and severity (S) one can ascertain whether a disease increases more by I relative to S or conversely. For this an exponential equation can be used

(James and Shaw, [illegible])

$$I = 100\ (1-r^2) \quad 0<r<1$$

I = Incidence

S = severity

$r = e(^1/_b)$

$b = \frac{y}{x}$ = slope

r - describes the increase in I relative to S.

The equation satisfies the condition that I = 0 when S = 0, and that as S increases, I also increases. A larger r value implies that disease increases relatively more by S than I, and conversely a smaller r value means disease increases more by I than S.

3.3 Curve fitting and transformations

The progress of a disease generally follows one of two courses - exponential or S-shaped (sigmoid) curve. The exponential growth curve is described as :

$$r_1 = \frac{1}{t_2-t_1} \quad \log_e \frac{x_2}{x_1} \quad (T^{-1})$$

t = time

x = disease [illegible]on ie. severity or intensity.

An exponential progress curve can be reduced to a straight line by plotting log x against t. The relative growth rate is given by the slope of the log transformed linear regression. However the exponential growth model has a limited value as it assumes the population increases to infinity and this is not the case as the pathogen usually runs out of host tissue as the season comes to an end, and the grasses senesce and the deciduous trees lose their leaves. Rather then most diseases follow the S-shaped course of increase. Disease progress curves (exponential; power curve; log; linear) were subjected to curve fitting tests to determine the best fit. Exponential curves were log transformed, and log 1/1-x plotted against time. The log phase of power curves or non-exponential curves were transformed into

straight lines by linear regression. The significance between two linear regressions was tested on the basis of comparing the two slopes involved. A small sample t-test for parallelism was employed, where the test statistic is computed :

$$T = \frac{\hat{b}_1 - \hat{b}_2}{S_{\hat{b}_1 - \hat{b}_2}}$$

$\hat{b}_1$ = least-squares estimate of the slope b_1, and n is the no. of observations.

$\hat{b}_2$ = least-squares estimate of the slope b_2, and n_2 is the no. of observations.

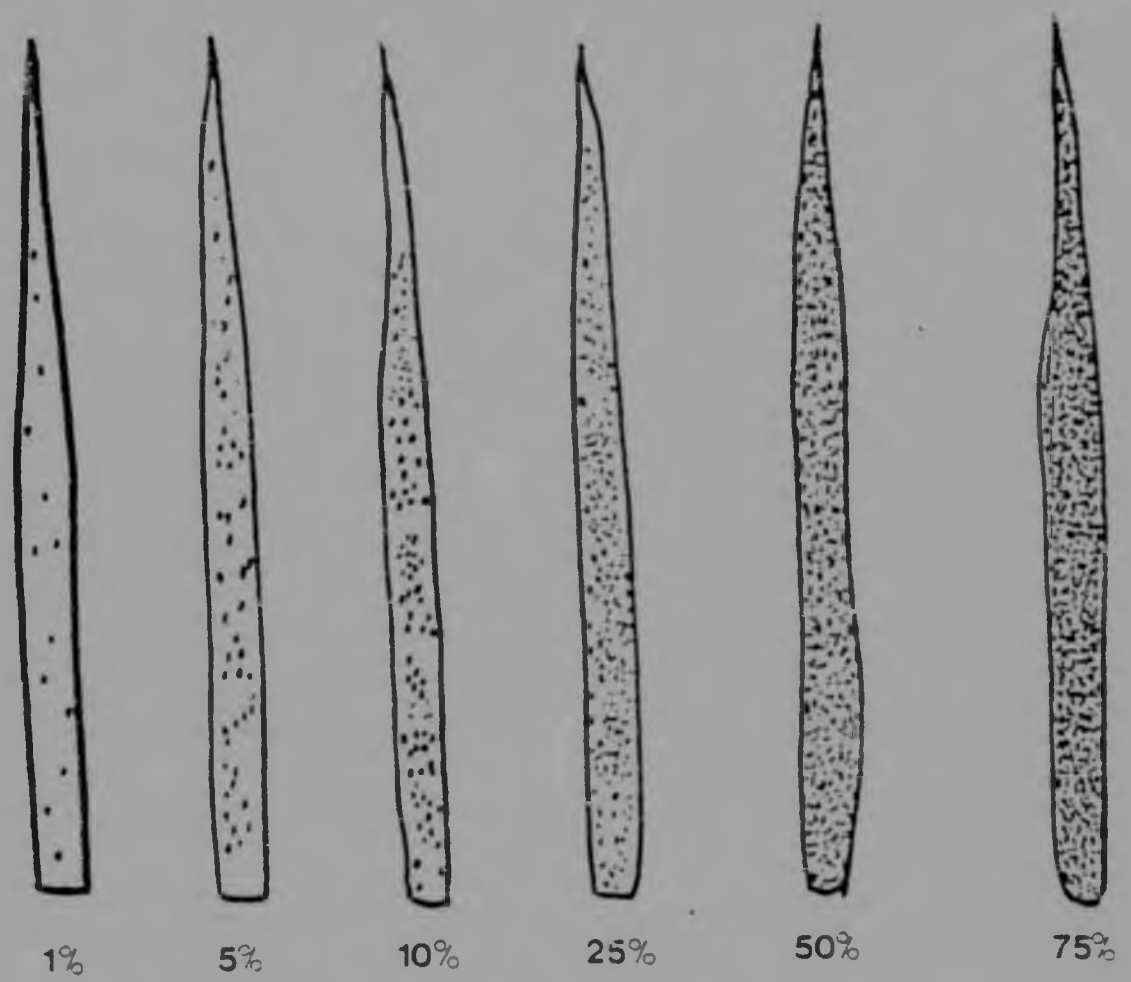
$S_{\hat{b}_1 - b_2}$ = estimate of the standard deviation of the estimated difference between slopes $(\hat{b}_1 - b_2)$.

The null hypothesis is given by $H_o : b_1 = b_2$. The test statistic is distributed as t with $n_1 + n_2 - 4$ degrees of freedom when H_o is true. Since one is only interested in the second phase (exponential phase) of the progressive leg (Fig. 14) only these figures were transformed. The transformation was based on the fact that the rate of increase of an infected area at any time (t) depends not only on the area already infected (x), but also on the leaf area remaining to be infected (1-x) (van der Plank, 1963) :

$$\frac{dx_t}{dt} = r \cdot x_t \ (1-x_t) \qquad (T^{-1})$$

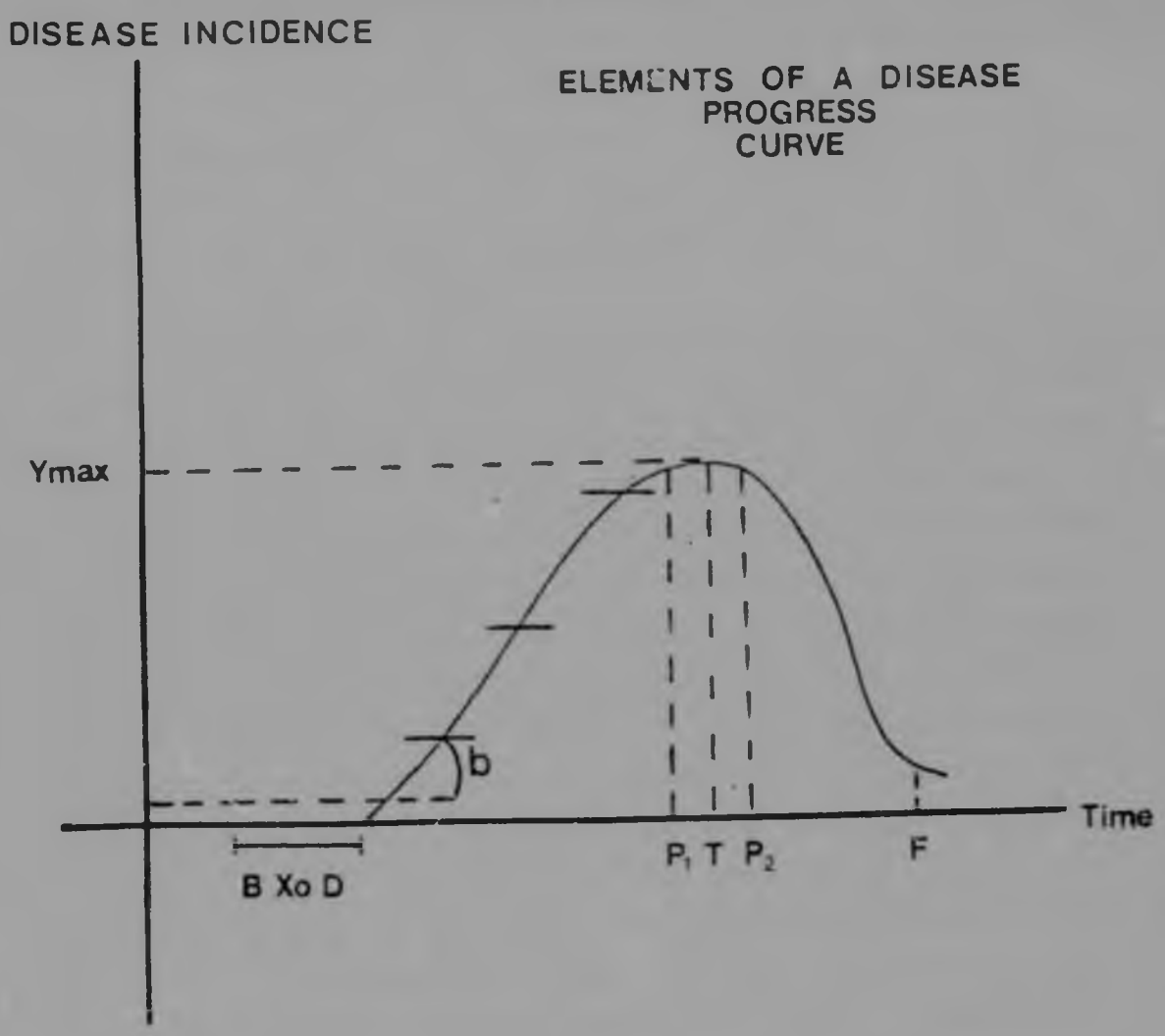
r = apparent rate of infection. (1-x) is the correction factor

$$\therefore \quad r = \frac{1}{t_2 - t_1} \left(\log_e \frac{x_2}{1-x_2} - \log_e \frac{x_1}{1-x_1} \right)$$



$$\text{Severity index} = \frac{\text{sum of all disease ratings}}{\text{total no. of ratings} \times \text{max. disease grade}}$$

Fig. 13 Disease assessment key for *D. eriantha* and *P. maximum*



Ymax = maximum disease incidence
X_0 = beginning of refoliation before first discernible symptoms
DP_1 or DT = length of progressive leg of the curve
P_1P_2 = duration of asymptote (plateau)
P_2F = duration of degressive leg of curve
b = regression co-efficient

Fig. 14 Elements of a disease progress curve

3.4 RESULTS

Incidence and severity data were collected during two growing seasons, 1978/79 and 1979/80. Results with standard errors are presented in Tables 2-4. The first leaf flushes occurred in September 1978 and October 1979 after the first spring rains and the growing season extended to March/April. Rainfall data is presented in Table 6 and other climatic data in Table 7 and 8. Graphs depicting seasonal climatic patterns are illustrated in Figs. B-I. Tables and figures are on pages 56-59.

The rates and patterns of lesion spread on *B. africana* are plotted in Figs. 15 and 16. Disease progress curves of rust on *D. erianthа* are represented in Figs. 17 and 18, and of tarspot on *P. maximum* in Figs. 19 and 20. Day zero was taken as the first day of disease recording and measurement. The initial lag phases of the epidemics were not observed in the field and only the subsequent phases measured. Smoothed untransformed graphs were plotted and linear regressions calculated (Table 5 A) for the progressive phase of non-linear curves. Exponential curves were log transformed (1/1-x). The relationship between the two simultaneous processes of incidence and severity increases was established for the three species. The r values (which define the increase in incidence (I) relative to severity (S)) were established (Table 5 B). The significance between the relative growth rates of epidemics was assessed by determining the significant differences between the slopes of the linear regressions. Tables and figures can be found on pages 62-76.

4.1 *B. africana*

The maximum incidence (31%) and severity (10.9%) of necrotic lesions was achieved in April 1979 of the 1978/79 growing season (Fig. 15). In contrast the maximum incidence (29%) and severity (5.2%) figures were attained at the beginning of January 1980 of the 1979/80 season (Fig. 16). The decline in severity of lesions in early January was due to the defoliation of *B. africana* trees as a result of an extensive caterpillar attack (Fig. A). A new flush of leaves occurred in mid-January as a result of heavy rains (152.5 mm) and a new growth cycle commenced. This would account for the interruption in the progress curve (Fig. 16).

3.4 RESULTS

Incidence and severity data were collected during two growing seasons, 1978/79 and 1979/80. Results with standard errors are presented in Tables 2-4. The first leaf flushes occurred in September 1978 and October 1979 after the first spring rains and the growing season extended to March/April. Rainfall data is presented in Table 6 and other climatic data in Table 7 and 8. Graphs depicting seasonal climatic patterns are illustrated in Figs. B-I. Tables and figures are on pages 56-59.

The rates and patterns of lesion spread on *B. africana* are plotted in Figs. 15 and 16. Disease progress curves of rust on *D. eriantha* are represented in Figs. 17 and 18, and of tarspot on *P. maximum* in Figs. 19 and 20. Day zero was taken as the first day of disease recording and measurement. The initial lag phases of the epidemics were not observed in the field and only the subsequent phases measured. Smoothed untransformed graphs were plotted and linear regressions calculated (Table 5 A) for the progressive phase of non-linear curves. Exponential curves were log transformed (1/1-x). The relationship between the two simultaneous processes of incidence and severity increases was established for the three species. The r values (which define the increase in incidence (I) relative to severity (S)) were established (Table 5 B). The significance between the relative growth rates of epidemics was assessed by determining the significant differences between the slopes of the linear regressions. Tables and figures can be found on pages 62-76.

4.1 *B. africana*

The maximum incidence (31%) and severity (10.9%) of necrotic lesions was achieved in April 1979 of the 1978/79 growing season (Fig. 15). In contrast the maximum incidence (29%) and severity (5.2%) figures were attained at the beginning of January 1980 of the 1979/80 season (Fig. 16). The decline in severity of lesions in early January 1980 was due to the defoliation of *B. africana* trees as a result of an extensive caterpillar attack (Fig. A). A new flush of leaves occurred in mid-January as a result of heavy rains (152.5 mm) and a new growth cycle commenced. This would account for the interruption in the progress curve (Fig. 16).



Fig. A Caterpillars (arrow) defoliating *B. africana* trees

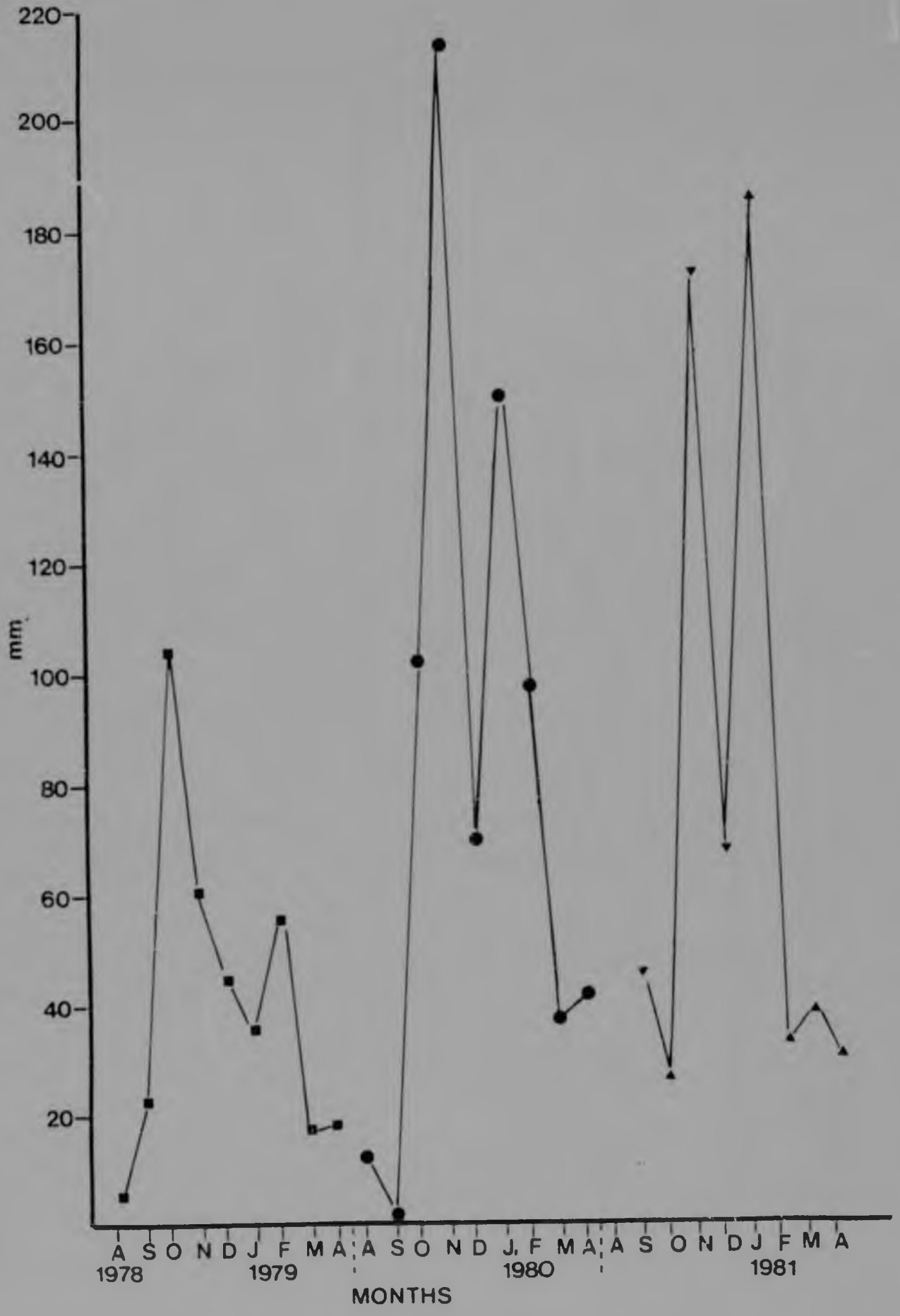


Fig. B Rainfall data from 1978 to 1981

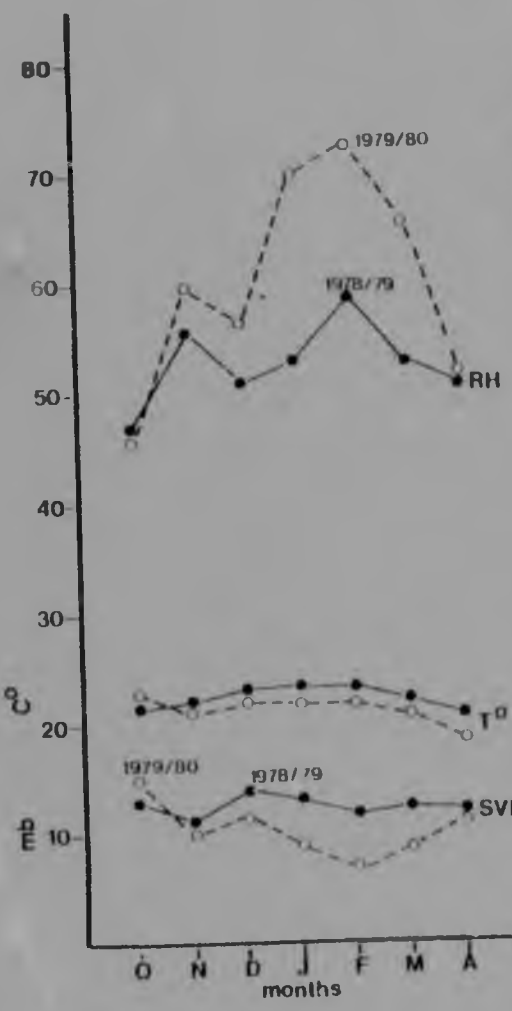


Fig.C Relative humidities(top) and saturation vapour pressure deficits (bottom)

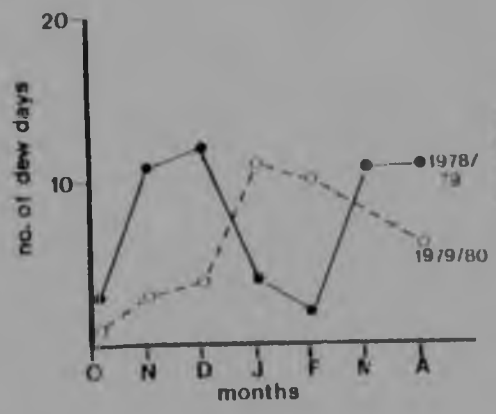


Fig.E No. of dew days

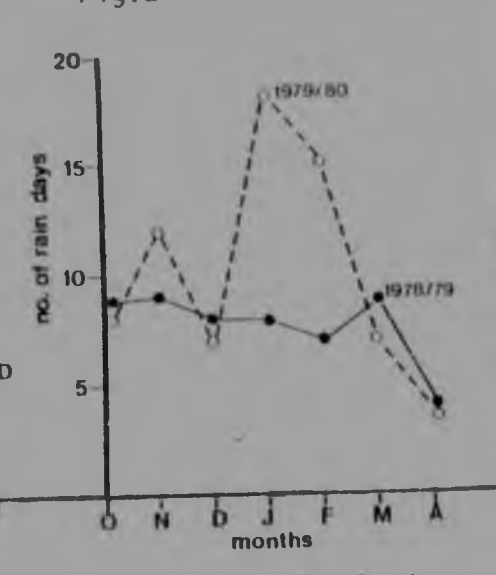


Fig.D No. of rain days

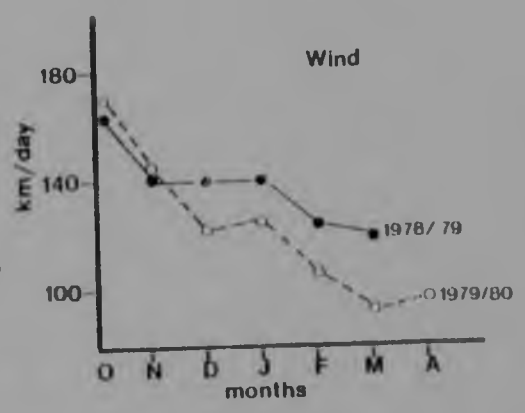


Fig.G Wind measurements(km/day)

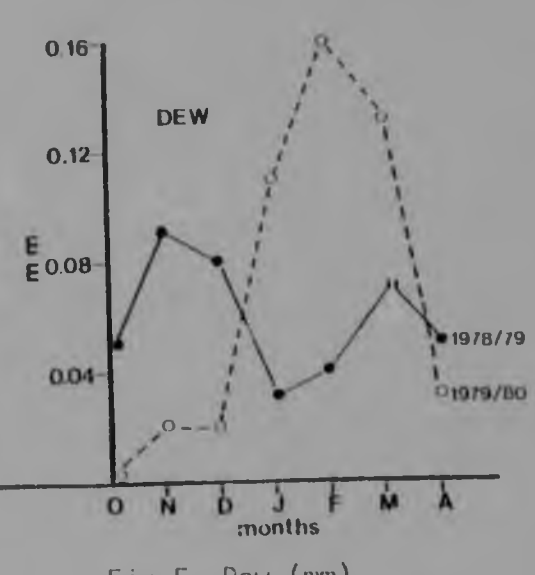


Fig.F Dew (mm)

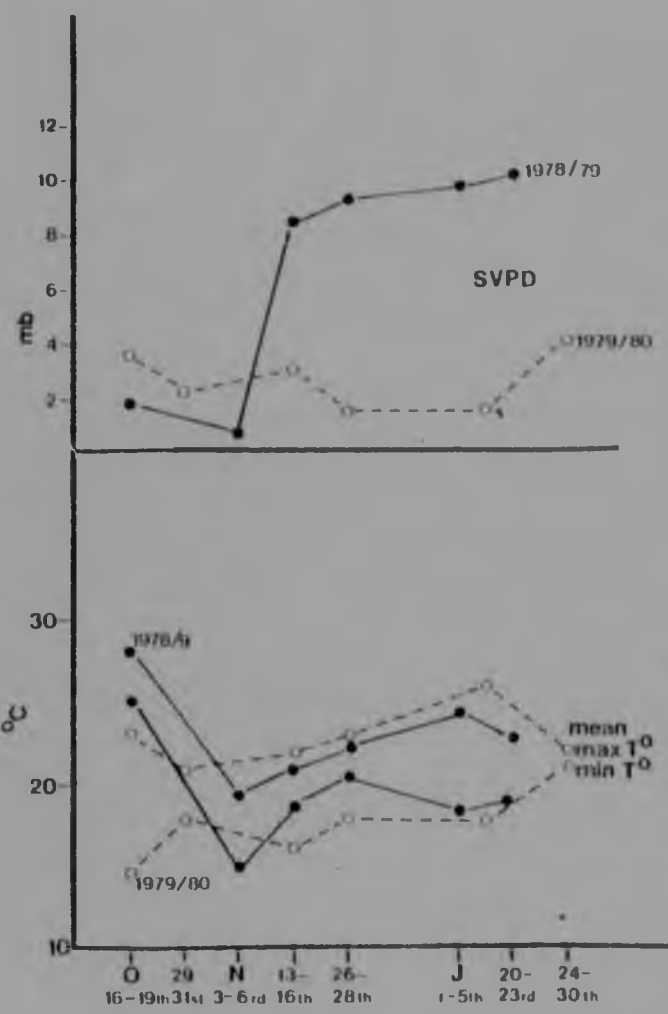


Fig.H (top) Lowest recorded saturation vapour pressure deficits. Fig.I Mean max and min temperatures

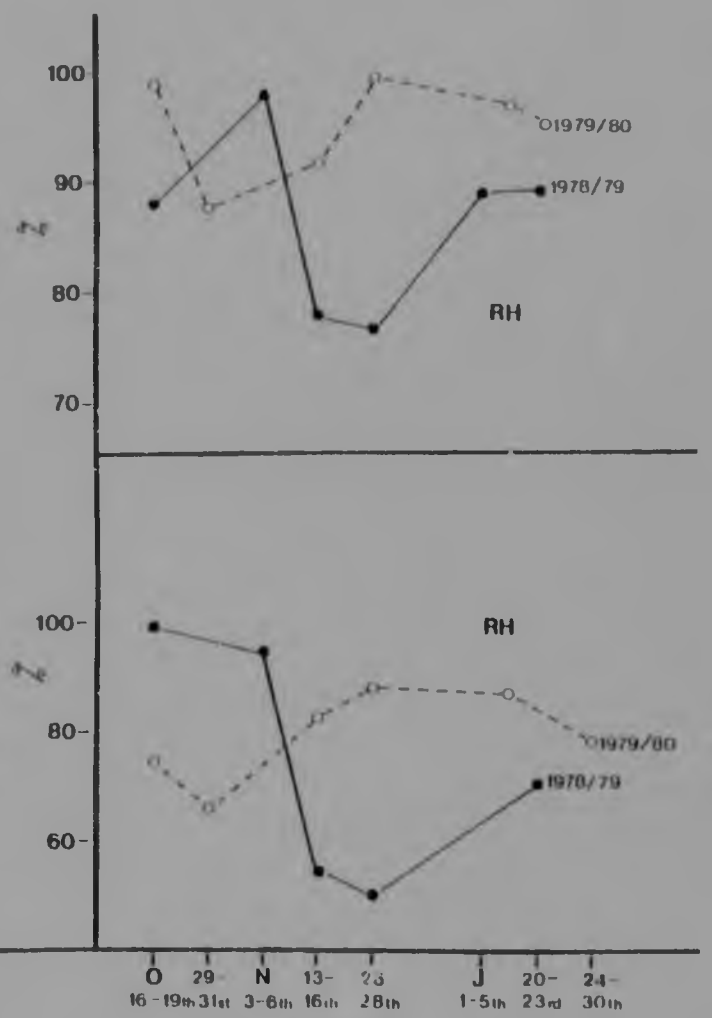


Fig.J(top) Maximum relative humidities recorded in the morning and afternoon (bottom)

The greater initial increase in incidence of lesions on *B. africana* in the 1979/80 growing season compared to 1978/79 may be attributed to a later leaf flush in September 1979 due to delayed spring rains.

Despite similar maximum incidence and severity indices for both growing seasons, the patterns, and relative growth rates of the two epidemics differ considerably. The structures of the epidemics are similar in that both curves represent discontinuous cycles where development of the necrotic lesions ceases due to senescence of the deciduous leaves at the end of the growth period. However the pattern is different in the 1979/80 growing season due to the death of the leaves in mid-season followed by a smaller secondary flush, which did not occur in the 1978/79 season. The initial relative growth rate (slope) in the incidence of lesions is much greater in the 1979/80 growing period, whilst towards the end of the growth period the relative growth rates (based on incidence) were similar for both seasons. The linear nature of the disease progress curves in 1978/79 indicates that lesion formation is not dependent on the availability of leaf tissue. However in the 1979/80 season, the logarithmic nature of the initial curve t_1-t_3 (Fig. 16) may possibly be a result of a decline in leaf tissue availability due to defoliation by caterpillars.

The relationship between incidence and severity was established (Figs. 21 and 22). The small value for r in the 1978/79 growing season (Fig. 21) indicates that the necrotic lesions increase relatively more by incidence than severity, as is the case in the initial period of the 1979/80 season (Fig. 22). However the growth of lesions after the new flush in January 1980 increased relatively more by severity than incidence.

4.2 *D. eriantha*

D. eriantha is a perennial grass, and the rust epidemic is discontinuous due to the life cycle of the grass where the leaves senesce towards the end of the growing season. The build up of *P. digitariae* is a result of a homogeneous infection chain where

one spore type (uredospore) infects the grass (ie. identical infection cycles, either on the same leaf blade or new leaves, follow one another).

The patterns of the rust epidemics differ between the two growth seasons. The disease progress curves for incidence and severity are linear in the 1978/79 season (Fig. 17) which indicates that neither leaf tissue availability nor host susceptibility is a limiting factor. However in the 1979/80 growing season the incidence of rust infection follows a logarithmic, assymmetrical pattern in the untransformed curves (Fig. 18). Severity increase for the initial period t_1-t_3 exhibited a slight exponential increase (r=0.93). A sudden decrease in severity occurred in late January 1980 (Fig. 18). This decline was followed by an increase in severity which occurred after the new flush of *D. eriantha* leaves. Maximum severity indices were attained in April (24%). The possible course of increase in severity (C_2), had senescence of some *D. eriantha* leaves followed by a secondary leaf flush not occurred, is indicated in Fig. 18. The maximum incidence of rust infection was 58% for both the 1978/79 and 1979/80 seasons, although the maximum was reached in December in 1978 whereas in the following season the maximum was reached later in the season in March. Maximum severity (14%) also occurred in December 1978, whereas the maximum (24%) was only attained in March 1980 the following season.

The relative growth rate of rust incidence was greater in 1978/79 than 1979/80 (determined by comparing the linear regression slopes; p=0.05) whereas the growth rate of the intensity or severity of infection throughout the season was greater in 1979/80 compared to 1978/79. The relationship between incidence and severity again illustrates that the rust infection of *D. eriantha* increases relatively more by incidence than severity in the 1978/79 season (Fig. 23) but this relationship behaves conversely in the later stages of disease development in 1979/80 (Fig. 24).

4.3 *P. maximum*

P. maximum is a perennial grass, and therefore as is the case in

Table 2 Incidence and severity data of *B. africana* (1978-1980)

TIME (DAYS)		INCIDENCE (%)	SEVERITY (%)
		OCTOBER 1978 - APRIL 1979	
t_1	1	7.9 ± 0.1	3.0 ± 0.1
t_2	11	13.9 ± 2.1	2.1 ± 0.3
t_3	25	14.4 ± 0.5	2.9 ± 0.4
t_4	35	17.0 ± 1.6	3.8 ± 0.7
t_5	50	19.5 ± 0.5	4.6 ± 0.2
t_6	65	19.4 ± 0.6	4.9 ± 0.3
t_7	115	20.0 ± 1.0	6.1 ± 0.2
t_8	135	22.0 ± 0.3	6.2 ± 0.3
t_9	150	25.0 ± 0.9	6.6 ± 0.5
t_{10}	170	31.0 ± 1.1	10.5 ± 0.3
t_{11}	190	31.0 ± 1.1	10.9 ± 0.2
		NOVEMBER 1979 - APRIL 1980	
t_1	1	9.30 ± 2.7	2.6 ± 0.6
t_2	30	27.0 ± 1.4	4.8 ± 0.9
t_3	50	29.0 ± 0.5	5.2 ± 0.1
NEW FLUSH			
t_4	75	1.90 ± 0.1	0.1 ± 0.1
t_5	90	4.80 ± 1.2	0.2 ± 0.3
t_6	120	7.40 ± 0.7	2.5 ± 0.3
t_7	150	10.0 ± 0.5	5.0 ± 0.4

Table 2 Incidence and severity data of *B. africana* (1978-1980)

TIME (DAYS)	INCIDENCE (%)	SEVERITY (%)
OCTOBER 1978 - APRIL 1979		
t_1 1	7.9 ± 0.1	3.0 ± 0.1
t_2 11	13.9 ± 2.1	2.1 ± 0.3
t_3 25	14.4 ± 0.5	2.9 ± 0.4
t_4 35	17.0 ± 1.6	3.8 ± 0.7
t_5 50	19.5 ± 0.5	4.6 ± 0.2
t_6 65	19.4 ± 0.6	4.9 ± 0.3
+ 115	20.0 ± 1.0	6.1 ± 0.2
t_8 135	22.0 ± 0.3	5.2 ± 0.3
t_9 150	25.0 ± 0.9	6.6 ± 0.5
t_{10} 170	31.0 ± 1.1	10.5 ± 0.3
t_{11} 190	31.0 ± 1.1	10.9 ± 0.2
NOVEMBER 1979 - APRIL 1980		
t_1 1	9.30 ± 2.7	2.6 ± 0.6
t_2 30	27.0 ± 1.4	4.8 ± 0.9
t_3 50	29.0 ± 0.5	5.2 ± 0.1
NEW FLUSH		
t_4 75	1.90 ± 0.1	0.1 ± 0.1
t_5 90	4.80 ± 1.2	0.2 ± 0.3
t_6 120	7.40 ± 0.7	2.5 ± 0.3
t_7 150	10.0 ± 0.5	5.0 ± 0.4

TABLE 3 Incidence and severity data and curve fitting analysis of rust-infected *D. eriantha*.

OCTOBER 1978 - FEBRUARY 1979			
TIME (DAYS)	INCIDENCE %	SEVERITY %	LINEAR CURVE FIT
t_1 1	11.6 ± 0.7	3.5 ± 0.2	INCIDENCE
t_2 15	23.3 ± 0.7	5.9 ± 0.1	r = 0.97
t_3 25	38 ± 1.5	8.4 ± 0.4	a = 0.12
t_4 45	2.3	10.6 ± 0.5	b = 0.01
			SEVERITY
t_5 55	57.0 ± 0.5	14.7 ± 0.2	
t_6 70	59.0 ± 0.6	16.0 ± 0.2	
t_7 85	50.0 ± 0.4	9.0 ± 0.2	r = 0.96
t_8 95	35.0 ± 0.6	7.0 ± 0.7	a = 0.03
t_9 105	24.0 ± 0.5	6.0 ± 0.6	b = 0.002
t_{10} 115	13.0 ± 0.2	5.0 ± 0.2	

NOVEMBER 1979 - APRIL 1980				
TIME (DAYS)	INCIDENCE %	LOGARITHMIC CURVE FITTING	SEVERITY %	
t_1 1	36.0 ± 1.6	r = 0.95	13.0 ± 1.3	
t_2 30	48.0 ± 2.8	a = 0.35	16.0 ± 1.8	
t_3 50	50.0 ± 2.4	b = 0.04	23.0 ± 0.9	log 1/1-x
t_4 75	52.0 ± 2.6	SEVERITY EXP-ONENTIAL CURVE FIT	14.0 ± 0.8	0.065
t_5 90	56.0 ± 2.8		19.0 ± 0.6	0.092
		r = 0.93		
t_6 120	58.0 ± 2.1	a = 0.12	23.0 ± 1.4	0.11
t_7 150	57.0 ± 0.9	b = 0.01	24.0 ± 0.2	0.119

Table 4 Incidence and severity data of *P. maximum* (1978/79 and 1979/80)

NOVEMBER 1978 - FEBRUARY 1979		
TIME (DAYS)	INCIDENCE %	SEVERITY %
t_1 1	2.7 ± 0.2	0.5 ± 0.02
t_2 10	14.1 ± 0.6	3.8 ± 0.2
t_3 30	36.5 ± 1.3	9.5 ± 1.0
t_4 40	44.5 ± 0.7	14.6 ± 0.8
t_5 70	47.0 ± 0.5	19.0 ± 0.6
t_6 90	51.0 ± 0.6	22.0 ± 0.9
t_7 100	45.0 ± 0.3	19.0 ± 0.2
t_8 115	10.9 ± 0.6	8.1 ± 0.4

JANUARY 1979 - APRIL 1980		
TIME (DAYS)	INCIDENCE %	SEVERITY %
t_1 1	12.0 ± 0.9	2.6 ± 0.1
t_2 25	28.0 ± 2.0	7.6 ± 0.7
t_3 40	57.0 ± 0.9	25.0 ± 1.2
t_4 70	61.0 ± 1.2	36.0 ± 0.6
t_5 100	67.0 ± 0.7	45.0 ± 1.3

Table 5 A Linear regression analysis of the progressive legs of disease progress curves.

1978/79 GROWING SEASON		
BURKEA INCIDENCE r = 0.85 a = 0.12 b = 0.001	DIGITARIA INCIDENCE r = 0.97 a = 0.12 b = 0.02	PANICUM INCIDENCE r = 0.77 a = 0.12 b = 0.01
SEVERITY r = 0.91 a = 0.02 b = 0.04	SEVERITY r = 0.96 a = 0.03 b = 0.002	SEVERITY r = 0.87 a = 0.02 b = 0.002
1979/80 GROWING SEASON		
BURKEA INCIDENCE t_1-t_3 r^2 = 0.90 a = 0.11 b = 0.004 t_4-t_7 r^2 = 0.97 a = -0.05 b = 0.001	DIGITARIA INCIDENCE r = 0.80 a = 0.41 b = 0.001	PANICUM INCIDENCE r = 0.82 a = 0.19 b = 0.01
SEVERITY t_1-t_3 r = 0.93 a = 0.03 b = 0.0005 t_4-t_7 r = 0.97 a = -0.06 b = 0.0007	SEVERITY t_1-t_3 r = 0.89 a = 0.12 b = 0.002	SEVERITY r = 0.92 a = 0.02 b = 0.004

Table 5 B. The relationships between incidence and severity for *B. africana*, *D. eriantha* and *P. maximum* (1978/79 and 1979/80 seasons)

SPECIES	SLOPE (b)	REGRESSION CO-EFFICIENT *
B. africana 1978/79	2.34	r = 1.53
1979/80	t_1-t_3 = 8.29 t_4-t_7 = 1.20	r = 1.13 r = 2.30
D. eriantha 1978/79	2.67	r = 1.45
1979/80	t_1-t_3 = 1.61 t_4-t_7 = 0.37	r = 1.86 r = 14.9
P. maximur 1978/79	4.01	r = 1.28
1979/80	1.09	r = 2.50

* $r = e^{(1/b)}$

Table 6. Rainfall data from the main weather station at Nylsvley (1978-1982).

YEAR AND MONTH	TOTAL RAINFALL (mm)	YEAR AND MONTH	TOTAL RAINFALL (mm)
August 1978	5.2	August 1980	-
September	23	September	46.5
October	104.7	October	27.9
November	60.9	November	173.9
December	45.3	December	67.8
January 1979	36.2	January	185.3
February	56.:	February	33.7
March	18.9	March	39.0
April	19.0	April	29.5
August 1979	12.5	August 1981	12.8
September	1.4	September	13
October	103.5	October	34.7
November	214.5	November	68.3
December	70.7	December	44.1
January 1980	152.5	January 1982	153.9
February	98.2	February	54.2
March	38		
April	42.6		

Table 7 Average monthly climatic data from October 1978 to April 1980 (taken from the synoptic summary charts at the Nylsvley weather station 2).

MONTHS	NO. OF DAYS OF RAIN	T° (°C)	RELATIVE HUMIDITY %	SATURATION VAPOUR PRESSURE DEFICIT (mb)	WIND (Km/day)	DEW (mm)	NO. OF DEW DAYS
OCTOBER 1978	9	21.5	47.4	13.4	162.2	0.05	3
NOVEMBER	9	22.0	56.4	11.4	140.2	0.09	11
DECEMBER	8	23.2	51.9	13.6	140.1	0.08	12
JANUARY 1979	3	23.4	53.4	13.3	140.0	0.03	4
FEBRUARY	7	23.7	59.0	11.9	123.1	0.04	2
MARCH	9	22.4	53.1	12.6	120.2	0.07	11
APRIL	4	20.8	51.5	11.8	108.3	0.05	11
OCTOBER 1979	8	22.7	46.1	14.7	169.8	0.00	1
NOVEMBER	12	21.6	59.6	10.3	144.4	0.02	3
DECEMBER	7	22.5	56.8	11.7	122.3	0.02	4
JANUARY 1980	18	22.2	66.9	8.8	123.5	0.11	11
FEBRUARY	15	22.3	72.5	7.3	106.0	0.16	10
MARCH	7	21.1	65.5	8.5	92.4	0.13	18
APRIL	4	18.5	51.6	10.2	95.5	0.03	6

Table 8 Selected climatic data from the Nylsvley weather station 2
(1978 - 1980)

MONTH	DAYS	RANGE MIN	RANGE MAX	MAX. RELATIVE HUMIDITY (%) MORNING	MAX. RELATIVE HUMIDITY (%) AFTERNOON	SATURATION VAPOUR PRESSURE DEFICIT (mb) MIN	SATURATION VAPOUR PRESSURE DEFICIT (mb) MAX
OCTOBER 1978	18-19th	27.8	24.5	88	99	1.8	4.3
NOVEMBER	3-6th	15.1	19.7	98	96	0.56	10.7
	13-16th	18.3	21.6	78	55	8.3	8.5
	26-28th	20.3	22.6	77	50	9.3	10.0
JANUARY 1979	1st-5th	18.3	24.5	89	51	8.8	9.0
	20-23rd	18.3	22.7	89	71	10.2	8.0
OCTOBER 1979	16-22nd	15.5	23.2	98	72	3.4	9.7
	29-31st	16.7	21.0	88	67	2.2	15.2
NOVEMBER	8-20th	16.3	22.9	92	83	3.2	11.0
	23-27th	18.1	23.0	99	88	1.4	10.4
JANUARY 1980	4-18th	17.7	25.9	96	87	1.7	11.9
	24-31st	20.4	22.4	95	78	4.2	11.1

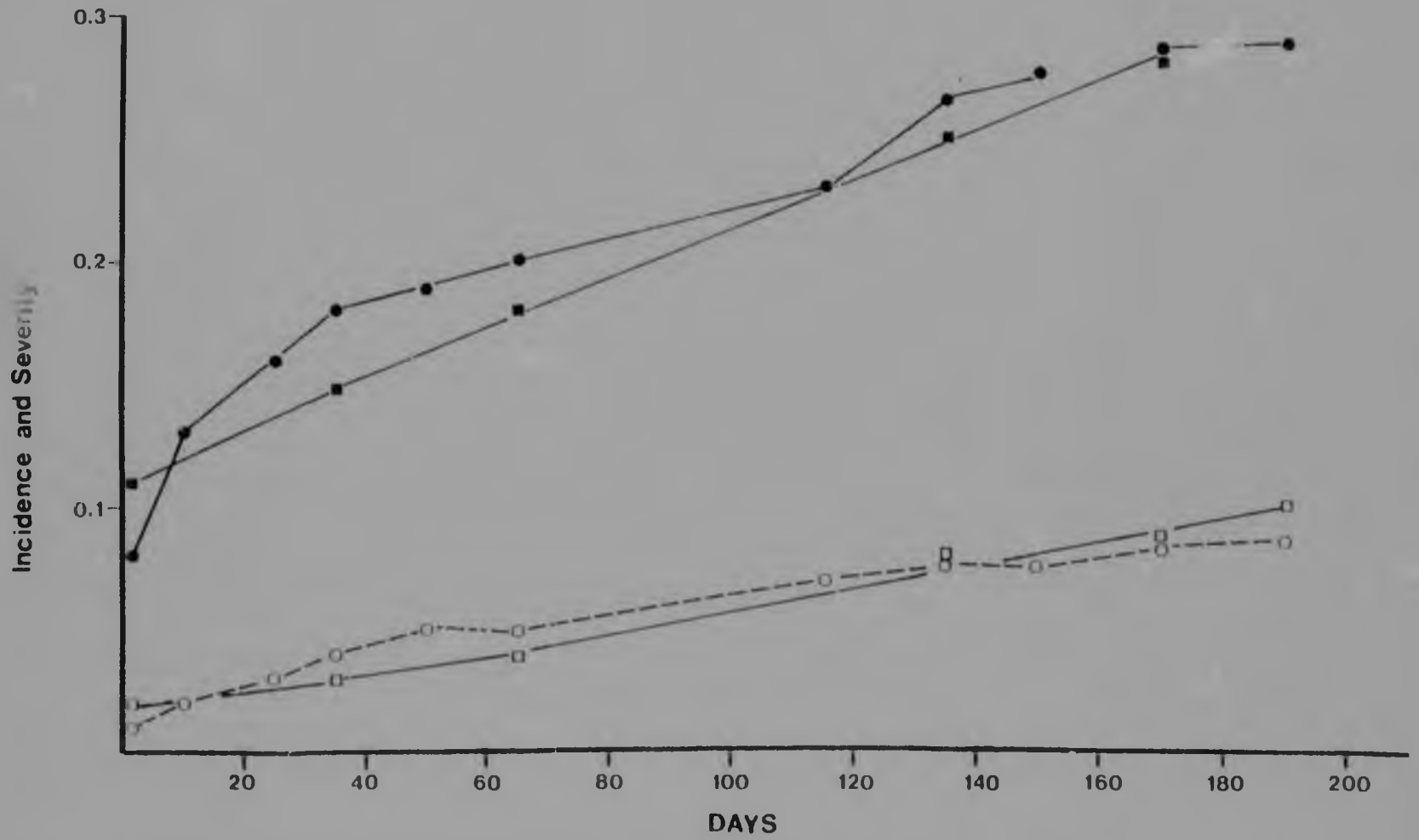


Fig.15 Incidence and severity of necrotic lesions on *B. africana* (1978/79)

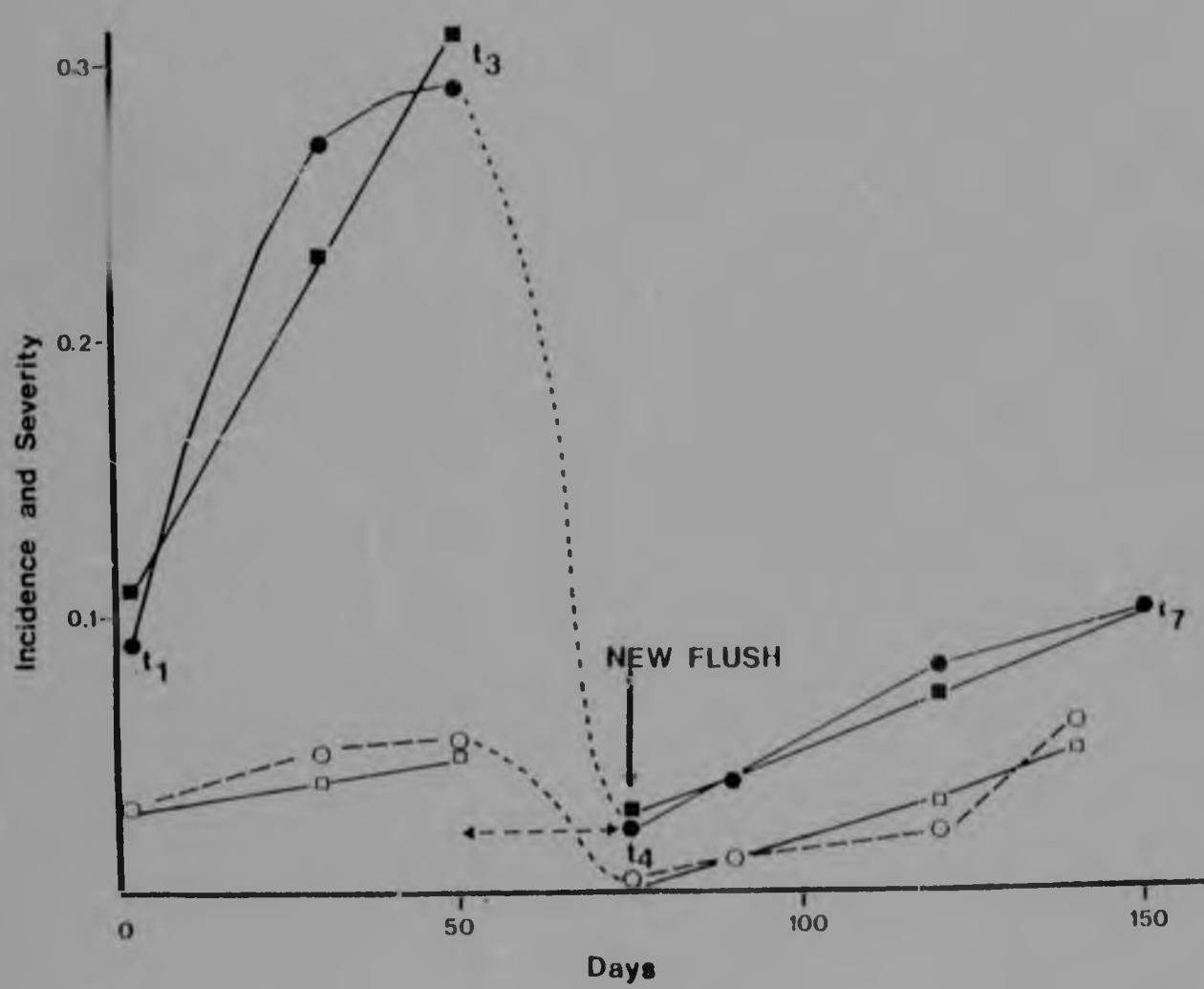
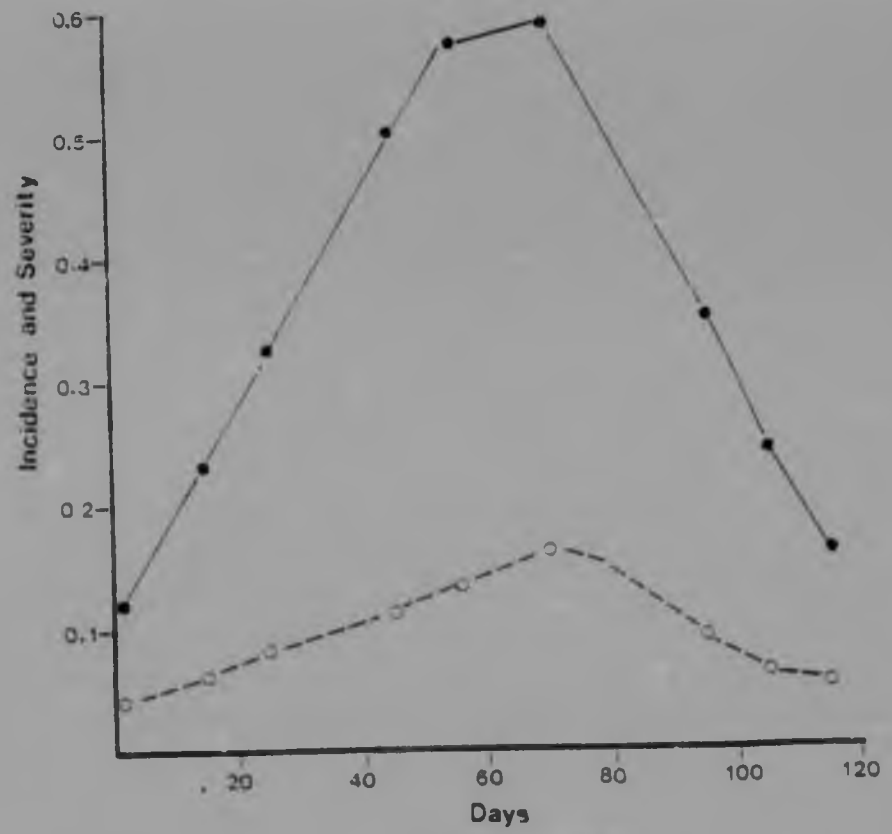


Fig.16 Incidence and severity of necrotic lesions on *B.africana* (1979/80)



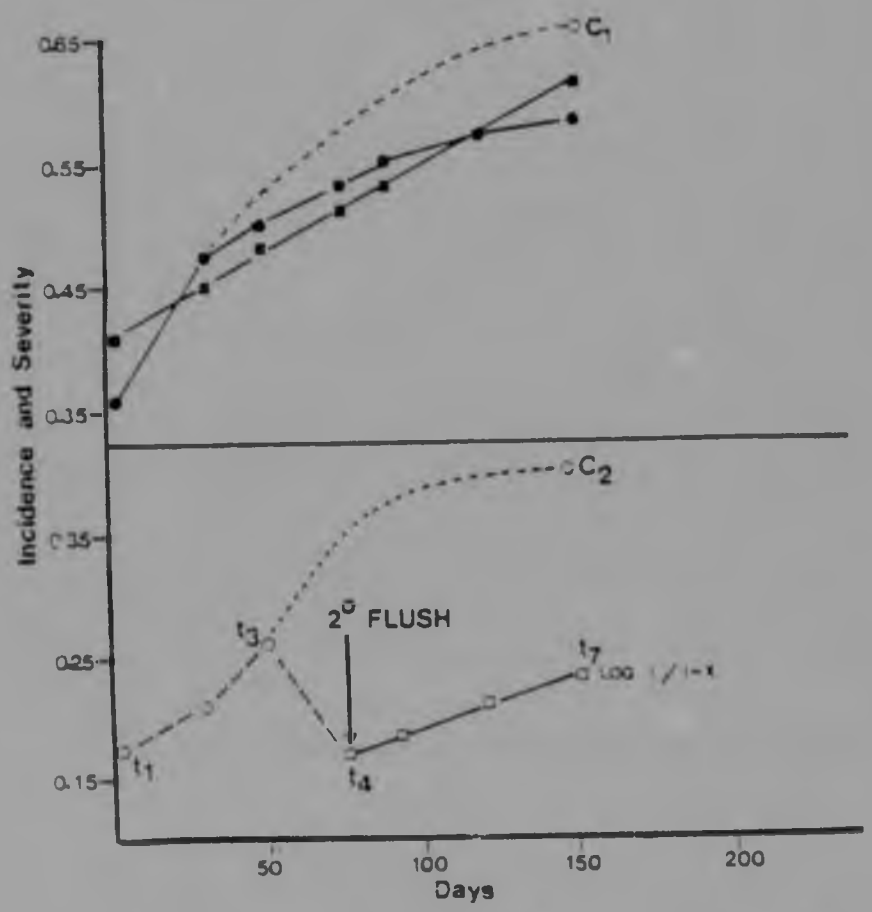
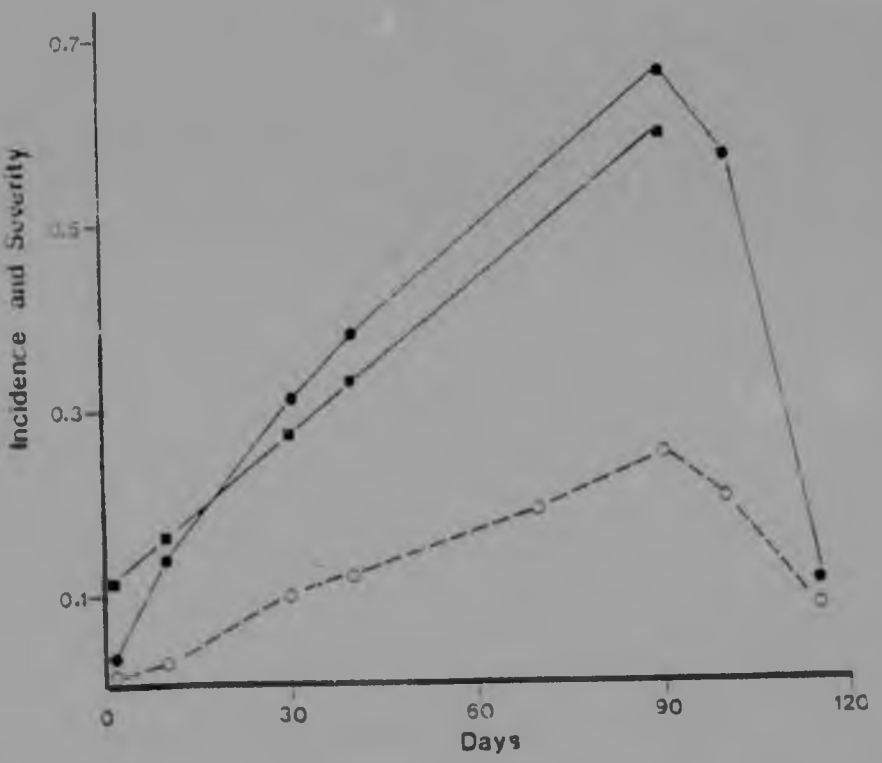


Fig.17(top) Incidence and severity of rust on *D riantha* (1978/79) and Fig.18(bottom) incidence and severity in the 1979/80 season



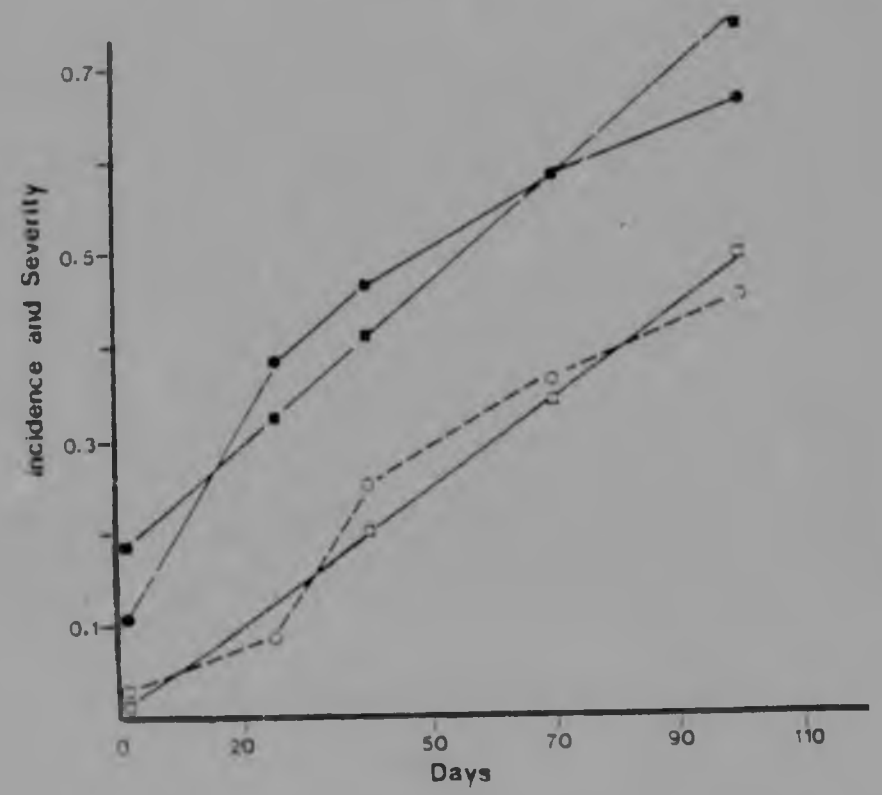
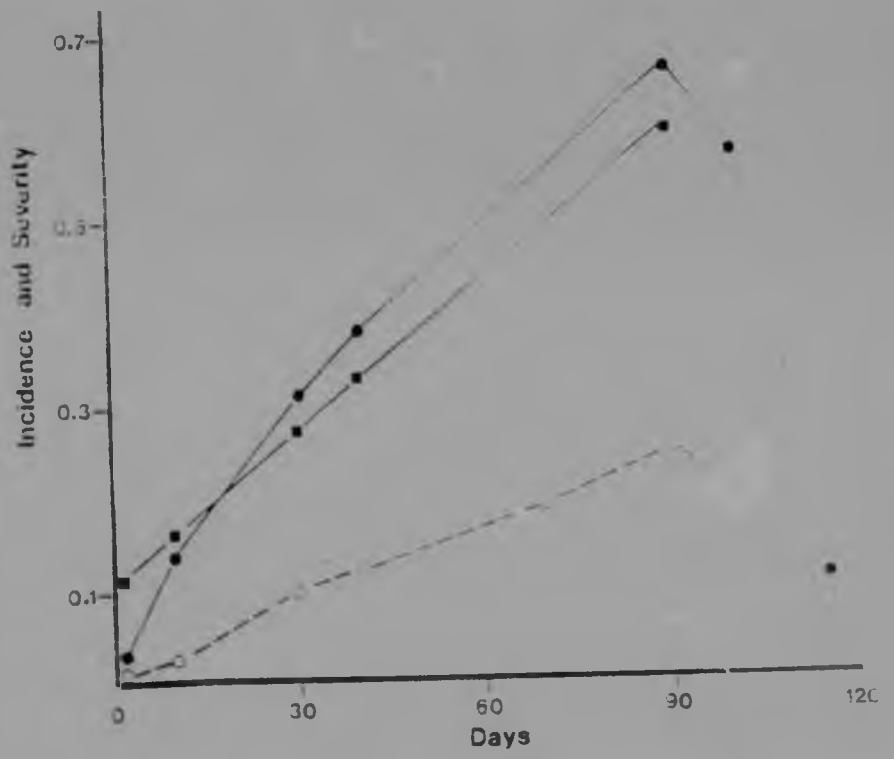


Fig.19 Incidence and severity of tarspot on *P.maximum* in the 1978/79 season (top) and Fig.20 (bottom) in the 1979/80 growing season



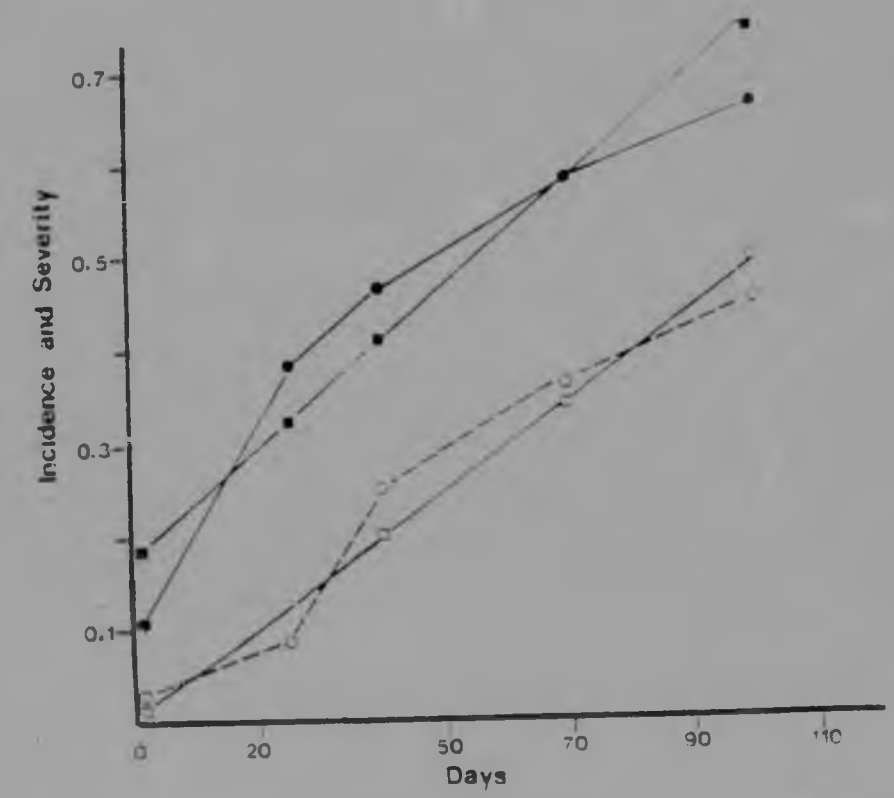
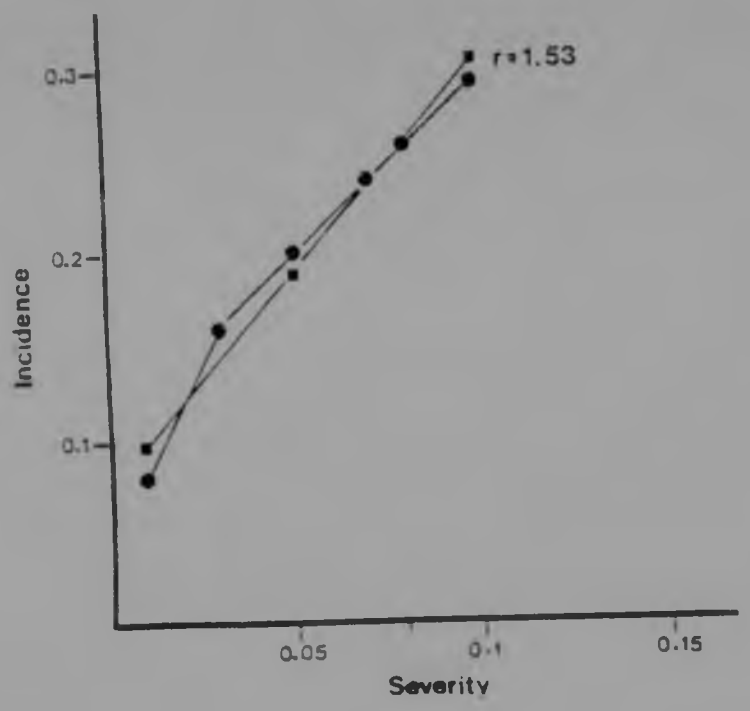


Fig.19 Incidence and severity of tarspot on *P. maximum* in the 1978/79 season (top) and [illegible] (bottom) in the 1979/80 growing season



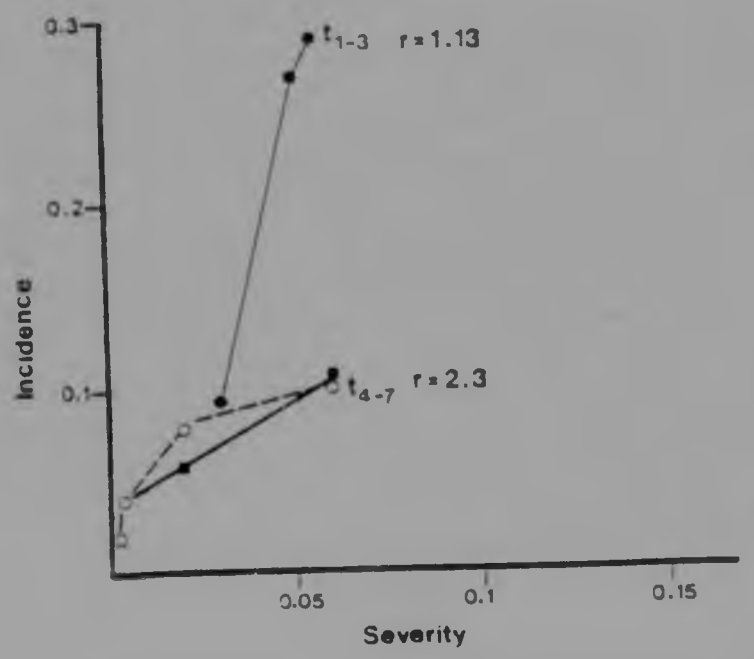
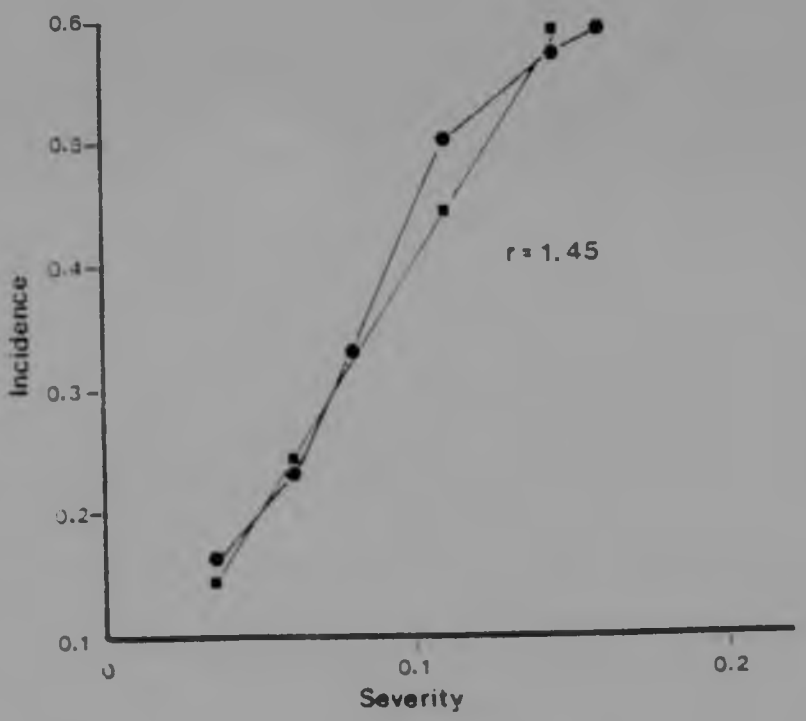


Fig.21 (top) Relationship between incidence and severity defined by the r values in necrotic *B.africana* leaves (1978/79) and Fig.22 relationship in the 1979/80 season



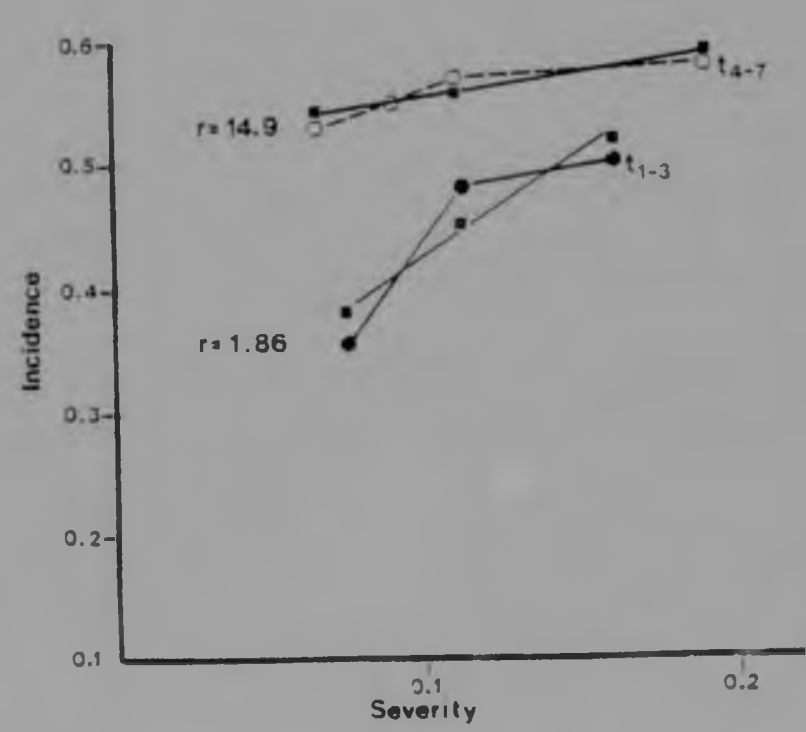
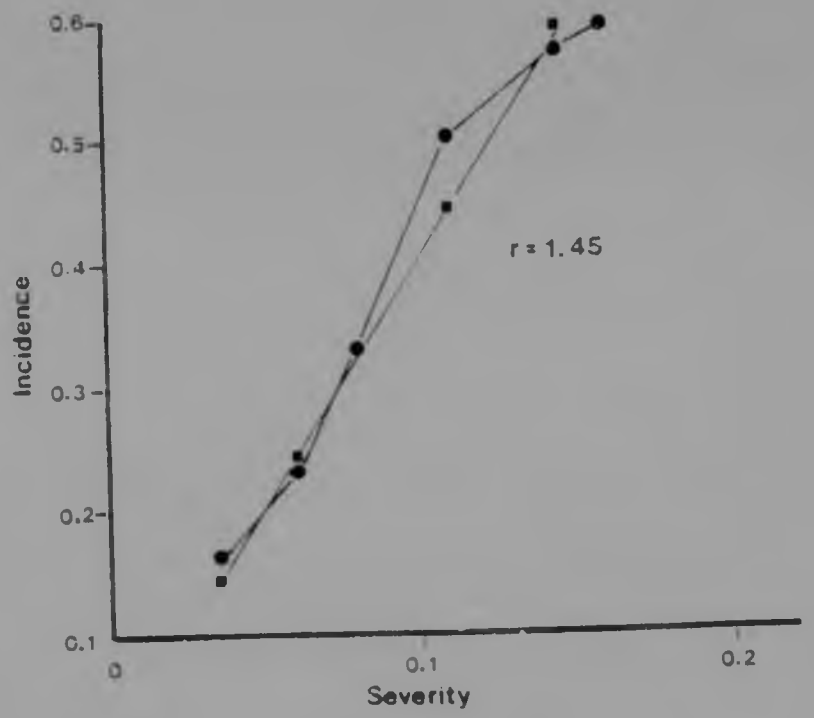


Fig.23 (top) Relationship between incidence and severity in rust-infected *D.eriantha* leaves (1978/79). Fig.24 Relationship between incidence and severity in the 1979/80 season



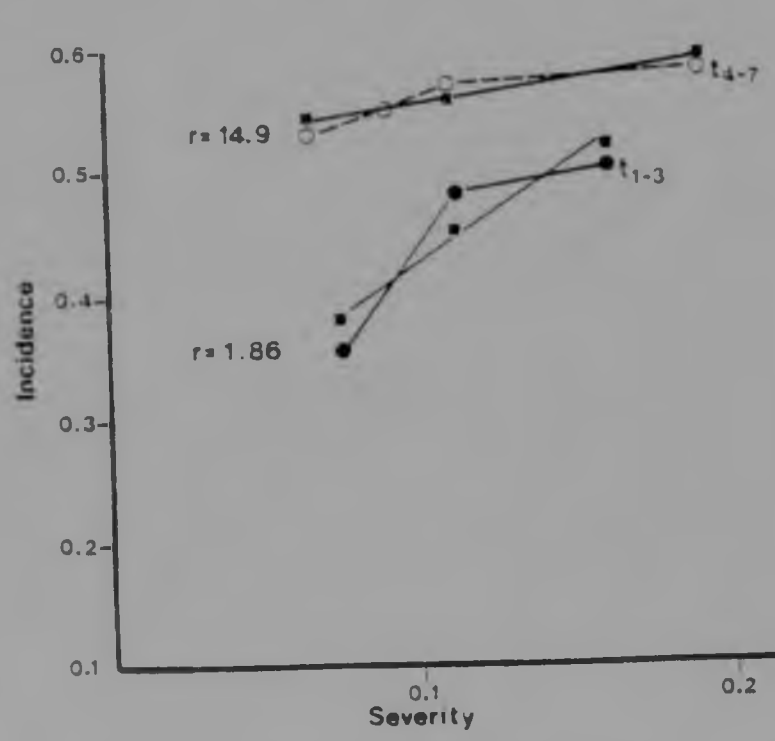
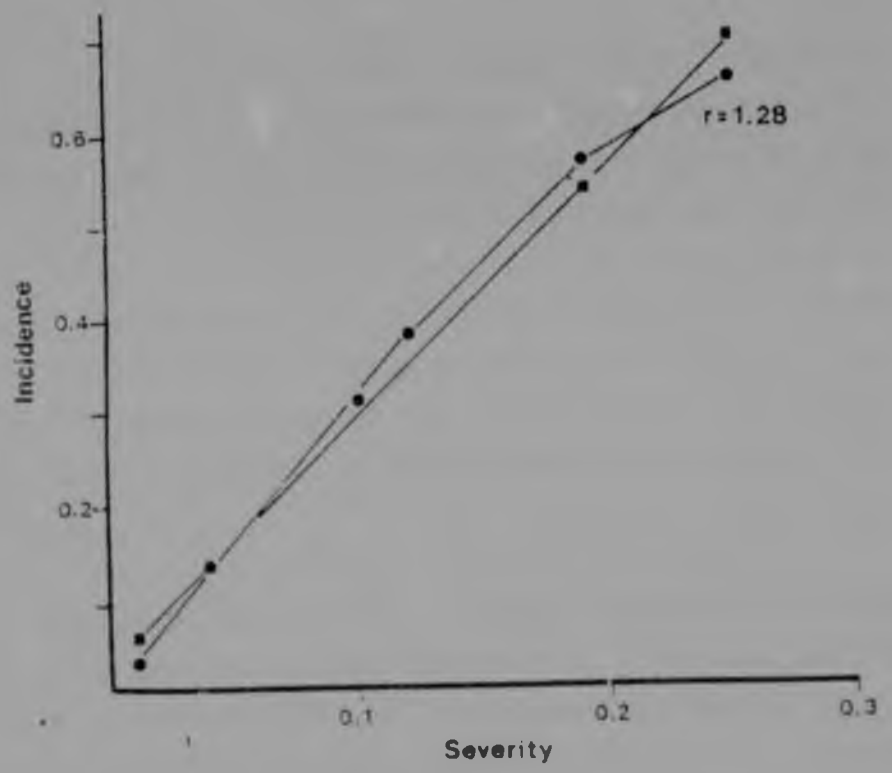


Fig.23 (top) Relationship between incidence and severity in rust-infected *D.eriantha* leaves (1978/79). Fig.24 Relationship between incidence and severity in the 1979/80 season



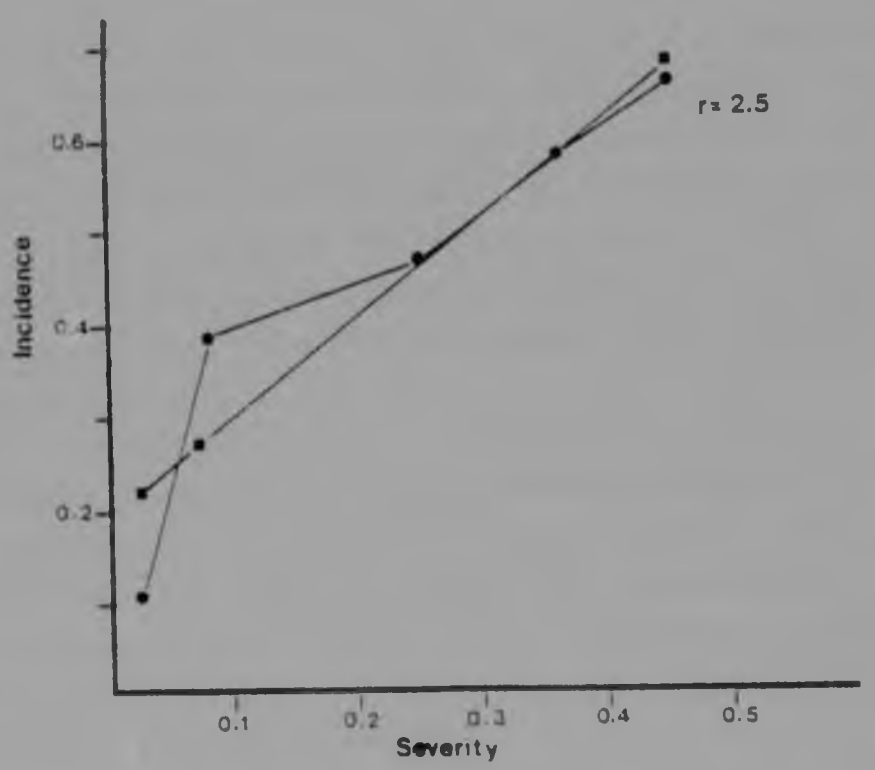


Fig.25 Relationship between incidence and severity in tarspot-infected *P.maximum* leaves (1978/79)
Fig.26 Relationship between incidence and severity during the 1979/80 growing season

D. eriantha, also has a discontinuous epidemiological structure where the disease cycle is terminated with senescence of the leaves. Tarspot on *P. maximum* exhibited a similar pattern to the rust infection on *D. eriantha* in that the incidence and severity increase was linear in the 1978/79 growing season (Fig. 19) which indicates that neither host susceptibility nor leaf tissue availability is a limiting factor in disease development. The untransformed disease progress curves in the 1979/80 season exhibited a slight logarithmic development in the incidence and severity of tarspot (Fig. 20).

The highest incidence and severity of disease occurred in February 1979 (51.4% and 22% respectively) whereas due to the late development of tarspot in the 1979/80 season maximum incidence (67%) and severity (45%) was only observed in April 1980 (Table 5). Despite differences in maximum incidence and severity figures the relative growth rates of tarspot were similar for both growing seasons.

The relative growth rate (b=0.02) in incidence of rust was greater than for tarspot (b=0.01) in the 1978/79 season. However in the following season (1979/80) tarspot showed a greater growth rate (b=0.01) than rust (b=0.001) with respect to incidence. In comparison to incidence, severity indices were similar for both diseases in the 1978/79 season (b=0.002) whereas in the 1979/80 season the growth rate of severity was greater for tarspot (b=0.004) than rust (0.002).

The relationship between incidence and severity of tarspot is defined by the r values. The smaller r value obtained in the 1979/80 season (r=1.28) compared to the 1978/79 season (r=2.5) indicates that the disease increased more by incidence relative to severity in 1978/79 (Fig. 25) but more by severity than incidence in the 1979/80 season (Fig. 26).

3.5 DISCUSSION

B. africana

Since the nature of the lesions on *B. africana* was not definitely

proved, it is not possible to explain the disease progress curves in terms of virus epidemics. However the pattern of lesion number and severity increase appears to follow an epidemiological pattern. The lesions were initiated from puncture wounds, typical of insect probing by leafhoppers and planthoppers which were isolated from *B. africana* trees (Williamson, 1978). Leafhoppers and planthoppers are known to transmit viruses (Thresh, 1978). The adult forms are winged and capable of spreading viruses to a greater extent than wingless arthropods.

The pattern of lesion development would therefore seem to depend not only on the nature and population features of the vectors, but also on the time of leaf emergence with respect to insect population buildup. Climatic conditions also appeared to influence the different patterns between the two seasons. The initial spread of lesions in the 1979/80 season (Fig. 16) was greater than in the 1978/79 season (Fig. 15) although the lesions appeared later on in 1979 than in 1978. It appears that the time of emergence of *B. africana* leaves at the beginning of the season is responsible for the initial pattern of lesion spread. The leaf flushes in the 1978/79 season occurred earlier than in 1979/80 due to early spring rains in September (23 mm) 1978 compared to 1.4 mm in September 1979. Less variation in extremes of rainfall allowed for a steady growth of leaves. Thus the growth rate of lesions followed a slower steady growth increase (Fig. 15). In contrast in the 1979/80 period, the initial increase of lesions occurred rapidly probably due to a larger insect population (leafhoppers and planthoppers) build-up before late emergence of the leaves. This was followed by a decrease in lesion incidence as a result of defoliation of *B. africana* trees by caterpillars. This was succeeded by a new flush and renewed lesion development. Defoliation and regrowth of leaves in *B. africana* in late January, accelerated by high rainfall throughout January to April therefore appears to be the principle factor controlling lesion spread in the 1979/80 season.

The relationship between incidence and severity of lesions appears

to be linear (Fig. 21) which indicates that the relationship between increase in the number of lesions and increase in intensity of lesions remains constant. The smaller r value (r = 1.13) for the initial growth period prior to defoliation by caterpillars (t_{1-3}) in the 1979/80 season compared to the previous season (r = 1.53) indicates that the spread of lesions increases more by incidence relative to severity in the 1979/80 season. However after defoliation (t_{4-7}) the high r value (r = 2.3) suggests that the severity of lesions increases to a greater extent relative to incidence.

The exponential equation used to describe the relationship between incidence and severity is useful in characterizing the relative importance of these two parameters, not reflected in progress curves (James and Shih, 1973).

If a virus is indeed involved, survival between seasons would be essential. Perennial weeds or other long-lived hosts either within the reserve or in adjacent uncultivated lands may function as overwintering hosts of viruses and would be important in maintaining the cycle of infection in deciduous crops. It is also possible that the natural vegetation at Nylsvley may itself be a breeding or overwintering site for vectors, and in fact be a source of infection for other crops in the agricultural areas around the reserve.

D. eriantha and *P. maximum*

The study of the epidemiology of the two fungal diseases, rust and tarspot, indicated several interesting patterns. In order to explain these patterns, it is necessary to relate them to environmental parameters as well as host features, such as growth, development and susceptibility, and pathogen attributes such as inoculum build-up, spore germination, inoculum potential and dispersal.

From the progress curves obtained for rust and tarspot infections, the linear nature of the majority of curves indicates that limiting

factors such as host susceptibility and tissue availability do not in most instances operate. In the case of non-linearity such as rust infection in the 1979/80 season, senescence of a large number of leaves occurred following a dry period in mid-December and this may have limited the amount of leaf tissue available for infection. This would explain the slow tailing off of the disease progress curve (Fig. 18).

Incidence was always higher than severity for both rust and tarspot throughout the seasons, despite the growth rate of severity being greater relative to incidence in certain cases e.g. (t_4-t_7) phase of the rust disease progress curve (Fig. 18). Higher incidence may possibly be due to partial resistance to disease of these naturally occurring grasses in the reserve, and the spread of disease being largely exodemic (infection occurs to a greater extent from spores being dispersed from leaf to leaf, than new infection cycles being established on the same leaf).

Environmental parameters

The influence of climatic parameters on host plant growth, spore germination and pathogen development is evident. Macro-climatic data was available from the meteorological station at Nylsvley for both seasons, but detailed micro-climatic data was not available for the period of this study. Although precise micro-climatic data is desirable for the explanation of causal relationships data from weather stations are often satisfactory since the two are interrelated.

Temperature, light and relative humidity are usually the most important meteorological factors influencing germination and germtube extension, and dew period has been found to influence appressorium and sub-stomatal vesicle formation (Mahindapala, 1978). Although most workers employ relative humidity measurements in germination studies, the duration of a desirable temperature and moisture regime is more informative. Dew is a microclimatic factor and an important source of moisture. Dew, which largely occurs in the dark will usually promote sporulation. The duration

of dew periods is more important than the amount deposited. Saturation vapour pressure deficit may be more meaningful in biological systems as it is the difference between the saturation and actual vapour pressure of a given volume of air.

The temperature range for uredospores is usually between 10-25°C, but peak germination temperature differs between species. *Puccinia sorghi* for example has the greatest germination success at 15°C (Mahindapala, 1978) whilst *Melampsora larici-populina* exhibits peak infection at 22°C (Spiers, 1978). Relative humidities between 95 - 100% are usually required for uredospore germination. Excessive temperatures (30 - 40°C) and light intensities can cause dehydration and prevention of spore germination (Sood and Wiese, 1974).

Climatic data are presented in Tables 6, 7 and 8. Table 6 presents average monthly rainfall measurements. Table 7 presents average monthly figures for temperature, relative humidity, saturation vapour pressure deficit, wind, dew and number of days of rain and dew in a month. Table 8 contains selected data from significant periods of high rainfall and moisture levels, minimum and maximum temperatures recorded for those periods, and maximum relative humidity and minimum saturation vapour pressure deficit measurements in the morning (8H 00) and afternoon (14H 00) for those dates.

September 1978 had a high rainfall (23mm) which resulted in leaf emergence in early September (Fig. B). In contrast rainfall in September 1979 was recorded at 1.4mm and the first leaf flush took place in early October. Number of days of rain was greater in October 1978 than 1979, but greater in January and February 1980 than the previous season (Fig. D).

Relative humidity and saturation vapour pressure deficit figures (means) were similar for October 1978 and 1979, but higher average relative humidities were recorded for the 1979/80 season (Fig. C). Saturation vapour pressure deficit figures were lower for the

1979/80 season, except for October, indicating higher moisture content in the air for 19/9/80. In addition the lowest saturation vapour pressure deficits, attained during the periods of high rainfall, were recorded in the 1979/80 season (except for October) (Fig. H).

Maximum relative humidities were recorded in the morning in October and November 1978 (88 and 98% respectively) and October and November 1979 (98 and 99% respectively) (Fig. J) although January 1980 had the greatest number of successive days where humidity exceeded 90%. Afternoon maximum relative humidities were 100% in October 1978 and 88% in November 1979 (Fig. J). Minimum saturation vapour pressure deficit figures were recorded in November 1978 (0.56) whereas in the 1979/80 season the minimum figure was attained in late November (1.4) (Table 8).

Dew measurements (Fig. F) and number of dew days each month (Fig. E) were greater in October/November 1978 than the following season. However maximum dew measurements (mm) and number of dew days were attained in January-March 1980 the following season. Average monthly wind (km/days) measurements were higher in October/November 1979 than 1978, but higher for the remainder of the growing season (December - April) in 1978/79 than 1979/80 (Fig. G).

Average monthly temperature figures followed identical patterns for both seasons (Fig. C), ranging between 18-23°C, although average temperature readings were slightly higher in October 1979 than 1978. Mean maximum temperature was higher in mid-October 1978 (27.8°C) than mid-October 1979 (22.5°C). Mean minimum temperature (14.5°C) was lower in October 1979 than October 1978 (24.5°C) (Fig. I).

D. eriantha

From the climatic data presented above, it appears as though the temperature conditions were ideal for uredospore germination for the entire 1978/79 and 1979/80 seasons (18-23°C). However October

1978 exhibited higher favourable temperatures than October 1979. This fact coupled with the high September 1978 rains resulting in an early leaf emergence and low saturation vapour pressure deficits, high relative humidities, greater dew measurements and number of dew days in October 1978, appears to be responsible for the earlier appearance of the rust infection in 1978 than in 1979. However the higher initial incidence of rust in November 1979 may be a result of a greater inoculum build-up before leaf emergence in October 1979, followed by high rainfall and favourable moisture conditions in November through to April 1980.

Senescence of some *D. eriantha* occurred in early January 1980 following a dry period in mid and late December. Exceptionally high rainfall in January through to April 1980 followed. A secondary leaf flush and re-infection was accompanied by high moisture conditions (Table 7 and 8), ideal temperatures for germination (17-26°C), and high dew measurements. The mid-season drought would account for the slow tailing off of incidence figures and decline in severity indices (Fig. 18) since only living blades were assessed. Had senescence of a proportion of *D. eriantha* tufts not taken place, the progress curves may have followed course C_1 and course C_2 (Fig. 18). Senescence commenced earlier in February 1979 than 1980, with lower recorded rainfall, relative humidity and dew measurements (Table 7). This accounts for a sharp decrease in incidence and severity due to senescence and limitation of leaf tissue.

Relationship between incidence and severity

The relationship between incidence of rust and severity in *D. eriantha* is reflected by the r values (Table 58). The rust infection appears to increase more by incidence than severity during the 1978/79 season ($r = 1.45$) whereas in the 1979/80 season the growth of the disease increased more by severity relative to incidence ($r = 1.86$ for the first leaf flush t_{1-3} and $r = 14.9$ for the secondary infection cycle following a secondary leaf flush in late January (t_{4-7}).

The difference in r values may be explained in terms of leaf tissue availability, spore germination and suitable climatic conditions. A smaller secondary leaf flush occurred in late January 1980. This was accompanied by a high rainfall and high moisture content in the air (70-9?% relative humidity, Table 8) as well as suitable temperatures (17-26°C). Subsequent re-infection was therefore accelerated by ideal climatic conditions but at the same time the younger leaves of the new flush were not as susceptible to infection as the more mature leaves. Results in this study have shown that the greater incidence of rust occurred later on in the 1978/79 season (December) when the leaves were mature and more susceptible to disease, and the amount of susceptible leaf tissue available for infection was not limiting. Therefore it appears as if suitable temperature and moisture conditions prompted secondary re-infection cycles on leaves already infected, and therefore severity or intensity increased to a greater extent relative to incidence (Fig. 18).

P. maximum

Incidence and severity of tarspot on *P. maximum* showed a continuous increase in growth rate, as was the case in rust-infected *P. maximum* in the 1978/79 season. Climatic patterns do not appear to have influenced leaf growth of *P. maximum* and this is reflected in the continuous growth of the disease progress curves (Figs. 19 and 20). However tarspot appeared later in the 1979/80 season (January 1980) than the previous season, where first visible symptoms were recorded in November 1978. In this study the limiting factor in the 1978/79 season appears to be senescence of leaf tissue. However in the 1979/80 season leaf growth continued late into April due to a high rainfall from January to April 1980 (Fig. 2), and consequently maximum incidence and severity figures were attained in early April before leaf senescence occurred towards the end of April (Fig. 20).

From these results, the importance of the stage of host plant growth at the time of infection with respect to disease development rates and patterns is evident. The late

tarspot fungus in January 1980 occurred when *P. maximum* was in a more advanced stage of leaf development. Aging of the leaves could have led to greater host susceptibility and this may explain the rapid development of the fungus in a shorter period.

The higher r value (r = 2.5) for tarspot in the 1979/80 season compared to the 1978/79 season (r = 1.28) indicates that tarspot increases more by incidence relative to severity in the 1978/79 season. Conversely severity increased to a greater extent relative to incidence in the 1979/80 season. The relationship between incidence and severity in the 1979/80 season is again reflected by the late appearance of the fungus, when mature *P. maximum* leaves may have been more susceptible to infection. However at the same time the number of immature leaves available for colonization may have declined. It is also possible that tne re-infection cycles occur more frequently on the same leaves than from infected to uninfected leaves.

Rainfall and temperature

From the results presented in this study, it appears that rainfall, in its inevitable relationship with free moisture essential for spore germination and leaf growth, is the critical factor affecting the development of fungi on the grasses *D. eriantha* and *P. maximum* in the reserve. In the field all sources of leaf wetness, such as dew and rain, must be considered as they serve the requirements for development of infection structures. The minimum wet period for pustule formation varies with temperature (Politowski and Browing, 1975), but temperatures between 15-25 C are generally required. These suitable temperature regimes were indeed present throughout the two growing seasons.

Susceptibility

Changes in disease development are not only influenced by environmental parameters, but also host factors. The principle limiting factor in this study appears to be susceptibility changes with leaf age and time of year, as was evident in tarspot infection of *P. maximum* in the 1979/80 season (Fig. 20). Tarspot appeared later on in the season and growth rates were initially high

probably due to greater host susceptibility as leaf age increased. Rates slowed down later on due to the commencement of leaf senescence. Aldwinkle (1975) demonstrated a different pattern with apple leaves infected with *Gymno-sporangium juniperi-virginianae* where decreases in lesion numbers were due to a decrease in susceptibility during the later part of the growth period. However when infectibility changes extend over the whole life of a plant part susceptibility usually increases with increasing leaf age e.g. oats infected with *Erysiphe graminis* (Jones and Hayes, 1971).

Final remarks

Even though the incidence of rust and tarspot on the grasses *D. eriantha* and *P. maximum* respectively does by no means reach explosive epidemiological proportions, the levels of disease are higher than one would expect in a natural environment. This study has demonstrated the influence of climate and significance of the stage of host development at the time of infection on the progress of disease. What it does not establish is many of the other important ecological aspects such as defoliation and grazing pressure effects on the vigour of grasses, which may change and in doing so alter susceptibility to disease.

Studies on plant diseases in natural populations have not received much attention in the past. Consequently this research has not only accomplished certain objectives stated previously, but has in its course revealed many exciting new aspects and raised several interesting questions with respect to plant pathogens in a natural ecosystem. Some of these will be discussed in Chapter 7, but salient features pertaining to this chapter will be mentioned below.

It is possible that the balance of co-existing host and pathogen populations has been disturbed by human interference. Cattle were introduced into the area many years ago (information on the exact period was not available, but farmers in the district have indicated at least 20-30 years if not more). Many cattle were

removed in 1973/74 when Nylsvley was proclaimed a nature reserve but approximately 300 head of cattle were kept in the reserve until 1978, after which they were removed. This coupled with the herbivore population such as impala, and other ungulates, resulted in a heavy grazing pressure being exerted on the grasses.

One is concerned with general productivity and stability in veld management, and over-grazing can lead to changes in species composition and introduction of undesirable species. Defoliation and grazing pressures can lead to reduction in the vigour of a grass species (Roberts et al., 1975). Decreased leaf areas, lower root carbohydrate reserves, reduced growth rates, less culms, less seeds and seedlings and reduced number of tillers are symptoms of reduced vigour on a seasonal basis. On a short term basis the decreased vigour of one species will reduce its competitiveness and undesirable or unpalatable grasses or weeds will appear.

D. eriantha and *P. maximum* are extremely palatable and heavily grazed by the herbivores and cattle at Nylsvley. Grazing pressure is the greatest on *D. eriantha* than the other grasses (Owen-Smith, 1982), although pressures have been reduced since removal of the cattle in 1978. Several agriculturists (pers. comm. ; unpublished) who visited Nylsvley postulated that the veld in the reserve had once been dominated by *D. eriantha* to a much greater extent than at present, and that the present *Eragrostis pallens* veld domination followed due to grazing pressures on *D. eriantha*. It seems possible that a reduction in vigour of *D. eriantha* could have occurred leading to greater susceptibility to rust disease. Certainly disease levels of rust (and tarspot) from a brief survey (although no data was collected intensively) appeared to be lower in the 1980/81 and 1981/82 season. However the 1981/82 season was a dry season in comparison to 1977/78 ; 1978/79 and 1979/80, and this may have partly contributed to lower infection levels.

Therefore it appears as if many factors must be taken into account when studying plant disease in a savanna ecosystem which supports a large population of not only herbivores but other consummers

such as insects and 'pathogens'. From this research several areas lacking in knowledge and that need to be studied, emerge. One needs to know the recovery rates of grasses after grazing and other pressures, and the effects not only on short term phenotypic characteristics but also on long term genotypic features. Can the reduction of vigour of a grass species which leads to short term phenotypic alterations also lead to long term genotypic and subsequent susceptibility changes? These and other exciting questions arise which need to be looked at in greater depth.

In addition the beneficial or detrimental role of pathogens in a natural ecosystem comes into view with respect to concepts such as biomass, mineral cycling, population dynamics and energy cycling. It may be postulated that pathogens are no longer 'pathogens' in a natural population, and may become regarded as 'co-existers'. The perspective of plant disease in natural environments will be discussed in Chapter 7, and the definition of pathogens in ecosystems and agrosystems reviewed in a different light.

4. CHAPTER FOUR DEVELOPMENTAL, MORPHOLOGICAL AND ULTRASTRUCTURAL STUDIES

4.1 LITERATURE REVIEW

4.1.1 Intercellular and intracellular structures and the host-pathogen interface

Biotrophic fungi produce a number of specialized feeding structures once they have entered a host plant. They also produce intercellular hyphae which spread through intercellular spaces and ramify through the leaf mesophyll tissue. The cell walls of rust intercellular hyphae are usually composed of two electron-opaque, fibrillar layers and commonly an amorphous outer layer (Rijkenberg and Truter, 1973; Muller et al., 1974) which has been suggested to have a role in the adhesion of the hyphae to other hyphae or host cells (Hardwick et al., 1971; Rijkenberg and Truter, 1973). Welch and Martin (1974) have postulated that *Cronartium ribicola* obtains host nutrients at the sites of host-hyphae adhesion, but Boyer and Isaac (1964) suggest that this outer layer protects the fungus from toxic host substances. Intercellular hyphae of all rusts are septate. The protoplasm of intercellular hyphae of rusts resemble those of other parasitic fungi (Bracker, 1967). Mitochondria with plate-like cristae, ribosomes and tubular and vesicular endoplasmic reticulum are present. Single membrane bound structures similar to microbodies (Frederick et al., 1968) have also been observed. Microbodies in vegetative mycelia often contain crystal lattices (Coffey et al., 1972a). Storage products in the cytoplasm are glycogen particles and lipid droplets (Coffey et al., 1972a).

When a pathogen invades a plant and establishes a parasitic relationship, it is entering into an association with its host. The host reacts to the invasion, and may exclude the pathogen and prevent it from developing (Bracker and Littlefield, 1973). On the other hand the host may provide conditions that are conducive to the development of the pathogen, which results in the establishment of the pathogen and consequent disease. The site of contact

between a pathogen and the host cell or protoplasm is known as the host-pathogen interface. The host-pathogen interface is one of the most significant yet elusive regions of a diseased organism. It is important because it is the region of direct interaction between a host and pathogen and thus is the zone through which materials that elicit responses in either partner are exchanged (Bracker and Littlefield, 1973). At any one time or place the interface may consist of any or all of the following

1. Normal host cell components
2. Normal pathogen components
3. Structures of the host or pathogen that are modified as a result of the interaction
4. Mixtures of materials or structures derived from both host and pathogen
5. Newly formed structures or materials that are not normally present in either host or pathogen

Several catagories of host-pathogen interface types can be distinguished (Dickinson and Lucas, 1977): intercellular relationships where the pathogen grows between the host cells; intracellular relationships where the pathogen grows partially within the host cell by means of intracellular haustoria e.g. biotrophic fungi; or intracellular relationships where the pathogen is entirely contained within the host cell e.g. viruses and mycoplasmas. Intercellular hyphae may be in direct contact with cell walls of the host or the walls may be separated by an extracellular matrix e.g. *Hypholoma fasciculare* growing on the cell wall of a tracheid of *Picea excelsa* (Schmid, 1966).

Intracellular associations encompass a wide variety of interface types. Two generalizations can be made with respect to intracellular symbionts (Bracker and Littlefield, 1973). The first is that the invading pathogen is surrounded by an additional membrane, which is the modified or invaginated host plasmalemma. The second generalization is that there is no single specialized infection structure to characterize the relationship between a pathogen and host cell. Often intracellular hyphae in disrupted host cells are surrounded by a sheath-like matrix, that appears in some cases to

be a fungal secretion separating the fungal wall from the degenerate host cell e.g. *Fusarium solani* f. *phaseoli* which penetrates dead cells of host hypocotyls (Reichle, 1965). Moribund cells, which are sometimes capable of responding to infection, may react to form a papilla on the inner surface of the cell wall (Hess, 1969). Similar wall appositions containing lignin or polysaccharide callose have also been noted at sites of penetration or surrounding the hypha (Mason, 1970). Wall degradation is of particular interest in relation to host penetration. Penetration by *Gymnoascus terrestris* is accompanied by dissolution of the host cell wall at the site of penetration (Hess, 1969), whereas general breakdown of host wall structure accompanies infection by other pathogens (Akai et al., 1971; Heath and Wood, 1969; Mercer et al., 1971). Commonly at the site of host wall penetration the fungal hyphae are constricted, and the fungal wall is in contact with the wall of the host (Reichle, 1965). Systemic smut fungi studied by Fullerton (1970) showed several types of interfaces. Hyphae penetrated host cells directly and were surrounded by the invaginated host plasmalemma. A collar-like wall apposition formed around hyphae near the host cell wall, and in some cases cytoplasmic vesicles were also found around the invading hypae in association with encasement formation.

Haustoria are distinctive fungal organs, representing the intercellular portion of a number of highly specialized pathogens. In spite of many ultrastructural studies, surprisingly little is known about the development, significance and role of interface components. Haustoria are distinct from intracellular hyphae which may continue to grow for some time after penetration and extend from cell to cell. Haustoria are usually only an extension of a cell (rusts, downy mildews) or may consist of one cell plus part of another cell (powdery mildews). The main haustorial body is connected via the haustorial neck to the haustorial mother cell which lies outside the host cell, attached to the surface (Bracker and Littlefield, 1973). The haustorium is surrounded by an extrahaustorial membrane or invaginated host plasmalemma, and a sheath or extrahaustorial matrix usually separates the membrane from the haustorial wall.

The extrahaustorial matrix is thought to consist partly of host and partly of fungal material and can be granular or contain layers of amorphous or fibrillar material (Calonge, 1969; Coffey et al., 1972a; Manocha and Shaw, 1967). The nuclei in aging haustoria sometimes degenerate. Lomasomes or multivesicular bodies are occasionally seen in the haustorial body (Hardwick et al., 1971; Coffey et al., 1972a) and their function has not as yet been definitely established. No published studies on rust haustoria have convincingly demonstrated cytoplasmic connection between the host and haustorial protoplasm (Littlefield and Heath, 1979). Often the haustorial mother cell adheres to the host wall with the aid of fungally secreted material (Heath, 1972 and Littlefield and Bracker, 1972). The interface before and during penetration sometimes includes wall appositions secreted by the host and laid down between the plasmalemma, and the wall adjacent to the fungal cell (Ehrlich et al., 1968). Sometimes small wall deposits form adjacent to penetration sites (Littlefield and Bracker, 1972). With powdery mildews, papilla formation at penetration sites is almost universal (Stanbridge et al., 1971). Where papillae and other appositions are formed they constitute a barrier beyond the host wall which must be penetrated (Ehrlich and Ehrlich, 1963). Great cytoplasmic activity has been described by Bushnell (1971) at the site of host penetration in *Erysiphe graminis*. Electron microscopy has also shown host organelles collected around penetration sites (Edwards and Allen, 1970). These organelles are involved at the interface during penetration and probably have a role in forming wall appositions or other secretions that either aid or combat the fungus in its penetration. Ultrastructural evidence suggests that penetration involves a combination of enzymatic degradation of host walls and a mechanical force.

Although viruses are intracellular, the particular location often depends on the type of virus and stage of pathogenesis. The capsids of most plant viruses are not enclosed by an envelope (Matthews, 1970). Viruses most commonly occur in the cytoplasm of the host, and some are found within or attached to organelles, or even in non-living cells of vascular tissue (Esau, 1968). Viruses in the

cytoplasm occur as individual dispersed virions or aggregates. They are also found within nuclei and less frequently in plastids e.g. TMV or in the lumina between membranes of the endoplasmic reticulum or nuclear envelope (Esau, 1968). There is also evidence to support the occurrence of virions in host vacuoles (Honda and Matsui, 1974). Virions may contact or be adsorbed onto various cellular membranes. Plant virus particles have been demonstrated within plasmadesmata linking adjacent host cells (Kitajima et al., 1969).

4.1.2 Ultrastructural changes

Once the pathogen has established itself, many morphological changes may manifest themselves. In haustorial relationships for example, there are surprisingly few changes in the ultrastructure of penetrated host cells, during the early stages of infection. Normal chloroplasts and mitochondria are present, although the host nucleus may be swollen. However, in later stages of infection there are visible changes in various organelles, such as the appearance of crystalline inclusions within microbodies. Many of these changes are superficially similar to ultrastructural changes in senescent and virus-infected cells. In intercellular relationships, various alterations of host cell walls and membranes occur (Bracker and Littlefield, 1973). As pathogens grow between host cells, cell walls may separate along the middle lamella (Akai et al., 1971), or be degraded or otherwise altered. Host-cell walls may be inordinately thickened (Heath and Wood, 1969) or extensive dark-staining wall-like or membraneous deposits may form on the inner side of the host cell wall adjacent to the plasmalemma (Bird, 1961). Wall appositions even occur in cells of bean tissue beneath points of contact with intercellular hyphae of *Uromyces phaseoli* var. *vignae* (Heath, 1972). Effects of intercellular pathogens upon the integrity of host cell membranes may result from diffusible substances produced by the pathogen or to deleterious reaction products of the host cells stimulated by materials from the intercellular pathogen. Wood et al (1972) has reviewed the effects of fungal and bacterial toxins upon host cell membranes. Victorin for example, produced by *Helminthosporium victoriae*,

causes extensive disruptions of the internal membrane systems of susceptible host cells (Luke et al., 1966). Damage to the host plasmalemma is regarded as the major cause of altered permeability (Hanchey and Wheeler, 1969). There have been many reports on the modifications of cell walls and plasmalemmas in cells infected with viruses.

The spread of plant viruses in hypersensitive hosts is limited by a resistant zone of cells which develops at the periphery of local lesions (Israel and Ross, 1967). Various substances have been found to be deposited in the necrotic zone and border of local lesions in virus-infected plants and also in non-specific hypersensitive reactions due to wounding or heat treatment (Faulkner and Kimmins, 1975; Hiruki and Tu, 1972). Wu and Dimitman (1970) and Hiruki and Tu (1972) have detected callose in the marginal tissue of virus lesions. Electron opaque substances, deposited along the cell wall and sometimes in the intercellular spaces, have been noted in lesion cells of *Gomphrena globosa* L. leaves infected with tomato bushy stunt virus (Appiano et al., 1977). Lignin and callose have also been detected in infected leaves e.g Wu (1973) obtained evidence for lignins in the resistant zone of *Nicotiana glutinosa* infected with a mild strain of TMV. The accumulation of toxic polyphenolic oxidation products is often thought to be responsible for necrogenic changes, although some studies have reported that many of these phenolics reach significant levels after the appearance of necrosis (Cabanne et al., 1971). Mechanical interruption of cellular continuity by deposition of callose is thought to reduce cell-to-cell movement of viruses or mycoplasmas. Several observations of membraneous proliferations of the plasmalemma or endoplasmic reticulum have also been made. Plasmalemmasomes or paramural bodies have been noted in leaf cells of *Chenopodium quinoa* Willd. infected with potato virus S. (Shulka and Hiruki, 1975), whilst the presence of myelin-bodies were detected in cucumber mosaic virus-infected tobacco leaves (Honda and Matsui, 1974). It has been suggested that increases in membraneous material and deposition of dense substances along the cell wall may be involved in virus localization, but there is still

much debate about whether the process of cell wall and plasmalemma modification is a host-cell response or a virus-induced response.

Many other modifications have been noted in infected cells. A reduction in the number and size of mitochondria is known to occur, and swollen mitochondria in rice plants infected with *[illegible] mimbeaus* have been reported (Horino and Akai, 1968). Degenerative changes in chloroplasts have also been noted (Sun, 1965; Matthews, 1973). For example, an increase in the number and size of osmiophilic granules and the appearance of abnormally large starch grains were reported by Tomlinson and Webb (1978). Disorganization of the thylakoid system and production of vesicles in the stroma periphery has also been demonstrated. In rust-infected leaves, chloroplasts have exhibited a reduction in the number of photosynthetic lamellae, and an increase in the development of a peripheral reticulum (Heath, 1974b). A marked increase in the number and/or size of plastoglobuli has also been reported by several workers (Coffey et al., 1972b).

The majority of ultrastructural modifications occur later on in the infection processes, and in the case of the rust fungi usually at the onset of sporulation (Manocha and Shaw, 1966b; Coffey et al., 1972b; Heath, 1974b; Abu-Zinada et al., 1975). Most frequently the observed response of the host tissue is a general disorganization of the cytoplasm and disruption of cell membranes occurs. Changes in nuclear structures have been noted e.g. an increase in the density of the interchromatin regions of the host nucleus has been reported for uredial infections of *Puccinia graminis* f. sp. *[illegible]* (Manocha and Shaw, 1966a) and *Uromyces fabae* (Abu-Zinada et al., 1975). Changes in the mitochondria and microbodies have been noted in rust-infected plants e.g. in the peripheral regions of uredial infections of *Puccinia helianthi*, atypical plate-like cristae and occasional crystals develop in the mitochondria, whilst the microbodies more frequently contain crystalline cores (Coffey et al., 1972b). Lipid bodies have been shown to increase in the cytoplasm of [illegible] infected with *Cronartium ribi-*

gels and tiny electron opaque deposits, suggested to represent tannin deposition, have been seen to develop uniformly throughout the cytoplasm (Robb et al.. 1975a).

4.1.3 Senescence and plant disease

Many of the changes in ultrastructure of cells in infected plants are associated with pathogen initiated or host-cell responses, but many may be attributed to aging or senescence. In discussing senescence and plant disease, senescence should be regarded as a developmental phase and should be viewed in context with earlier phases of development (Farkas, 1978). Disease induced senescence may be included among the stress-induced phenomena, where the concept of stress involves mechanical and biochemical damage (Farkas, 1978). The physiological age of a leaf depends on both the age of the entire plant and on the absolute age of a particular leaf as related to the other. In virus-induced local lesions for example, the lesion number usually depends on the age of the leaves (Kiraly et al., 1968), whilst the size of the lesions is greatest in younger leaves (Weststeijn, 1976). The biochemical changes induced by infection also depend on the age of the leaf. Nonspecific changes in proteins triggered by mechanical injury or degradative processes, have been reported, and these changes play a role in the induction of senescence (Farkas, 1978). Senescence, in a large number of cases, is causally correlated with the high metabolic rate of the host-parasite complex at the infection centres. Metabolic sinks arise at the infection sites and lead to a depletion of metabolites and thereby premature senescence of nearby tissues. The dramatic increase in respiration in rust- and mildew-infected leaves is due partly to a contribution by the fungal spores and mycelia in the invaded tissues, and partly to an increase in the host's metabolic activity in the infection centres and sometimes nearby vicinity. High respiratory rates in tissues infected with biotrophic parasites may be due to a high ATP-consumption, which would consequently supply a suitable phosphate acceptor (ADP) which is required for synthetic processes by the host and parasite, especially during the sporulation phase (Farkas. 1978). Toxins can cause respiratory increases. Senes-

cent tissues tend to be rich in peroxidases which contribute to the acceleration of aging and lesion formation. A decrease in photosynthetic activity is usually associated with senescence. The photosynthetic apparatus in biotrophic infections usually remains relatively intact initially to supply metabolites for the parasites (Montalbini and Buchanan, 1974), but in the later stages of the disease the photosynthetic activities decline, and the chloroplasts begin to show signs of damage. Chloroplast RNA synthesis also decreases in senescent leaves (Tani et al., 1973). A number of major enzyme changes in diseased tissues reflect the accelerated aging associated with disease. In rust infections, for example, RNAase activity increases in senescing leaves, and stress enzymes, amongst which are the first two hydrogenases of the hexose monophosphate shunt, peroxidases and phenol oxidases, are also known to increase in infected leaf tissue. Lysosomal enzymes (nucleases, proteases and esterases) involved in the breakdown of nucleic acids and proteins, increase during aging. Hormonal changes may also play a role in senescence. Indoleacetic acid and cytokinins accumulate in the infection centres of leaves attacked by biotrophic parasites and may be responsible for the transport of metabolites to the infection sites and the early senescence of the other parts of the leaf. Stimulation of ethylene formation can also induce leaf and fruit senescence. Diseased plant tissues sometimes exhibit increased permeability suggesting damage to the cell membranes due to a general wound response (Thilo and Nienhaus, 1975 in Kiraly et al., 1978).

Farkas (1978) points out the caution that is needed in claiming specificity in host-parasite relationships. Some phenomena are stress-induced whilst other changes are specific pathogen-induced responses.

4.1.4 Uredospore development

The ultrastructure and host-pathogen relationship of the uredial stage of rust fungi has been studied by many workers (Manocha and Shaw, 1967; Littlefield and Bracker, 1972; Heath, 1974; Hardwick et al., 1975). However little work has been done on the

actual formation process of the uredospores. Uredospore ontogeny has been examined by a few workers (Ehrlich and Ehrlich, 1969; Hughes, 1970; Muller et al., 1974), mainly at the light microscope level, but also at the electron microscopical level. Most uredospores develop from successive new growing points on a sporogenous cell (Hughes, 1970). The primordial cells give rise to basal cells which cut off uredospore initials each of which, in turn, divides to form a uredospore and a sporophore. In some cases the sporophores elongate and at the abscission stage extend beyond the developing uredospores (Muller et al., 1974). In *Kernkampella breyniae-patentis* uredospores are liberated by a break across the middle of the pedicel, and the sporogenous cell then grows through the persistent half of the pedicel and produces a new uredospore at the apex of the proliferation. This phenomenon is repeated, and the old, lower parts of several earlier pedicels appear as collars around the base of newly forming uredospores (Rajendren, 1970). Rijkenberg and Truter (1974) showed that pycniospore sporogenesis in *Puccinia sorghi* is annellophoric.

The definition of annellations is that they are scars marking the points of attachment of previously formed conidia in basipetal sequence (Hughes, 1953). Hammill (1971) extended the definition of annellations to include new aspects such as annellations on annellophore necks do not invariably result each time in a conidium and annellophores are capable of shortening in certain conidial formations e.g. in *Scopulariopsis koningii* (Oud). Vuill. instead of invariably lengthening.

4.2 AIMS

In order to study the physiological and ecological impact of plant disease it is first essential to understand the cytological relationship between the host and parasite. The ultrastructural research hoped to accomplish several goals:-

1. Determination of the influence of a hypersensitive reaction resulting in localized lesion formation, on the cytology of *B. africana*, and to ascertain the nature of the substances (deposited in the semi-necrotic and necrotic zones) detected in TEM micro-

graphs.

2. Characterization of the host-pathogen interface of *D. eriantha* infected with the rust *P. digitariae* and *P. paspalicola*-infected *P. maximum*, which has not been examined previously. This research did not attempt a detailed study of infection processes. Even though much research has been carried out on rust infections, virtually no ultrastructural work has been reported on rusts of naturally occurring grasses. *P. paspalicola* has been studied extensively from a taxonomic point of view, but little is known about the relationship with its hosts at an electron-microscope level.

3. The effect of the two fungal diseases on the ultrastructure or morphology of their respective grass hosts *D. eriantha* and *P. maximum*. A study of the cytological alterations due to disease often corresponds to the physiological responses, and may assist in the understanding of host-parasite relationships.

4. An electron microscope study of *P. digitariae* infecting *D. eriantha* revealed several interesting features with respect to uredospore sporogenesis. The presence of 'annellation-type' structures was noted during a preliminary examination and consequently evoked further investigation as to whether or not uredospore ontogeny was annellophoric. A similar type of ontogeny has only been reported once (at the light microscope level), in *Kernkampella breyniae-patensis* where the sporophore apex grows through the old persistent sporophore resulting in 'annellation-type' structures being formed from the old sporophore walls which are forced aside to allow for new growth (Rajendren, 1970). This research was aimed at describing a new type of uredospore formation occurring in *P. digitariae* Pole Evans.

4.3 METHODS

3.1 Light microscopy

3.1.1 Frozen sections

Leaf segments were sectioned using a freezing microtome (Photax Model 2). The sections (10-15 µm) were mounted in glycerine jelly for support and some leaf segments were decolorized in alcohol for 5 min before sectioning.

3.1.2 Wax sections

Segments (1-2 mm^2) from necrotic, semi-necrotic and unaffected

areas of . *africana* were fixed in FAA (formalin-acetic acid-alcohol) and then dehydrated in a graded alcohol series. The samples were rinsed in 3 changes of 100% butanol - the first and second changes were for 1h each and the last change overnight. The material was then transferred to a mixture of 1:1 paraffin oil:butanol for one and a half hours, at 60 °C followed by two changes of semi-melted paraffin wax for an hour each. The sections were left overnight in a third change of pure melted wax at 60 °C. Final embedding was completed by replacing the molten wax with good quality wax (melting point 56 °C). Sections (10-15 µm) were cut on a Spenser Rotary microtome and placed on a clean slide (with a light application of Haupts' adhesive) ready for histochemical tests.

3.2 Fluorescence microscopy and histochemistry

Frozen and wax sections were used for several histochemical tests. Control sections were left unstained.

3.2.1 Aniline-blue for callose detection

Leaf sections were placed in a drop of 0.1% aniline-blue solution (in 0.1N K_3PO_4, pH 9.5) for 2h and viewed under ultraviolet light using a Reichert Univar Microscope, fitted with a blue excitor filter 18X(3-5FITC 490 + 2GG 400)6b and an absorption filter (18XGG9 + OG515/VG). Callose should appear bright yellow in the stained material but should not be visible in the unstained preparations.

3.2.2 Phloroglucinol for lignin

Leaf tissue was treated with a drop of 1% (w/v) phloroglucinol in 70% ethanol for 5 min, followed by 1N HCl. Lignin containing aromatic aldehydes should stain bright red-violet. Lignin also fluoresces naturally under dark-field, giving a bright yellow colour (primary fluorescence).

3.3 Transmission electron microscopy (TEM)

Transmission electron microscopy was employed to study leaf tissues at the ultrastructural level. Material was collected from Nylsvley Nature Reserve and leaf tissue sections (1-2 mm^2) cut out with a sharp razor blade. Leaf samples included areas of necrotic and adjacent semi-necrotic tissue in the case of *B. africana* and clypei

areas from *P. maximum*. In the case of *D. eriantha*, leaf sections were cut from the yellow fleck areas (early stage of fungal development), immature and mature sporulating pustules. Due to the hard nature of grass leaves, the sections were embedded in 1% agar before dehydration, as this seemed to facilitate cutting of the resin blocks. Leaf segments were fixed in 4% glutaraldehyde in sodium cacodylate buffer (pH 7.2) for 6h at 4 °C. The tissue was then rinsed with 0.5M Na cacolydate buffer and post-fixed with 2% osmium tetroxide in buffer for 3h at 4 °C. Fixed material was dehydrated in a graded ethanol series and embedded in Spurr's resin.

Sections were cut on a Reichert 'OM03' ultramicrotome using glass knives made with a LKB type 7801B knifemaker. Specimens were stained with a 2% solution of uranyl acetate made up in 50% ethanol for 20 min, post-stained in lead citrate for 10 min and viewed in the JEM-100S electron microscope.

4.4 RESULTS

4.1 *B. africana*

4.1.1 Transmission electron microscopy (TEM)

Examination of the leaf tissue of *B. africana* revealed several cytomorphological disturbances in necrotic and semi-necrotic mesophyll cells. Non-necrotic mature mesophyll cells (Fig. 27 A) exhibited a large nucleus, chloroplasts, mitochondria and the cytoplasm was packed with ribosomes. In contrast, mesophyll cells from the necrotic zone were characterized by degeneration of the cytoplasm and cellular organelles, and the appearance of large numbers of vesicular bodies (Fig. 27 B). Cell wall thickening (Fig. 28 A) was often detected in semi-necrotic mesophyll cells. Paramural bodies (Fig. 28 B), plasmalemmasomes (Fig. 28 C) and myelinic bodies (Fig. 28 D) resulting from membrane proliferation were noted in necrotic and semi-necrotic cells, and were often seen to develop opposite plasmodesmata. These structures were not detected in non-necrotic mesophyll cells. The chloroplasts exhibited the greatest extent of damage in necrotic leaf tissue. The chloroplasts in younger mesophyll tissue adjacent to the

LEGENDS

bc - basal cell
bo - boundary formation
bsc - bundle sheath cell
c - collar
cl - chloroplast
Clp - clypeus
cr - cristae
cw - host cell wall
E - epidermis
f - fertile
H - rust haustorium
Hw - fungal cell wall
Ih - intercellular hyphae
ir - tarspot intracellular hyphae
lo - lipid droplet
Ll - lamellae
ln - lignin
lo - lomosomes
m - mesophyll
Mb - myelinic body
mt - mitochondrion
N - nucleus
NNT - non-necrotic tissue
NZ - necrotic zone
P - pustule
Pl - plasmalemma
Pls - plasmalemmasome
sg - starch grain
SNZ - semi-necrotic zone
sp - sporophore
spi - spine
St - stroma
sth - starch
su - suberin
sw - sporogenous cell wall
u - uredospore
ui - uredinial initial
Vb - vascular bundle

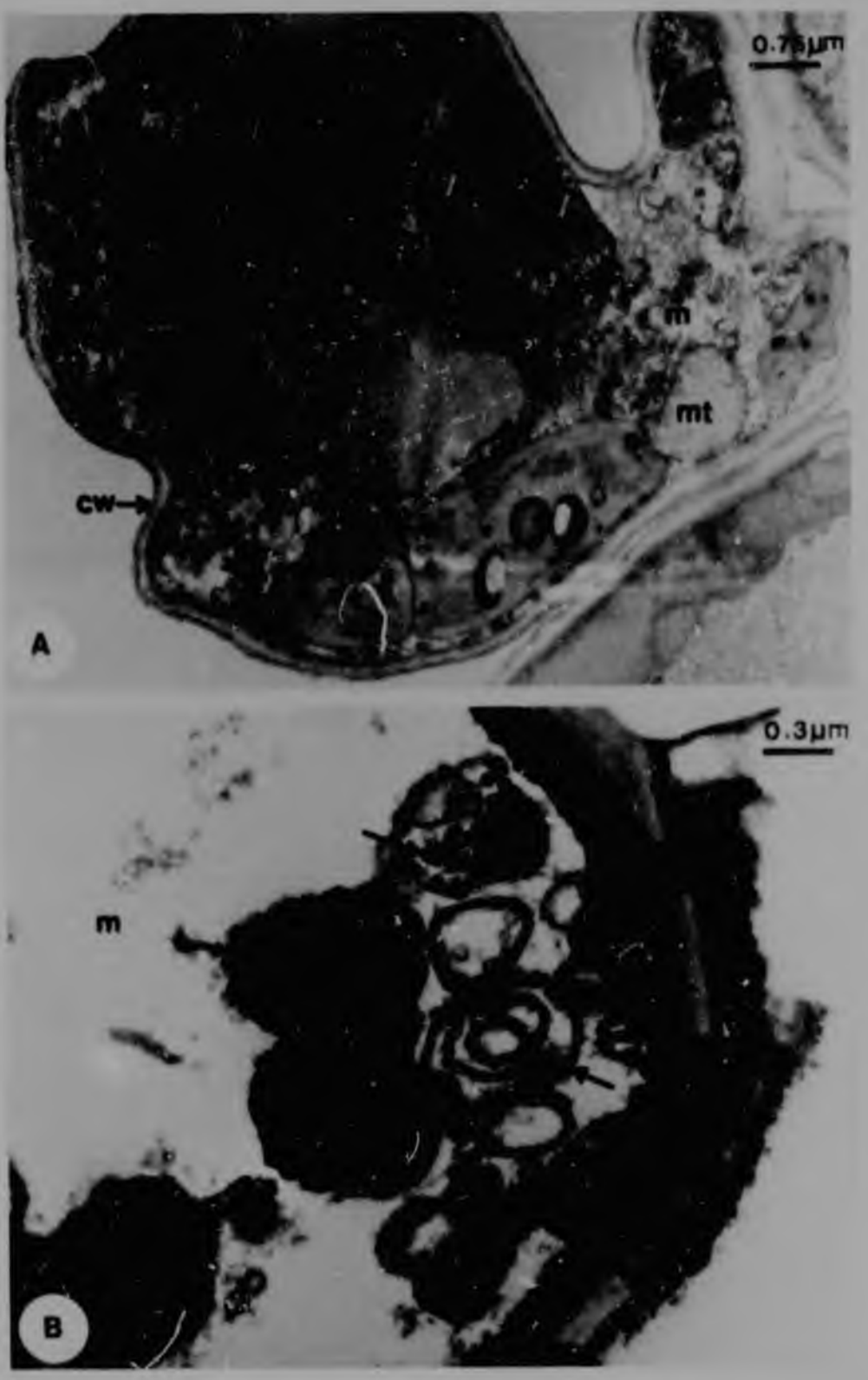
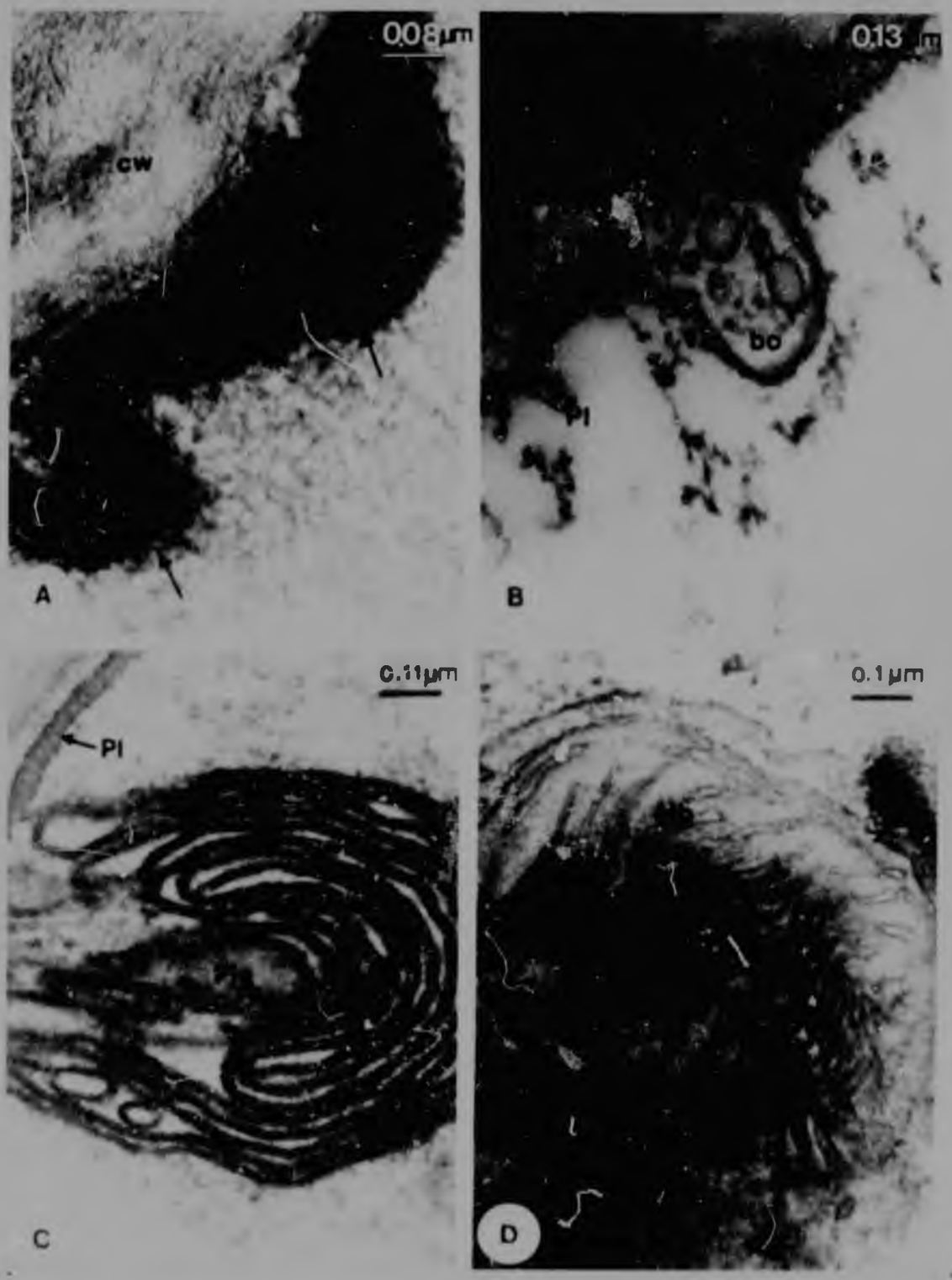


Fig.27 A. TEM micrograph of a transverse section through a healthy *E. africana* mesophyll cell. Note the large nucleus, mitochondria, and chloroplasts with a few lipid bodies.
B. In contrast a necrotic mesophyll cell exhibiting breakdown of cellular organelles and large numbers of membraneous vesicles.



Figs.28 A-D are High power TEM micrographs of sections through *B. africana* leaf tissue. A. Electron-dense deposition along mesophyll cells in the areas adjacent to the lesions. B. Boundary formation. C. Plasmalemmasome. D. Myelinic body. Figs.B-C-represent membraneous proliferation of the plasmalemma and in Fig.D the endoplasmic reticulum.

necrotic areas contained large lipid bodies, and exhibited disruption of the lamellae (Fig. 29 B), in contrast to the healthy chloroplasts (Fig. 29 A), whilst in the mature mesophyll cell chloroplasts, starch grains were degraded (Fig. 29 C). In advanced necrotic cells, the chloroplasts became totally disorganized, revealing disrupted lamellae and membranes, and large lipid bodies (Fig. 29 D).

4.1.2 Fluorescence microscopy and histochemistry

The presence of callose deposits on cell walls can be detected by yellow fluorescence under ultraviolet (uv) illumination when staining with aniline-blue. Unstained cross-sections through non-necrotic (Fig. 30) and necrotic (Fig. 33) leaf tissue exhibited autofluorescence of various substances. Lignin fluoresced bright yellow, suberin fluoresced orange, whilst starch in the chloroplasts fluoresced dark orange/red (Fig. 31). Stained sections taken through healthy tissue (Fig. 31) exhibited similar fluorescence as unstained material, indicating that the fluorescing substance was not callose, but lignin. The necrotic and semi-necrotic areas fluoresced bright yellow (Fig. 32). Control sections (Fig. 34) were unstained and viewed without uv, and no fluorescence was visible in comparison to Fig. 35 which was viewed under uv. The presence of lignin deposition in necrotic and semi-necrotic leaf areas was confirmed by phloroglucinol staining. Lignin stained bright red-violet in the necrotic tissue (Fig. 37 A) as opposed to unstained sections (Fig. 36) and healthy leaf tissue (Fig. 37 B).

4.2 *D. eriantha*

Penetration of *D. eriantha* leaves usually occurred through stomata, with the germ tube forming an appressorium over a stoma (Fig. 10 F). Intercellular vegetative hyphae ramified throughout the intercellular spaces of the leaf mesophyll (Fig. 38 B). The site of contact between a pathogen and host cell or protoplasm is known as the host-pathogen interface. In the case of *P. digitariae* infected-*D. eriantha*, the haustorial body appeared to be surrounded

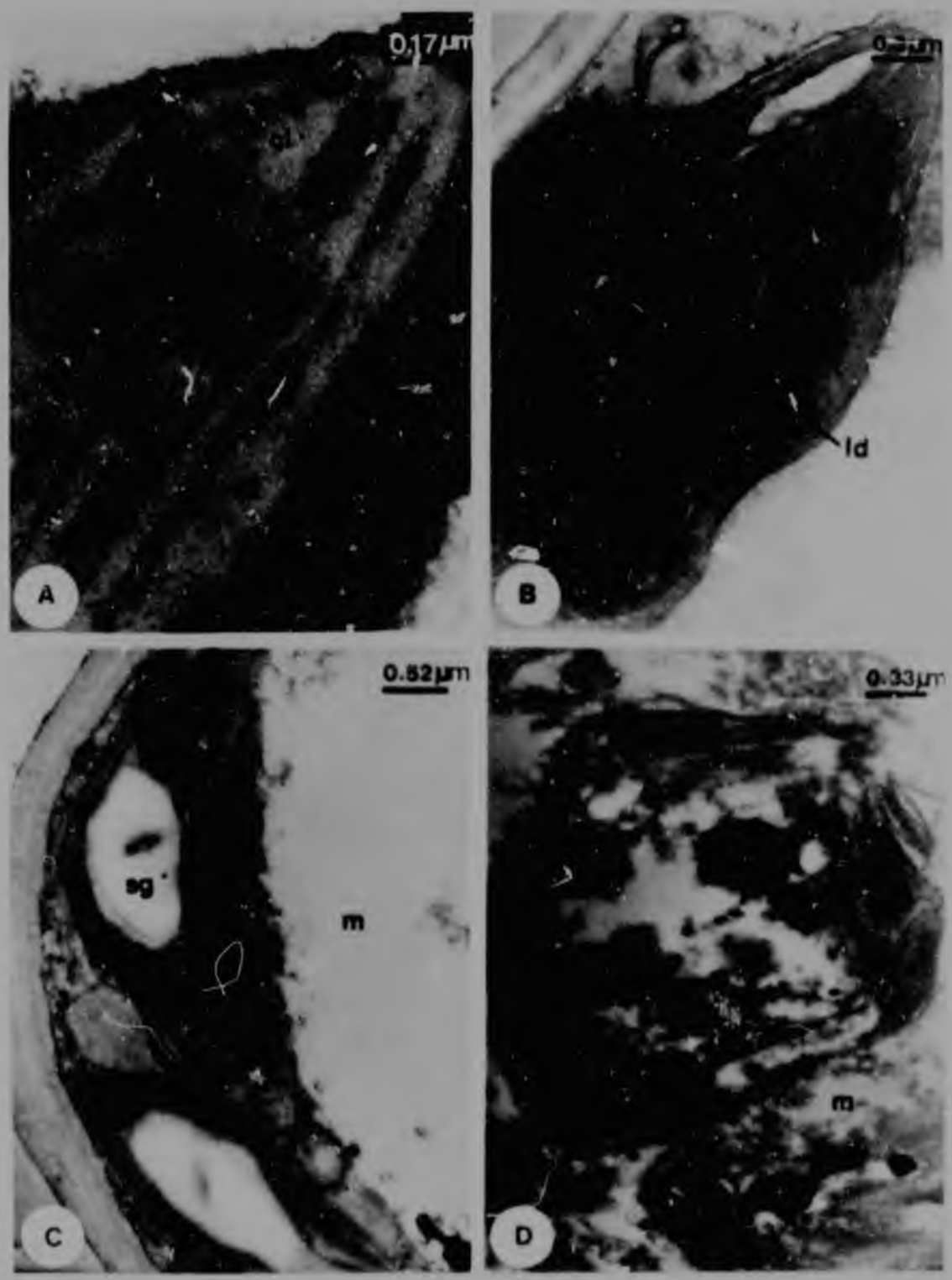
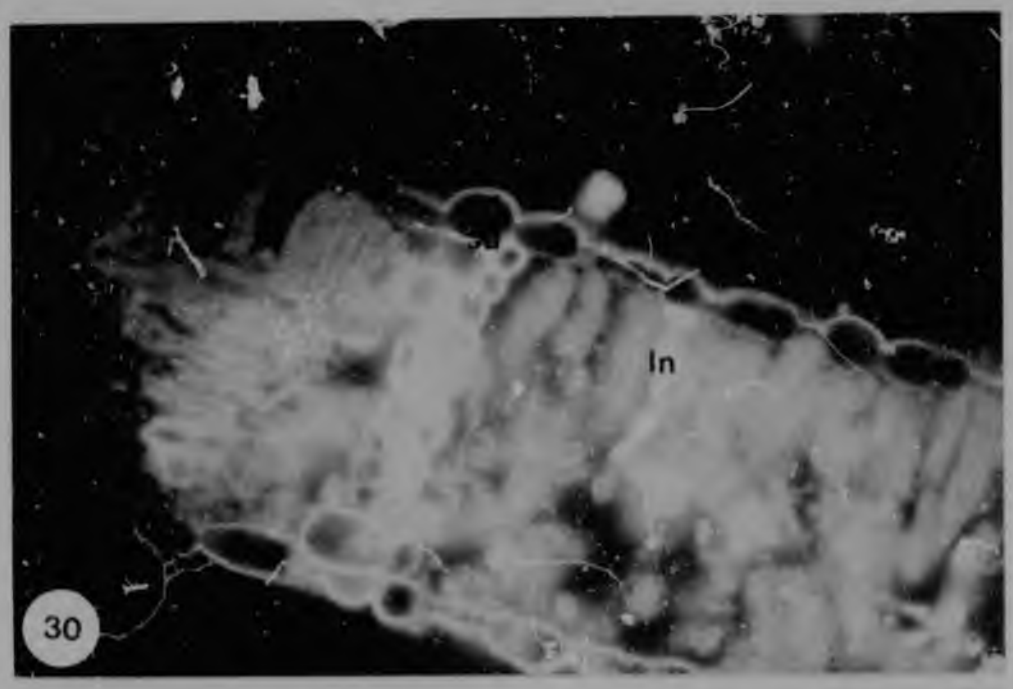


Fig.29 A-D are TEM micrographs of transverse sections through *B. africana* chloroplasts. A. A young chloroplast with intact organized grana and stroma lamellae. B. Young chloroplast from chlorotic area around lesion, showing disruption of lamellae system by large lipid bodies. C. Chloroplast from mature semi-necrotic mesophyll cell, exhibiting a large starch grain and number of lipid droplets. D. Degenerated chloroplast from necrotic lesion cell.



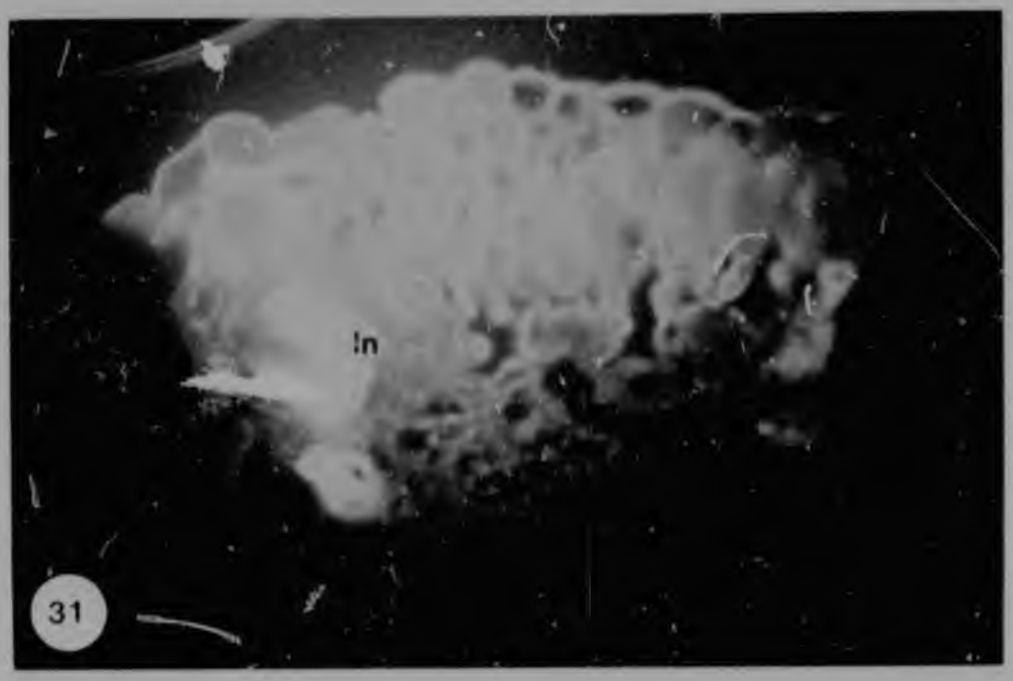


Fig.30 Unstained cross-section through non-necrotic *B. africana* leaf tissue exhibiting autofluorescence of lignin (yellow), suberin (orange), and starch in chloroplasts (orange/red) under UV. Fig. 31 Aniline-blue stained section through healthy leaf tissue exhibiting similar fluorescence as in unstained sections.



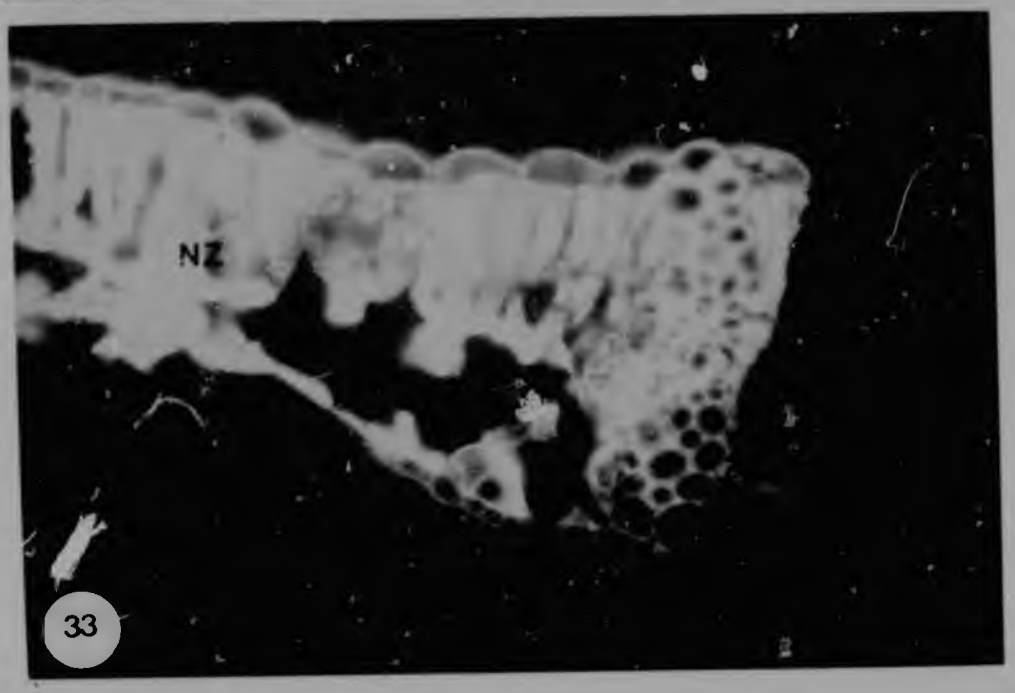


Fig.32 Aniline-blue stained cross-section through necrotic and semi-necrotic zones. Bright yellow fluorescence can be observed under UV. Fig.33 Unstained section through necrotic leaf tissue exhibiting yellow fluorescence (+UV).



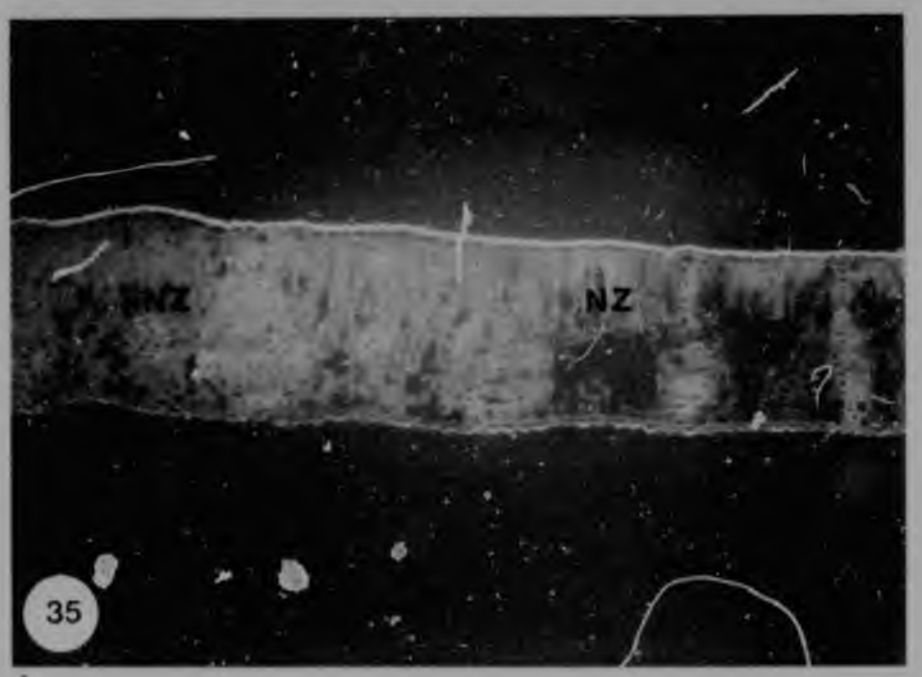
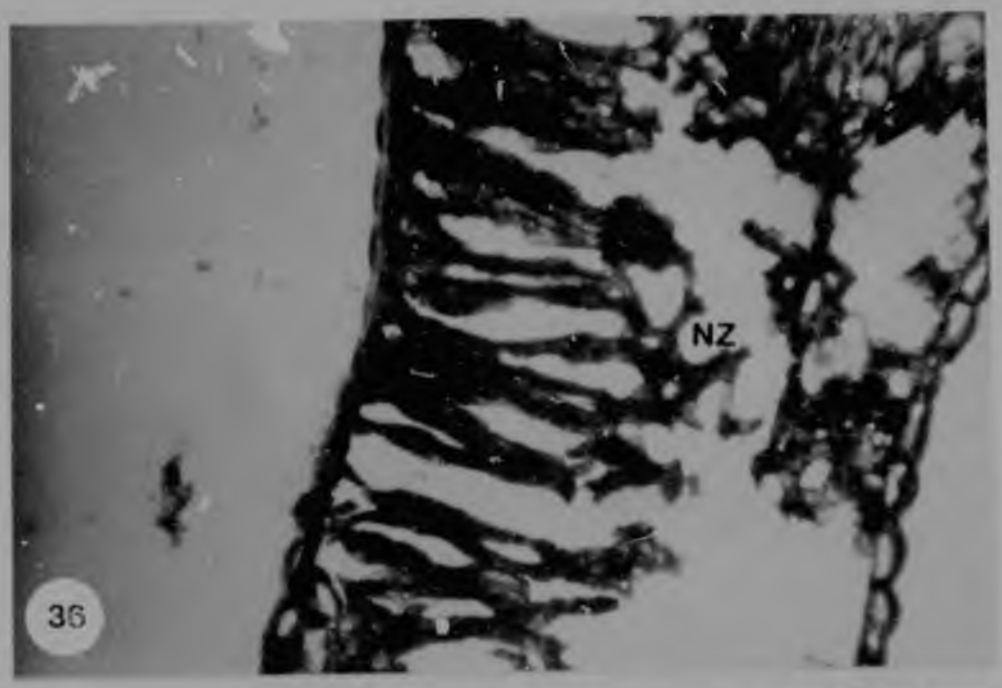


Fig.34 Control section through necrotic tissue of *B. africana* (-UV; unstained). Fig.35 Section taken through necrotic and semi-necrotic tissue (+UV; unstained).



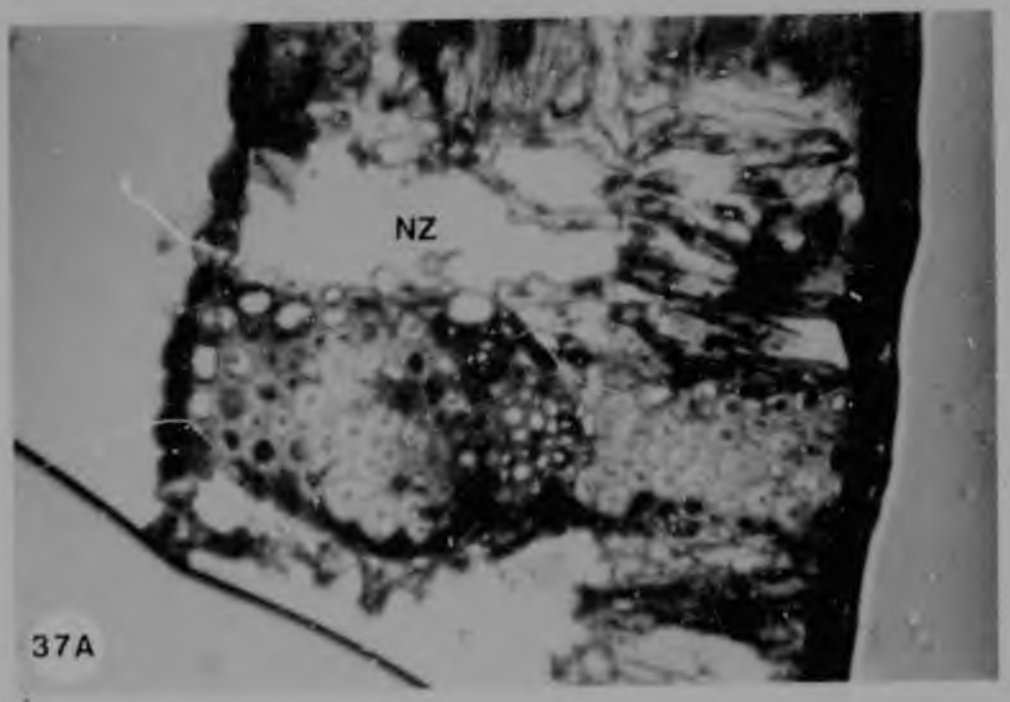


Fig.36 Cross-section (LM) through necrotic leaf tissue of *B. africana* (unstained) and Fig. 37 stained with phloroglucinol. Note the bright red-violet stain in Fig.37A.

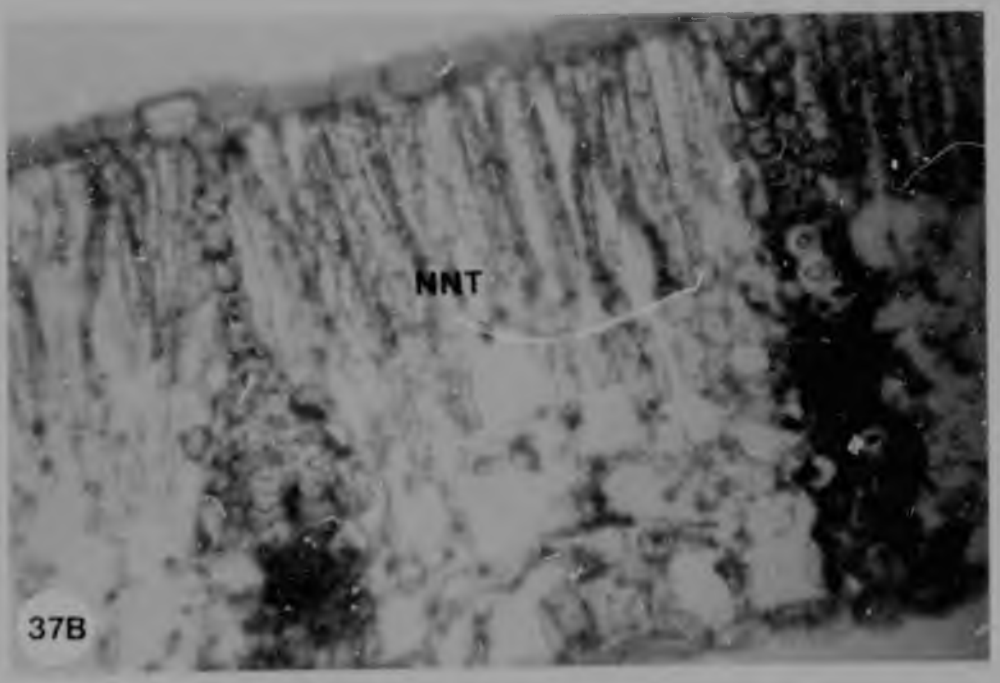


Fig.37 B. Non-necrotic leaf tissue of *B. africana* stained with phloroglucinol. No red-violet colour was visible.

by the invaginated host plasmalemma (Fig. 38 A). Although continuity of the membrane with the host plasmalemma was not demonstrated, the haustorial membrane did not appear to differ from those described by other workers (Littlefield and Bracker, 1972; Littlefield, 1979). This intracellular haustorium was found to be surrounded by a sheath-like matrix between the fungal cell wall and host plasmalemma. It is uncertain whether this extrahaustorial matrix is partly a fungal or partly a host secretion. The haustoria contained many mitochondria which exhibited highly convoluted tubular cristae (Fig. 41 F). Lomosomes and myelin-like structures were detected in the cytoplasm, closely associated with the fungal cell wall (Fig. 38 A).

Disruption of leaf tissue, following rust infection, is evident in Fig. 39 D, compared to healthy tissue (Fig. 39 C). The nature of the thick walls of these structures (arrows) in Fig. 39 D suggests that they may be haustoria. TEM, indeed, confirmed the presence of haustoria (Figs. 38 A and 40 B) and it appears likely that disruption of the leaf tissue (Fig. 39 D) may have resulted from penetration of haustoria and ramification of intercellular hyphae (Fig. 38 B). Healthy mesophyll chloroplasts were characterized by a normal lens-shape, well developed stromal and granal lamellae and small lipid droplets (Fig. 40 A). Disorganization of the mesophyll (Fig. 38 A) and bundle sheath chloroplasts took place during the later stages of infection, with the chloroplast lamellae becoming disrupted and formation of large lipid bodies and starch grains occurring. Other cytological changes were manifested as swollen, densely staining nuclei (Fig. 40 B) and swollen mitochondria. Mitochondrial counts were made of serial sections through healthy and rust-infected mesophyll and bundle sheath cells (Table 3). Statistical analysis (t-tests) were undertaken in order to determine whether or not the differences in mitochondrial types between healthy and infected mesophyll and bundle sheath cells were significant. Four types of mitochondria were observed. The healthy mitochondria (mt_0) from the mesophyll (Fig. 41 C) and bundle-sheath cells (Fig. 41 A) were oval-shaped with many invaginated tubular cristae. The second mitochondrial type (mt_1) was swollen with a decreased number of narrow cristae (Fig. 41 B).

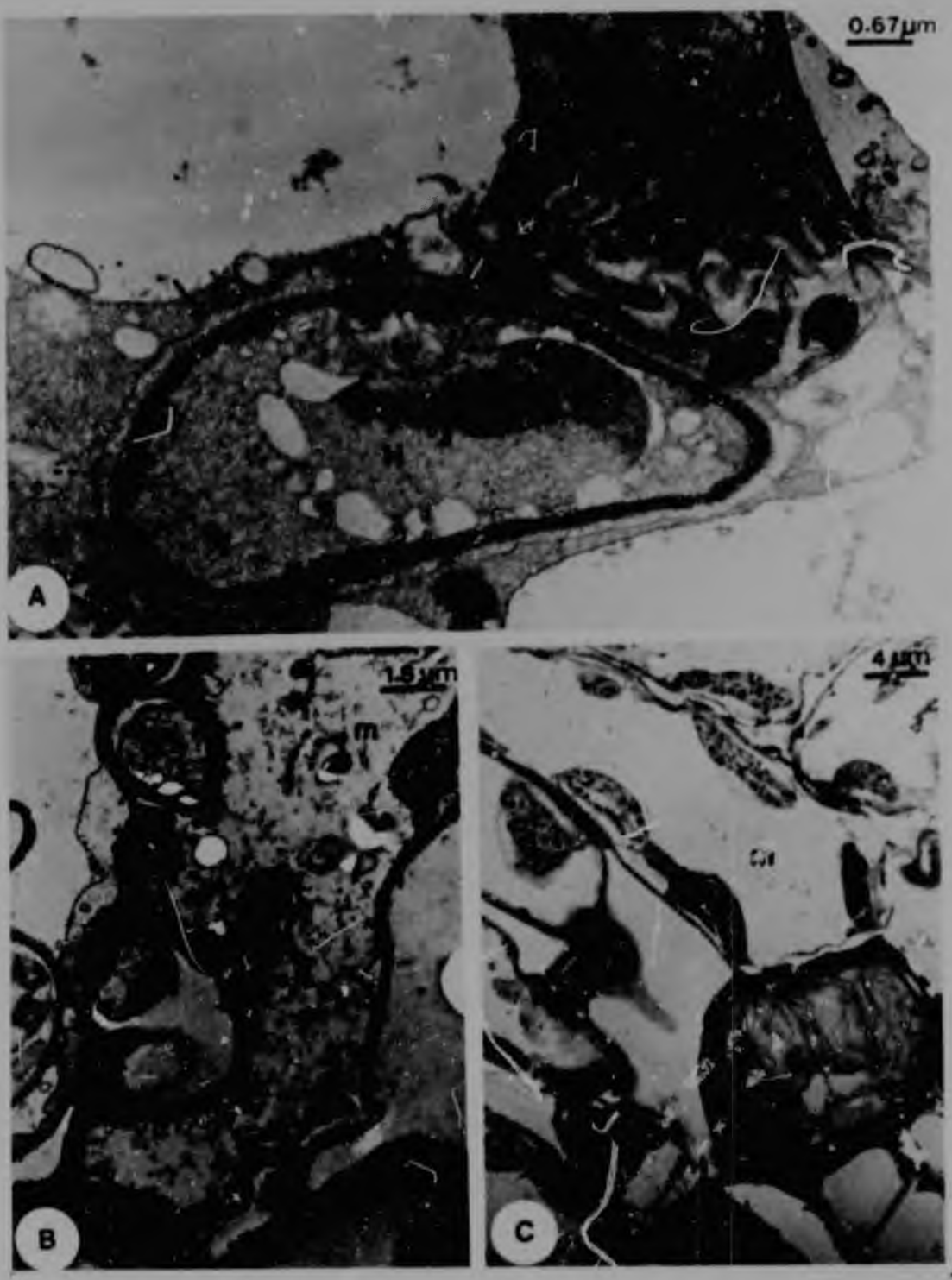


Fig.38 A. TEM micrograph of an intracellu'ar haustorium of *P. digitariae* infecting *D. eriantha*. The haustorium is surrounded by a membrane (solid arrow) resembling the host plasmalemma and sheath-like matrix (open arrow). Note disorganization of mesophyll chloroplast. B. Intercellular hyphae ramifying throughout intercellular spaces. C. Healthy mesophyll tissue.

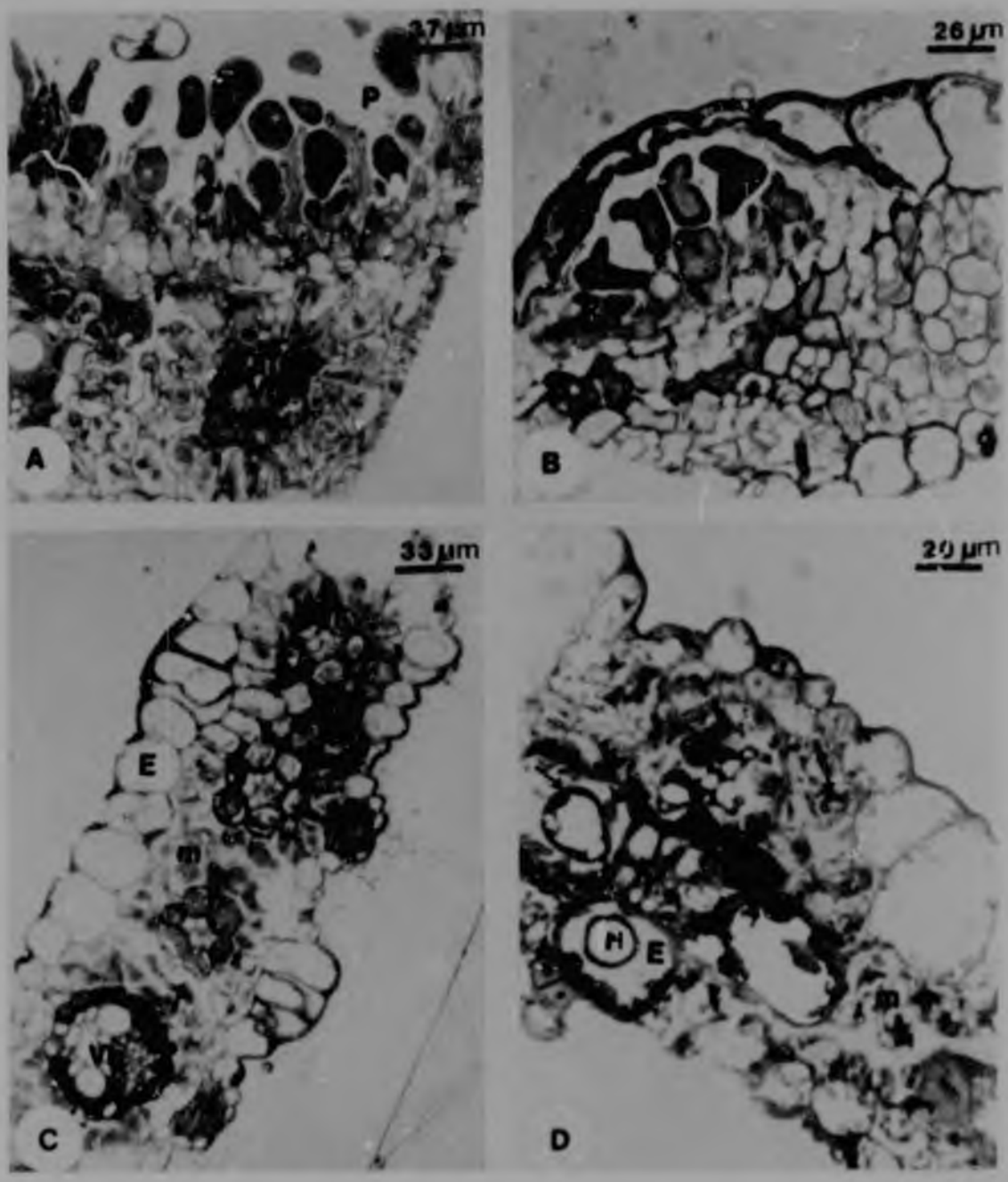


Fig.39 A-D. Toluidine-blue semi-thin transverse sections through *D. eriantha* leaf tissue. A. Mature pustule exhibiting uredospores being released, and fertile layer. B. Immature uredosorus. No peridium was visible although the proximal epidermis cell wall appears thickened. C. Healthy leaf tissue. D. Disruption of mesophyll tissue by the rust-fungus. Note the intracellular haustoria.

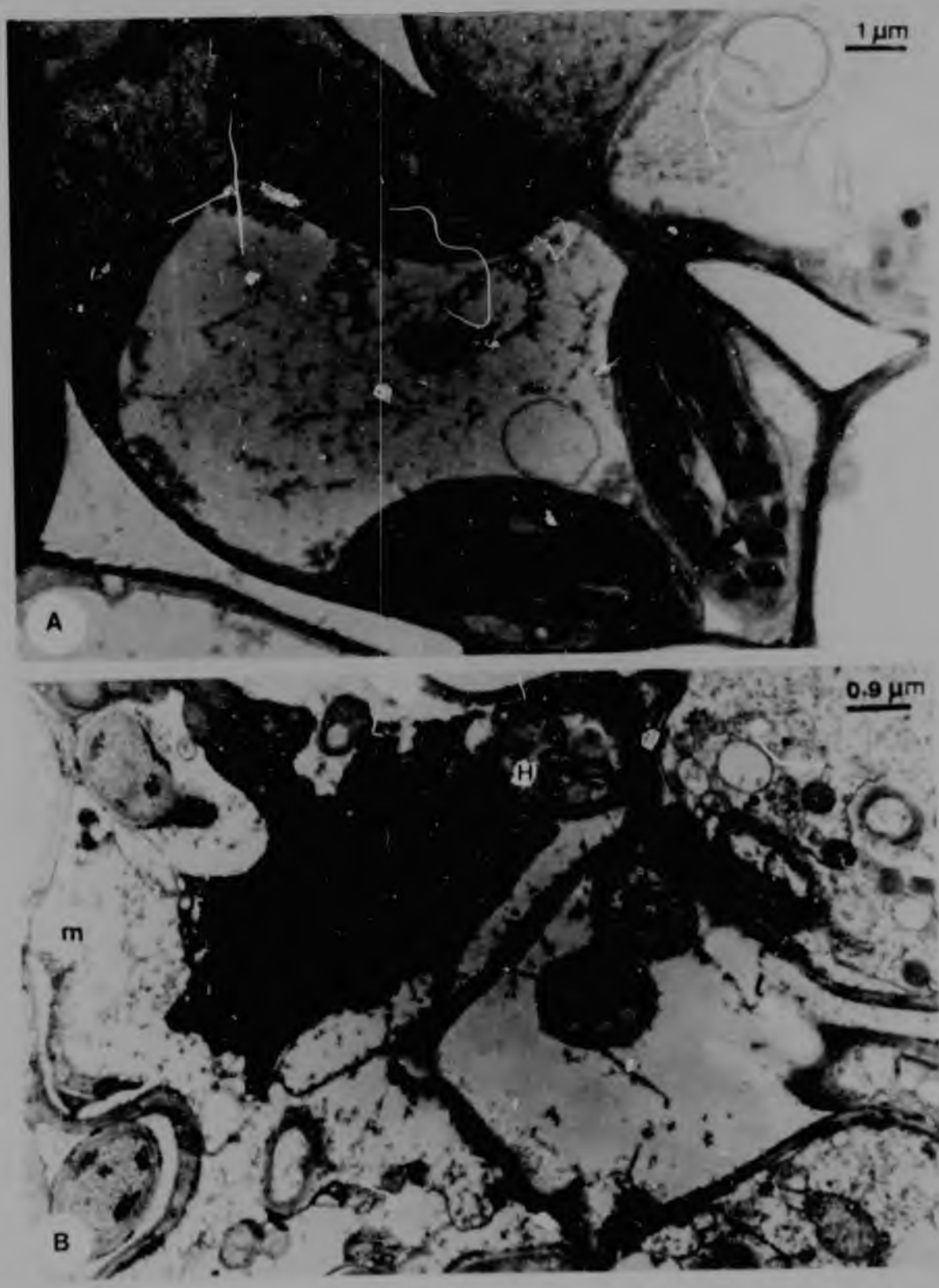


Fig.40 A. TEM section through a healthy *D. eriantha* mesophyll cell showing normal lens-shaped chloroplasts and few small lipid droplets. B. Section through rust-infected mesophyll cells. The cells contained a number of intracellular haustoria and the nucleus appeared swollen and densely staining in comparison to the nucleus in the uninfected mesophyll cell (A).

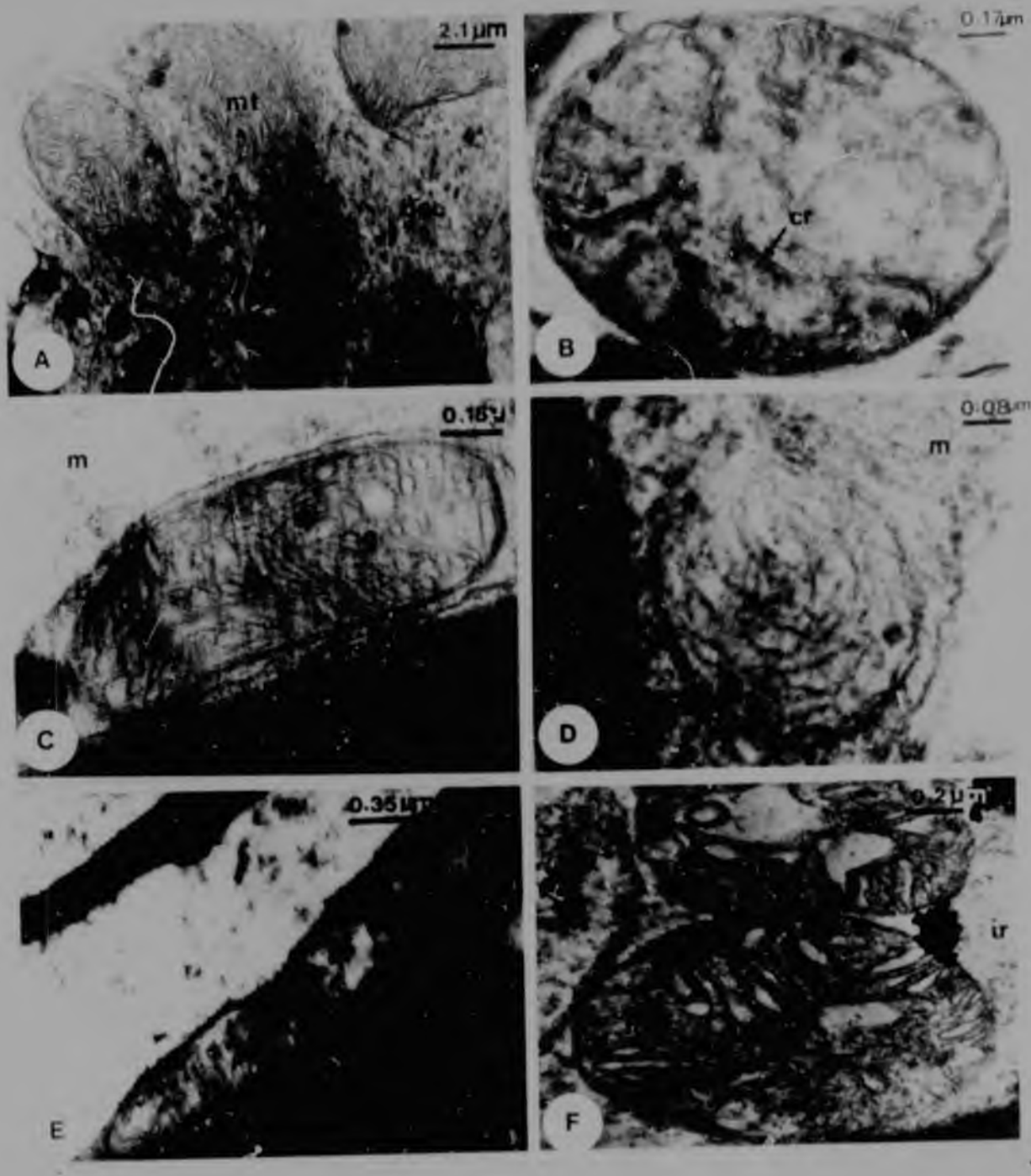


Fig.41 A. Mitochondria (mt_0) from healthy *D. eriantha* bundle sheath cells. B. Swollen mitochondrion (mt_1) in rust-infected *D. eriantha* bundle sheath cells. C. Mitochondrion with many cristae in healthy mesophyll cell. D. Rounded off mitochondria (mt_3) with the cristae and outer membranes losing their integrity. E. Elongated mitochondrion (mt_2) along the cell wall in mesophyll cells invaded by haustoria. F. Haustorium mitochondrion with well-developed tubular cristae.

Table 9. Distribution of different types of mitochondria in healthy and rust-infected *D. eriantha*.

COUNTS	TYPES OF MITOCHONDRIA*				TOTAL COUNTS
	mt_o	mt_1	mt_2	mt_3	
Control leaves-Bundle sheath cells	120 (80)**	12 (8)	14 (9.3)	4 (2.7)	150
Control leaves-Mesophyll cells	158 (79)	+25 (12.5)	8 (4)	9 (4.5)	200
Rust-infected leaves-Bundle sheath cells	11 (7.9)	90 (64.2)	- -	39 (29.7)	140
Rust-infected leaves-Mesophyll cells	17 (9.4)	+18 (10)	97 (53.9)	48 (26.7)	180

* mt_o: Intact mitochondria in healthy bundle sheath cells (Fig. 41A) and mesophyll cells (Fig.41C)

mt_1: Swollen mitochondria (with decreased no. of cristae) in mesophyll cells, observed during the stages of post-sporulation (Fig.41B)

mt_2: Elongated mitochondria (with an increase in the no. of cristae) in rust-infected mesophyll cells prior to sporulation (Fig.41E)

mt_3: Swollen mitochondria with a reduced no. of cristae. The cristae have become contracted (Fig.41D)

** Figures in parentheses represent the percentages of mitochondria.

Note: 5 leaf sa ples of each healthy and infected leaves were used for counting.
Differences proved significant at p = 0.05 except +.

In mesophyll cel s invaded by haustoria, the mitochondria (mt_2) appeared elongated along the cell wall (Fig. 31 E). The mitochondria (mt_3) in mesophyll and bundle sheath cells during the post-sporulation stages, were rounded with the cristae and outer membranes losing their integrity (Fig. 41 D). From the mitochondrial counts the majority of mitochondria in the healthy cells appeared to be of the mt_o type (80%), whilst types mt_1, mt_2 and mt_3 were forms appearing as a result of rust development in *D. eriantha*, the differences being statistically significant ($p = 0.05$). The number of mitochondria of the mt_1 type increased from 8% to 64% in infected bundle sheath cells, whilst the number of mitochondria of type mt_2 increased from 4% in healthy to 54% in infected mesophyll cells. The degenerating mitochondria (mt_3) were detected in rust-infected tissue during the later stage of infection (post-sporulation). The number of mt_3 mitochondria increased from 2.7% in healthy bundle sheath cells to 30% in infected cells, whilst the number increased from 4.5% in healthy to 26.7% in infected mesophyll cells.

The mesophyll cells (Fig. 42 A) below the basal cells (Fig. 42 B) in the fertile layer (from which the sporophores/spores are formed, Fig. 42C) showed complete degeneration of the protoplasm, and were packed with large numbers of starch grains.

The sporogenous zone of developing uredospores, or the fertile layer (Fig. 43 A) as it is sometimes called, was composed of basal cells which varied in size and shape. These basal cells (Fig. 42 B) were characterized by dense, ribosome-packed cytoplasm and numerous large vacuoles. The basal cell gave rise to a uredinial initial which divided to form a sporophore and uredospore distally, and the sporophore elongated beyond developing uredospores at the adscission stage (Fig. 43 B). Figs. 43 B and E also reveal the presence of the remnants of an old sporophore wall forming a collar around the developing sporophore wall. It appeared as if in some cases the sporophore remained attached to the sporogenous or basal cell below, and the sporophore wall split either at its distal apex in the centre (Fig. 43 C, arrow 1) causing inner folds to occur laterally or split on both sides at the top of the sporophore wall forming straight collars (Fig. 41 B and 43 A).

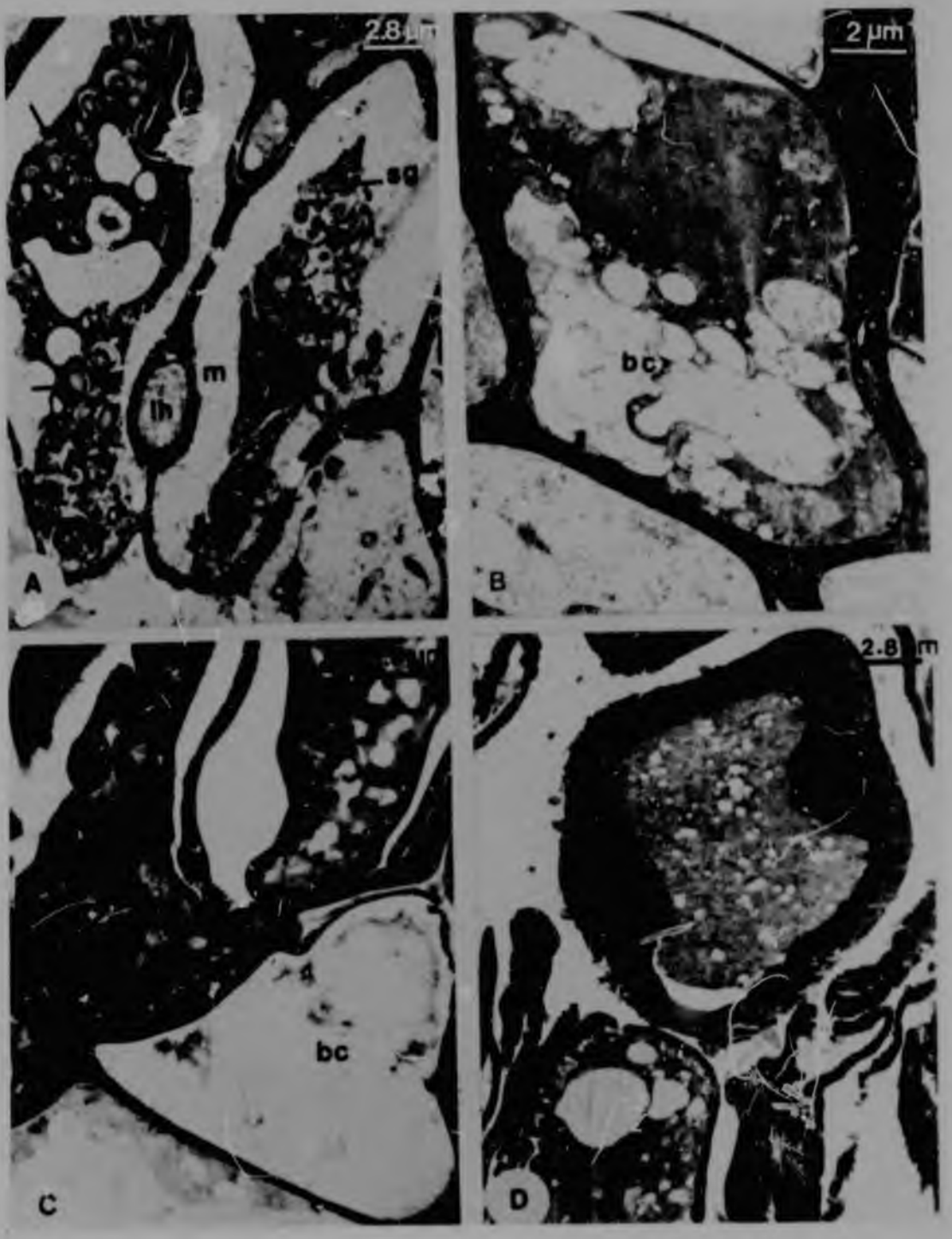


Fig.42 A-D TEM micrographs of rust-infected *D. eriantha*. A. Mesophyll cells below the basal cells (B) in the fertile layer from which sporophores/spores (C) are formed. The mesophyll cell protoplasm has degenerated and the cells are packed with large starch grains (arrows). D. Mature released uredospore with thick walls and spines.



Figs.43 A-E TEM of developing rust pustules on *D. eriantha*. A. Pustule (low power) showing uredospores, collars formed around old sporophores and fertile layer. B. High power of remnant collars (arrow) around sporophore and basal cell below. C. Inner folds of old sporophore wall caused by splitting of wall at its distal apex (arrow 1). D. Remainder of old sporophore wall (arrow) can clearly be observed above uredinial initial below. E. High power of collars pushed laterally aside.

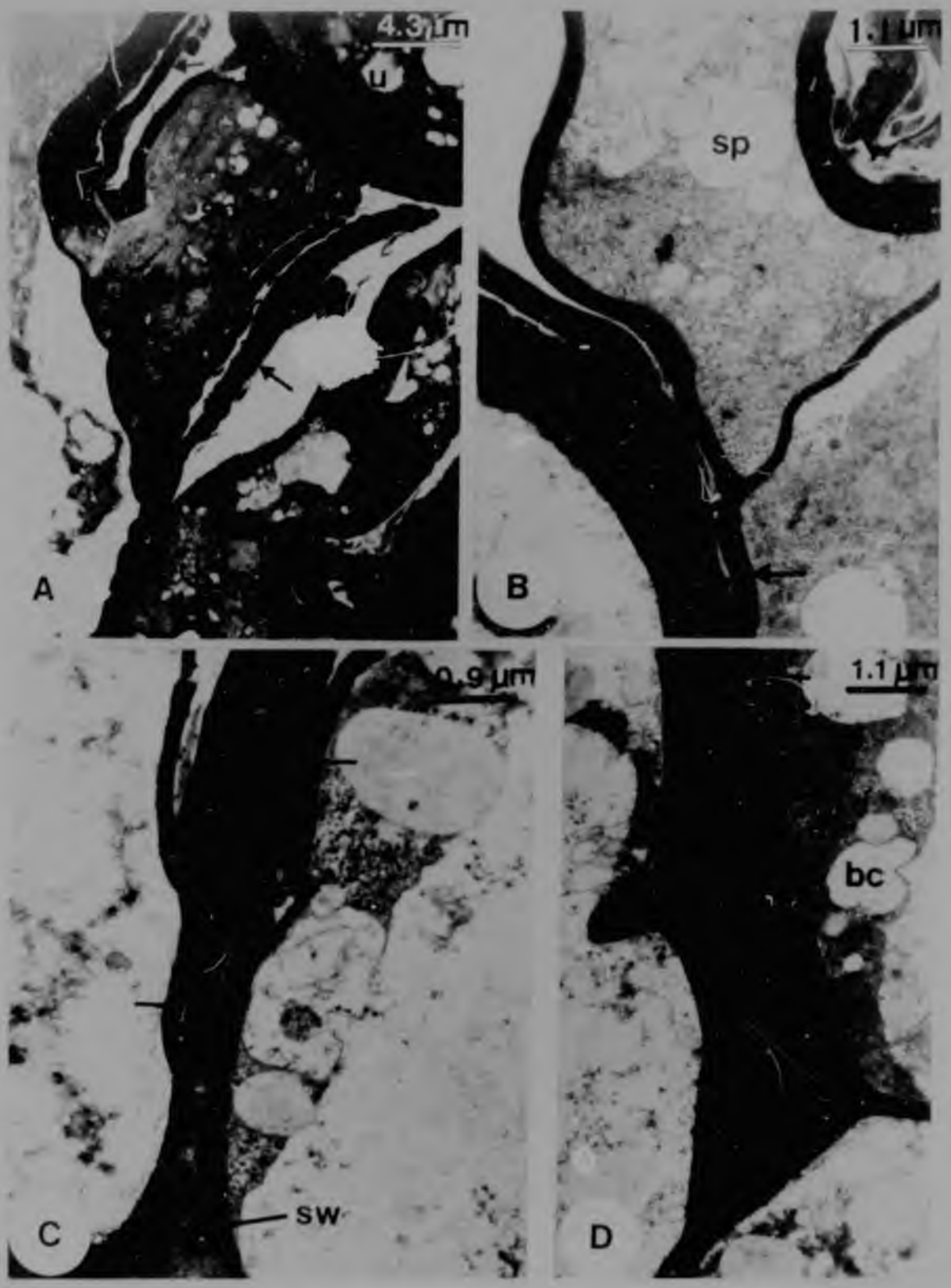


Fig.44 A-D Uredospore ontogeny of *P. digitariae*. A. High power TEM micrograph of basal cell, sporophore and collars. B. and D. illustrate that the new wall growth occurs from further down the inner sporogenous cell wall (arrows). C. Laterally displaced septa that had occurred between sporogenous cell and persistant sporophore (arrows).

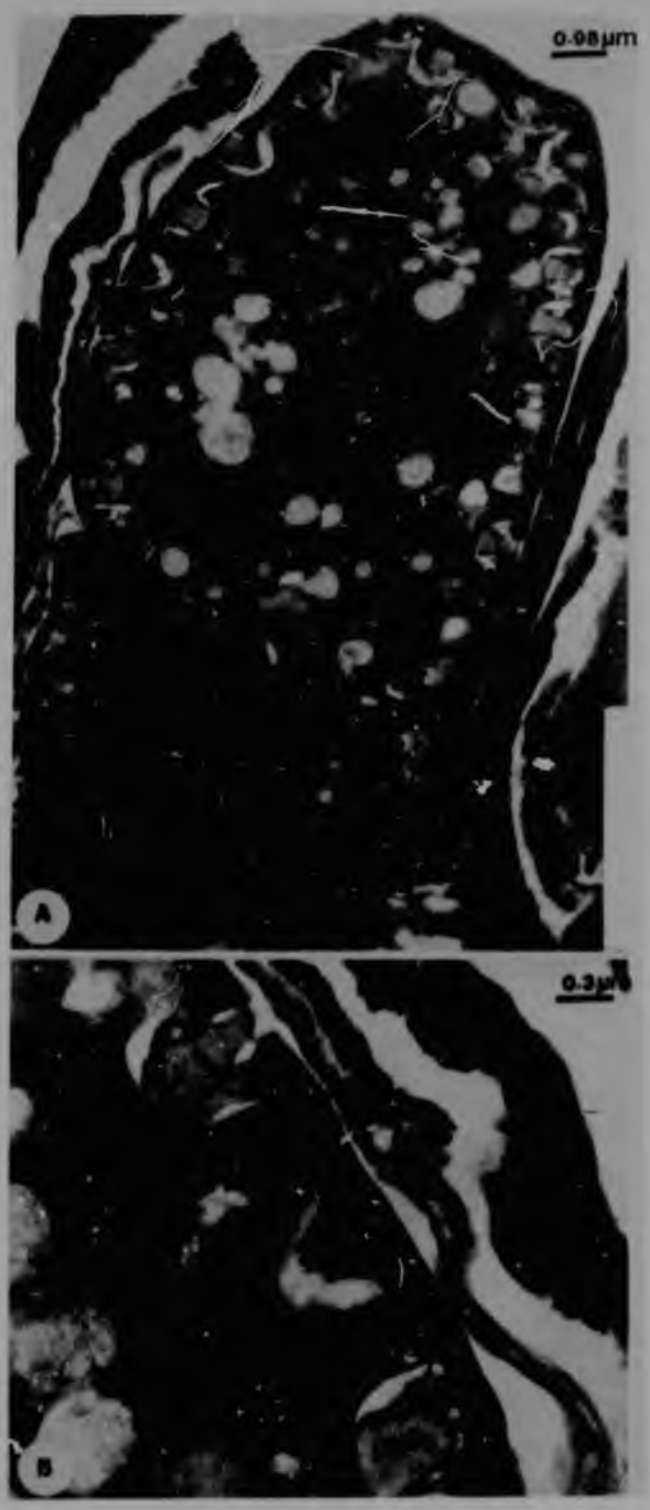
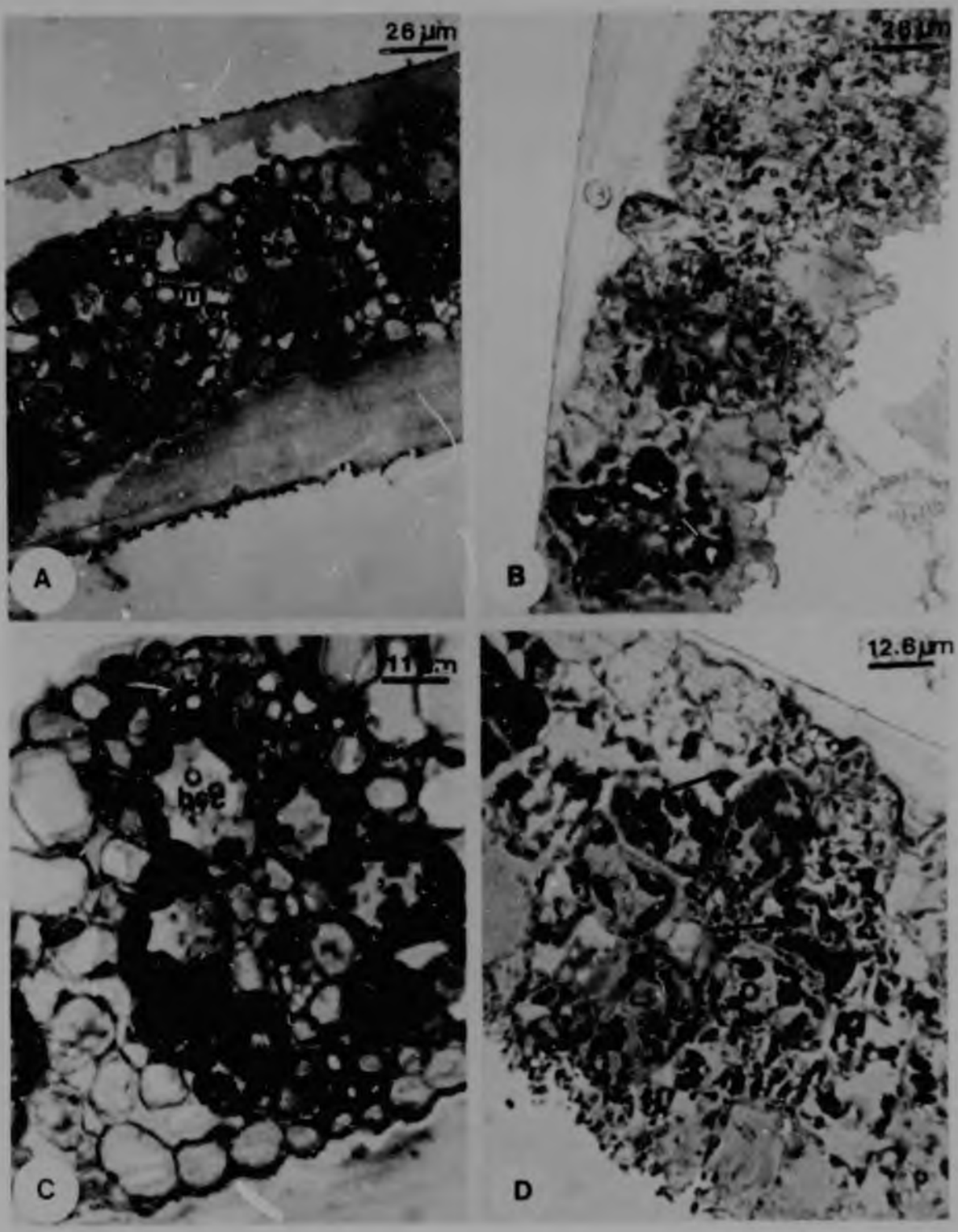


Fig.45 A. Uredospore of *P. digitariae* exhibiting dense cytoplasm and lipid droplets. B. Spine development in uredospores. The spines contain fibrillar materials and are initiated as small electron-lucent areas outside the plasmalemma at the inner face of the thin wall of the immature uredospore.

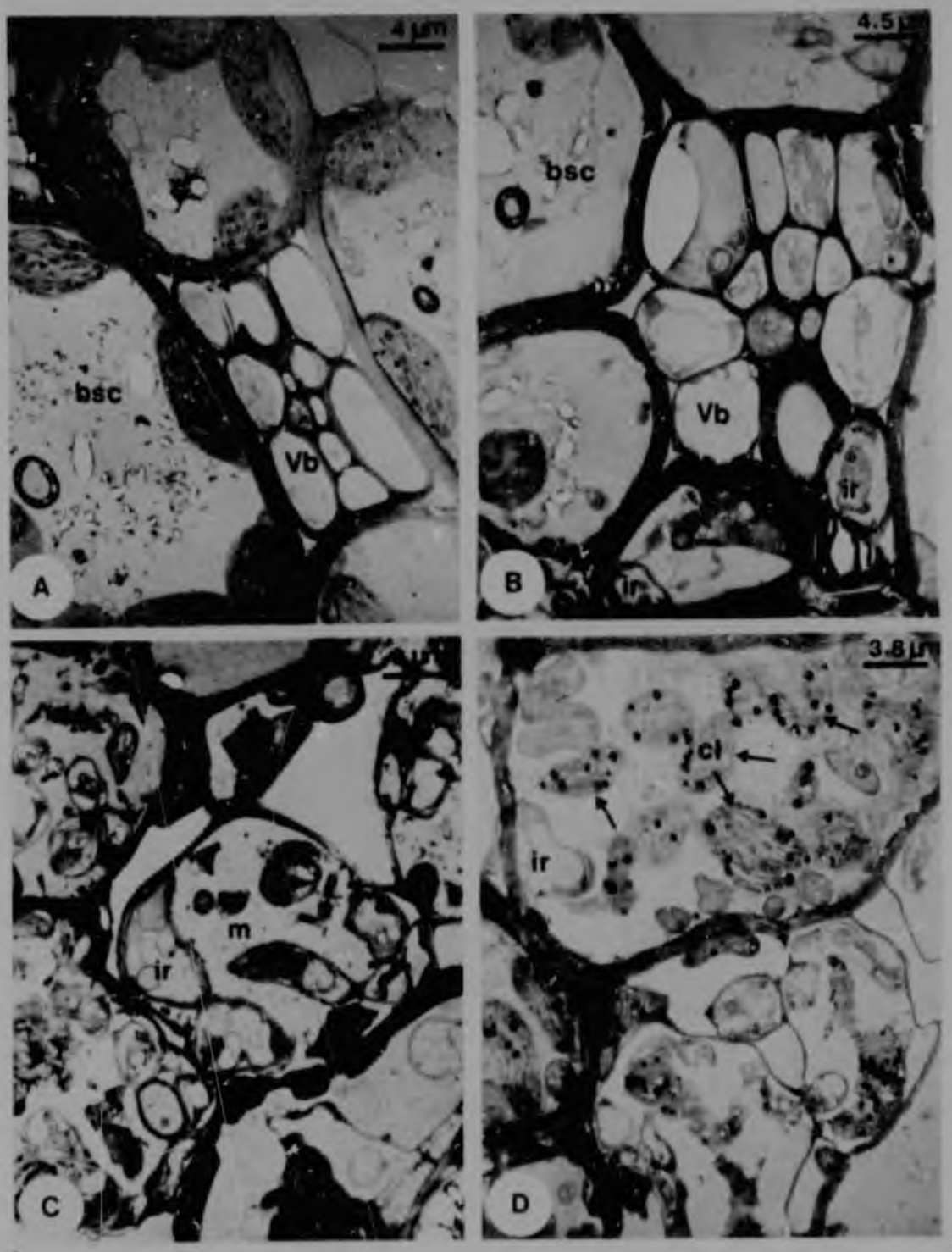


Figs. 46 A-D Toluidine-blue stained semi-thin transverse sections through *P. maximum* leaf tissue. A. Healthy leaf tissue. B. Disintegration of mesophyll due to tarspot infection. C. High power of healthy bundle sheath cells with centrifugal chloroplasts. D. Disrupted bundle sheath cells in tarspot-infected tissue with the chloroplasts having become randomly displaced.

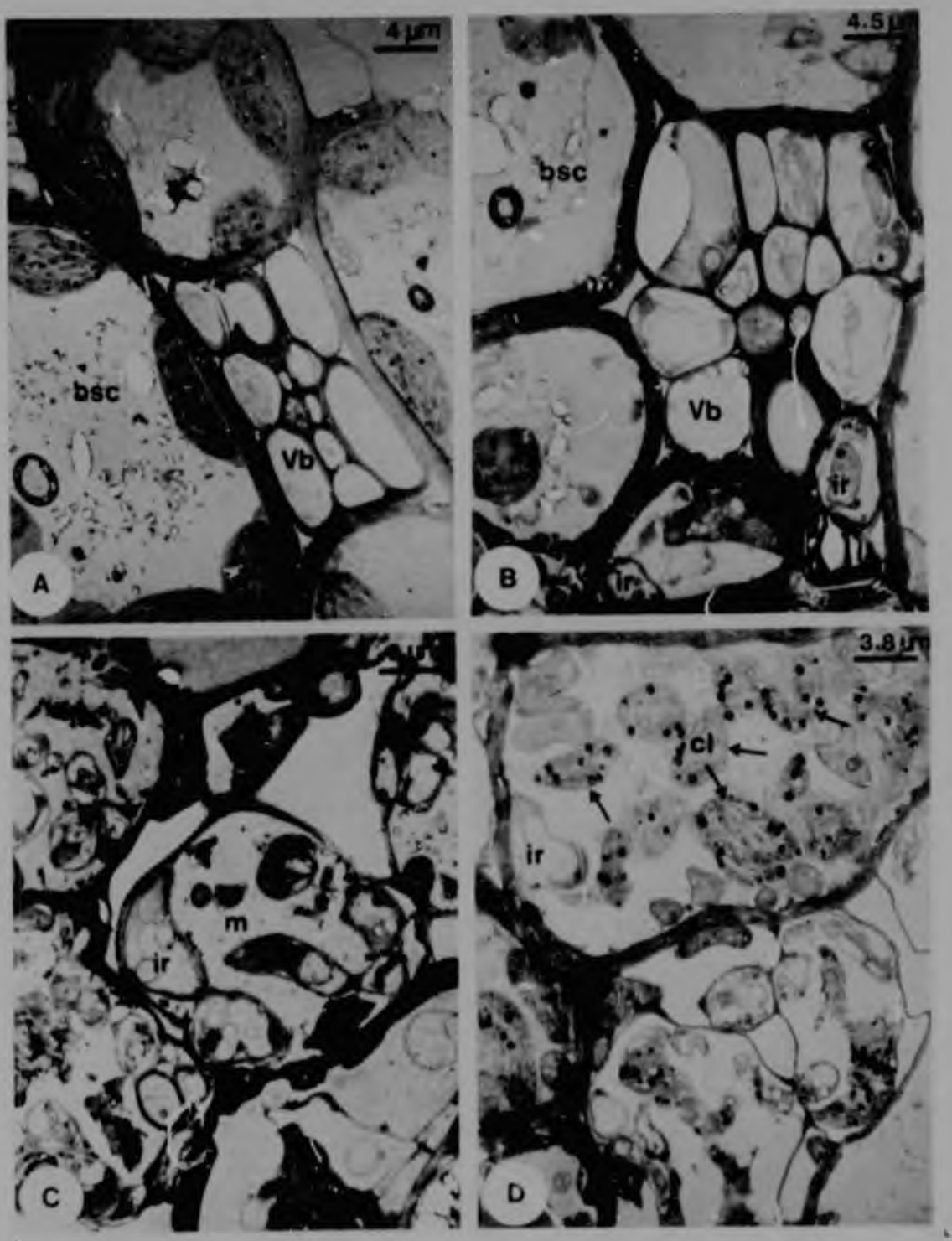
In the latter case the distal remnants of the sporophore wall were pushed aside when the new sporophore elongated (see arrow Fig. 43 B). Consequently the sporogenous cell wall extended through the previous sporophore and cut off another uredinial initial resulting in the formation of collars around the newly-formed sporophore. The new uredinial initial with the remainder of the old sporophore wall could be observed clearly · Fig. 43 D. High power TEM micrographs illustrated clearly that new wall growth occurred from further down the inner sporogenous cell wall (arrows Figs. 44 B and D). When this occurred the septum between the sporogenous cell and persistent sporophore was laterally displaced (arrows Fig. 44 C). However in some instances the sporophore or pedicel did become detached from the sporogenous cell, and was displaced by newly formed uredinial initials either at the same point or at new adjacent sites on the sporogenous cell. The young uredospores rapidly grew to a mature size and were marked by increased density of the cytop'asm, increased accumulation of lipid droplets, spine development (Figs. 45 A and B) and wall thickening (Fig. 42 D). Spine formation was essentially similar to that described for other rust fungi (Thomas and Isaac, 1967; Ehrlich and Ehrlich, 1969; Manocha and Wisdom, 1971). The uredospores were formed under the epidermis (Fig. 39 B) and were liberated when the epidermis erupted (Fig. 39 A). No evidence of a peridium was visible. At the time of spore abscission it appeared as if the septum everted laterally (open arrow Fig. 43 C) probably exerting some mechanical pressure.

4.3 *P. maximum*

Colonies of *P. paspalicola* were found to develop only in the tissue of the leaf blades of *P. maximum* and the clypeus or stromatic structure consisted of densely packed dark hyphae. TEM micrographs revealed the presence of intracellular mycelia in the mesophyll cells (Fig. 47 C), bundle sheath cells (Fig. 49 A) and occasionally in the vascular tissue (Fig. 47 B). The tissue surrounding the colonies became disrupted during the later stages of infection when the fungus had discharged its spores.
This disintegration of mesophyll tissue can be seen clearly in



Figs.47 A-D TEM micrographs of healthy and tarspot-infected *P. maximum* leaf tissue. A. High power of healthy bundle sheath cells. B. Bundle sheath cells with displaced chloroplasts due to intracellular hyphal penetration. C. Intracellular hyphae in mesophyll cells. D. High power of chloroplasts in bundle sheath cells. Note the high number of lipid droplets and loss of lens-shape and centrifugal position.



Figs.47 A-D TEM micrographs of healthy and tarspot-infected *P. maximum* leaf tissue. A. High power of healthy bundle sheath cells. B. Bundle sheath cells with displaced chloroplasts due to intracellular hyphal penetration. C. Intracellular hyphae in mesophyll cells. D. High power of chloroplasts in bundle sheath cells. Note the high number of lipid droplets and loss of lens-shape and centrifugal position.

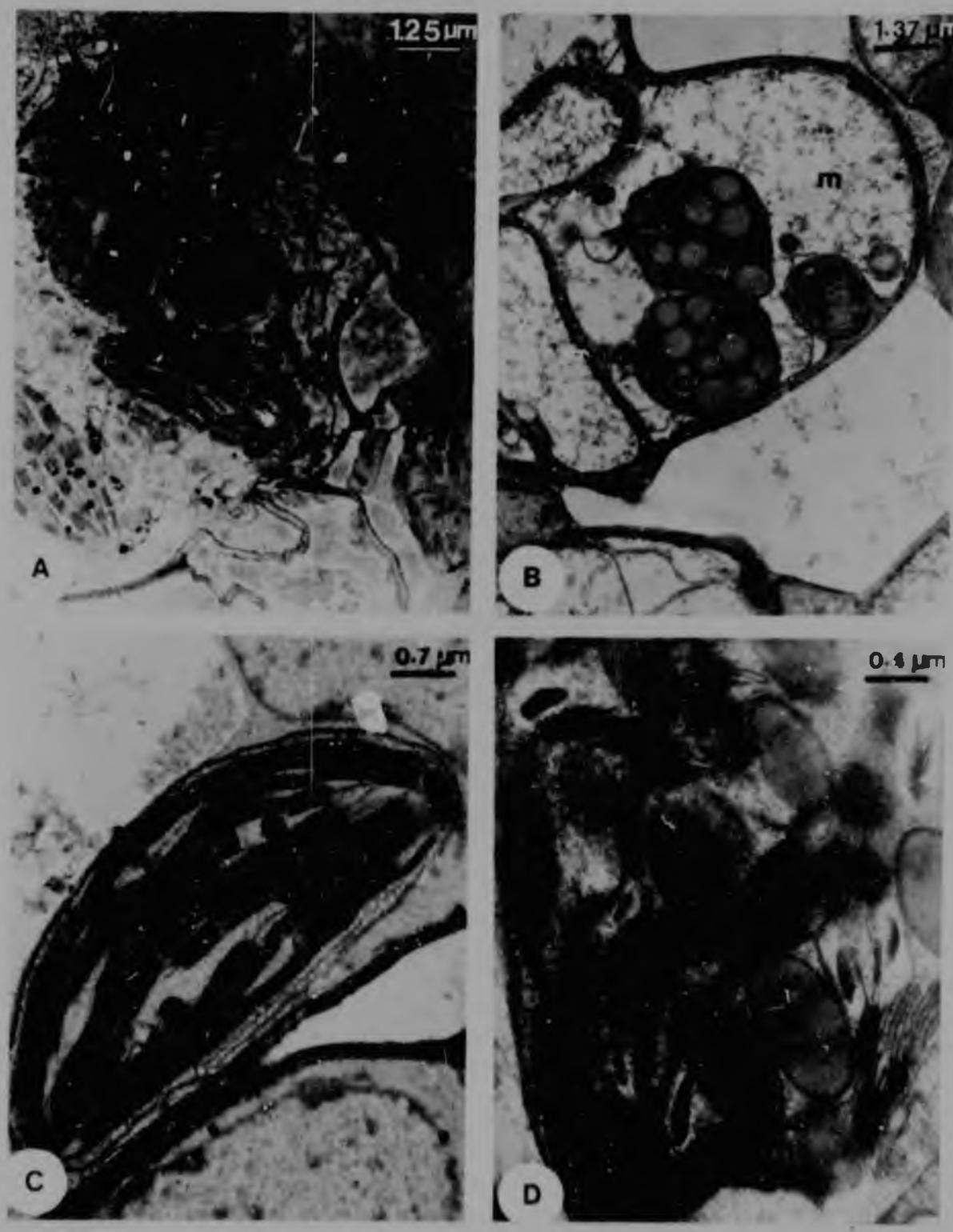


Fig.48 A. Chlorplasts in healthy bundle sheath cells. C. Chloroplast in a healthy mesophyll cell. Healthy chloroplasts exhibit a lens-shape with well developed stroma and grana lamellae. Figs.B and D are chloroplasts from tarspot-infected tissue. B. Note the large lipid bodies distorting the chloroplasts. D. Disruption of the lamellae and chloroplast membrane was often observed.

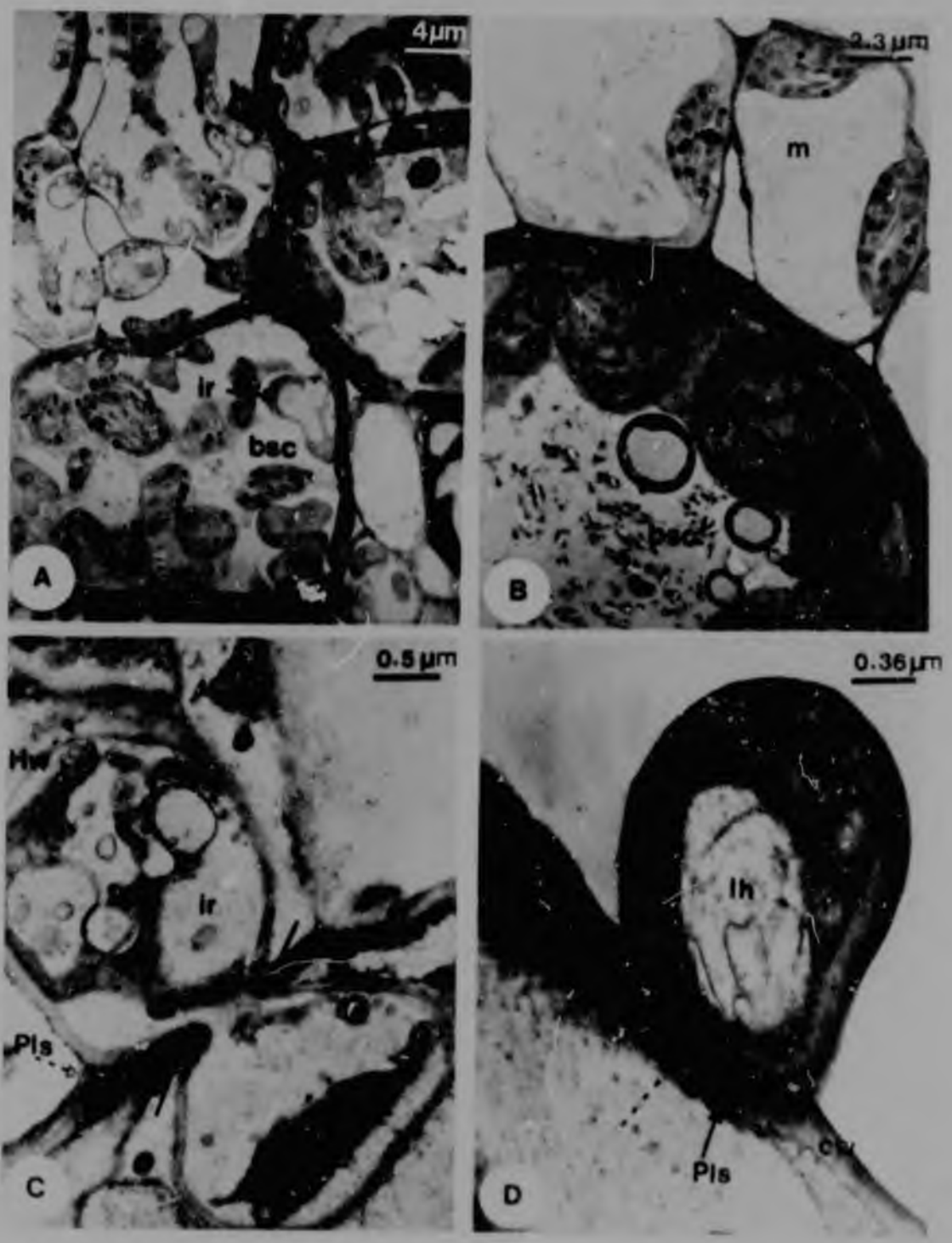


Fig.49 A. High power TEM micrograph of bundle sheath cells from tarspot-infected tissue. B. BSC from healthy leaf tissue. C. Intracellular penetration by hyphae. The plasmalemma (Pls) is invaginated and there appears to be an electron-dense deposit on the host wall around the areas of penetration. D. Intercellular hyphae closely appressed to the host cell wall. Note the electron-dense band (open arrow) between host and fungal walls.



Fig.50 A. TEM of densely packed intercellular hyphae forming the clypeus. B. The host-pathogen interface of *P. maximum* and *P. paspalicola*. There does appear to be some deposition between the host and intracellular hypha cell wall (arrow)

Fig. 46 B compared with the healthy tissue in Fig. 46 A (toluidine-blue stained cross-section). Disruption of the tissue was partially due to the intracellular penetration of the hyphae (Figs. 47 A-D). The chloroplasts in healthy bundle sheath cells were arranged centrifugally around the perimeter of the cells (Figs. 46 C and Fig. 47 A). However in infected tissue the chloroplasts become randomly dispersed in the bundle sheath cells (Fig. 46 D and Fig. 47 B and D). The chloroplasts in healthy mesophyll (Fig. 48 A) and bundle sheath (Fig. 48 C) cells appeared lens-shaped with well-developed stromal and granal lamellae. However in tarspot-infected tissue, the chloroplast membranes appear to become distorted by large starch grains. Large lipid bodies were also observed, and may cause lamellae disruption, or alternatively these bodies may result from disruption of the lamellae themselves. Often the integrity of the chloroplast membrane was lost (Fig 48 B and D; Fig. 47 D). The host-pathogen interface included the walls of both host and pathogen, with the deposition of some wall apposition between the host cell and fungal cell wall (Fig. 50 B). The intracellular hyphae were loosely surrounded by the invaginated host plasmalemma, and sometimes there appeared to be an electron-dense deposition on the host cell wall around the areas of penetration (Fig. 49 C). The intracellular hyphae at the penetrating site were closely appressed against the host cell walls, and although no wall apposition was apparent between host and pathogen, there did appear to be an electron-dense band between the two cell walls (Fig. 49 D).

4.5 DISCUSSION AND CONCLUSIONS

Even though the precise nature of the lesions on *B. africana* was not established in this study, the destruction of green photosynthetic tissue in the form of localized necrosis has an effect on the cytological features of leaf tissue, and consequently on the physiological properties of *B. africana* leaves.

Many reports have been made on the modifications of cell walls and plasmalemmas in cells infected with viruses. Israel and Ross (1967) suggest that the spread of viruses in hypersensitive hosts is limited by a resistant zone of cells which develops at the periphery of local lesions. Secondary wall thickening, similar

to that observed in TEM micrographs of *B. africana* (Fig. 28 A), has been seen to occur within the resistant zone (Tu and Hiruki, 1971; Wu, 1973). Membrane proliferations of the plasmalemma or endoplasmic reticulum, as detected in *B. africana* (Fig. 28 B, C, and D), has been associated with virus localization (Honda and Matsui, 1974; Shulka and Hiruki, 1975). Despite these suggestions that pathogens such as viruses may induce a hyper-sensitive reaction resulting in local lesion formation and cell wall alterations, many of these host cell reactions are in some cases a general response to injury.

Numerous studies have reported metabolite accumulation around necrotic lesions (Shimomura and Dijkstra, 1975; Stobbs et al., 1977). Fluorescence of substances such as lignin and callose has been detected in many virus-induced lesions and boundary areas. Indeed the results in this study reveal fluorescence in the necrotic and semi-necrotic zones in *B. africana*, although no deposition of callose was evident. Shimomura and Dijkstra (1975) demonstrated the deposition of callose in 'Samsun' tobacco leaves infected with tobacco mosaic virus before actual lesion formation. The fluorescence weakened however with progressive browning of the tissue, and disappeared when the tissue became completely necrotic (3-4 days after inoculation). This disappearance of callose after lesion formation may explain the failure to detect callose in *B. africana* since the tests were carried out on leaves where lesion formation had already been completed. Lignin deposition appears to take place later once the lesions are formed.

Therefore despite the similarity of cellular features in *B. africana* and many virus-infected tissues, it appears that the responses of *B. africana* to necrosis should be regarded, until definite evidence of a virus infection is obtained, as a general hypersensitive reaction of the leaf tissue to injury.

Chloroplast destruction in *B. africana* necrotic tissue may be a consequence of leaf senescence. Alterations in chloroplasts in the semi-necrotic mesophyll cells of *B. africana* such as large

starch grains displacing chloroplast contents (Fig. 29 B, C and D), have been reported by several workers in virus-infected leaves (Sun, 1965; Cohen and Loebenstein, 1975; Tomlinson and Webb, 1978). An increase in the size and number of osmiophilic granules in *B. africana* was also detected. Similar changes have been observed in TMV-infected tobacco leaves (Carroll and Kosage, 1969). However these modifications in chloroplasts do not only occur in virus infections, but also in other pathogen diseases such as rust-infection (Heath, 2974b). Sometimes the changes are a result of general cellular disturbances and are not specific pathogen-induced responses.

The haustoria of *P. digitariae* in *D. eriantha* were similar to most of those described for the uredial stages of rust fungi (Littlefield and Heath, 1979). The host-pathogen interface can be described as the site of contact between a pathogen and the host cell or protoplast. It is important because it is the region of direct interaction between a host and its pathogen and thus is the area through which materials, that elicit responses in either partner, are exchanged (Bracker and Littlefield, 1973). In the case of *P. digitariae*, as with most documented haustoria (Buchnell, 1972), the haustorium appears to be surrounded by the invaginated host plasmalemma, which resembles those described by Littlefield and Bracker (1972). The presence of an extrahaustorial matrix was also detected (Fig. 38 A). There is increasing interest in the role of the extrahaustorial sheath and its bounding membrane in the host-pathogen interaction. Recent evidence suggests that the sheath is of host origin (Manocha, 1975). Littlefield and Bracker (1972) found the sheath membrane to differ structurally and chemically from the host plasmalemma and thus it may be a unique product of the host-pathogen interaction. The sheath membrane has been shown to interact with host cytoplasmic vesicle membranes (Harder, 1978).

The fine-structural response of the host cells of *D. eriantha* to rust-infection exhibited several features reported by other workers (Manocha and Shaw, 1966; Van Dyke and Hooker, 1969) in susceptible plants. A considerable increase in the density of the inter-chromatin and chromatin was noted (Fig. 40 B). These observations have been made in bean leaves infected with *Uromyces fabae* (Abu-Zinada et al.,

1975). This increase in nuclear density could be associated with enhanced protein synthesis as shown by Bhattacharja et al. (1965), in the presporulation stage of infection.

In the current study of *D. eriantha*, chloroplast destruction only took place in the later stages of infection. In agreement with other findings (Van Dyke and Hooker, 1969) the internal lamellar structure was not affected in the earlier stages (3-4 days after inoculation). Disintegration of the thylakoids and increase in the volume of the plastoglobuli were similar to that reported by Mlodzianowski and Siwecki (1975) in *Populus tremula* L. leaves infected with *Melampsora pinitorqua* Braun. Rostr. The distortion of the chloroplast lamellae may be due to the presence of these large lipid bodies. Alternatively the disruption of the lamellae themselves may lead to the accumulation of lipid. The ultrastructural changes in the chloroplasts were generally similar to those that occur following infection of wheat, flax and sunflower by rust fungi (Shaw and Manocha, 1965; Coffey et al., 1972b). Starch appeared to accumulate in chloroplasts in cells penetrated by haustoria, but in the later stages of infection (7-9 days after inoculation) starch was sometimes degraded. This degration could be attributed to fungal enzyme activity, resulting in glyogen formation similar to that observed in rust-infected flax and sunflower.

Unlike the reports of the absence of fine-structural changes in mitochondria in rust-infected mesophyll cells (Abu-Zinada et al., 1975; Mlodzianowski and Siwecki, 1975), appa ent changes in mitochondria were noted in rust-infected cells of *D. eriantha* leaves during the later stages of sporulation (Fig. 41 A-F). In necrotic cells the mitochondria appear to lose their membrane integrity, and in some cells they appear swollen or elongated. It is possible that these features are a consequence of specimen preparation difficulties,

but since all the leaf samples were collectively prepared for TEM in the identical manner, this appears unlikely, the mitochondria as shown in Fig.41F having a normal appearance. T-tests indicated significant differences between the mitochondrial types ($p = 0.05$) and add weight, or support, the hypothesis that these adaptations may be a result of infection.

The elongated appearance of the mitochondria in rust-infected mesophyll cells (Fig.41E) could result from the plane of sectioning, and if viewed from a different plane at 90° to the field of view, may appear round with a small diameter. However, a large number of cells were counted from several leaf samples and analysed statistically. Perhaps, however, closer attention to the plane of sectioning should be given before definite conclusions are made.

Despite negative reports by Abu-Zinda et al. (1975) and Mlodzianowski and Siwecki (1975) degenerative mitochondria have been reported in other diseases such as rice infected with *Cochliobolus miyabeanus* (Horino and Akai, 1968). The swelling of mitochondria in *D. eriantha* may be associated with the stimulated respiratory rates during presporulation which will be discussed later (5.4.1.4).

There appear to be three phases of disease in rust-infected *D. eriantha*. In the first phase (early flecking) the morphology of the cytoplasm and organelles does not differ significantly from that of healthy cells. The second phase (3 days after inoculation until sporulation) is characterized by changes in the fine-structure of the chloroplasts, nuclei and mitochondria. In the third stage of disease (post-sporulation), the mesophyll cells and bundle sheath cells exhibit features of senescence and protoplasm degeneration.

From the electron microscopical studies carried out in this research it appears as if uredospore ontogeny in *P. digitariae* is unusual. The process of spore formation can be termed annellophoric in a sense, although this term is usually restricted to certain conidial formations in the Fungi Imperfecti (Kendrick, 1971). Rajendren (1970) has reported a similar type of uredospore sporogenesis in *Kernkarpella breyiae-patentis*, where the sporogenous tip grows through the old persistent sporophore. Hennen and Figueiredo also reported a spore ontogeny, in *Intrapes paliformis* Hennen & M.B. Figueiredo, gen. nov., resembling that of Rajendren (1970), except that the first spore in *I. paliformis* is produced endogenously. However, these studies were only done at the light microsopical level and it is not possible from other drawings or photographs to establish the exact nature of the new sporogenous cell growth. According to Rajendren's study the sporogenous cell apex extends distally. However, in this case of *P. digitariae*, the extension does not necessarily involve the sporogenous cell apex (septum exposed by spore abscission), but involves new wall growth from the inner sporogenous cell wall, pushing the half septum laterally. This type of uredospore ontogeny has not been reported, although Rijkenberg and Truter (1974) have shown that pycnial ontogeny of *Puccinia sorghi* is annellophoric. It would be preferable to call the old sporophore walls 'collars' rather than annellations since this term is usually used in conjunction with conidia. According to the terminology (Kendrick, 1971) an annellophore (or annellate conidi-

ogenous cell) is 'typically a conidiogenous cell producing a single terminal blastic con idium and by percu rent vegetative proliferations (annellations) a succession of similar conidia'. An annellation is 'a ring-like or cylindrical portion of an annellide produced between successive conidia'. The successive formation of 'collars' or old sporophore walls hardly fits this description.

The interaction of *P. paspalicola* with host plants has not been studied at the TEM level in the past, and it was interesting to observe some similar features in the interface between this fungus and leaf cells of *P. maximum* and the haustorial penetration into mesophyll cells of *D. eriantha*. The feeding structures of both rust and tarspot are intracellular, although less specialization of the intracellular hyphae occurs in the case of *P. paspalicola* compared to specialization of haustorial structures in *P. digitariae*. The presence of an electron dense layer at the site of penetration of intracellular structures (Fig. 49 D) is similar to the mucilagenous layer between the haustorial mother cell and host cell wall in wheat infected with *Puccinia graminis*. Tarspot hyphae penetrate in a similar manner to rust hyphae in that the hyphal tips swell in the manner of appressoria when in contact with a host cell wall, and constrict to form a slender hypha (as fine as an infection peg in rusts) which penetrates the cell wall and swells again on the other side of the newly invaded cell.

Although the intracellular hyphae of tarspot are surrounded by the invaginated host-plasmalemma and some wall apposition between the fungal and host wall exists, the extrahaustorial sheath of rust haustoria and their close association with cellular organelles seem more highly specialized than in the case of tarspot.

Unlike the rust uredosori which develop from sporogenous or basal cells in the fertile layer, hyphae of tarspot invade epidermal cells, laying the foundation of the clypeus which develops independently of the perithecium (Fig. 12 C). The perithecium of *P. paspalicola* is initiated from the dense mass of intercellular hyphae. As these intercellular hyphae become densely packed so

the mesophyll cells lose their identity so that in some areas they appear to contain only fungal tissue. In this study disruption of the chloroplasts and cellular disorganization in tarspot-infected leaf tissue is considerable once the perithecia have been formed and is similar to those changes observed in rust-infected *D. eriantha*. These changes were only observed in the clypeus and adjacent leaf tissue of *P. maximum* whereas leaf tissue away from the areas of fungal invasion appeared normal.

Several of these ultrastructural modifications can be associated with physiological disturbances in leaf tissue. In the following chapter some of the implications of organelle alterations will be discussed. The host-parasite interaction of *P. maximum* and *P. paspalicola* is of special interest since it has not been studied previously and comparisons with the more severe rust disease of *D. eriantha* will prove informative since tarspot has in the past been neglected since it is considered to be economically unimportant (Parbery, 1967).

EPIDEMIOLOGICAL, MORPHOLOGICAL, AND PHYSIOLOGICAL STUDIES OF SELECTED PLANT DISEASES AT NYLSVLEY

Marie Emma Christine Rey

Volume II

A THESIS SUBMITTED TO THE FACULTY OF SCIENCE, UNIVERSITY OF THE WITWATERSRAND, JOHANNESBURG, IN FULFILMENT OF THE REQUIREMENTS FOR THE DEGREE OF DOCTOR OF PHILOSOPHY.

July, 1982

Volume II

PART II OF TWO VOLUMES

This thesis is presented in two volumes.

Volume I contains Chapters one, two, three and four; Tables 1-9; Figures 1-50 and A-J

Volume II contains Chapters five, six, and seven; the references; Tables 10-25; Figures 51-114

TABLE OF CONTENTS

	PAGE
CHAPTER FIVE PHYSIOLOGY	136
5.1 LITERATURE REVIEW	136
1.1 General introduction	136
1.2 Fungal physiology	137
1.3 Photosynthetic and respiratory metabolism	138
1.3.1 Photosynthesis	138
1.3.2 C_4 photosynthesis	141
1.3.3 Chlorophyll	142
1.3.4 Respiration	143
1.4 Nitrogen metabolism	145
1.4.1 Total nitrogen and nitrates	145
1.4.2 Nitrogen metabolism, photosynthesis and photo-respiration	148
5.2 AIMS	150
5.3 METHODS	150
3.1 Photosynthesis	150
3.1.1 Gross photosynthesis	150
3.1.2 Net photosynthesis	155
3.1.3 Photosynthetic enzymes	163
1.3.1 Enzyme extraction	163
1.3.2 Ribulose - 1.5 - biphosphate carboxylase *in vitro* assay	163
1.3.3 Phosphoenolpyruvate carboxylase	166
1.3.4 NADP and NAD-malic dehydrogenase	166
1.3.5 NADP and NAD-malic enzyme	166
1.3.6 Alanine aminotransferase and aspartate amino transferase	166
1.3.7 Phosphoenolpyruvate carboxykinase	167
1.3.8 Chlorophyll	167
3.1.4 Respiration	167
1.4.1 Dark respiration	167
1.4.2 Succinate dehydrogenase	168
3.1.5 Chlorophyll	168
5.3.2 Nitrogen metabolism	168
3.2.1 Nitrates	168
3.2.2 Total nitrogen	170

PAGE

5.4 RESULTS 170
5.4.1 Photosynthesis and respiration 170
4.1.1 Gross photosynthesis 170
4.1.2 Net photosynthesis 179
4.1.3 C_4 photosynthetic enzymes 183
4.1.4 Respiration 190
1.4.1 Dark respiration 190
1.4.2 Succinate and NAD-malate dehydrogenase 190
4.1.5 Chlorophyll 194
5.4.2 Nitrogen metabolism 202
4.2.1 Nitrates 202
4.2.2 Total nitrogen or crude protein 202
5.4.3 Estimation of the overall effect of pathogens on primary productivity of the grass layer 210
5.4.4 Biomass 216
5.5 DISCUSSION 217

CHAPTER SIX 230
6.1 LITERATURE REVIEW 230
1.1 Nutrients and plant disease 230
1.2 Methodology 232
6.2 AIMS 234
6.3 MATERIALS AND METHODS 234
3.1 Autoradiography 234
3.1.1 Feeding leaves with D-(6-^{3}H) glucose before spore inoculation 234
3.1.2 Feeding leaves with labelled glucose after infection 236
3.2 Sugar analysis 236
3.2.1 Extraction procedure 236
3.2.2 Sugar detection 237
3.3 Staining procedures 239
6.4 RESULTS 241
4.1 Autoradiography 241
4.1.1 Feeding *D. eriantha* leaves with D-(6-^{3}H) glucose before spore inoculation 241
4.1.2 Feeding *D. eriantha* leaves, exhibiting mature pustules with ^{3}H-glucose 252

PAGE

4.2 Sugar analysis 252
6.5 DISCUSSION 259

CHAPTER SEVEN FINAL DISCUSSION 266
7.1 General discussion 266
1.1 Identification of pathogens 266
1.2 Epidemiology 266
1.3 Ultrastructural studies 267
3.1 Morphological changes 267
3.2 Uredospore ontogeny 269
1.4 Photosyhthesis and related processes 270
1.5 Nitrogen metabolism 272
1.6 Sugar analysis 272
1.7 Autoradiography 273
7.2 A perspective of plant disease in a natural ecosystem .. 274
2.1 Introductory note 274
2.2 Co-evolution of the rusts 274
2.3 Photosynthesis, primary production and pathogens ... 278
7.3 Concluding remarks 281

FIGURE INDEX

Fig. 51 Scheme illustrating the proposed reaction of the three types of C_4 pathways. 153

Fig. 52 Shimshi apparatus for measuring photosynthesis. 154

Fig. 53 Cuvette for holding leaf specimens 154

Fig. 54 Resporse of gross photosynthesis to $^{14}CO_2$ exposure time. 157

Fig. 55 Open-system used to measure net photosynthesis using an Infra Red Gas Analyser. 158

Fig. 56 Response of gross photosynthesis to radiation. 159

Fig. 57 Resistance (secs cm^{-1}) vs. time (secs). 160

Fig. 58 Leaf temperature correction factor for resistance. 160

Fig. 59 Daily photosynthetic run of *D. eriantha* taken from 7.30 a.m. through to 4.30 p.m. 161

		PAGE
Fig. 60	Daily photosynthetic run of *P. maximum* taken from 8.00 a.m. tnrough to 5.00 p.m.	162
Fig. 61	Response of increasing CO_2 flow rates on CO_2 efflux which was passed through leaf chamber.	164
Fig. 62	Diagram of the open system used to measure the effect of increasing CO_2 concentration on net photosynthesis in healthy and rust-infected *D. eriantha* leaves.	165
Fig. 63	Standard curve for nitrate (µmoles KNO^{-3}) measurements.	169
Fig. 64	Gross photosynthetic rates of necrotic and non-necrotic *B. africana* leaves (1978/79).	172
Fig. 65	Gross photosynthetic rates of necrotic and non-necrotic *B. africana* leaves (1979,80).	172
Fig. 66	Gross photosynthesis in healthy and rust-infected *D. eriantha* leaves (1978/79).	175
Fig. 67	Gross photosynthesis in healthy and tarspot-infected *P. maximum* (1978/79).	175
Fig. 68	Gross photosynthesis in healthy and rust-infected *D. eriantha* leaves (1979/80).	176
Fig. 69	Gross photosynthesis rates in healthy and rust-infected *D. eriantha* (1980/81).	176
[illegible]	Gross photosynthesis in healthy and tarspot-infected *P. maximum* leaves (1979/80 and 1980/81).	178
[illegible]	Net photosynthetic rates of healthy and rust-infected *D. eriantha* leaves (1980/81 and 1981/82).	131
[illegible]	Response of healthy and rust-infected *D. eriantha* leaves to increasing CO_2 concentrations.	182
[illegible]	Dark respiration rates measured in healthy and rust-infected *D. eriantha* leaves (1981/82).	185
[illegible]	Net photosynthesis in healthy and tarspot-infected *P. maximum* leaves (1981/82).	185
Fig. 74	C4 photosynthetic enzymes (RuBP carboxylase; PEP carboxylase; NADP-malic enzyme and NADP-malate dehydrogenase) in healthy and rust-infected *D. eriantha* leaves (1980/81).	187

PAGE

Fig. 75 C_4 photosyntnetic enzyme activities (PEP carboxykinase; Aspartate aminotransferase and Alanine aminotransferase) in healthy a rust-infected *D. eriantha* leaves (1980/8 .

Fig. 76 C_4 photosynthetic enzyme activities (RuBP PEPC; NADP-ME and NADP-malic dehydrogena in healthy and rust-infected leaves (1981/82).

Fig. 77 C_4 photosynthetic enzyme activities PCK; Aspartate aminotransferase and Alanine am transferase) in healthy and rust-infecte *D. eriantha* leaves (1981/82).

Fig. 78 C_4 photosynthetic enzyme act vit es NADP-ME and NADP-malic dehydrogenase healthy and tarspot-infected leaves (1980/81).

Fig. 79 C_4 photosynthetic enzyme in healthy and tarspot-infected *P. maximum* (1980/81), and the dark respiration enzymes NAD-malate dehydrogenas and succinate dehydrogenase.

Fig. 80 Dark respira ion enzyme activities (succ dehydrogenase and NAD-malate dehydrogenase in healthy and rust-infected leaves (1980/81).

Fig. 81 Dark respirat.on enzyme activities (succinate dehydrogenase and NAD-malate dehydrogenase in healthy and rust-infected *D. eriantha* leaves (1981/82).

Fig. 82 Chlorophyll content of necroti and non-necrot *B. africana* leaves (1978/79).

Fig. 83 Chlorophyll content of necrotic and non-necrot *B. africana* leaves (1979/80).

Fig. 84 Chlorophyll content of healthy and rust-infecte *D. eriantha* leaves (1979/80). 20

Fig. 85 Chlor phyll a . b ratio in healthy and rust- nfecte *D. eriantha* leaves (1980/81).

Fig. 86 Chlorophyll content of healthy and tarspot-inf ted *P. maximum* leaves.

Fig. 87 Nitrate measurements in healthy and rust- nfected *D. eriantha* leaves (1981/82).

Fig. 88 Nitrate measurements in healthy and tarspot-infected *P. maximum* leaves (1981/82).

		PAGE
Fig. 89	Total nitrogen content of necrotic and non-necrotic *B. africana* leaves.	209
Fig. 90	Total nitrogen content of healthy and rust-infected *D. eriantha* leaves (1979/80).	213
Fig. 91	Total nitrogen content of healthy and rust-infected *D. eriantha* leaves (1980/81).	213
Fig. 92	Total nitrogen content of healthy and tarspot-infected *P. maximum* leaves (1979/80).	214
Fig. 93	Total nitrogen content of healthy and tarspot-infected *P. maximum* leaves (1980/81).	214
Fig. 94	Photosynthetic model of the host-parasite system of *D. eriantha* - *P. digitariae* prior to and at the time of sporulation.	220
Fig. 95	Diagram of the High Pressure Liquid Chromatography system employed to separate sugars.	238
Fig. 96A	Transverse section (LM) through a *D. eriantha* leaf 4 after uredospore inoculation.	243A
Fig. 96B	Germinating uredospore on leaf surface.	243B
Fig. 97	Aniline blue-safranin stained transverse section through *D. eriantha* leaf tissue 21h after uredospore inoculation.	244
Fig. 98	Penetration of rust fungus occurring directly through the epidermis.	244
Fig. 99	Penetration of epidermal cells by *P. digitariae*.	245
Fig. 100	Penetration peg from the epidermis into the intercellular space below.	245
Fig. 101	Penetration through stomata of *D. eriantha* by *P. digitariae*.	246
Fig. 102	Malachite green-acid fuchsin-martius yellow stained section through *D. eriantha* leaf tissue.	246
Fig. 103	Transverse section through *D. eriantha* leaf tissue depicting the infection hyphae closely adhering to host mesophyll.	247
Fig. 104	Suspected haustoria staining red/brown with toludine blue-safranin stain.	247
Fig. 105 A-C	Phase contrast autoradiographs of transverse sections through *D. eriantha* fed with labelled glucose.	248

		PAGE
Fig. 89	Total nitrogen content of necrotic and non-necrotic *B. africana* leaves.	209
Fig. 90	Total nitrogen content of healthy and rust-infected *D. eriantha* leaves (1979/80).	213
Fig. 91	Total nitrogen content of healthy and rust-infected *D. eriantha* leaves (1980/81).	213
Fig. 92	Total nitrogen content of healthy and tarspot-infected *P. maximum* leaves (1979/80).	214
Fig. 93	Total nitrogen content of healthy and tarspot-infected *P. maximum* leaves (1980/81).	214
Fig. 94	Photosynthetic model of the host-parasite system of *D. eriantha* - *P. digitariae* prior to and at the time of sporulation.	220
Fig. 95	Diagram of the High Pressure Liquid Chromatography system employed to separate sugars.	238
Fig. 96A	Transverse section (LM) through a *D. eriantha* leaf 4h after uredospore inoculation.	243A
Fig. 96B	Germinating uredospore on leaf surface.	243B
Fig. 97	Aniline blue-safranin stained transverse section through *D. eriantha* leaf tissue 21h after uredospore inoculation.	244
Fig. 98	Penetration of rust fungus occurring directly through the epidermis.	244
Fig. 99	Penetration of epidermal cells by *P. digitariae*.	245
Fig. 100	Penetration peg from the epidermis into the intercellular space below.	245
Fig. 101	Penetration through stomata of *D. eriantha* by *P. digitariae*.	246
Fig. 102	Malachite green-acid fuchsin-martius yellow stained section through *D. eriantha* leaf tissue.	246
Fig. 103	Transverse section through *D. eriantha* leaf tissue depicting the infection hyphae closely adhering to host mesophyll.	247
Fig. 104	Suspected haustoria staining red/brown with toludine blue-safranin stain.	247
Fig. 105 A-C	Phase contrast autoradiographs of transverse sections through *D. eriantha* fed with labelled glucose.	248

		PAGE
Fig. 106 A-C	Dark field autoradiographs. A. Low power of ^{3}H-glucose labelled rust-infected *D. eriantha*. B. Labe in healthy leaf tissue. C. Control leaf tissue fed with unlabelled glucose.	249
Fig 107 A	LM autoradiograph of rust-infected *D. eriantha* leaves, exhibiting intense label accumulation in mesophyll cells. B. Incorporation of ^{3}H-glucose into fungal haustoria and haustorial walls.	250
Fig. 108	Dark field autoradiographs. A. Label accumulates intensely in mesophyll cells in areas of rust-infection. B. ^{3}H-glucose incorporated into suspected fungus haustorial cell walls.	251
Fig. 109 A	LM autoradiograph illustrating the intense silver grains in infection hyphae of *P. digitariae*. B. Incorporation of ^{3}H-glucose in infection peg and sub-stomatal vesicle in rust-infected tissue.	
Fig. 110	A and B. Dark field autoradiographs of sections through penetrating structures of *P. digitariae* infecting *D. eriantha*.	
Fig. 111 A-C	Phase contrast autoradiographs of rust-infected *D. eriantha* leaves fed with ^{3}H-glucose.	255
Fig. 112 A	Dark field autoradiograph of rust pustule fed with ^{3}H-glucose, with a few silver grains in the uredospore. B. Healthy *D. eriantha* leaf tissue showing greater incorporation into mesophyll and vascular bundle cells.	256
Fig. 113	Sugar content of healthy and rust-infected *D. eriantha* (1981/82).	258
Fig. 114	Sugar content of healthy and tarspot-infected *P. maydis* (1981/82).	258

LIST OF TABLES

PAGE

10. Gross photosynthetic rates of *B. africana* (1978/79 and 1979/80 seasons). 171
11. Gross photosynthetic rates of healthy and rust-infected *D. eriantha* and healthy and tarspot-infected *P. maximum* (1978/79). 173
12. Gross photosynthetic rates of healthy and rust-infected *D. eriantha* (1979/80 and 1980/81). 174
13. Gross photosynthetic rates of healthy and tarspot-infected *P. maximum* (1979/80 and 1980/81 season). 177
14. Net photosynthetic rates and dark respiration of healthy and rust-infected *D. eriantha* (1980/81;1981/82). 180
15. Net photosynthetic rates of healthy and tarspot-infected *P. maximum* (1981/82). 184
16. C_4 photosynthetic and respiration enzymes in healthy and rust-infected *D. eriantha* (1980/81;1981/82 season). 186
17. C_4 photosynthetic and respiration enzyme activities of healthy and tarspot-infected *P. maximum* (1980/81). 191
18. Chlorophyll content of *B. africana* leaves (1978/79 and 1979/80 season). 197
19. Chlorophyll content of healthy and rust-infected *D. eriantha* (1979/80;1980781) and chlorophyll a:b ratios (1979/80). 200
20. Chlorophyll content of healthy and tarspot-infected *P. maximum* and chlorophyll a:b ratios (1979/80). 204
21. Nitrates in healthy and infected leaves of *D. eriantha* and *P. maximum* (1981/82 season). 206
22. Percentage total nitrogen of healthy and necrotic *B. africana* leaves (1979/80). 208
23. Percentage total nitrogen of healthy and rust-infected *D. eriantha* leaves (1979/80 and 1980/81 seasons). 211
24. Percentage total nitrogen in healthy and tarspot-infected *P. maximum* leaves (1979/80 and 1980/81 seasons). 212
25. Average percentage sugar content of healthy and fungal-infected leaves of *D. eriantha* and *P. maximum* (1981/82). 257

APPENDIX 282b

LIST OF ABBREVIATIONS

ADP - adenosine 5' - diphosphate
ATP - adenosine 5' - triphosphate
BSA - Bovin Serum Albumin
C - carbon
chl - chlorophyll
CO_2 - carbon dioxide
DTT - dithiothrietol
EDTA - ethylenediaminotetraacetic acid
g - gram
h - hour
H_2O - water
IRGA - Infra Red Gas Analyser
kPa - kiloPascals
l - litre
LM - light microscopy
m - metre
M - molar
MAX - maximum
mb - millibars
MIN - minimum
min - minute
mCi - milliCurie
ME - malic enzyme
mE m^{-2} s^{-1} - micro-Einsteins metre^{-2} sec^{-1}
mg - milligram
$MgCl_2$ - magnesium chloride
ml - millilitre
mM - millimolar
$MnCl_2$ - manganese chloride
N - nitrogen
NAD - nicotinamide adenine dinucleotide
NADH - reduced nicotinamide adenine dinucleotide
NAD-MΔ - NAD-malic dehydrogenase

NADP - nicotinamide adenine dinucleotide phosphate
NADPH - reduced nicotinamide adenine dinucleotide phosphate
NH_4^+ - ammonium
nm - nanometre
NO_2^- - nitrite
NO_3^- - nitrate
O - oxygen
OAA - oxaloacetic acid
PCK - PEP caryboxykinase
PEP - phosphoenolpyruvate
PEPC - PEP carboxylase
PPO - 2,5-Diphenyloxazole
POPOP - 1,4-bis-2-(-5-phenyloxazdyl)-benzene
3-PGA - 3-phosphoglyceric acid
ppm - parts per million
RH - relative humidity
RuBP - ribulose-1-5-biphosphate
RuBPC - RuBP carboxylase
SEM - scanning electron microscopy
SVPD - saturation vapour pressure deficit
Tricine - N-tris (hydroxymethyl)methyl-glycine
T^o - temperature
TEM - transmission electron microscopy
Tris - Tris (hydroxymethyl)aminomethane
µCi - microCuries
µ - micro
µl - micolitre
µm - micrometre
v/w - volume per weight
x g - revolutions per minute

5. CHAPTER FIVE PHYSIOLOGY

5.1 LITERATURE REVIEW

1.1 General introduction

Infections of plants by viruses, fungi or bacteria usually bring about changes in biochemical and morphological processes in their hosts. Foliar diseases of forage crops occur worldwide and are a major factor contributing to poor quality forage (Hanson, 1965). Similarly it may be predicted that foliar diseases could influence the nutritional quality of important feeding plants in a natural ecosystem which supports a number of grazing herbivores. From an ecological standpoint pathogens may act as consumers utilizing part of the energy fixed by plants and thus accelerate the cycling of minerals in the system. Viruses and fungi are able to alter the rates of production processes such as photosynthesis and respiration, and the rate of transfer of standing live to standing dead biomass (Bollard and Matthews, 1953). As well as reduced rates in photosynthesis, chlorophyll content is also affected (Singh and Gupta, 1975), as are protein synthesis and transpiration rates (Hussain and Kelman, 1959). Plants infected by different pathogens often exhibit similar physiological symptoms, and sometimes some of the gross changes in physiological processes represent a non-specific response to cellular damage. On the other hand a number of responses are specific reactions to pathogens which may produce toxins, or induce host responses in a specific manner.

The rusts (Uredinales) and powdery mildews (Erysiphaceae) include the causal organisms of many of the most important plant diseases (Shaw, 1967). Cereal plants infected with rusts and mildews have reduced root growth and grain yield (Doodson et al. 1964; Large, 1966). Nutrient movement is one of the processes which rusts can influence to a large extent. In rusted bean plants for example it appears that nutrients are translocated from younger uninfected leaves to infected leaves (Zaki and Durbin, 1965; Livne and Daly, 1966). Host nutrients accumulate at the sites of infection assuring that these obligate parasites have an adequate supply of nutrients for their

development (Shaw and Samborski, 1956; Johnson et al., 1966). In contrast non-infected plants exhibit a flow of sugars and amino acids from mature to younger developing parts of the plant. Since rusts develop as local infections, the ratio of invaded to uninvaded host tissue changes progressively as the parasite develops and also varies with the frequency of infections (Shaw, 1967). When the frequency is low, localized physiological changes may be so diluted as to be undetectable if measurements are made on entire leaves. Even though infections are localized, substances emanating from them may alter the physiology of the entire plant.

1.2 Fungal physiology

Fungal structures such as mycelia and spores are able to metabolize some of their own nutrients, whereas other nutrients have to be obtained from the host. Fungi are capable of excreting activators of host enzymes, as well as excreting starch hydrolyzing enzymes (Scott, 1972). Host sugars are taken up by rust fungi and converted to polyols after uptake (Livne, 1964; Smith et al., 1969). Hexoses such as glucose and fructose are taken up by rust fungi and converted in compounds such as chitin, fatty acids and glucomannon, whilst amino acids are also absorbed by fungal mycelia although some are synthesized by the fungi themselves. Howes and Scott (1972) have shown that axenic cultures of wheat - stem rust fungus can synthesize glutamic acid, lysine and arginine from glucose. Reisener et al., 1970 (in Burrell and Lewis, 1977) have shown that 70 percent of the alanine of the spores is synthesized by the mycelium from glucose obtained from the host. Uredospores have a complement of enzymes for intermediary metabolism (Staples and Wynn, 1965). Trehalose and other sugar alcohols, are characteristic fungal components (Prentice and Cuendet, 1954) together with sugars, free and protein amino acids, fatty and organic acids, and most of the intermediates of the tricarboxylic acid (TCA) cycle except α-Ketoglutaric dehydrogenase, (McKillican, 1960, Tulloch, 1960. Staples et al., 1962). There is also evidence for the presence of all the enzymes of the Embden - Meyerhof-Parnas (EMP) Pathway except pyruvic dehydrogenase and all those of the pentose phosphate pathway (PPP) (Caltrider and Gottlieb, 1963). The key enzymes of the glyoxylate cycle, isocitratase and malate synthetase are also present

development (Shaw and Samborski, 1956; Johnson et al., 1966). In contrast non-infected plants exhibit a flow of sugars and amino acids from mature to younger developing parts of the plant. Since rusts develop as local infections, the ratio of invaded to uninvaded host tissue changes progressively as the parasite develops and also varies with the frequency of infections (Shaw, 1967). When the frequency is low, localized physiological changes may be so diluted as to be undetectable if measurements are made on entire leaves. Even though infections are localized, substances emanating from them may alter the physiology of the entire plant.

1.2 Fungal physiology

Fungal structures such as mycelia and spores are able to metabolize some of their own nutrients, whereas other nutrients have to be obtained from the host. Fungi are capable of excreting activators of host enzymes, as well as excreting starch hydrolyzing enzymes (Scott, 1972). Host sugars are taken up by rust fungi and converted to polyols after uptake (Livne, 1964; Smith et al., 1969). Hexoses such as glucose and fructose are taken up by rust fungi and converted in compounds such as chitin, fatty acids and glucomannan, whilst amino acids are also absorbed by fungal mycelia although some are synthesized by the fungi themselves. Howes and Scott (1972) have shown that axenic cultures of wheat - stem rust fungus can synthesize glutamic acid, lysine and arginine from glucose. Reisener et al., 1970 (in Burrell and Lewis, 1977) have shown that 70 percent of the alanine of the spores is synthesized by the mycelium from glucose obtained from the host. Uredospores have a complement of enzymes for intermediary metabolism (Staples and Wynn, 1965). Trehalose and other sugar alcohols, are characteristic fungal components (Prentice and Cuendet, 1954) together with sugars, free and protein amino acids, fatty and organic acids, and most of the intermediates of the tricarboxylic acid (TCA) cycle except α-Ketoglutaric dehydrogenase, (McKillican, 1960, Tulloch, 1960, Staples et al., 1962). There is also evidence for the presence of all the enzymes of the Embden - Meyerhof-Parnas (EMP) Pathway except pyruvic dehydrogenase and all those of the pentose phosphate pathway (PPP) (Caltrider and Gottlieb, 1963). The key enzymes of the glyoxylate cycle, isocitratase and malate synthetase are also present

(Frear and Johnson, 1961). Studies on the metabolism of ^{14}C - labelled substrates emphasize the importance of the PPP and glyoxylate cycle, as the latter may function in the conversion of fat to carbohydrate in germinating uredospores. Carbohydrates (Gottlieb and Caltrider, 1962) and chitin (Shu et al. 1954) are the major components synthesized during germination. White and Ledingham (1961) have shown the cytochrome system to be present in fungi. Even though obligate parasites such as the rusts do possess most physiological processes, certain substances are nevertheless essential for growth and development. Uredospores for example are unable to utilize exogenous substrates at rates approaching those of saprophytic fungi. A stimulation of certain metabolic processes is achieved only from the interaction of the parasite with a susceptible host.

1.3 Photosynthetic and respiratory metabolism

1.3.1 Photosynthesis

Any pathogen which attacks green aerial tissue is likely to affect crop yield in some form or the other (Shaw, 1963). In a susceptible host some parasites including the rust fungi, develop vigorously sporulating pustules with a minimum of necrosis before sporulation. There is however an early chlorosis at infection sites which produces a characteristic yellow flecking, but later on the retention or resynthesis of chlorophyll surrounding the infection sites results in the formation of 'green islands'. Photosynthesis may in some cases be stimulated in the early stages of infection to supply substances for the parasite but eventually decreases due to chlorosis and senescence of the leaves (Doodson et al. 1975). The remaining leaf tissue can in some instances have an enhanced photosynthetic efficiency to compensate for loss in area eg. *Botrytis* on bean leaves (Dickinson and Lucas, 1977). Changes in photosynthesis in rust - infected leaves have been studied by many workers (Livne, 1964; Doodson et al. 1965; Edwards, 1970). They have shown that overall photosynthetic activity declines in infected leaves at the later stages of infection. Raggi (1978) for example demonstrated a decrease in photosynthesis in the primary leaves of Pinto III bean leaves infected with *Uromyces appendiculatus* var. typica. Raggi (1980) demonstrated an increase in the CO_2 compensation point in rust infected bean leaves from the

flecking stage to reach a maximum at the sporulation stage. The increase in the CO_2 compensation point was accompanied by an increase in respiration and progressive decrease in photosynthesis. Ragg suggests however that photorespiration did not contribute to the increase in the CO_2 compensation point, and that the CO_2 output in the light seemed to be mainly a mitochondrial process, since the release of CO_2 in healthy compared to infected leaves in the light was unaffected by increasing the O_2 concentration from 0 percent to 20 percent.

Initial stimulation of photosynthesis in plants during the early stages of rust and mildew infections has been noted by several workers (Livne, 1964; Scott and Smillie, 1966). Edwards (1970) detected a stimulation in photosynthesis in mildew infected barley, at high CO_2 concentrations up to 60h after inoculation. This observation raises the important question as to why photosynthesis is apparently stimulated in infected leaves at high CO_2 concentrations. Two possibilities exist, first that glycollate metabolism may be impaired in infected leaves especially at high CO_2 concentrations thus giving an apparent increase in photosynthesis and second, that the fungus causes partial closure of stomata which at high CO_2 concentrations would have little effect on the rate of photosynthesis. Mitchell (1979) found the rate of apparent photosynthesis and chlorophyll content declined progressively three days after inoculation of wheat cv. Little Club with *Puccinia graminis* f. sp. tritica Eriks. & Henn. Dark respiration increased during late flecking and sporulation on rust-infected first leaves whereas there were no differences in rates of photorespiration between healthy and infected leaf tissues. The rates of apparent photosynthesis expressed on a chlorophyll basis showed a small decline in activity in infected leaves compared with healthy. Since the differences in combined photorespiration and dark respiration between healthy and infected leaves during sporulation were less the 0.96mg $CO_2 dm^{-2} h^{-1}$, Mitchell concludes that the rise in respiratory activity would not have caused an appreciable depression of photosynthetic activity. These results provide evidence that infection by a biotrophic pathogen may directly influence the carbon cycle or dark reaction of photosynthesis. Studies of

carbon relations of many rusts and powdery mildew infection have shown that the carbon available to the parasite for its growth and sporulation may be increased by stimulation of host photosynthesis (Yarwood, 1967) and higher carbon fixation in the dark (Zaki and Mirocha, 1964). A fine balance is achieved between obligate parasite and host, as opposed to non-obligate parasite infections where chlorophyll in leaves and photosynthesis decline rapidly. For its survival, the pathogen must reproduce as prolifically as possible before death of the colonized tissue. In the case of maize leaves infected with *Helminthosporium carbonum* Ullstrup for example, the conversion of ribose 5-phosphate to ribulose -1,5-biphosphate (RuBP) is stimulated until the appearance of symptoms (Malca, et al., 1964) and fixation in the dark may increase (Kuo and Scheffer, 1970). However this is not always the case. Malca and Zscheile (1963) demonstrated a reduction in phosphoenolpyruvate (PEP) carboxylase activity and malic acid content in corn seedlings infected with *Helminthosporium* leaf spot disease, and Rowe and Reid (1979a) showed a decline in RuBP carboxylase (RuBPC) activity per milligram protein in a susceptible barley variety infected with *Helminthosporium teres*. They also demonstrated an increase in PEP carboxylase activity as infection developed and contrary to Malca and Zscheile (1963) they found an increase in malic enzyme activity as early as 24h after inoculation, while at seven days the activity was three to four times that of controls. In comparison. the resistant barley variety (C.I. 5791) exhibited stimulated CO_2 fixation, PEP carboxylase and malic enzyme activity and a decline in RuBPC activity only at 24h after inoculation. As the infection progressed the differences between healthy and infected plants diminished. Changes in fixation patterns may be explained on the basis of changes in relative levels of substrates and co-factors in infected tissue, especially those shared by the photosynthetic and non-photosynthetic carbon fixation pathways e.g. PEP and intermediates such as the dicarboxylic acids (Daly and Krupka, 1962; Livne and Daly, 1962). There could also be additional demands on existing substrate pools e.g. ribose-5-phosphate levels (a precursor of RuBPC) might be depleted by increased nucleotide synthesis (Whitney et al., 1962). Such changes could be either pathogen mediated, a host mediated response to pathogenesis or a function of the

host-parasite interaction. In barley infected with *Helminthosporium teres*, quantitative analysis of the early products of $^{14}CO_2$ fixation in the light indicated that carbon entered predominantly via the Calvin cycle in infected and healthy plants, but in susceptible infected plants β-carboxylation increased (Rowe and Reid, 1979a). Increased β- carboxylation could result in the replenishment of pools of acid intermediates depleted by the increased synthetic activity. Increases in malic enzyme and PEP carboxylase activity were also demonstrated by Rowe and Reid (1979a) in *Helminthosporium teres* - infected barley. Since both the host and pathogen contained an active malic enzyme, they might contribute components to a combined enzyme system peculiar only to the host-parasite complex. Host involvement is indicated by changes in enzyme activity outside the vicinity of the fungus. Both a fungal and stimulated host malic enzyme were found to be involved in the enhanced β-carboxylation in rusted tissue (Rick and Mirocha, 1968). The increase in PEP carboxylase was less localized in *Helminthosporium* - infected barley, and since stimulation occurred in uninvaded tissue of point-inoculated leaves it appears as if the increase is more a result of host stimulation than a co-operative effect between the enzymes of host and parasite. Changes in translocation patterns may influence the net carbon accumulation in infected plants. Rowe and Reid (1979b) demonstrated that the amount of carbon fixed in the dark, although showing a fourfold increase in infected compared to healthy leaves, did not compensate for the reduction in photosynthetically fixed carbon in the light period. Products of fixation were largely retained by the infected leaf rather than transported to other healthy parts. This retention of photosynthate by infected leaves, may bring about reductions in the photosynthetic rate by feedback mechanisms (Durbin, 1967). In monocotyledons the translocation stream is not as readily interrupted as in dicotyledons (Edwards, 1971).

1.3.2 C_4 photosynthesis

The requirement for energy by plants from photochemical reactions for carbon assimilation depends on the pathway of carbon flow from CO_2 to organic products. In C_3 plants atmospheric CO_2 is fixed directly through the Calvin - Benson pathway with all the reactions of the pathway occurring in a common chloroplast type in the leaf mesophyll

cells (Edwards et al., 1970). However in C_4 plants (species having Kranz anatomy ie. with a bundle sheath around the vascular tissue) both the C_4 pathway and Calvin Cycle exist, whereby O_2 inhibition of photosynthesis is eliminated. The C_4 pathway shuttles CO_2 from the atmosphere to the Calvin - Benson pathway (Black, 1973; Hatch, 1971). In addition different types of C_4 pathways exist in various C_4 species, based on differences in the mechanism of decarboxylation of C_4 acids (Fig. 51). C_4 acids may be decarboxylated through NADP-malic enzyme (NADP - ME), NAD-malic enzyme (NAD - ME) or phosphoenolpyruvate carboxykinase (PCK) (Gutterrez et al., 1974; Hatch et al., 1975). Both *D. eriantha* and *P. maximum* are C_4 plants (Ellis, 1977). *D. eriantha* belongs to the NADP - ME group where malate is the principle acid formed. *D. eriantha* has a single bundle sheath, and the chloroplasts lack well developed grana and are centrifugally arranged. This grass is suspected to be a PCK type. *P. maximum* on the other hand is a PCK type where aspartate is chiefly formed. The bundle sheath is double, and the chloroplasts have well-developed grana and are centrifugally arranged. There is evidence that partitioning occurs with PEP carboxylase being confined to the mesophyll cell chloroplasts and malate and asparatate being transported to the bundle sheath chloroplasts where they are decarboxylated. The CO_2 released is refixed via RuBP carboxylase in the Calvin Cycle (Slack et al., 1969; Kanai and Edwards, 1973; Ku et al., 1974). Another theory is that primary carboxylation occurs in the mesophyll cytoplasm whilst the Calvin Cycle is localized in the mesophyll chloroplasts, and bundle sheath chloroplasts store starch formed from sugars produced in the mesophyll chloroplasts (Baldry et al., 1971; Coombs, 1976).

1.3.3 Chlorophyll

Decreases in photosynthesis later on in infection can also be attributed to changes in organelle structures. Cytological studies of wheat leaves have shown that the size of chloroplasts is reduced and membrane breakdown occurs after infection with rusts (Shaw and Manocha, 1965; Manocha and Shaw, 1966). Chlorophyll content can also be influenced by disease. Singh and Gupta (1975) have shown a reduction in chlorophyll in Cynodon Mosaic Virus - infected Bermuda Grass, and Borah et al. (1977) demonstrated a decrease in chlorophyll a and b in the tea

leaves (*Camellia sinensis* (L.) O. Kuntze infected with rust *Cephaleuros parasiticus*. Decreases in chlorophyll content may be due to the inhibition of synthesis (Crosbie and Mathews, 1974) rather than the destruction of pre-existing pigments, or to the degeneration of chloroplast structure (Heath, 1974b). Whatever the cause of reduction in chlorophyll is, it is important because of its obligate involvement in photosynthesis, both as a light-absorbing antenna and as a photochemically active pigment.

1.3.4 Respiration

Increased respiration rates in rust infected plants may mask the true events of photosynthesis during infection. The importance of an adequate carbohydrate supply for development of rusts in susceptible hosts has been realized by many workers (Scott, 1972). The developing fungus requires energy for growth and this comes from intermediates of respiratory or photosynthetic pathways. As early as 1934, Yarwood reported a 50 percent increase in respiration in clover leaves infected with *Erysiphe polygoni* compared with that in non-infected leaves. The relative contributions of host and pathogen to the rise in respiration has been a controversy for many years (Shaw, 1963; Daly 1967). However it does appear as if the increase is partly due to the fungus and partly due to the stimulation of host tissue in the adjacent areas (Bushnell and Allen, 1962; Scott and Smillie, 1966). In rust infections, respiration increases usually begin with the appearance of visible infection flecks and rise to a maximum at the time of sporulation (Daly et al., 1961). Generally these symptoms are confined to the environs of infection centres and a few millimeters beyond the limits of parasite development, but other effects such as hormonal changes, may influence the entire plant (Shaw, 1963). Changes in respiration may be due to either quantitative changes in existing pathways or alternatively qualitative changes (Scott, 1972). Included among the many proposals is the suggestion that a non-cytochrome system of terminal oxidases is activated in infected tissue which may account for increased oxygen consumption. Many workers have reported an increase in the activity of soluble oxidases *in vitro*, including phenoloxidase, ascorbic acid oxidase, peroxidase and catalase (Maxwell and Bateman, 1967; Farkas and Kiraly, 1968; Retig,1974). Brenneman and Black (1979) however present evidence which indicates

that the increase in respiration in tomato leaves infected with *Phytophthora infestans* is due to a large extent to the additive effect of the fungus rather than stimulation of host respiration. They showed that the effect of respiratory inhibitors such as azide, malonate or arsenite on control tissue was no different to inoculated tissue. They also showed no difference between healthy and infected tissue in catalase and cytochrome oxidase activities. Another proposal is that partial uncoupling of oxidative phosphorylation occurs in the later stages of development of infections on susceptible plants preventing the formation of ATP and other synthetic reactions, and accelerating glycolysis and oxidation (Shaw and Samborski, 1957). However this appears to contradict the evident synthetic activities and accumulation of substances at the infection sites (Billett and Burnett, 1977). Enzyme assays on extracts of rusted and mildewed leaves suggest that the PPP plays a role in the increased respiratory activity of infected leaves (Kiraly and Farkas, 1962: Scott and Smillie, 1962). Daly et al. (1957; 1961) put forward the suggestion that the C_6/C_1 ratio of infected tissue fell sharply after sporulation in rust-infected wheat, safflower and bean. They pointed out that this may be a result of one or both of the separate ratios of the fungus and host decreasing, or alternatively due to the fact that the ratio of fungal to host tissue is initially too small to exert a measurable effect on the overall C_6/C_1 ratio until after sporulation has begun. An increase in activity of the PPP would result in increased amounts of NADH. This reduced co-enzyme could consequently function in synthetic reactions such as lipid synthesis. However if NADPH reoxidation results in oxygen consumption, electrons have to be transferred to NAD. One possible mechanism for such an electron transfer may be that catalysed by the malic enzyme. Enhanced activities of this enzyme have been found in rust-infected bean leaves (Mirocha and Rick. 1967). Such a system would allow a shuttle of reducing power from the outside to the inside of the mitochondria. NAD has been found to increase in rust-infected leaves in a pattern similar to that of oxygen uptake which appears to be consistent with the view that increased oxygen consumption ocurs via the mitochondrial oxidative pathways.

Evidence bearing on the involvement of the TCA and glyoxylic acid

cycles in rust-infected tissues has been presented (Daly and Krupta, 1962). Larger increases in succinic, malic, citric and fumaric acids as well as aspartic and glutamic acids have been reported to occur in rust-infected wheat and bean leaves. The extent of the increases depended apon the stage of development of the rust, and was greater at sporulation than early flecking, though a marked increase in malate was characteristic of flecking.

1.4 Nitrogen metabolism

4.1 Total nitrogen and nitrates

Many investigations have been carried out on the qualitative and quantitative changes in the composition of free amino acids in plant tissue during infection, but with varying results (van Andel, 1966). The stage of disease development as well as the growing conditions of the plants may be important factors in determining results. Nitrogen metabolism is important, not only in its influence on photosynthesis, but also in its involvement in susceptibility of the host to infection. This conclusion is supported by the correlation between total nitrogen or amino acids of the plant and susceptibility to disease (Weinhold, 1964). Application of asparagine or glycine to wheat leaves has been found to promote rust infection (Gassner and Hassebrauk (1933) in van Andel, 1966). Amino acids are important sources of both nitrogen and sulphur for fungi (Burrell and Lewis, 1977). An increase in the content of certain amino acids is often accompanied by a decrease in a number of others, so that the composition of the amino acid pool must be changed considerably (Hrushovetz, 1954 and Lowther, 1964). As the disease progresses, in most cases the amino acid content of the tissue starts to decrease (Shaw and Colotelo, 1961). Shaw (1961) has reviewed the work that has been done in rust-infected wheat and indicates that there are considerable differences in behaviour between susceptible and resistant wheat varieties. Shaw and Colotelo (1961) found that total nitrogen and protein nitrogen increased in susceptible wheat (Little Club) whereas decreases occurred in resistant varieties (Khapli). Virus diseases can also influence nitrogen metabolism. Singh and Gupta (1975) noted a reduction in crude protein in Bermuda grass infected with Cynodon Mosaic Virus, whereas Mukherjee et al. (1979) found an

increase in protein nitrogen, total nitrogen and nitrate reductase activity as a result of cucumber mosaic virus infection of tobacco var. white barley leaves. Increases in nitrate reductase activity may result from increased nitrate uptake, whilst increases in protein and total nitrogen following inoculation may be due to the synthesis of virus proteins. Foliar diseases may reduce forage quality by inducing higher levels of undesirable constituents and by reducing the amount of desirable constituents. Mainer and Leath (1978) for example have shown a twenty five percent reduction in crude proteins in alfalfa leaflets rated at 80 percent infection with *Phoma medicaginis* or *Stagonospora arenaria* whereas in orchard grass, crude protein was significantly reduced at an infection level of twenty percent. Thus crude protein was reduced in proportion to disease severity. The ratio of soluble to insoluble nitrogen may change in infected leaves, or even in different areas of the leaves. Uritani and Stahmann (1961) demonstrated that some soluble proteins increased in tissue adjacent to the infection site, whilst others decreased in sweet potato infected with black rot. The leaf-to-root distribution of free amino acids can change in infected plants eg. Hodges and Robinson (1977) showed a disproportionate decrease of amino acids in roots of *Bromyces striiformis*-infected *Poa pratensis*.

The relationship between nitrates and protein synthesis in infected leaves is variable. Stubbs and Walbran (1963) reported the accumulation of nitrates under low nitrogen nutrition in barley-yellow dwarf virus infected oats, to a level toxic to livestock, even though dry weight of infected leaves decreased. A high nitrate level in infected plants grown under low nitrogen conditions may suggest that the virus is interfering with the transformation of nitrate to protein in the plant. Increased nitrate levels have also been reported in some rust-infections. Piening (1972) showed an accumulation of nitrate above 2000 ppm in leaf rust-infected rye, which proved toxic to cattle.

Infection of leaves by rust fungi ususally leads to an increase in their amino acid composition (Shaw and Colotelo, 1961; Raggi,1974, Borah et al., 1978), or a change in the ratio of soluble to insoluble nitrogen.

Indeed Shaw and Coletelo (1961) found total nitrogen, protein nitrogen and soluble nitrogen increased per gram fresh wt. in susceptible Little Club wheat. Differential changes in the concentration of individual amino acids were also noted as early as two days after inoculation. Large increases in asparagine, serine, alanine and glutamine occurred in infected leaves. Such changes may reflect changes in the activity of enzymes concerned with amino acid metabolism, although transport and accumulation of these compounds may also be involved. Increases in the activities of glutamic dehydrogenase and glutamine synthetase were demonstrated in Little Club plants. Glutamine has often been found to show the greater increase, and this amino acid is important in its role in linking nitrogen and carbohydrate metabolism. Rohringer (1974) has shown that uredospores are also rich in glutamine, and has drawn attention to the fact that glutamine is a precursor of glucosamine which after acetylation becomes n-acetylglucosamine, the building unit of chitin. According to Farkas and Kiraly (1961) production of NH_4 by the fungus would stimulate glutamine synthesis, but the accumulation of NH_4 or urea in the tissue after infection would be toxic to plant and parasite. Kiraly (1964) also points out the relationship between nitrogen and phenol metabolism in wheat. Samborski and Shaw (1956) indicated that soluble N is translocated into rust-infected wheat leaves and is retained in infection or pustule areas. Increases in the total nitrogen concentration have also been reported by Colonge (1967) in barley infected with *Puccinia hordei* Otth. The results indicated that the barley rust was able to synthesize or alternatively caused the host to synthesize extra nitrogenous material.

In considering the changes in the amino acid pool, it is important to remember that the pool consists of four components namely the vacuolar and cytoplasmic 'pools' of both host and parasite. The haustoria of fungi are in contact with the cytoplasm of the host, and the parasite may thus draw a supply of amino acids from the cytoplasmic pool rather than the less available amino acids in the vacuoles. Not only are amino acids such as alanine and serine (Burrell and Lewis, 1977) absorbed by the fungi, but some amino acids are synthesized by rust fungi themselves. Staples and Stahmann (1963) showed that *Uromyces*

phaseoli (Rebent) Wint. or bean rust, synthesizes some proteins when growing in the host plant, whilst alanine is both absorbed and synthesized by *Puccinia graminis* on wheat (Reisener et al. 1970 in Burrell and Lewis, 1977).

There have been many explanations for the changes in nitrogen metabolism in rust-infected leaves. One possibility for total nitrogen increase is the induced synthesis of protein in the host as indicated by the increase in RNA content of the nucleoli of rust-infected wheat cells (Shaw , 1962). Increases in amino acids in tea leaves after infection with *Cephaleuros parasiticus* (red rust) may be of pathogen origin since *C. parasiticus* depends apon the host for its nitrogen nutrition (Vidyasekaran and Parambaramani 1971). Borah et al. (1978) postulate that the increase in amino acids in variegated tea leaves is likely to be due to the increased concentration of proteolytic enzymes contributed both by the plant and pathogen, while Raggi et al. (1974) are of the view that infection reduces incorporation of amino acids into proteins, resulting in an accumulation of inorganic nitrogen. Decreases in amino acid content in infected leaves can sometimes be attributed to utilization by the pathogen. In some cases protein amino acids are found to increase simultaneously with free amino acids (Jones, 1963), suggesting that either amino acids are translocated from other parts of the host to the infected tissue or aminoacids as well as protein synthesis is stimulated. On the other hand Shaw and Colotelo (1961) intepret changes in protein composition as fluctuations between leaf and pathogen amino acid compositions at different stages of development of the disease.

4.2 Nitrogen metabolism, photosynthesis and photorespiration

Both carbon and nitrogen skeletons are required for the synthesis of amino acids. The response of N metabolism to photosynthesis has been studied in C_3, C_4 and intermediate grasses (Bolton and Brown, 1980). Photosynthesis was found to increase in a linear fashion with increases in leaf nitrogen content in *P. maximum* (C_4), *P. miliodes* Nees ex Trin. (intermediate) and *Festuca arundinacea* Schreb. (C_3). In other cases apparent photosynthesis has been shown to level off at high N supply levels (Nevins and Loomis, 1970). Ryle and Hesketh

(1969) also showed a decrease in the rate of C assimilation by a N deficiency in *Zea mays*. Grossman and Cresswell (1973) indicated that a change from nitrate to ammonia as the N source increased the photosynthetic rate of *Zea mays*, and the CO_2 compensation point increased when NH_4 was the sole nutrient as opposed to nitrate nitrogen. Nitrogen metabolism is also linked to photosynthetic enzyme activities. The close relationshio between leaf N and photosynthesis may result from a large proportion of leaf protein being accounted for by RuBPC protein. As much as fifty percent of the soluble leaf protein in C_3 plants may be invested in RuBP carboxylase (Brown, 1978). Consequently this would have an influence on photosynthesis since RuBPC is one of the regulatory enzymes in photosynthesis. Plants with C_4 pathway of CO_2 assimilation apparently utilize N more efficiently than C_3 species because they generally have higher apparent photosynthetic rates and lower leaf N concentrations. Wilson (1975) showed that *Panicum maximum* Jacq. fixed CO_2 at higher rates than a C_3 grass (*Lolium perenne* L.). Photorespiration is also influenced by N levels. Fair et al. (1973a) showed that CO_2 compensation point was correlated with the ratio of nitrate reductase to RuBPC activity. At elevated CO_2 concentrations *Hordeum vulgare* (C_3) had increased levels of RuBPC whilst glycolate oxidase and nitrate reductase were suppressed. Andreeva et al. (1975) demonstrated that an increase in N supply stimulated glycolate oxidase activity in beans and maize, whilst Cresswell et al. (1974) showed that an increase in NH_4 or nitrate led to an increase in PEPC, RuBPC and RuBPO in the C_4 species *Eragrostis* and *Themeda*. Higher levels of nutrient N led to a greater ratio of RuBPO to RuBPC for C_4 plants. These results indicate that RuBPO and hence photorespiration is increased with the addition of N. Nitrogen also appears to influence carbonydate matabolism. Platt et al. (1977) reported that the addition of NH_4 could result in the diversion of CO_2 away from sugars into amino acid biosynthesis and that pyruvate kinase and PEPC were activated by NH_4. Amory (1981, pers. comm.) has also indicated that N starvation leads to a decrease in aspartate and alanine amino transferase. Nitrogen therefore is important as a regulatory factor in the photosynthetic capacity of forage grasses.

5.2 AIMS

The physiological studies were undertaken with several objectives:-

1) To obtain a better understanding of host-parasite interactions at a micro-level.
2) To study the host-pathogen relationship of *P. maximum* - *P. paspalicola* which has not been researched with respect to physiological aspects.
3) To determine the physiological changes due to plant disease on the two selected grass species at Nylsvley, which have not been previously studied, and to assess the impact of necrosis on *B. africana*.
4) To estimate the effect of fungal pathogens on C_4 photosynthesis and hence the primary production of the grasses *D. eriantha* and *P. maximum*. The different nature of C_4 photosynthesis compared to C_3 photosynthesis provides a unique system not only for studying the effect of pathogens on photosynthesis, but also for achieving a better understanding of the recently developed ideas on photosynthesis and its relationship with nitrogen metabolism and photorespiration.

5.3 METHODS

3.1 Photosynthesis and respiration

3.1.1 Gross photosynthesis

Apparatus

Gross photosynthetic rates were measured in the field using an adaptation of the Shimshi method (Shimshi, 1969). This method is based on the measurement of radioactive carbon dioxide assimilated by illuminated leaves. After a fixed exposure the leaf is killed and the amount of $^{14}Co_2$ incorporated is determined. This method is subject to two inherent errors. The first error is due to isotope discrimination against ^{14}C in the multi-enzyme system of photosynthetic carbon fixation. A kinetic isotope effect is achieved (reaction rate constant changes) when ^{14}C is mixed with a ^{12}C- gas mixture. The relative rates of diffusion of $^{14}CO_2$ and $^{12}CO_2$ are in the ratio of approximately 1:1.02, and therefore in species showing appreciable photorespiration an apparent discrimination would be mainly due to the dilution of the $^{14}CO_2$ by respiratory $^{12}CO_2$.

however this is not significant in C_4 plants with low photo-respiration and Yemm and Bidwell (1969) have shown that the discrimination in maize (C_4) is only 2 percent. The second error results from the dilution of ^{14}C and ^{12}C mixtures by respiratory $^{12}CO_2$. However using short exposure times (± 20 seconds) only a little $^{14}CO_2$ will be present in the respiratory $^{12}CO_2$. Also these errors become less significant in the current study which is concerned with comparisons between healthy and infected leaves under identical conditions.

In the Shimshi apparatus (Fig. 52) employed, an aliquot of barium ^{14}C - carbonate (50mCi/mM; 1.83Ci/mM CO_2) was placed in a reaction vessel and $^{14}CO_2$ generated by acid blown into the reaction vessel. The generated $^{14}CO_2$ was forced into a cylinder by compressed carbon-dioxide free air. The compressed air was admitted until the pressure in the cylinder had reached the desired value. This system enabled the concentration and specific activity of the CO_2 to be calculated. The gas cylinder was attached to a leaf chamber which consisted of two symmetrical valves made from perspex and held in tongs. When clamped on a leaf, a valve was depressed by the clamping action and the CO_2 was released. The leaf chamber satisfied the conditions of air tightness; uniform illumination; sufficient turbulent air movement to reduce diffusion gradients to an accepted level; and prevention of an excessive rise in leaf temperature during measurement (Sestak et al., 1971)

Sampling

Exposure time used was 20 seconds. A short exposure time is desirable since leaf chambers cause changes in the conditions of the enclosed leaf. Sources of errors (such as 'dead time' which is the interval between turning on of the labelled gas and it reaching the leaf, and that between turning off and disappearance of all traces of the gas; and the time that diffusion processes within the leaf and its boundary layer are in a non-steady state) are reduced to a minimum at exposure times of 15 - 20 seconds (Austin and Langdon, 1967). The leaves were held perpendicularly to the sun to minimize radiation angle effects. Radiation was measured using a LI-170 quantum meter (micro-Einsteins m^{-2} sec^{-1}). The leaf discs were

punched out using cork borers designed as the exact measurement of the discs, and placed immediately in 10mℓ of 95 percent ethanol. The $^{14}CO_2$ was extracted by boiling the alcohol for 1h and then removing the leaf discs and evaporating the alcohol to dryness. Following this step, 2mℓ alcohol was added to the residue, 0.5 mℓ removed and added to 15mℓ scintillation fluid (2:1 by volume of toluene containing 5g PPO + 0.1g POPOP/litre and Triton X 100,. The samples were counted for 10 min on a Packard TRI-CARB scintillation spectrophotometer.

Calculations

The aim of the calculation was to express CO_2 uptake in mg CO_2 dm^{-2} h^{-1}.

$$CO_2 \text{ uptake} = \frac{(44.X)}{(10^3 S)} \times \frac{(180)}{(\text{disc area})\ (dm^2)} \times 1.02$$

180 = exposure time (20 seconds) in 1h
1.02 = correction factor for $^{14}CO_2$ vs $^{12}CO_2$ discrimination
$10^3 S/44$ = cpm/mg CO_2 as 1 mole = 44mg CO_2
Disc area for tree chamber = 0.0177 dm^2
Disc area for grass chamber = 0.0135 dm^2
X = cpm for leaf disc = 1.83 X 10^3 μCi/mM CO_2
S = specific activity of labelled air =
4.0626 X 10^6 dpm/mM CO_2 (2.22 X 10^6 dpm/mM CO_2)

Because of age differences and different temperature and radiation conditions in the field, sampling techniques of the plants were of great importance. Shimshi (1969) points out the significance of standardization of leaf age, degree of exposure to illumination, and time of sampling. In order to minimize radiation effects leaves were always held perpendicular to the sun and measurements were only made on hot, cloudless days. Since photosynthetic rates change throughout the day (Fig. 56) gross photosynthesis was measured approximately between 7.30 - 9.30 am (steady rates) and averages of groups of data calculated. The relationship between gross photosynthesis

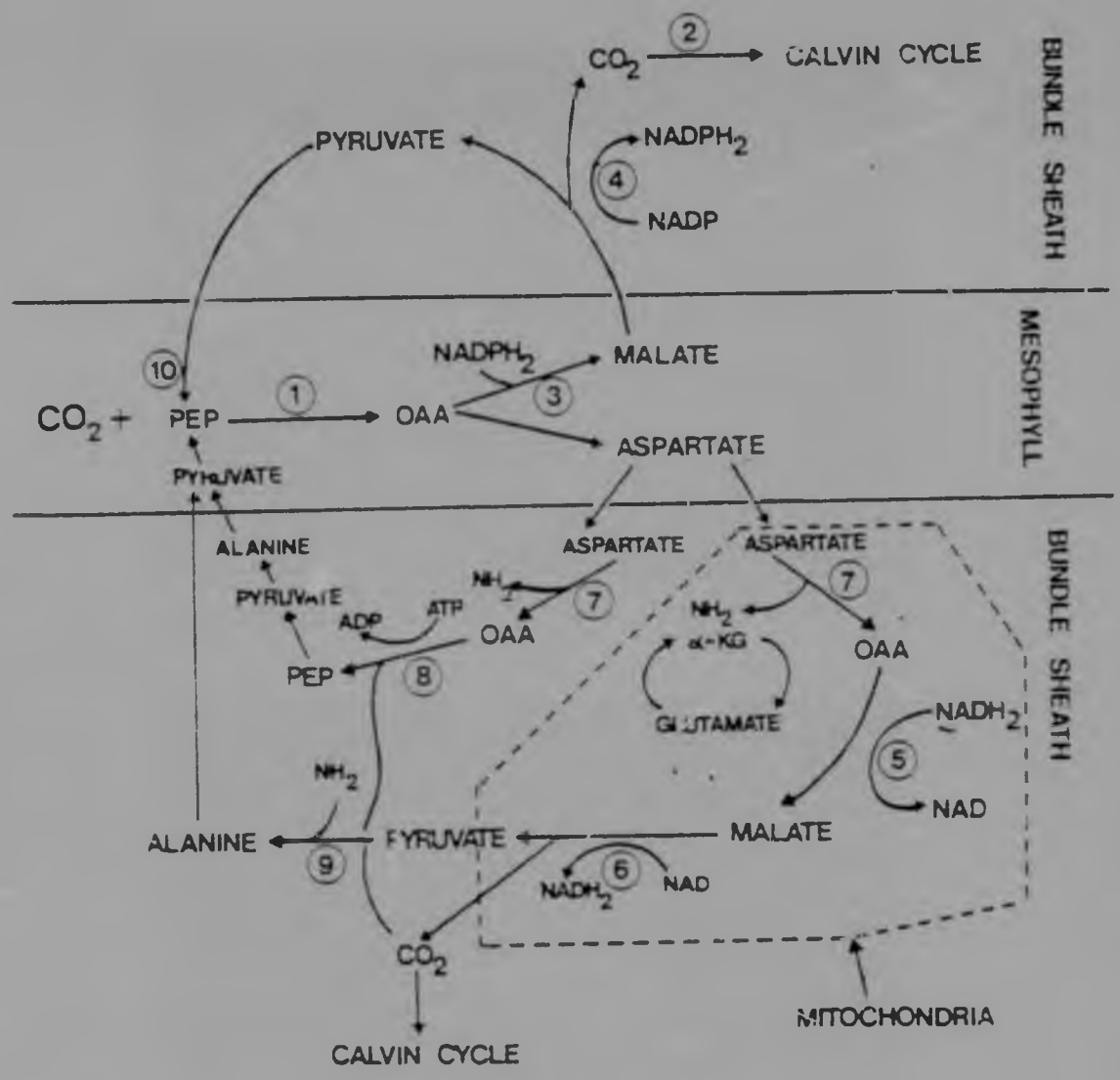


Fig. 51 Scheme illustrating the proposed reactions of the three types of C. pathways.

Enzymes: 1, PEP carboxylase ; 2. RuBP carboxylase;
3, NADP-malate dehydrogenase; 4, NADP-malic enzyme;
5, NAD-malate dehydrogenase; 6, NAD-malic enzyme;
7, Aspartate aminotransferase; 8, PEP carboxykinase;
9, Alanine aminotransferase; 10, pyruvate Pi dikinase





Fig.52 Shimshi apparatus for measuring gross photosynthesis. C- $^{14}CO_2$ gas cylinder, CL - clamp, arrow - leaf chamber. Fig.53 Cuvette for holding leaf specimens. Wj - water jacket, lc - leaf chamber, solid arrows - air inlet, open arrows - water inlet.

and exposure time of $^{14}CO_2$ was also established (Fig. 54). Healthy and infected leaves were sampled one after the other and averages of pairs estimated. In this way variations due to time were minimized. In order to standardize the leaf age effects, leaf blades were chosen on the same tufts and if possible in the same position up the leaf sheath. Several replicates were taken for each leaf sample. Paired - T tests were carried out on the data to test for the significance between healthy and infected leaves.

3.1.2 Net photosynthesis

Net photosynthetic rates were measured in the field using an Infra-Red Gas Analyser (Series 225 Gas Analyser, The Analytical Development Co. Ltd., England). An open-system was used, with the IRGA calibrated on differential, and measuring the difference in CO_2 concentrateion between the atmosphere (320 - 340 ppm) and the CO_2 leaving the cuvette containing the leaf sample (Fig. 55). The cuvette used was designed to take four to six leaves and had a water jacket to control leaf temperature (Fig. 55). The flow rate was regulated using a Fischer and Porter-Type10A 3200 flow meter (0.5 - 1.5 ℓ min^{-1}). Leaf temperature was measured using a thermocouple and automatically recorded on a linear recorder. Radiation was measured ($\mu E\ m^{-2}\ sec^{-1}$) above the cuvette and below the perspex in order to determine the radiation attenuation factor. Resistance was assessed using a ventilated diffusion porometer (Cayuga Model VPIC). The relationship was established between resistance (secs cm^{-1}) and the time (secs) measured on the porometer (Fig. 57) and the leaf T° correction factor taken into account (Fig. 58). Leaf area was determined with a planimeter. Sampling was carried out in pairs (similar to gross photosynthetic measurements) between 7.00 - 11.00 am and 3.00 - 5.00 pm. Leaf samples were allowed to run for the entire day in order to establish the daily photosynthetic pattern as well as the radiation and temperature respo[illegible]igs. 59 and 60). Photosynthetic rates (mg CO_2 dm^{-2} h^{-1}) were calculated as follows.-

$$PN = FR \times \frac{60 \times \text{ppm } CO_2}{LA \times 10^6 \times 22.4} \times 44 \times \frac{273}{T^{\circ}+273} \times \frac{840\ KPa}{1013}$$

KEY FOR GRAPHS AND HISTOGRAMS

GENERAL

Graphs

Healthy

Infected

Histograms

Healthy

Infected

EPIDEMIOLOGY

Incidence

1. Smoothed untransformed

2. Linear regressions

Severity

1.

2.

SPECIFIC

Graphs

Healthy
Infected

1 – 5%

10%

25%

50–75%

50%

75%

Histograms

HEALTHY

Infected

1 – 5%

10%

25%

50–75%

f – flecking
s – sporulation
ps – post– sporulation

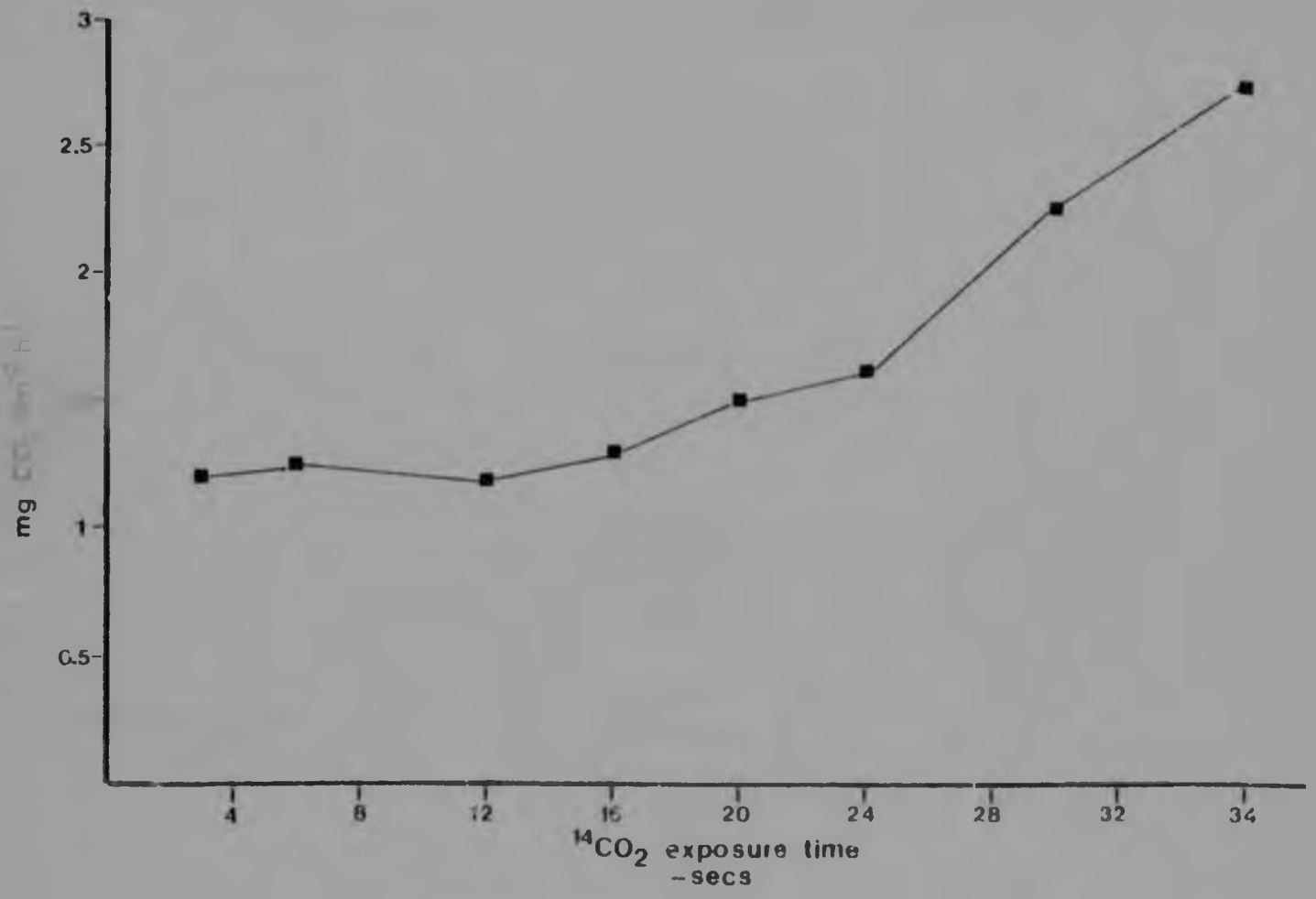


Fig.54 Response of gross photosynthesis to $^{14}CO_2$ exposure time

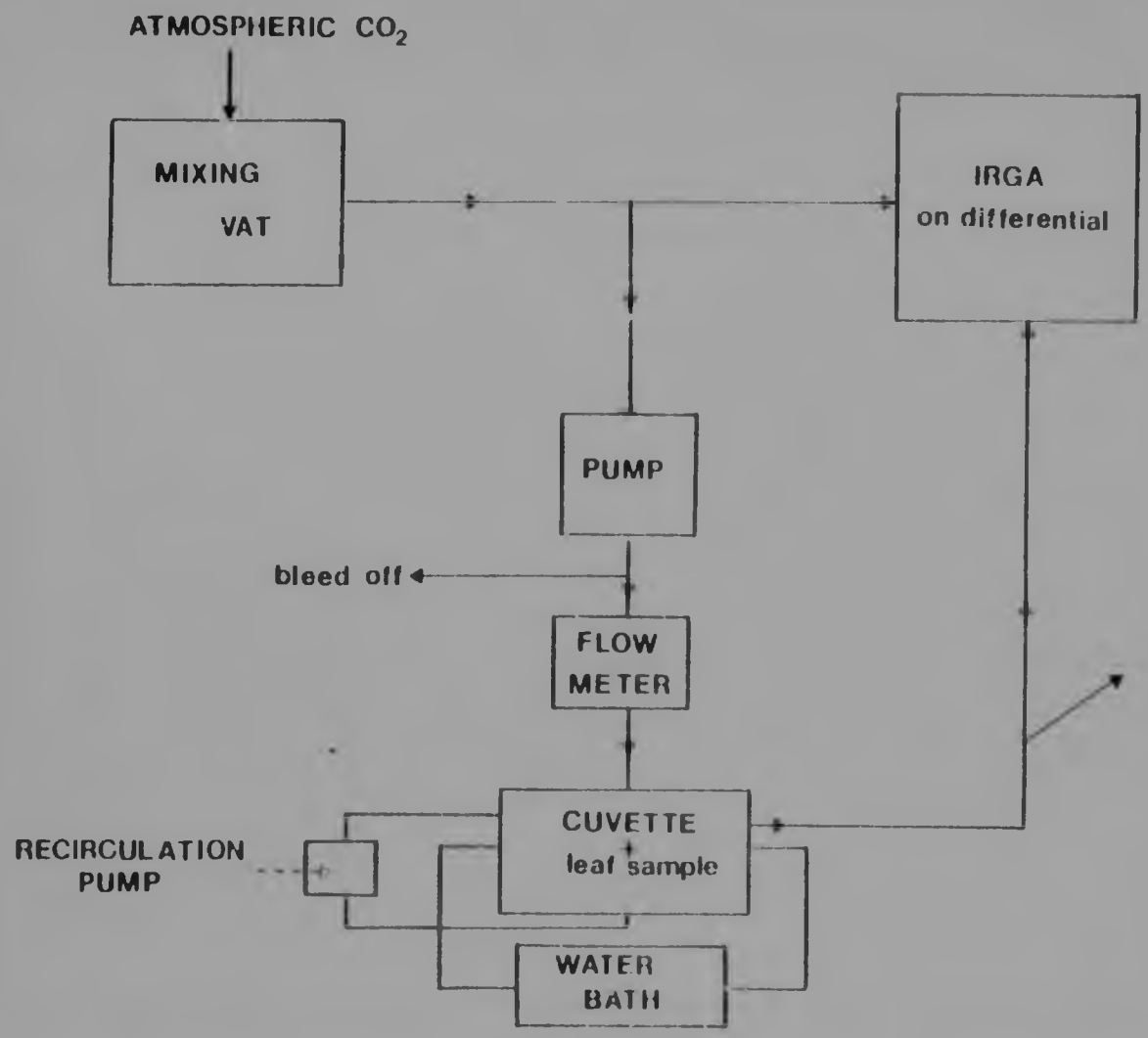


Fig.55 Diagram of the open-system used to measure net photosynthesis using an Infra Red Gas Analyser (IRGA)

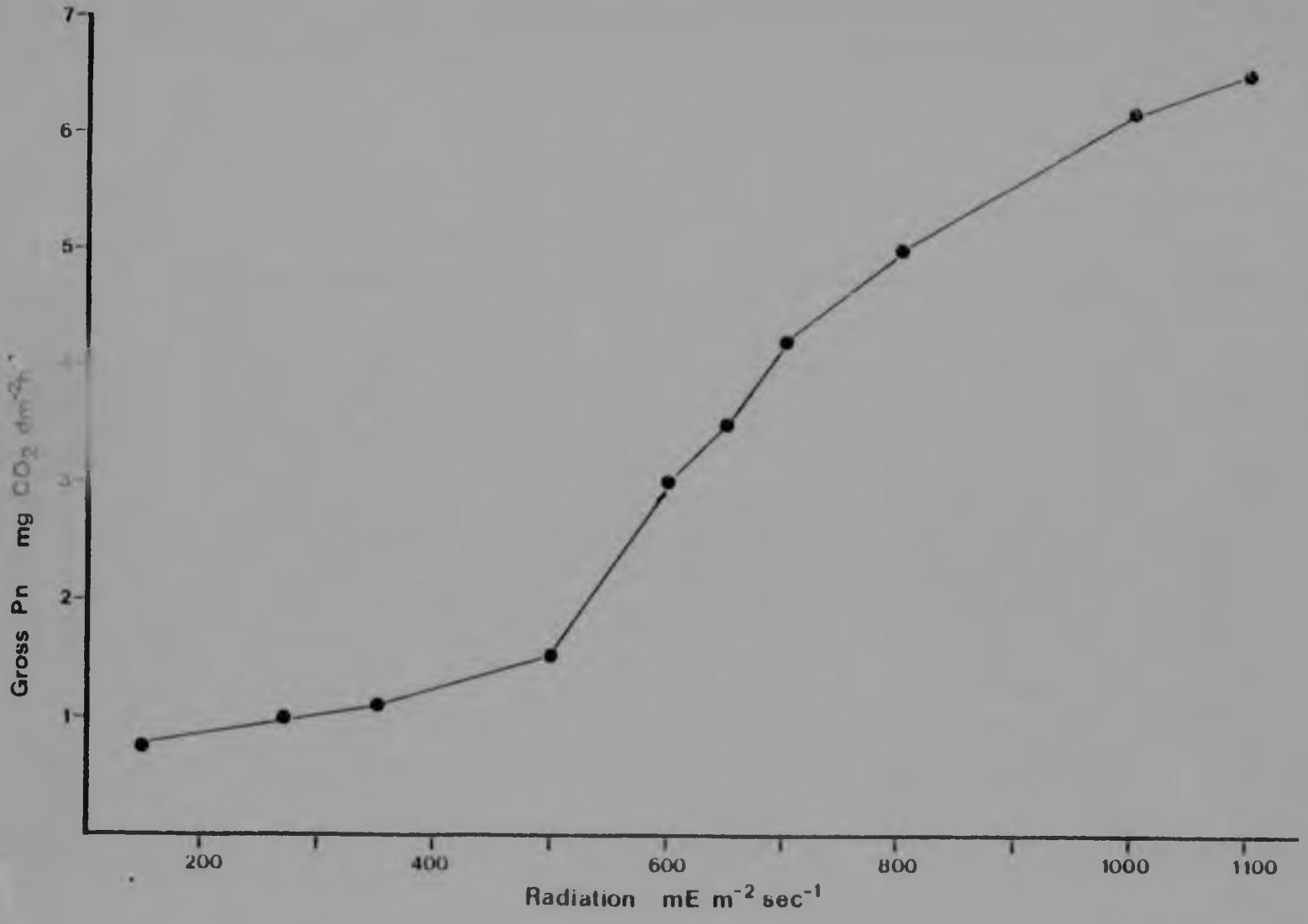


Fig.56 Response of gross photosynthesis to radiation

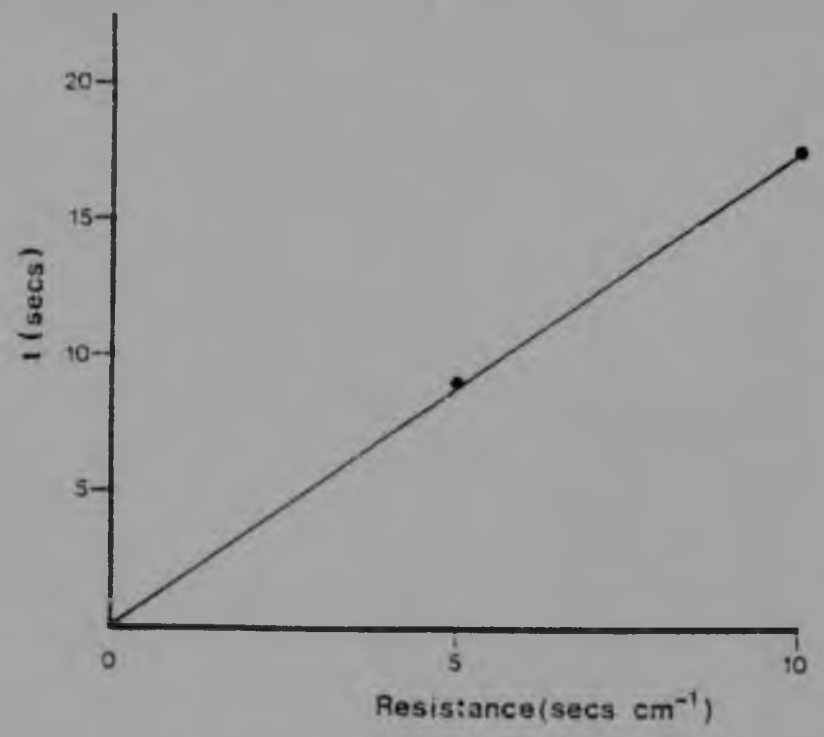


Fig.57 Resistance(secs cm^{-1}) vs time(secs)

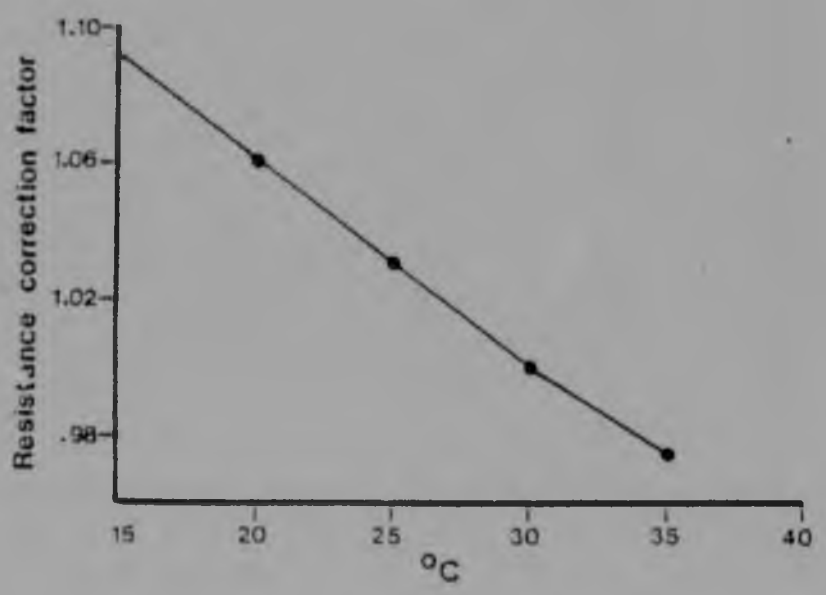


Fig.58 Leaf temperature correction factor for resistance

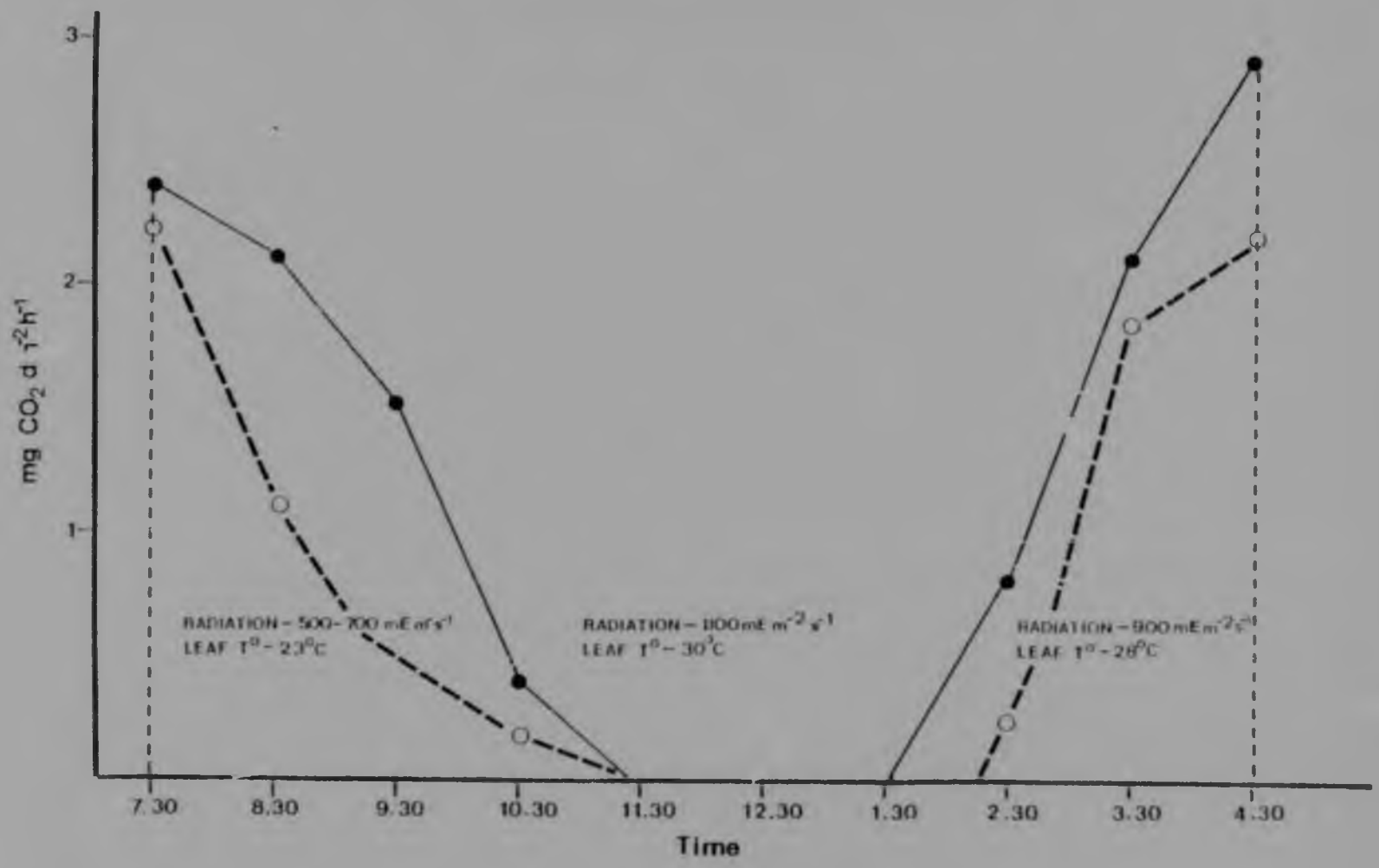


Fig.59 Daily photosynthetic run of *D.eriantha* taken from 7.30am through to 4.30pm

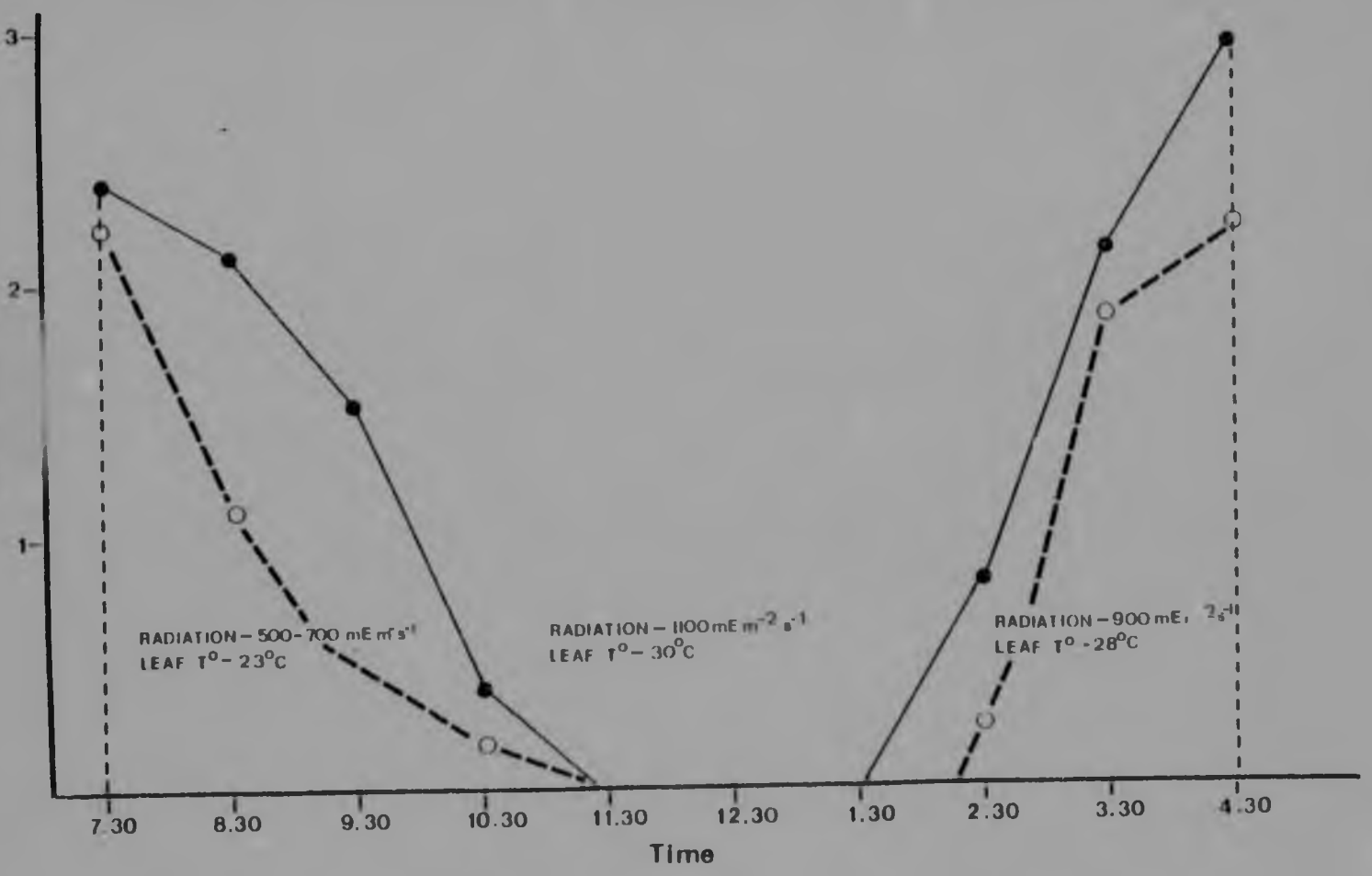


Fig.59 Daily photosynthetic run of *D.eriantha* taken from 7.30am through to 4.30pm

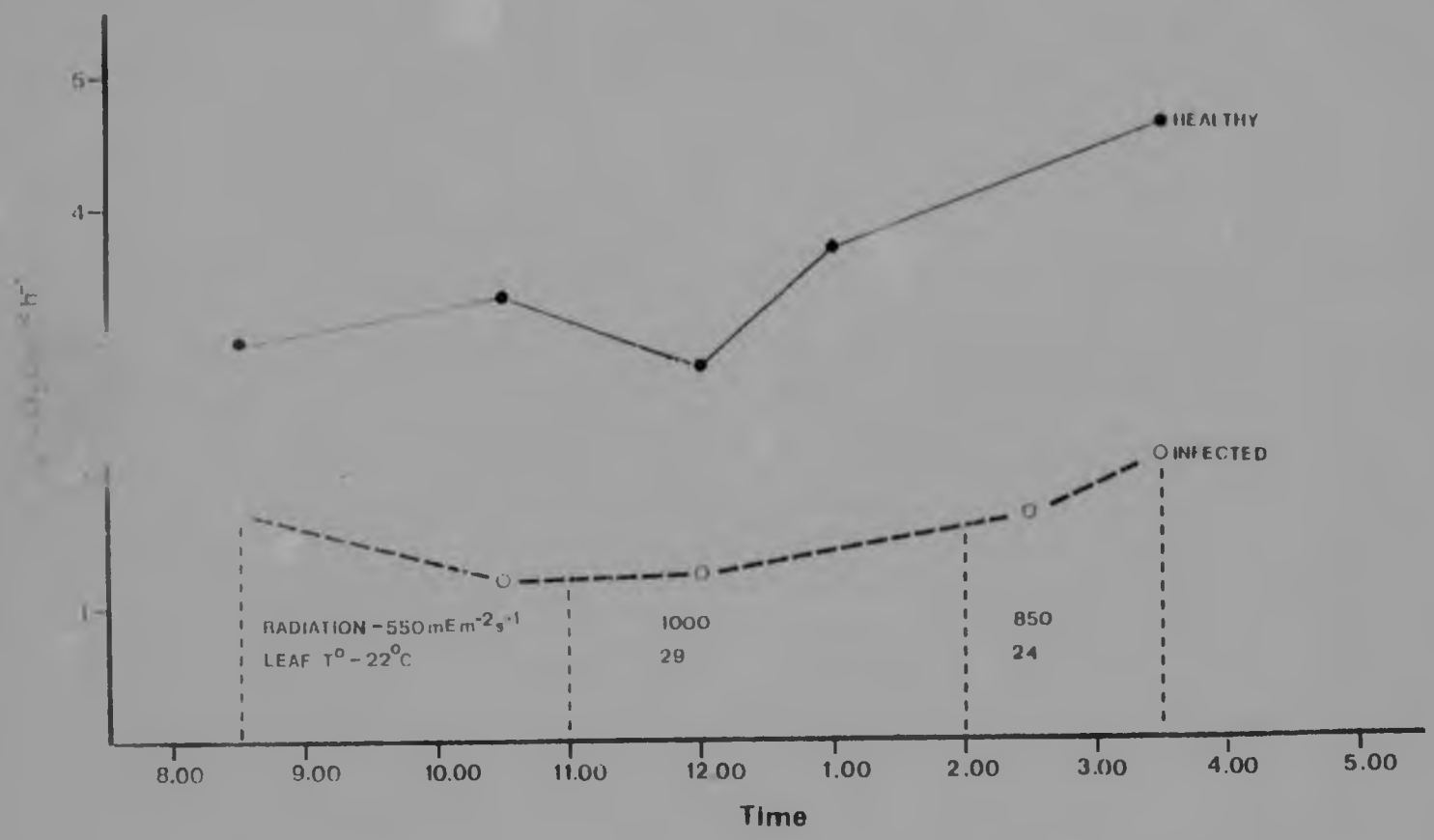


Fig.60 Daily photosynthetic run of *P. maximum* taken from 8.00am through to 5.00pm

FR = flow rate (litres min $^{-1}$)

ppm CO_2 = ppm/division x number of divisions on recorder scale

LA = leaf area (dm^2)

$\frac{273}{273+T°}$ = Temperature correction factor

$\frac{840 \text{ KPa}}{1013}$ = Pressure conversion from sea level to atmospheric pressure at Nylsvley.

Response of net photosynthesis to different CO_2 concentrations

The comparison of the response of net photosynthesis to increasing CO_2 concentrations between healthy and rust-infected *P. arundinacea* leaves was carried out by mixing N_2 gas with CO_2 gas (1000 ppm) in varying proportions (Fig. 61). A similiar open - system was employed, but instead of passing atmospheric CO_2 through the cuvette the specified gas mixture (proportions controlled by flow meters) was passed over the leaf samples (Fig. 62).

3.1.3 Photosynthetic enzymes

1.3.1 Enzyme extraction

Grass tufts were collected at Nylsvley early in the morning to avoid water stress conditions. The tufts were dug out carefully to avoid disturbing the soil around the roots and placed with water in plastic bags, and immediately transported to the laboratory where assays were performed. Leaf tissue (2g) was ground in a mortar and pestle with 5mℓ chilled grinding medium (50mM Tris-HCl buffer with pH 7.8, 1mM EDTA, 5mM DTT, 2mM Mg Cl_2, 10mM mercaptoethanol, and 1 percent (W/V) BSA) on ice, squeezed through two layers of miracloth and centrifuged for 15 minutes at 10 000 x g at 4°C, and the supernatant used for the enzyme assays.

1.3.2 Ribulose - 1,5 - biphosphate carboxylase *in vitro* assay

The assay employed was based on a method by Bjorkman (1968) modified by A. Amory (pers. comm.). The enzyme extract (50µℓ) was incubated with 300µℓ reaction mixture containing 200µℓ buffer of 150mM Tris - HCl (pH 8.0), 0,5mM EDTA (pH 8.0), 15mM $MgCℓ_2$ and 15mM DTT, and 100µℓ of 20µmole $NaH^{14}CO_3$ (0.5 Ci/µmole) for six minutes in a scintillation

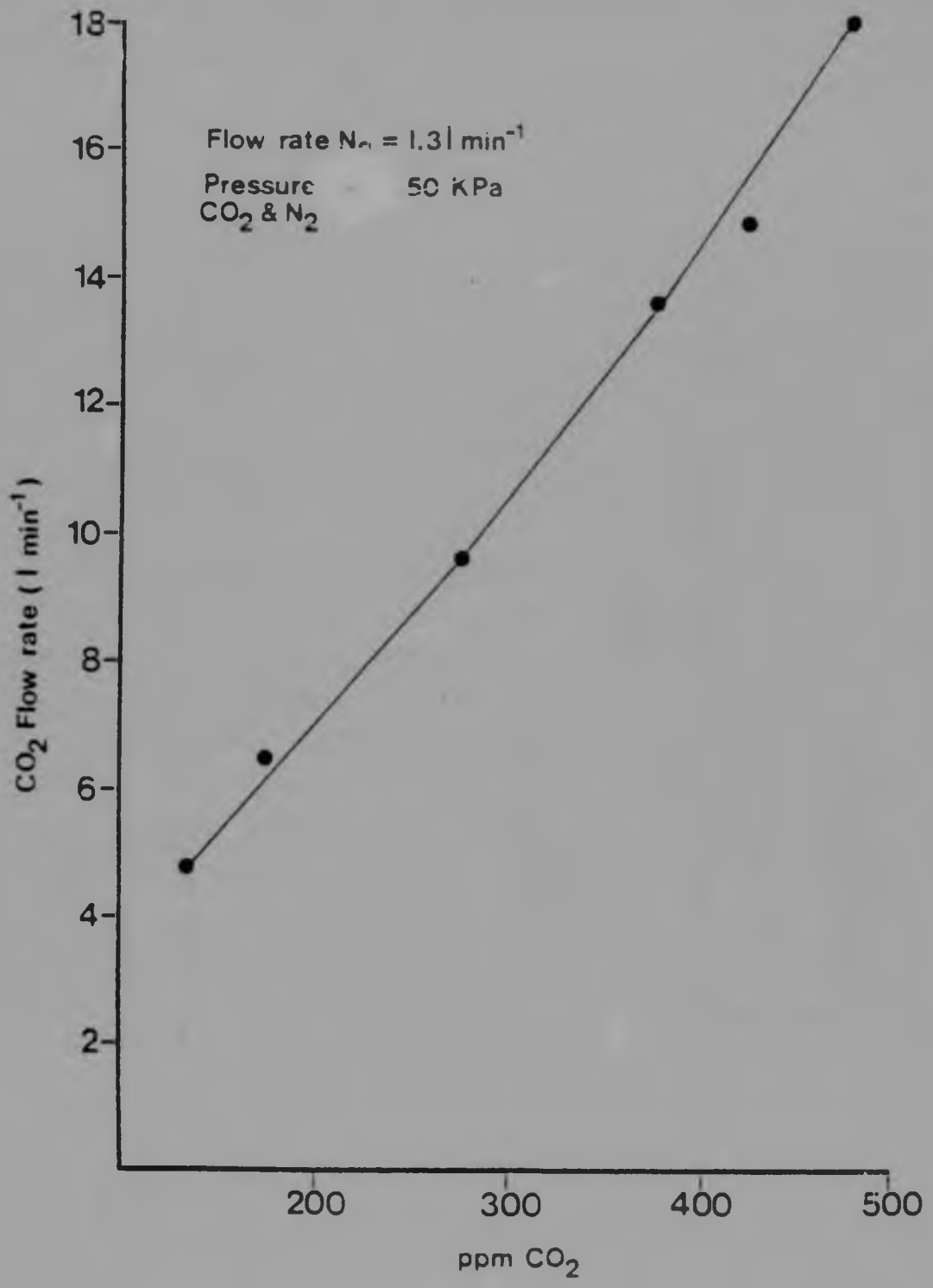


Fig.61 Response of increasing CO_2 flow rates on CO_2 efflux which was passed through the leaf chamber

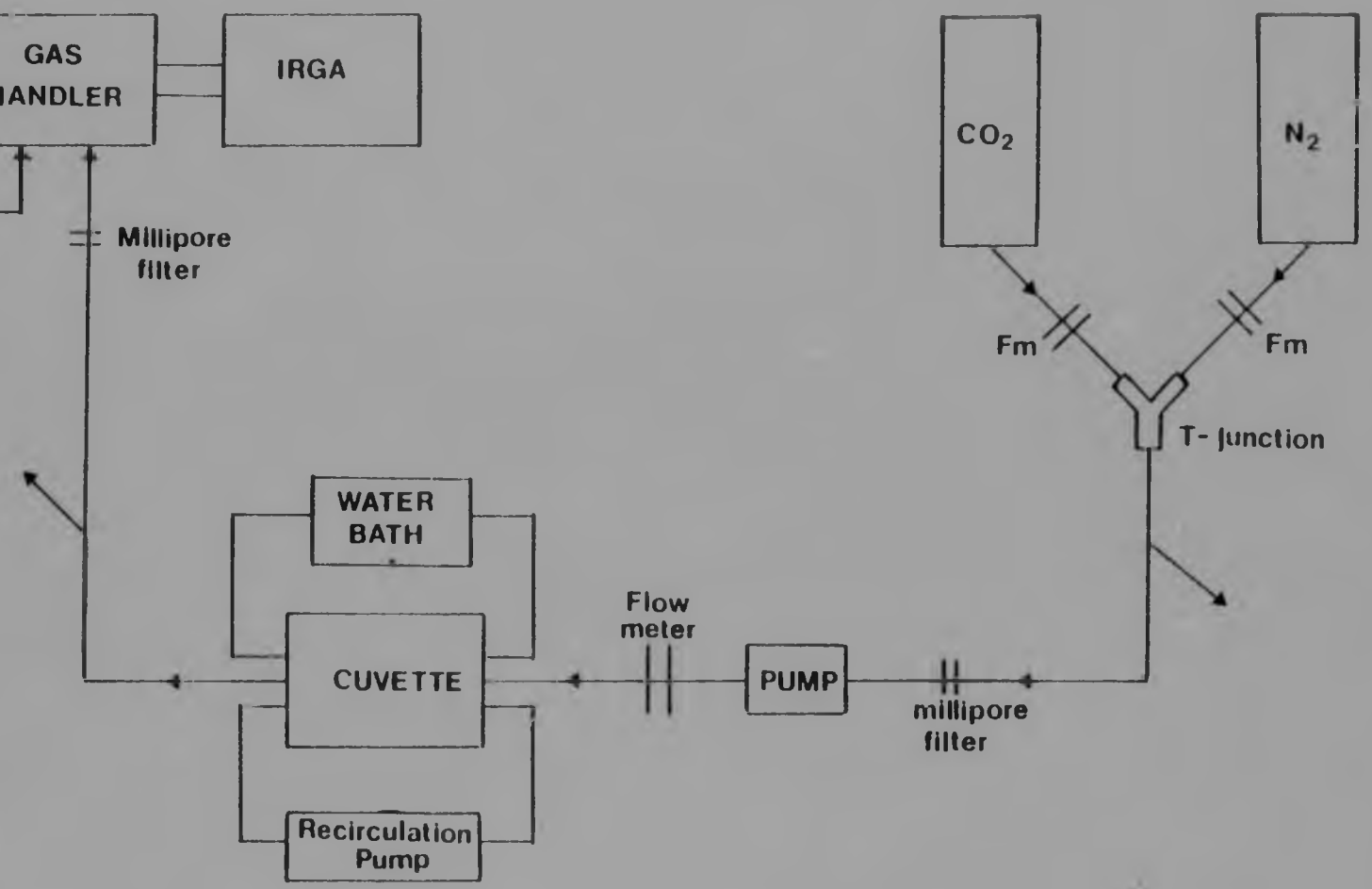


Fig.62 Diagram ofthe open-system used to measure the effect of increasing CO_2 concentration on net photosynthesis in healthy and rust-infected *D.eriantha* leaves

vial. The reaction was initiated with 100µℓ 10mM RuBP and stopped after four minutes with 6N acetic acid. The vials were then air dried and 500µℓ water and 10mℓ scintillation fluid (Lips and Beevers, 1966) added to the residue. The amount of labelled carbon incorporated was measured in a Packard TRI-CARB scintillation spectrophotometer. The control samples lacked either substrate (RuBP) or enzyme. Assays were run in triplicate and counted for 10min each.

1.3.3 Phosphoenolpyruvate (PEP) carboxylase

The activity of PEP carboxylase was determined using a method by Maruyama et al. (1966). The enzyme extract (200µℓ) was added to a reaction buffer (containing 50mM Tris-HCℓ, pH 7.5, 2mM $Mgcl_2$, 10mM $KHCO_3$, 5mM glutathione, 0.15mM NADH, 4mM PEP and 40µg malate dehydrogenase). The reaction was started by the additon of NADH. The blanks contained no NADH and/or PEP.

1.3.4 NADP and NAD malic dehydrogenase

NADP and NAD malic dehydrogenase activities were determined by the method of Raghavendra and Das (1978). The reaction mixture (total volume 3mℓ) contained 25mM Tris - HCL buffer (pH 8), 1mM EDTA, 10mM 2- mercaptoethanol, 0.2mM NADPH or NADH, and enzyme extract. The reaction was started with the addition of 0.5mM OAA. The blank contained no NADPH or NADH. Reaction was read at 340nm (UV) on a Beckman Model 25 spectrophotometer.

1.3.5 NADP and NAD malic enzyme

The activities of NADP and NAD-ME were measured using the method of Raghavendra and Das (1978). The reaction mixture (total volume 3mℓ) contained 25mM Tris - HCl buffer (pH 8), 0.5mM EDTA, 0.25mM NADP or NAD, 2mM DTT, enzyme extract and 2.5mM malate. The reaction was initiated with the addition of malate. The blank contained no NADP or NAD. The oxidation of NADP/ NaD was read at 340nm.

1.3.6 Alanine aminotransferase and aspartate aminotransferase

The activities of alanine aminotransferase (linked to the lactic dehydrogenase) and asparatate amino transferase (linked to malic dehydrogenase) were assayed spectrophotometrically according to Edwards and Gutierrez (1972). The reaction mixture for both enzymes (final volume

3mℓ) contained 50mM Tricine (pH 8.0), 0.03mM pyridoxal phosphate, 0.1mM NADH, 2mM EDTA, 2.5mM ∝-ketoglutarate and enzyme extract. For alanine aminotransferase 2.5mM alanine and 5µℓ lactic acid was added to the reaction vessel. For aspartate aminotransferase 50µℓ malic dehydrogenase and 2.5mM aspartate was added to the reaction mixture. The reactions were initiated with alanine and aspartate respectively, and the blanks contained no NADH.

1.3.7. Phosphoenolpyruvate carboxykinase

The activity of PEP carboxykinase was assayed radioactively according to the method of Edwards et al. (1971). The reaction was run in scintillation vials (total volume 500µℓ). The vials contained 50mM Tris - HCl buffer (pH 6), 5mM ADP, 10mM PEP, 5mM DTT, 5mM $MnCl_2$, 6mM $NaH^{14}CO_3$ (0.5 Ci/µmole) and enzyme extract (100µℓ). Two blanks were run with each assay - one without PEP and the other without ADP. The reaction was initiated with PEP and then stopped after 6 min with 200µℓ 6N acetic acid. The samples were air dried, and the residues redissolved with 500µℓ water and 10mℓ scintillation fluid. All assays were carried out in triplicate. The ^{14}C incorporated into the acid stable compounds was counted in a Packard TRI - CARB scintillation spectrophotometer for 10 min.

1.3.8 Chlorophyll

The amount of chlorophyll was determined according to the method of Arnon (1949). An aliquot (0.1mℓ) of enzyme extract was diluted in 80 percent (V/V) acetone (final volume 3mℓ), and read at 652 nm in an Eel spectrophotometer.

$$\text{Chlorophyll (mg)} = \frac{\text{absorption (652)}/100}{34.5}$$

3.1.4 Respiration

1.4.1 Dark respiration

Dark respiration activities were measured on an Infra Red Gas Analyser at night in the field, using similar methods employed in net photosynthetic measurements.

1.4.2 Succinate dehydrogenase

Succinate dehydrogenase (Kreb Cycle enzyme) activities were measured according to the method of Hiatt (1961). The enzyme extraction procedure was similar to that employed for the other enzyme assays, except that 0.4 M sucrose as added to the grinding medium. The sediment (from centrifugation) was resuspended in 20mℓ buffer and centrifuged again at 10 000g for 15 min. The reaction mixture (3mℓ) contained 0.05M potassium phosphate buffer (pH 7.4), 0.04M Na succinate, 0.01M Na cyanide, 0.0003 M Na 2,6 - dichlorophenolindophenol (DCPP) and 0.3mg/mℓ PMS. The initiaterwas PMS at room temperature, and the reduction of Na 2,6 - DCPP measured at 600nm.

3.1.5 Chlorophyll

Chlorophyll measurements for healthy and infected leaves were made according to the method of Arnon (1949). Leaf tissue was weighed out or area measured and homogenized in 25mℓ of 80 percent acetone. The extract was filtered through a millipore filter and the absorbance read at 645nm and 663nm using acetone as a blank.

$$\text{Chlorophyll } (\text{mg } g^{-1} \text{ or mg } dm^{-2}) = \frac{20.2\ D_{645} + 8.02\ D_{663}}{g \text{ or } dm^2}\ \text{mg} \times \frac{25\ \text{mℓ}}{1000\text{mℓ}}$$

5.3.2 Nitrogen metabolism

3.2.1 Nitrates

Nitrates were assayed using the salicylic acid method (Cataldo et al., 1975). The leaves were dried at 70°C and 0.2 - 0.5 g of crushed tissue added to 10mℓ distilled water and left to stand for 1h. Five millilitres of chloroform were added, the tubes shaken for 1 min and centrifuged at 10 000 x g for 5 min. The supernatant was used for the assay. An aliquot (0.2mℓ) of sample was mixed with 0.8mℓ 5 percent (W/V) salicylic acid in concentrated H_2SO_4 in a 50ml erlenmyer flask and left to stand at room T°. After 20 min, 19mℓ of 2N NaOH was added to raise the pH to 12. The yellow colour was measured at an absorbance of 410nm and absorbance plotted against µmoles KNO_3^-. A series of standard KNO_3^- solutions (0.1 - 1.25 µmoles) was made in order to obtain a standard curve. (Fig. 63).

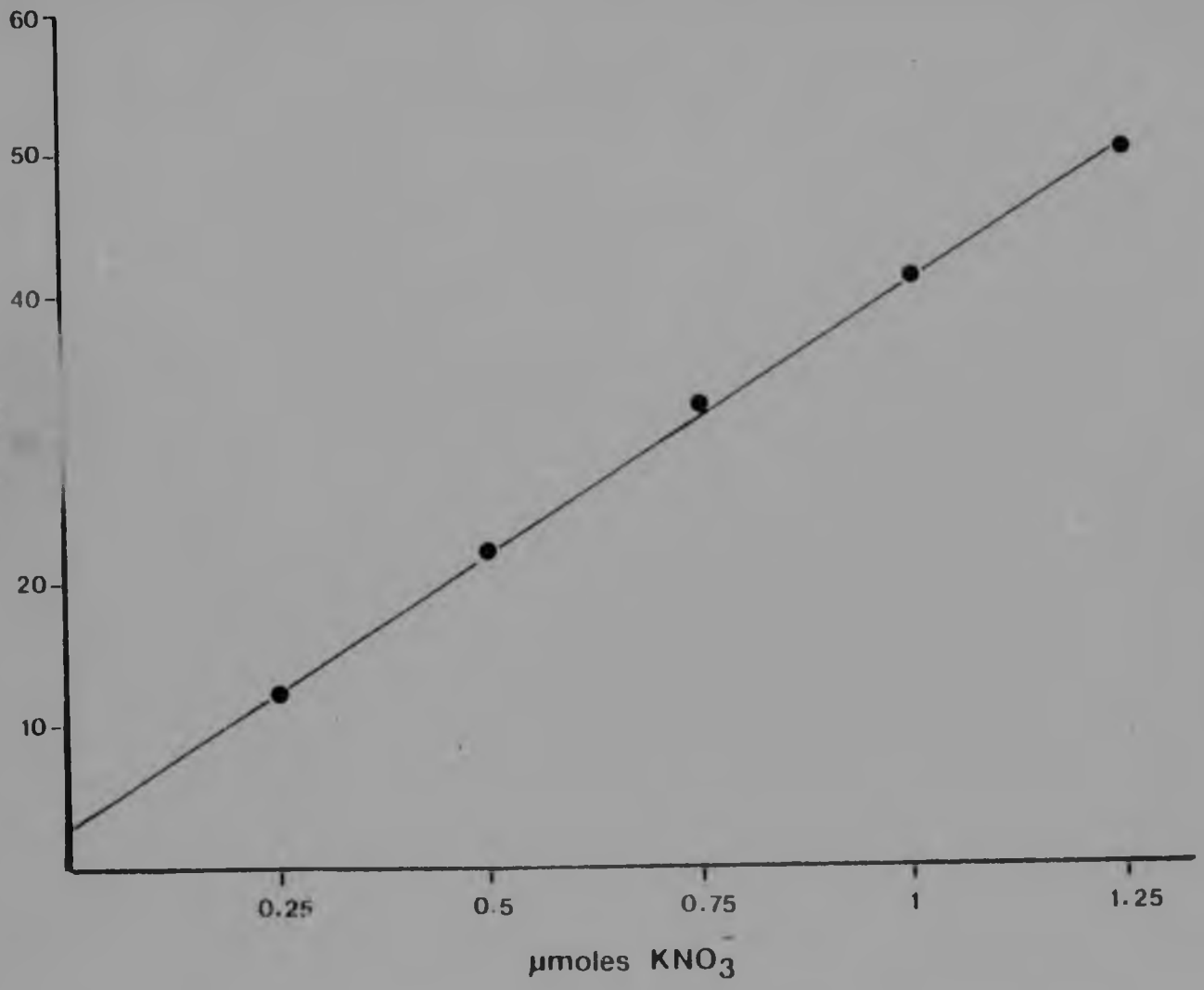


Fig. 63 Standard curve for nitrate (µmoles KNO_3^-) measurements

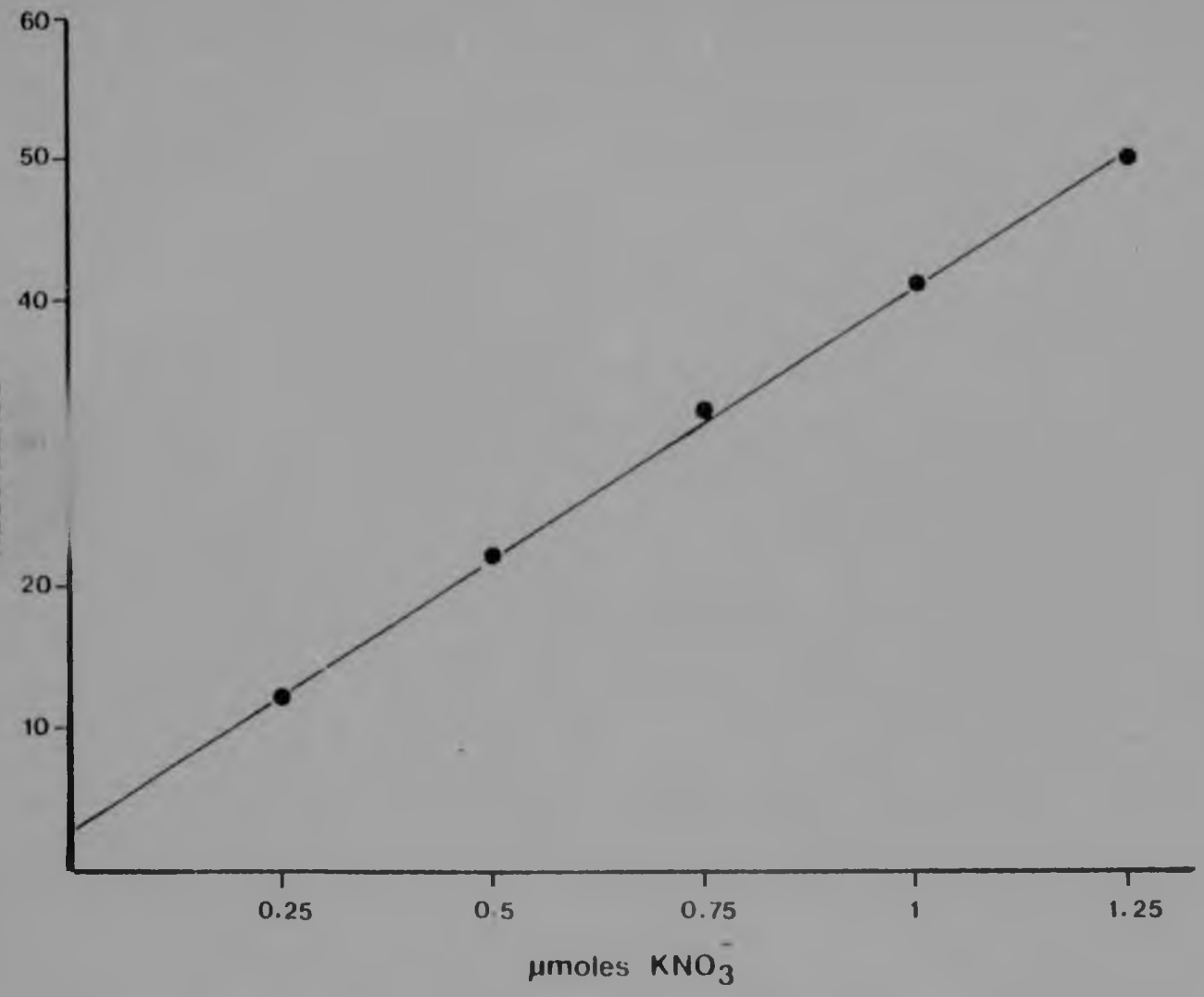


Fig. 63 Standard curve for nitrate (μmoles KNO_3^-) measurements

3.2.2 Total nitrogen

Total nitrogen was measured using the automatic Kjeldahl method based on the standard method (Association of Official Analytical Chemists, 1970) at the Food Research Institute, CSIR. Crude protein was calculated as 6.25 X total nitrogen.

5.4 RESULTS

4.1 Photosynthesis and respiration

Gross photosynthetic rates recorded for *B. africana* were similar to those reported by P. Ferrar at Nylsvley. The net photosynthetic rates of *D. eriantha* and *P. maximum* were low in comparison with other world-wide C_4 grasses ($30mgCO_2dm^{-2}h^{-1}$). but were comparable to other studies (both on single leaves and whole plants) carried out at Nylsvley. Research performed, in the laboratory, on *D. eriantha* and *P. maximum*, also indicated a low maximum photosynthetic rate (e.g. $6mgCO_2dm^{-2}h^{-1}$) in young plants (10-15 days) at night/day temperatures of 12°/28°C.

4.1.1 Gross Photosynthesis

B. africana

Gross photosynthetic rates are presented in Ta-le 10. The difference in gross photosynthetic rates between non-necrotic and necrotic (1-10%) leaves proved insignificant (p = 0.05) (Figs. 64 and 65). However at the 25% level of necrosis gross photosynthetic rates (2.4 mg $CO_2dm^{-2}h^{-1}$) decreased in comparison to non-nectrotic leaves (3.5 mg $CO_2dm^{-2}h^{-1}$).

D. eriantha

Data are recorded in Table 11 (1978/79) and Table 12 (1979/80; 1980/81). Gross photosynthetic rates were unaffected in the early stages of rust-infection (Figs. 66, 68 and 69) characterized by yellow flecking. However at a later stage of the disease ie. at the onset of sporulation photosynthetic rates appeared to decrease. Reductions in rust-infected grasses were more significant (p = 0.05) in heavily infected leaves (50-75%) than leaves exhibiting a lower level of infection (<10%). During the post-sporulation period gross photosynthetic rates declined rapidly until senescence occurred (Fig. 6 For example in February 1980 rates decreased from 3.3 in healthy to 0.6 mg $CO_2dm^{-2}h^{-1}$ in 50-75% rust-infected leaves following sporogenesis (Table 12).

P. maximum

Gross photosynthetic rates are presented in Table 11 (1978/79) and Table 13 (1979/80 ; 1980/81). Similar results were obtained in tarspot-

Table 10 Gross photosynthetic rates (mg CO_2 $dm^{-2}h^{-1}$) of *E. africana* (1978/79;1979/80 season).

MONTHS	1978/79		1979/80	
	HEALTHY	NECROTIC	HEALTHY	NECROTIC
OCTOBER	2.0 ± 0.12	1-5% 1.7 ± 0.15	-	-
NOVEMBER	3.8 ± 0.14	1-5% 3.4 ± 0.15	2.9 ± 0.30	1-5% 2.3 ± 0.40
DECEMBER	3.7 ± 0.30	1-5% 3.6 ± 0.37	2.8 ± 0.27	1-5% 2.6 ± 0.18
FEBRUARY	2.8 ± 0.35	10% 2.4 ± 0.21	3.3 ± 0.40	10% 2.5 ± 0.50
MARCH	3.1 ± 0.30	10% 3.0 ± 0.36	3.5 ± 0.10	5% 2.8 ± 0.28 10% 2.6 ± 0.18 25% 2.4 ± 0.07
APRIL	2.6 ± 0.40	10% 2.? ± 0.11	2.3 ± 0.43	50% 1.3 ± 0.12

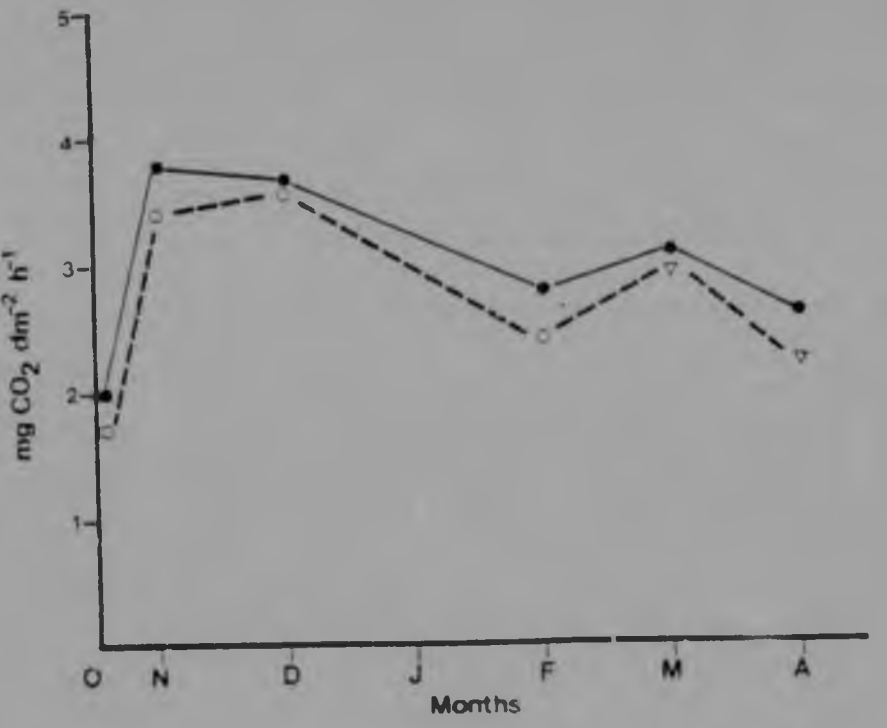


Fig.64 Gross photosynthetic rates of necrotic and non-necrotic *B.africana* leaves (1978/79)

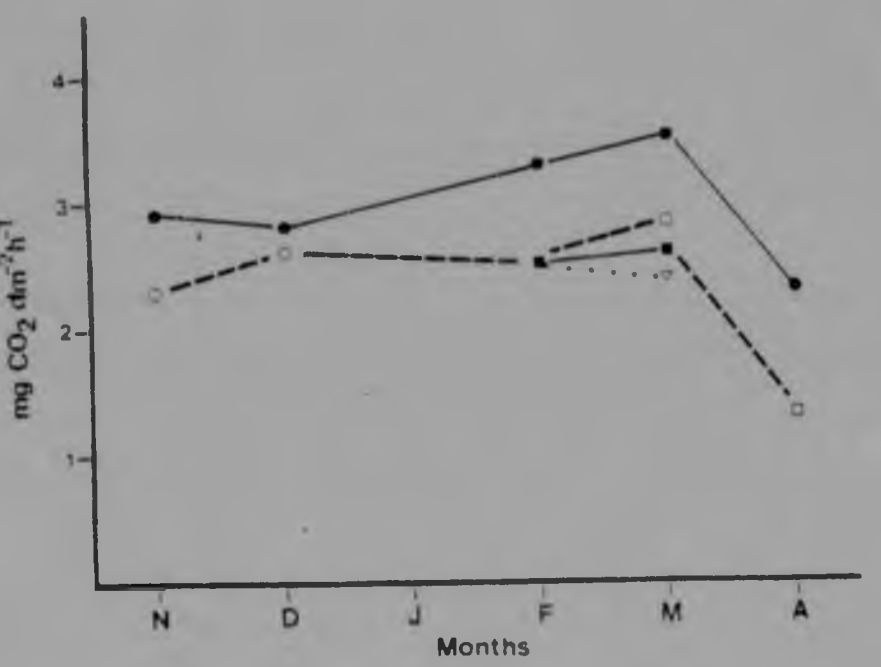


Fig.65 Gross photosynthetic rates of necrotic and non-necrotic *B.africana* leaves (1979/80)

Table 1. Gross photosynthetic rates (mg CO_2 $dm^{-2} h^{-1}$) of healthy and rust-infected *D. eriantha* and healthy and tarspot-infected *P. maximum* (1978/79).

MONTH	HEALTHY	RUST-INFECTED *D. eriantha*	
NOVEMBER	4.1 ± 0.08	1-5% flecking	3.9 ± 0.20
DECEMBER	5.3 ± 0.20	1-5% flecking	4.9 ± 0.13
	4.1 ± 0.06	25% sporulating	1.9 ± 0.17
DECEMBER	4.1 ± 0.08	sporulating	
		10%	4.5 ± 0.10
		25%	3.5 ± 0.08
		50%	2.4 ± 0.06

MONTH	HEALTHY	TARSPOT-INFECTED *P. maximum*	
NOVEMBER	3.8 ± 0.12	5%	3.6 ± 0.14
DECEMBER	3.4 ± 0.10	10%	3.0 ± 0.01

Table 12 Gross photosynthetic rates (mg CO_2 $dm^{-2}h^{-1}$) of healthy and rust-infected *D. [illegible]antha* (1979/80 and 1980/81).

MONTH	HEALTHY	INFECTED	
1979 NOVEMBER	2.6 ± 0.5	10% flecking	2.6 ± 0.30
DECEMBER	1.9 ± 0.3	Flecking	
		1%	2.0 ± 0.10
		5%	2.0 [illegible]
		10%	1.9 ± 0.10
		Sporulating	
		50%	1.0 ± 0.02
1980 JANUARY	1.6 ± 0.2	Flecking	
		1-5%	[illegible] ± 0.40
		10%	[illegible] ± 0.22
		Spor[illegible]ting	
		25%	0.8 ± 0.1[illegible]
		50-75%	0.3 ± 0.08
FEBRUARY	3.3 ± 0.2	Sporulating	
		1-5%	2.[illegible] ± 0.04
		10%	1.7 ± 0.12
		25%	0.9 ± 0.12
		Post-sporulation	
		50-75%	0.6 ± 0.08
MARCH	2.5 ± 0.3	Sporulating	
		1-5%	1.3 ± 0.2[illegible]
		10%	1.2 ± 0.15
		25%	0.9 ± 0.06
		Post-sporulation	
		50-75%	0.5 ± 0.05
OCTOBER	3.4 ± 0.4	Flecking	
		1-5%	3.2 ± 0.38
		Sporulating	
		25%	1.5 ± 0.03
		50%	0.8 ± 0.09
NOVEMBER	3.5 ± 0.9	Flecking	
		1-5	2.9 ± 2.00
		Sporulating	
		25%	2.3 ± 1.20
		50-75	1.3 ± 0.10
DECEMBER	4.5 ± 2.0	Sporulating	
		10%	[illegible] ± .50
		50-75	[illegible].1 ± 0.88

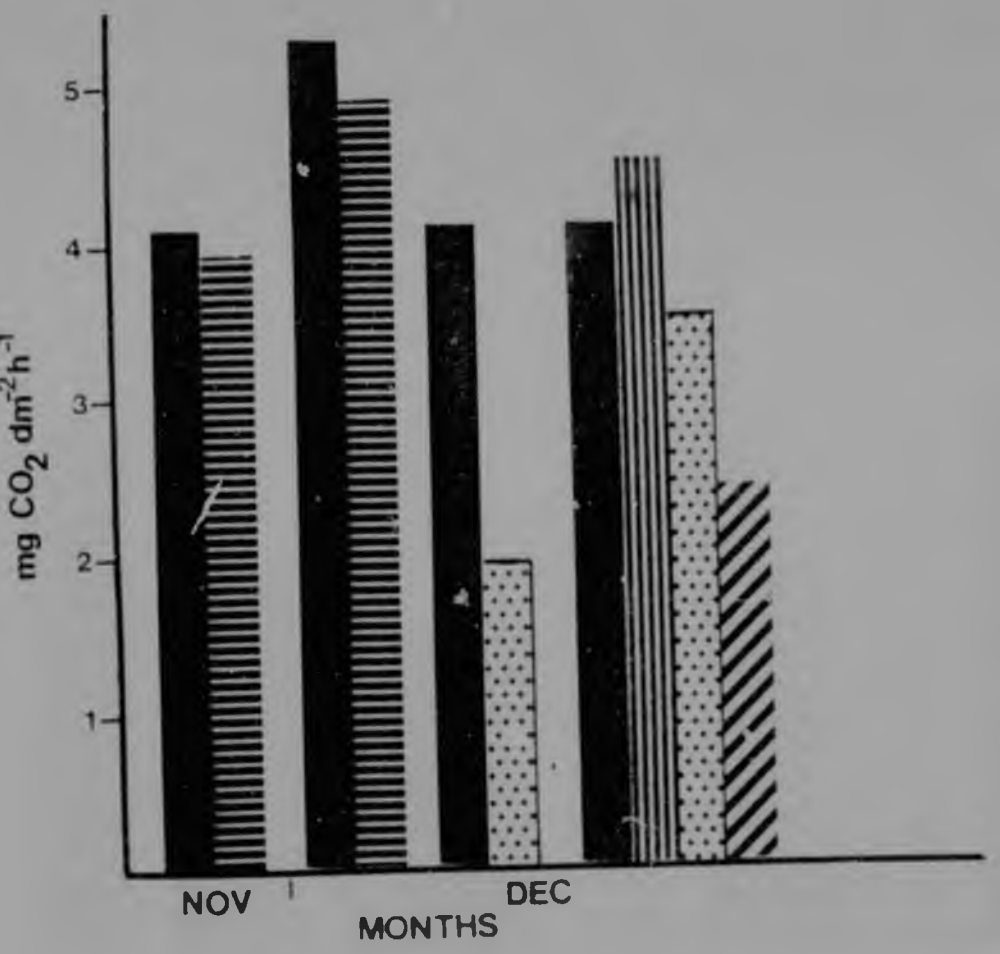


Fig.66 Gross photosynthesis in healthy and rust-infected *D.arianta* leaves (1978/79)

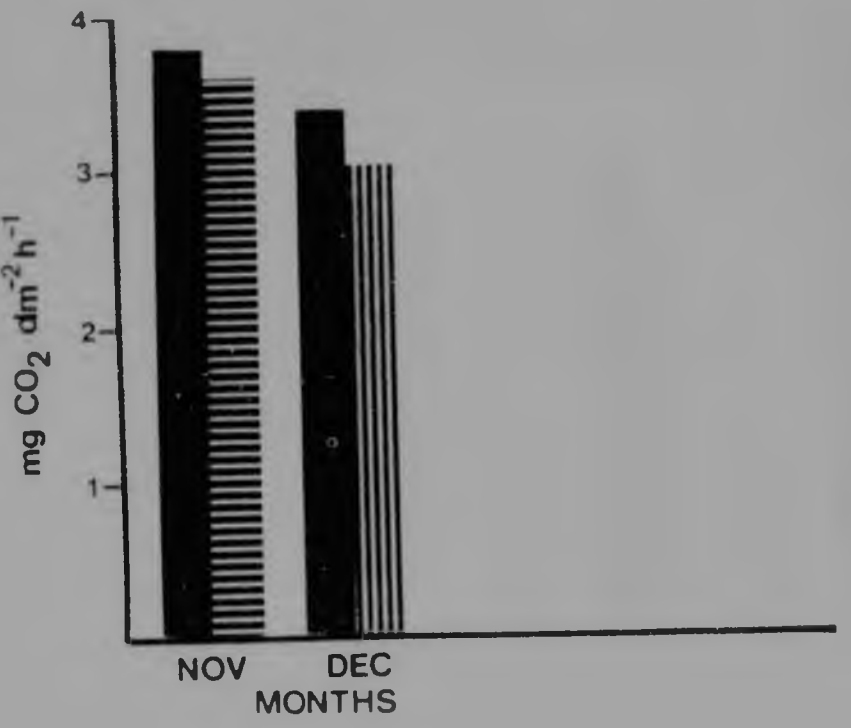


Fig.67 Gross photosynthesis in healthy and tarspot-infected *P.maximum* leaves (1978/79)

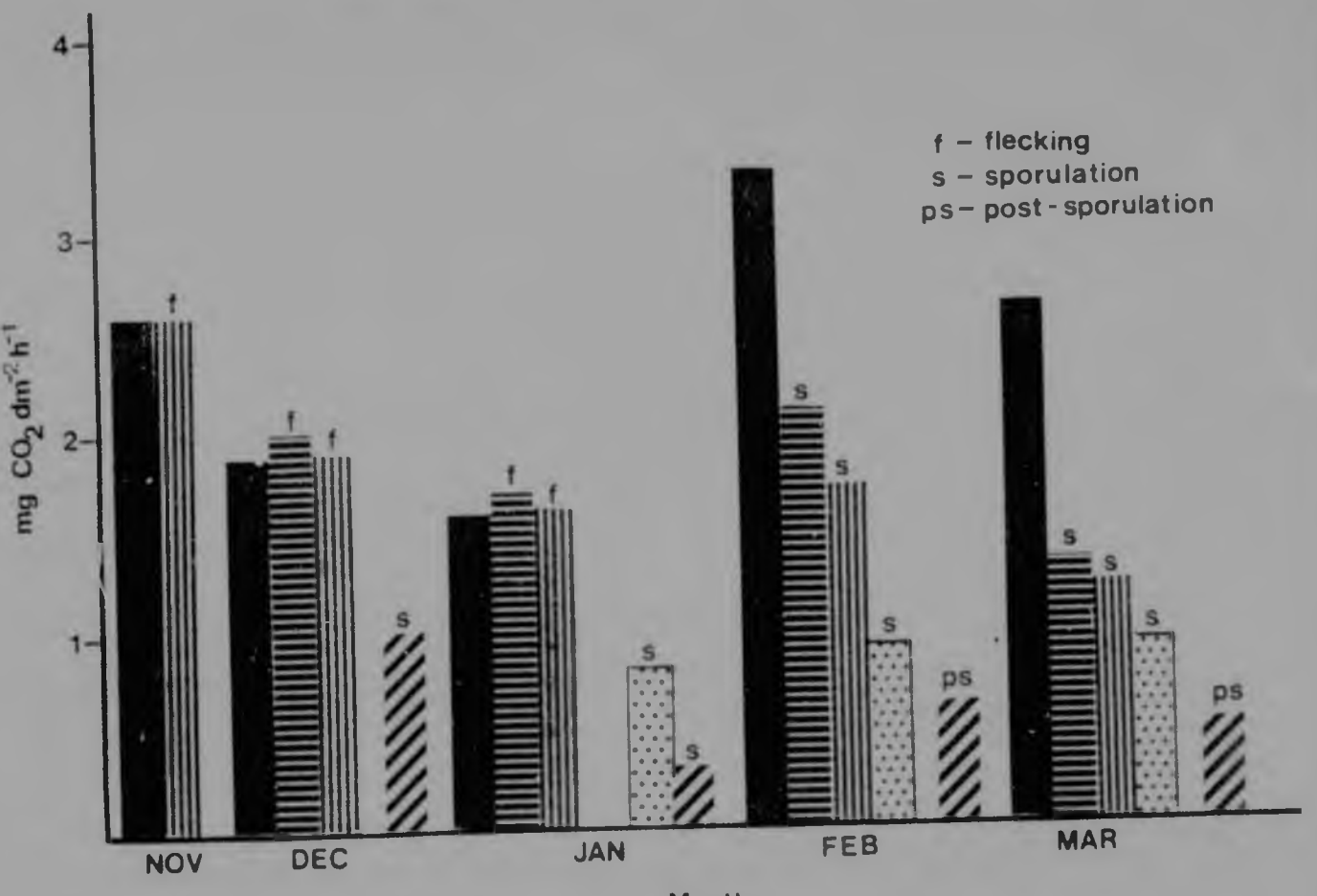


Fig. 68 Gross photosynthesis in healthy and rust-infected *D.eriantha* leaves (1979/80)

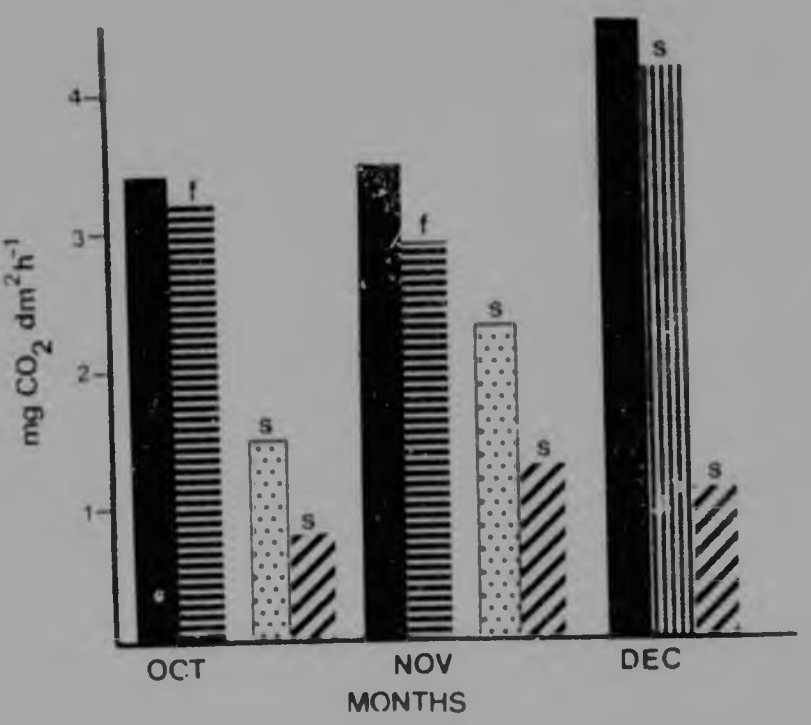


Fig.69 Gross photosynthetic rates in healthy and rust-infected *D.eriantha* (1980/81)

Table 13 Gross photosynthetic rates (mg CO_2 dm $^{-2}$ h $^{-1}$) of healthy and tarspot - infected *P. maximum* (1979/80 and 1980/81 season).

MONTH	HEALTHY	INFECTED
1980 JANUARY	1.6 ± 0.25	1-5% 1.5 ± 0.58
FEBRUARY	2.1 ± 0.70	1-5% 2.0 ± 0.10 10% 1.8 ± 0.04 25% 0.8 ± 0.03
MARCH	2.2 ± 0.13	1-5% 2.1 ± 0.07 10% 1.1 ± 0.10 25% 0.7 ± 0.04 50-75% 0.5 ± 0.02
NOVEMBER	2.2 ± 0.90	1-5% 1.9 ± 0.40 25% 1.6 ± 0.20

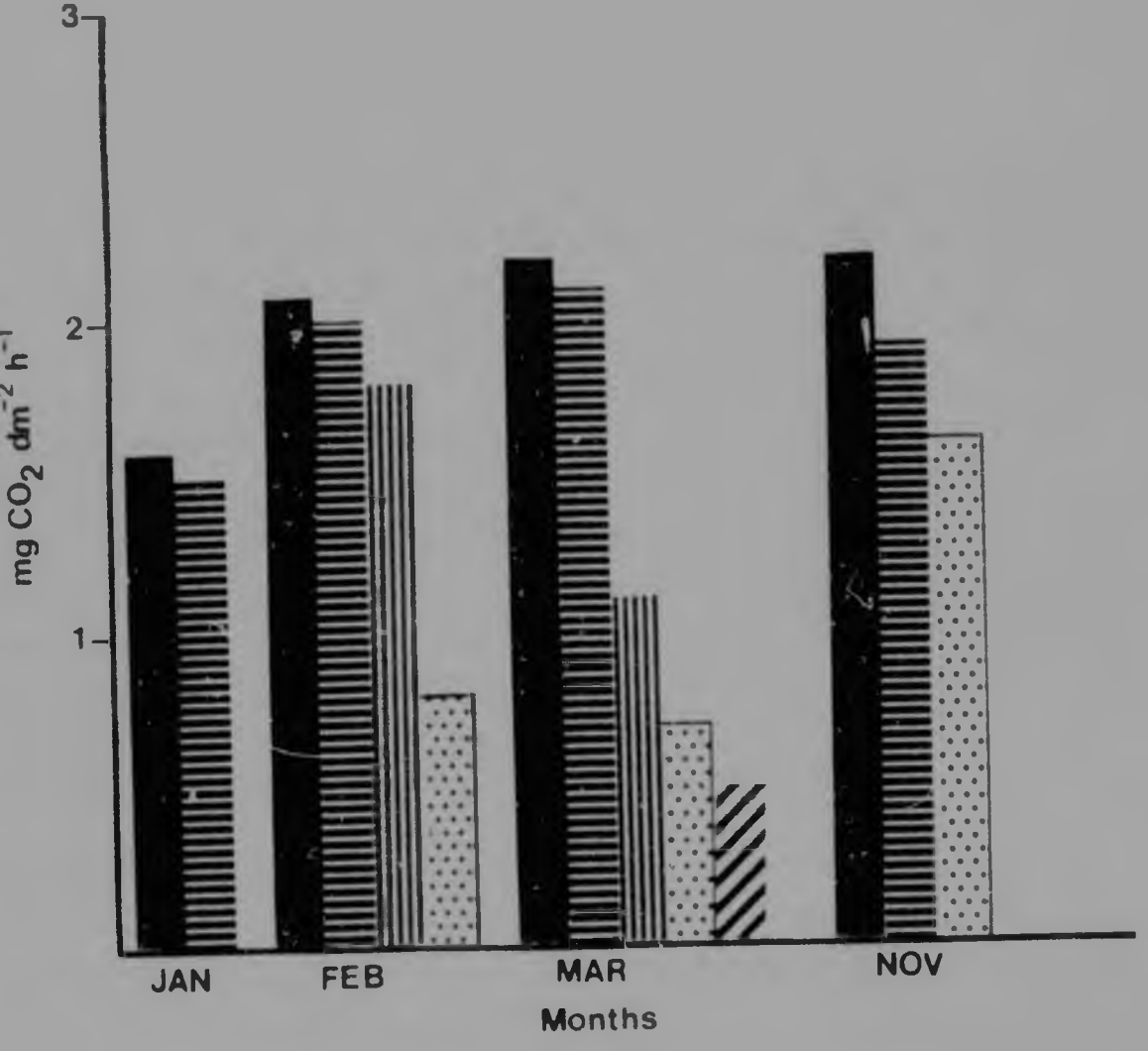


Fig.70 Gross photosynthesis in healthy and tarspot-infected *P. maximum* leaves (1979/80 and 1980/81)

infected leaves as in rust-infected *D. eriantha*. Gross photosynthesis was unaffected at low intensities of infection (1-10%) but decreased at higher levels of disease (>10%) (Figs. 67 and 70). Paired T-tests showed the differences between healthy and tarspot-infected *P. maximum* to be highly significant ($p = 0.05$) in heavily infected leaves (50-75%). The reductions in gross photosynthesis were less dramatic in *P. maximum* (Figs. 67 and 70) than in the case of *D. eriantha* (Figs. 66, 68 and 69).

4.1.2 Net Photosynthesis

D. eriantha

From Fig. 59 it appeared as if *D. eriantha* ceased to photosynthesize in the mid-day, probably due to closure of stomata under water stress. The net photosynthetic rates presented in Table 14 and illustrated in Fig. 71A are taken from measurements in early mornings and afternoons. No significant difference was observed between healthy and rust-infected leaves during the early flecking stage. In some cases net photosynthetic rates were even increased to a small extent in flecked leaves e.g. in January 1982 rates increased from 3.2 in healthy to 3.4 mg $CO_2 dm^{-2} h^{-1}$ in infected leaves (Table 14). however paired T-tests revealed significant differences between healthy and heavily infected (> 25%) leaves. Photosynthetic rates decreased in leaves exhibiting >10% sporulating pustules, with a positive correlation between net photosynthesis and degree of infection.

The effect of increasing CO_2 concentrations on net photosynthesis of healthy and rust-infected *D. eriantha* is illustrated in Fig. 71B. Leaf temperature and resistance measurements, and radiation regimes were kept as constant as possible for each pair of photosynthetic runs on healthy and infected leaves. However the conditions varied between pairs of runs resulting in different photosynthetic rates. Therefore it was decided not to average the replicates. However the response of photosynthetic rates in healthy and infected leaves to changing CO_2 concentrations were similar in all experiments, and only one comparison is depicted in Fig. 71B.

Net photosynthesis increased in both healthy and infected *D. eriantha* leaves as the CO_2 concentration was increased from 120 to 420ppm in healthy leaves and from 110 to 362ppm in infected plants (Fig. 71B), but dropped after CO_2 concentrations exceeded 420ppm. However the response was more significant in infected leaves (25% flecking) in comparison to healthy leaves.

Table 14 Net photosynthetic rates and dark respiration (mg CO_2 $dm^{-2}h^{-1}$) of healthy and rust-infected *D. eriantha* (1980/81;1981/82).

MONTH	HEALTHY	RUST-INFECTED	
1980 NOVEMBER	2.2 ± 0.5	1-5% early flecking	2.2 ± 0.4
DECEMBER	2.0 ± 0.6	50-75% sporulating	0.7 ± 0.2
1981 FEBRUARY	2.2 ± 0.2	1-5% early flecking	1.8 ± 0.3
	2.5 ± 0.1	25% sporulating	1.0 ± 0.4
DECEMBER	3.0 ± 0.5	25% sporulating	1.9 ± 0.4
1982 JANUARY	3.2 ± 0.6	10% flecking	3.4 ± 0.5
		25% sporulating	1.9 ± 0.4
		50-75%	1.2 ± 0.1
DARK RESPIRATION			
1980 DECEMBER	1.9 ± 0.4	10% flecking	2.5 ± 0.5
	2.3 ± 0.4	50-75% sporulating	3.5 ± 0.1
1981 JANUARY	2.3 ± 0.4	10% sporulating	2.2 ± 0.2
	2.0 ± 0.3	25%	3.1 ± 0.4
		50-75%	3.8 ± 0.2

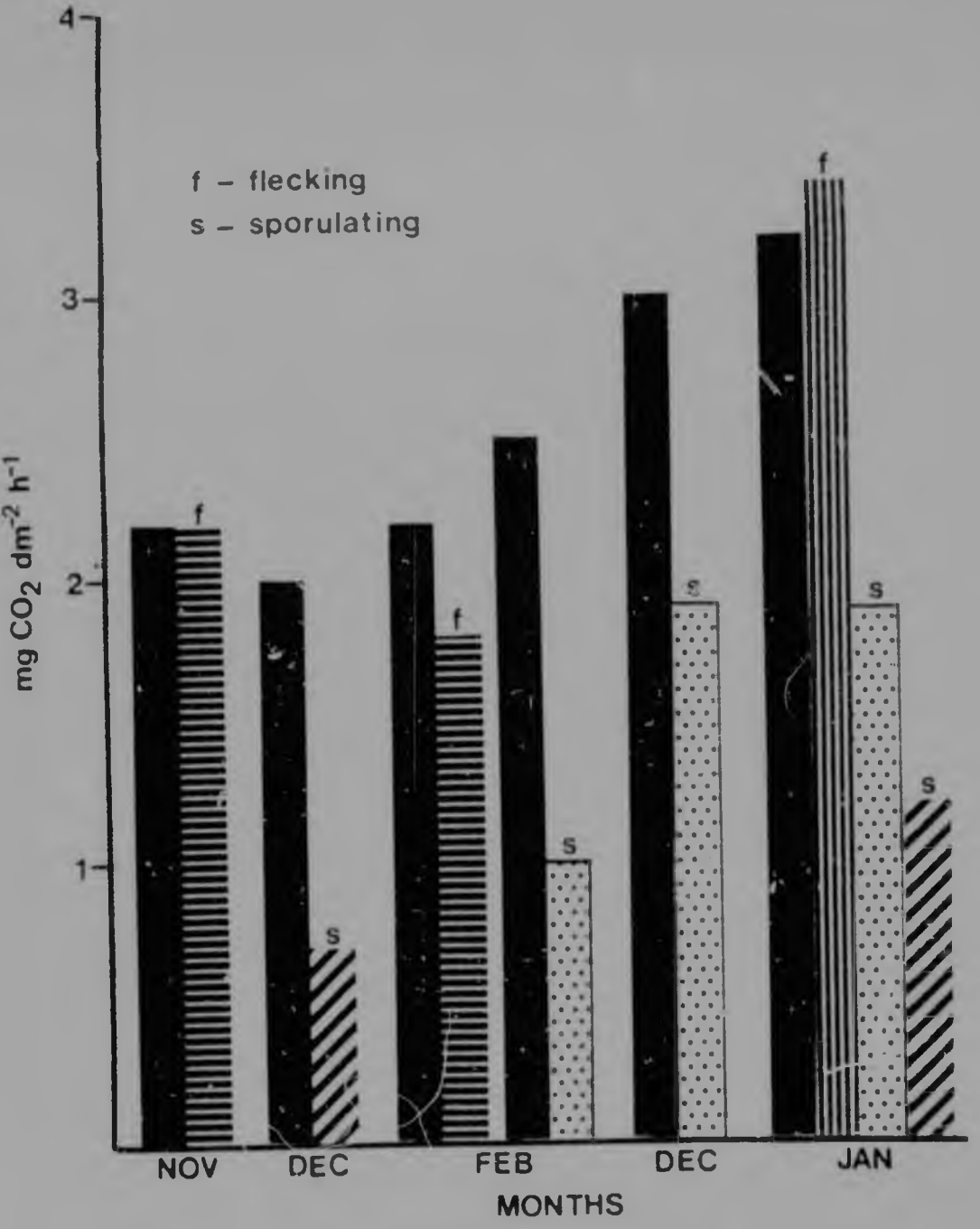


Fig.7' A Net photosynthetic rates of healthy and rust-infected *D. ...antha* leaves (1980/81 and 1981/82)

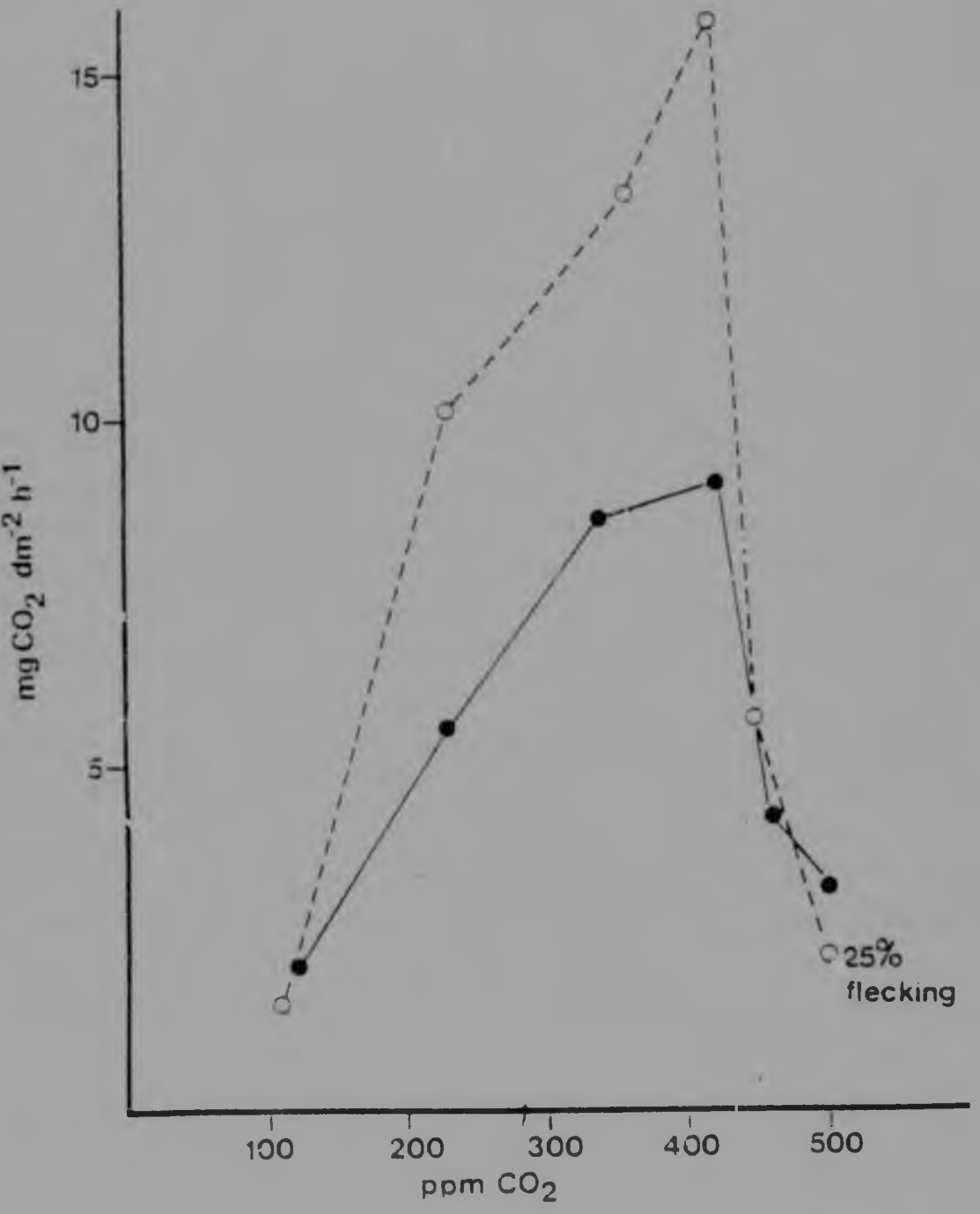


Fig.71 B Response of healthy and rust-infected *D.eriantha* leaves to increasing CO_2 concentrations

P. maximum

From the daily photosynthetic runs of *P. maximum* (Fig. 60), it appeared as though this grass was not influenced by water stress and photosynthesis continued during the mid-day period, even though rates dropped slightly probably due to partial stomata closure at mid-day. This is understandable since *P. maximum* is a shade plant.

Results are presented in Table 15 and Fig. 73. Net photosynthetic rates declined in tarspot-infected leaves (Fig. 73). However differences only became significant ($p = 0.05$) when infection levels exceeded 10%. There was a similar pattern to that of rust-infected *D. eriantha*, where a positive correlation occurred between net photosynthesis and extent of infection.

4.1.3 C_4 photosynthetic enzymes

Fig. 51 illustrates the C_4 photosynthetic pathways.

D. eriantha

Photosynthetic enzyme activities are recorded in Table 16. Enzyme rates of healthy and rust-infected leaves are illustrated in Figs. 74 and 75 in the 1980/81 season and experiments were repeated in the 1981/82 season (Figs. 76 and 77).

This grass is considered to be chiefly a malate former ie. NADP-malic enzyme (NADP-ME) type (Fig. 51). C_4 photosynthetic enzyme studies demonstrated NADP-ME and NADP-malic dehydrogenase activities in healthy leaves, but there was no trace of these enzymes in sporulating leaves (Figs. 74 and 76). However stimulation of the alanine forming pathway enzymes aspartate aminotransferase, PEP carboxykinase (PCK) and alanine aminotransferase was observed in sporulating leaves (10-25%) (Figs. 75 and 77). However once sporogenesis ceased, these enzymes decreased in activity during post-sporulation until senescence occurred. These results indicate a shift from the malate to the alanine forming pathway in sporulating leaves.

The carboxylating enzymes PEP carboxylase (PEPC) and RuBP carboxylase (RuBPC) increased in activity during the early stages of infection

Table 15 Net photosynthesis (mg CO_2 dm $^{-2}h^{-1}$) of healthy and tarspot-infected *P. maximum* (1981/82).

MONTH	HEALTHY	TARSPOT-INFECTED
1981 FEBRUARY	4.4 ± 0.75 4.3 ± 0.70 2.1 ± 0.10	10% 3.8 ± 0.80 25% 2.3 ± 0.40 50% 0.5 ± 0.20
1982 JANUARY	3.6 ± 0.13 4.2 ± 0.30 1.2 ± 0.20	10% 3.7 ± 0.27 25% 2.9 ± 0.10 10% 1.3 ± 0.20
FEBRUARY	3.0 ± 0.60 2.2 ± 0.05	25% 1.6 ± 0.02 25% 0.7 ± 0.05

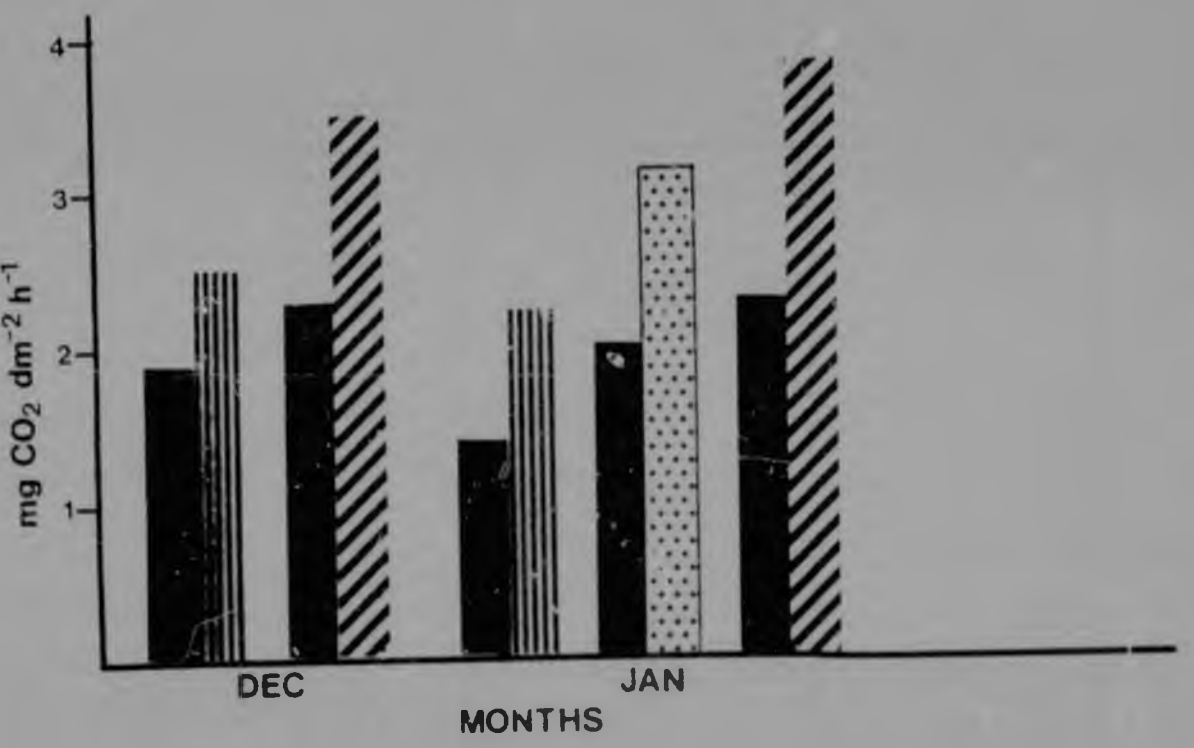


Fig.72 Dark respiration rates measured in healthy and rust-infected *P.eriantha* leaves(1981/82)

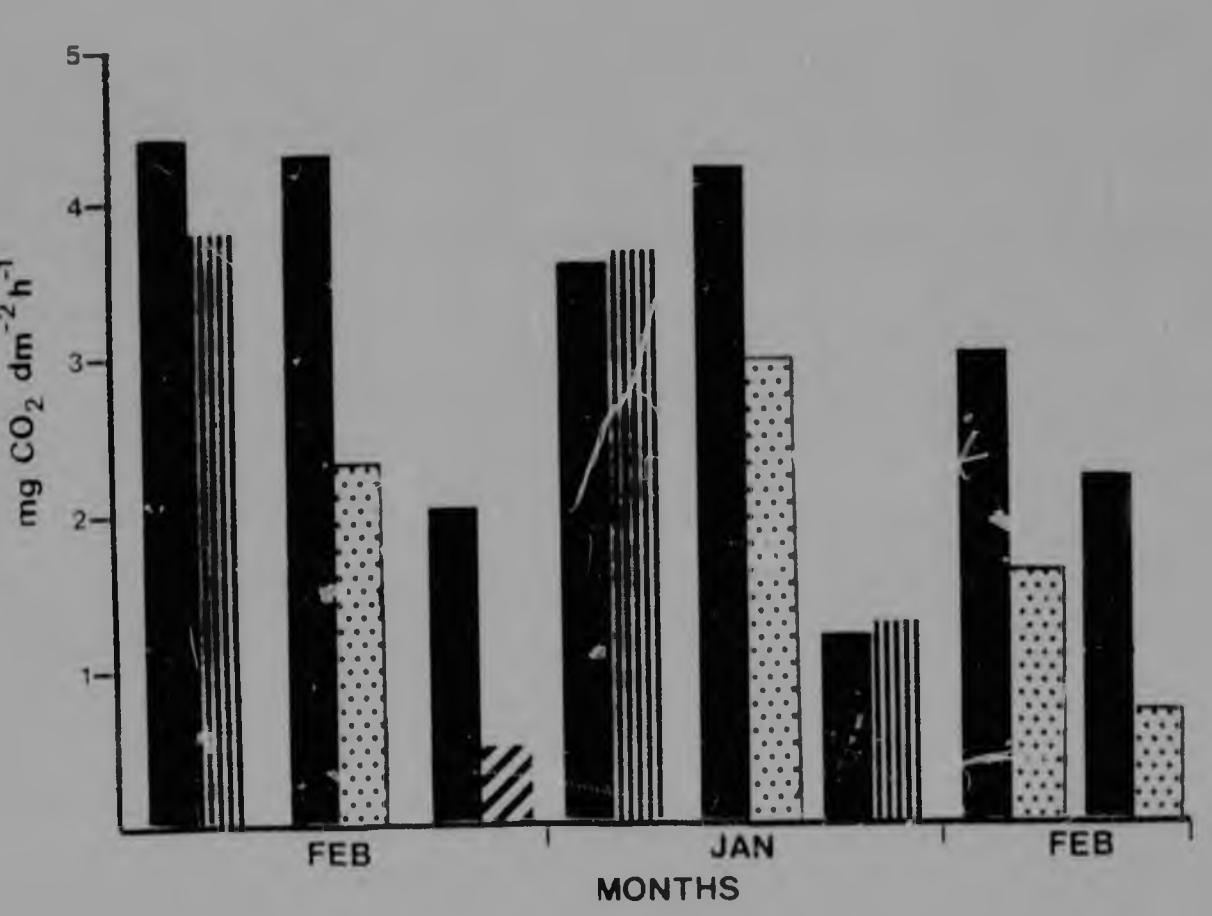


Fig.73 Net photosynthesis in healthy and tarspot-infected *P.maximum* leaves (1981/82)

Table 16 C_4 photosynthetic and respiration enzyme act[illegible]
of healthy and rust-infected [illegible] 1980/81; 1981/82 seasor

ENZYME	1980/81		1981/82	
	HEALTHY	RUST-INFECTED	HEALTHY	RUST-INFECTED
Succinate dehydrogenase (µmoles NAD mgchl^{-1} min^{-1})	34 ± 2.8	flecking 10% 39.0 ± 2.6 sporulating 25% 50.9 ± 2.9 50% 59.5 ± 0.8	[illegible]	sporulating 25% 22.2 ± Post-sporulation
NAD-malate dehydrogenase (µmoles NAD mgchl^{-1} min^{-1})	17.[illegible] ± 0.6	flecking 10% 28 ± 13 sporulating 25% 68 ± 5 Post-sporulation 50% 39 ± 12	[illegible] 22.6 ±	78.5 ± Post-spor[illegible]
RuBP carboxylase (µmoles CO_2 mgch[illegible]	5.3 ± 0.6	sporulating 10% 18.6 ± 0.7 25% 28.6 ± 0.7	[illegible] ± 0.6 8.5 ± 0.3	sporulating 50-75% 51.4 ± Post-sporulati[illegible] 50-75% 7.3 ± 0.9
PEP carboxylase (µmoles CO_2 mgchl [illegible]	6.8 ± 0.5	sporulating 10% 7.8 ± 1.1 25% 27.7 ± 2.0	36.4 ± [illegible] 57.1 ± [illegible]	sporulati[illegible] 25% 53.2 ± 50-75% 106.8 ±
NADP-malic enzyme (µmoles NADP mgchl^{-1} min^{-1})	5.0 ± 0.5	-	4.2 ± 0.5	-
NADP-malic dehydrogenase (µmoles NADPH mgchl^{-1} min^{-1})	1.3 ± 0.2	-	1.6 ± 0.3	-
Alanine aminotransferase (µmoles NAD mgchl^{-1} min^{-1})	0.8 ± 0.1	sporulating 10% 3.2 ± 0.7 25% 2.8 ± 0.3 50% 6.9 ± 0.9	3.0 ± 0.2 2.8 ± 0.2	sporulating 25% 8.3 ± Post-sporulation 50-75% 0.9 -
Aspartate aminotransferase (µmoles NAD mgchl^{-1} min^{-1})	5.0 ± 0.4	sporulating 10% 30.3 ± [illegible] 25% 33.8 ± 0.5 50% 23.3 ± 0.9	3.9 ± 0.3 5.4 ± 0.4	sporulating 10% 9.0 ± Post-sporulation 50-75% 4.[illegible]
PEP carboxykinase (µmoles CO_2 mgchl^{-1} m[illegible]	60.0 ± 2.0 44.0 ± 3.0 63.5 ± 2.1	flecking 10% 66.0 ± 2.5 sporulating 25% 59.0 ± 3.2 Post-sporulation 50-75% 63.0 ± 1.8	9.8 ± 0.8	sporulating 25% 21.0 ± Post-sporulation 25% 3.8 ± [illegible] 50% [illegible] ±

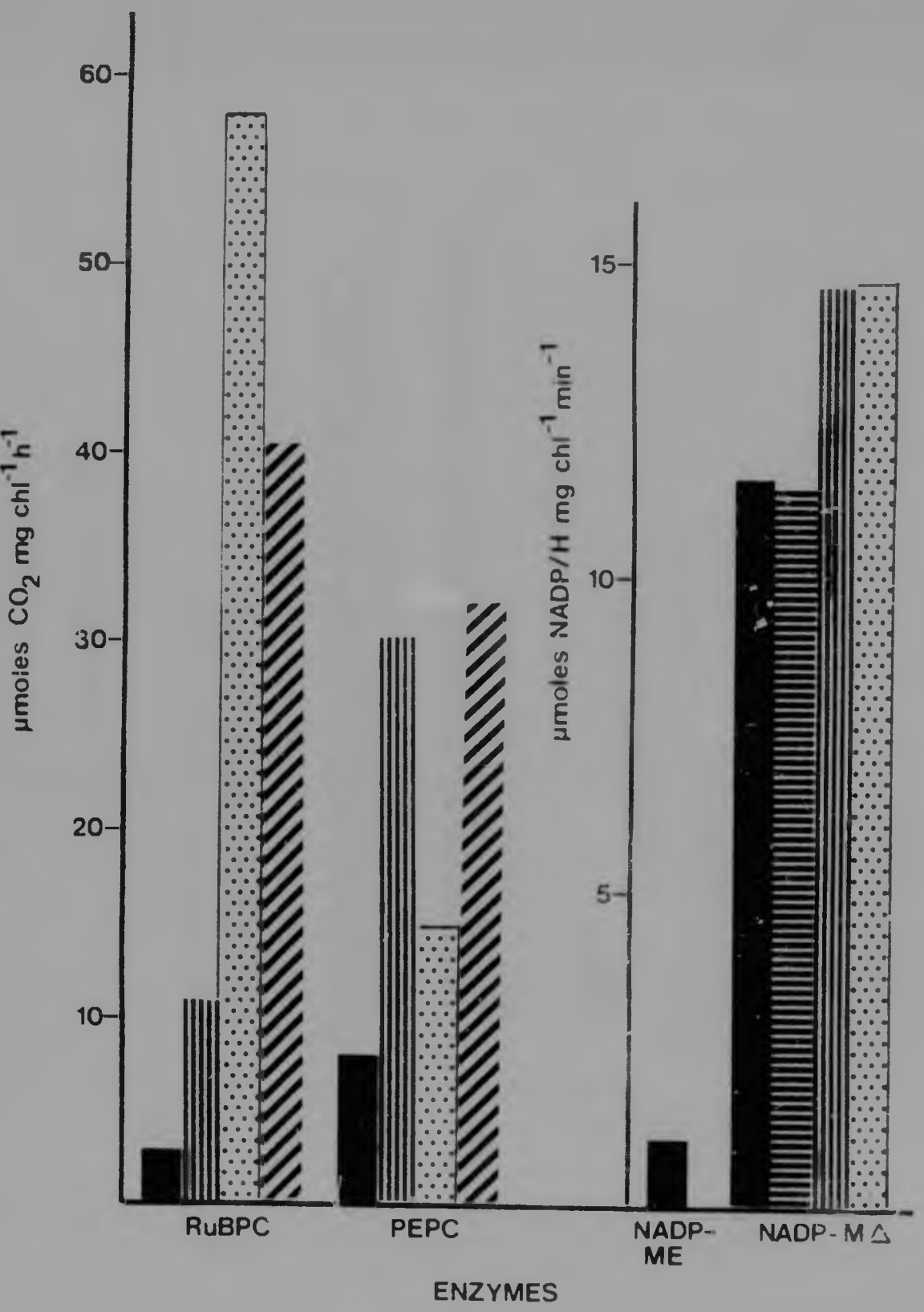


Fig.74 C_4 photosynthetic enzyme activities (RuBP carboxylase; PEP carboxylase; NADP-malic enzyme and NADP-malate dehydrogenase) in healthy and rust-infected *D.eriantha* leaves (1980/81)

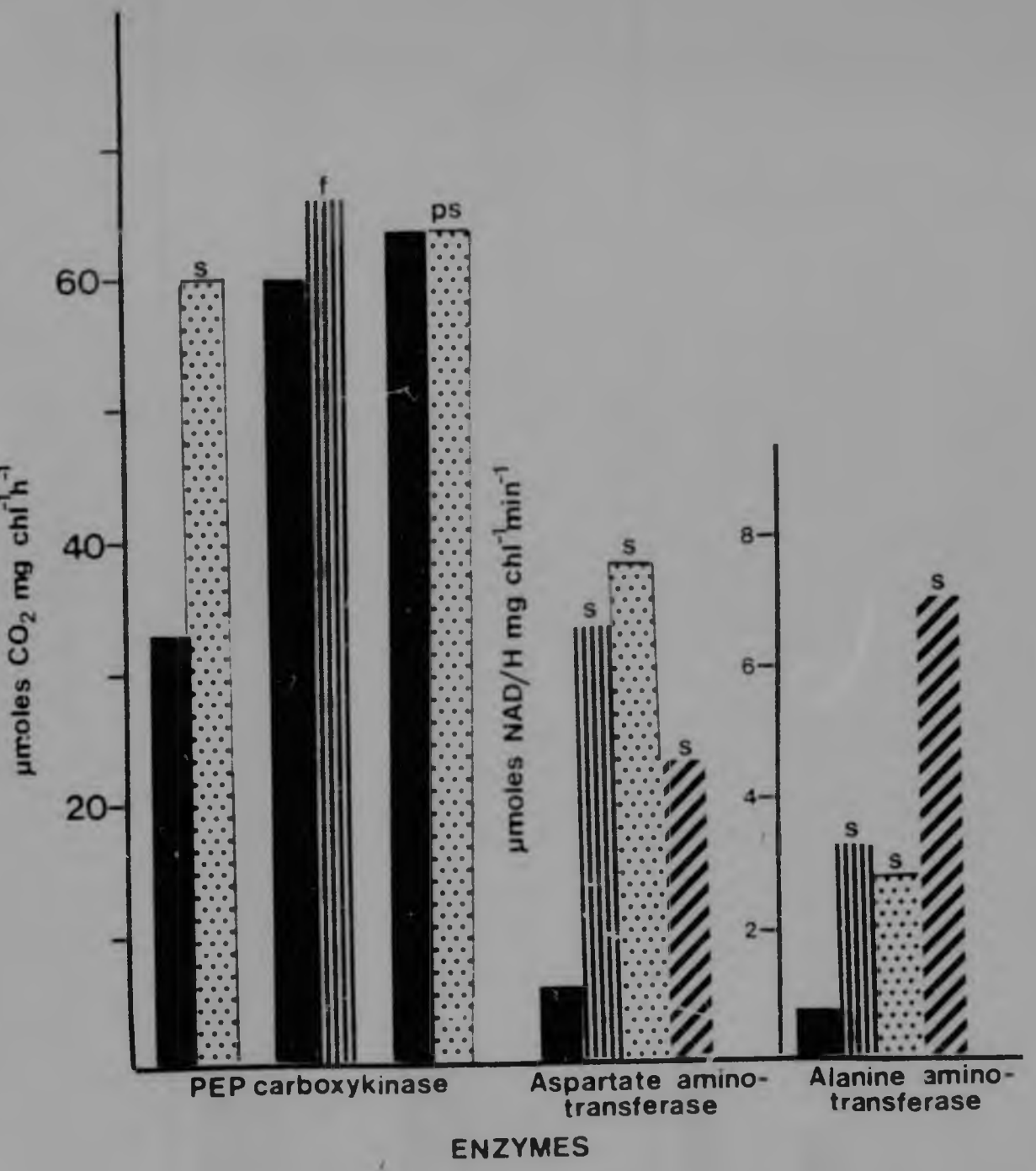


Fig.75 C_4 photosynthetic enzyme activities (PEP carboxykinase; Aspartate amino-tranferase and Alanine aminotransferase) in healthy and rust-infected *D.eriantha* leaves (1980/81)

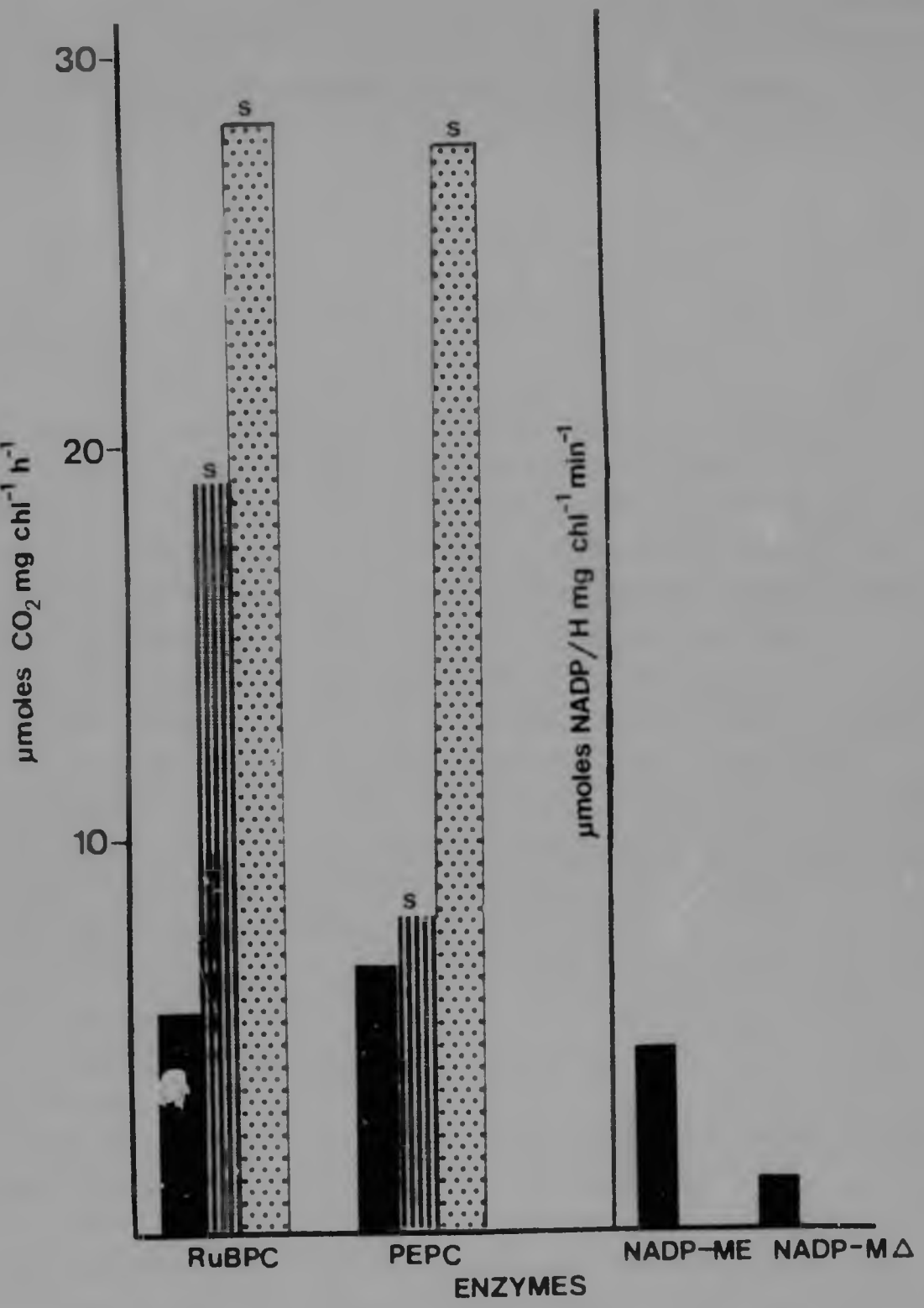


Fig.76 C_4 photosynthetic enzyme activities in healthy and rust-infected *D.eriantha* leaves (1981/82)

(late flecking and early sporulation), but enzyme activity decreased after sporogenesis (Figs. 74 and 76). Leaves with higher levels of infection (50-75%) showed greater stimulation in enzyme activities than the less infected leaves (<25%) at p = 0.05 significant level (Table 16).

P. maximum

Photosynthetic enzyme rates are depicted in Table 17 and Figs. 78 and 79.

P. maximum possesses malate forming enzymes but is a suspected PCK-type, although extremely low levels were detected in this study. NADP-malic enzyme activity was extremely low in healthy leaves (1.1umoles mg $chl^{-1} min^{-1}$) but no activity was detected in tarspot-infected leaves (Fig. 78). There was small change in NADP-malic dehydrogenase activity from healthy to infected leaves (Fig. 78). The respiratory enzyme NAD-malic dehydrogenase increased markedly in activity in tarspot-infected leaves (10-25%) (Fig. 79), as did RuBPC and PEPC rates (Fig. 79). Enzyme rates increased to a greater extent in RuBPC than PEPC (p = 0.05). A small change in alanine aminotransferase was noted between healthy and tarspot-infected leaves (1-25%). Asparatate aminotransferase rates decreased in infected leaves (Fig. 79).

4.1.4 Respiration

1.4.1 Dark respiration

D. eriantha

Results are presented in Table 14. Experimental data revealed that dark respiration rates increased from 1.9 mg CO_2 $dm^{-2}h^{-1}$ in healthy *D. eriantha* leaves to 2.5 in leaves exhibiting 10% flecking (Fig. 72). Dark respiration continued to increase into the sporulation stage of infection, and the most significant stimulation was observed in heavily infected leaves (50-75%).

1.4.2 Succinate and NAD-malate dehydrogenase

D. eriantha

The respiratory enzymes (Kreb Cycle) succinate dehydrogenase and

Table 17 C_4 photosynthetic and respiration enzyme activities of healthy and tarspot-infected *P. maximum* (1980/81).

ENZYME	HEALTHY	TARSPOT-INFECTED
Aspartate amino transferase (μmoles NADH $mgchl^{-1}$ min^{-1})	73.6 ± 3.0	1-5% 35.5 ± 6.0 10% 42.2 ± 3.0 25% 23.7 ± 3.5
Alanine aminotransferase (μmoles NAD $mgchl^{-1}$ min^{-1})	9.6 ± 0.9	1-5% 8.8 ± 1.0 10% 8.6 ± 0.6 25% 7.1 ± 0.6
NADP-malic enzyme (μmoles NADP $mgchl^{-1}$ min^{-1})	1.1 ± 0.2	-
NAD-malic dehydrogenase (μmoles NAD $mgchl^{-1}$ min^{-1})	39.4 ± 3.0	1-5% 43.5 ± 13.0 10% 90 ± 17.0 25% 120 ± 33.0
NADP-malic dehydrogenase (μmoles NADPH $mgchl^{-1}$ min^{-1})	11.6 ± 1.3	1-5% 11.5 ± 1.4 10% 14.5 ± 2.0 25% 14.6 ± 1.1
RuBP carboxylase (μmoles CO_2 $mgchl^{-1}$ h^{-1})	3.0 ± 0.1	10% 10.6 ± 1.4 25% 58.3 ± 1.6 50% 40.5 ± 1.8
PEP carboxylase (μmoles CO_2 $mgchl^{-1}$ h^{-1})	8.1 ± 0.4	10% 29.9 ± 2.0 25% 14.7 ± 2.3 50% 32.2 ± 1.9
Succinate dehydrogenase (μmoles NAD $mgchl^{-1}$ min^{-1})	8.5 ± 0.8	10% 12.2 ± 1.0 25% 15.6 ± 0.5 50% 23.3 ± 0.9

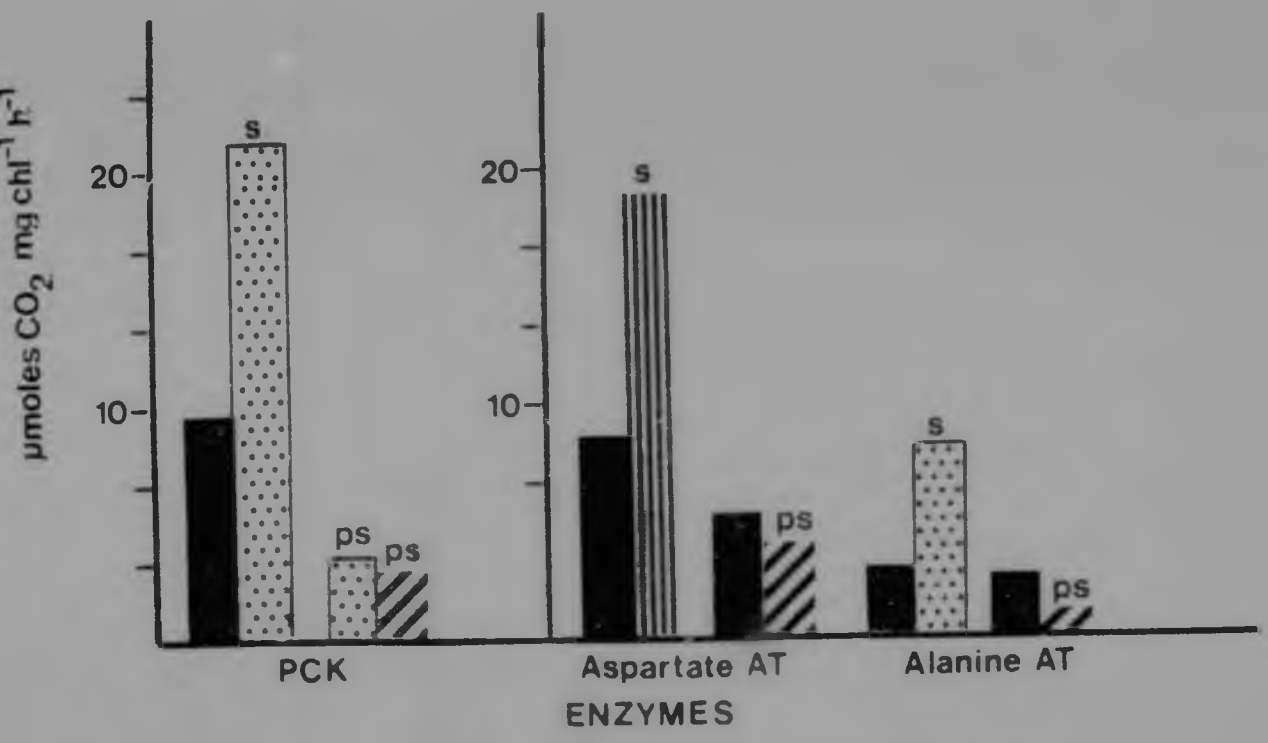


Fig.77 C_4 photosynthetic enzyme activities in healthy and rust-infected *P. antidotale* leaves (1981/82)

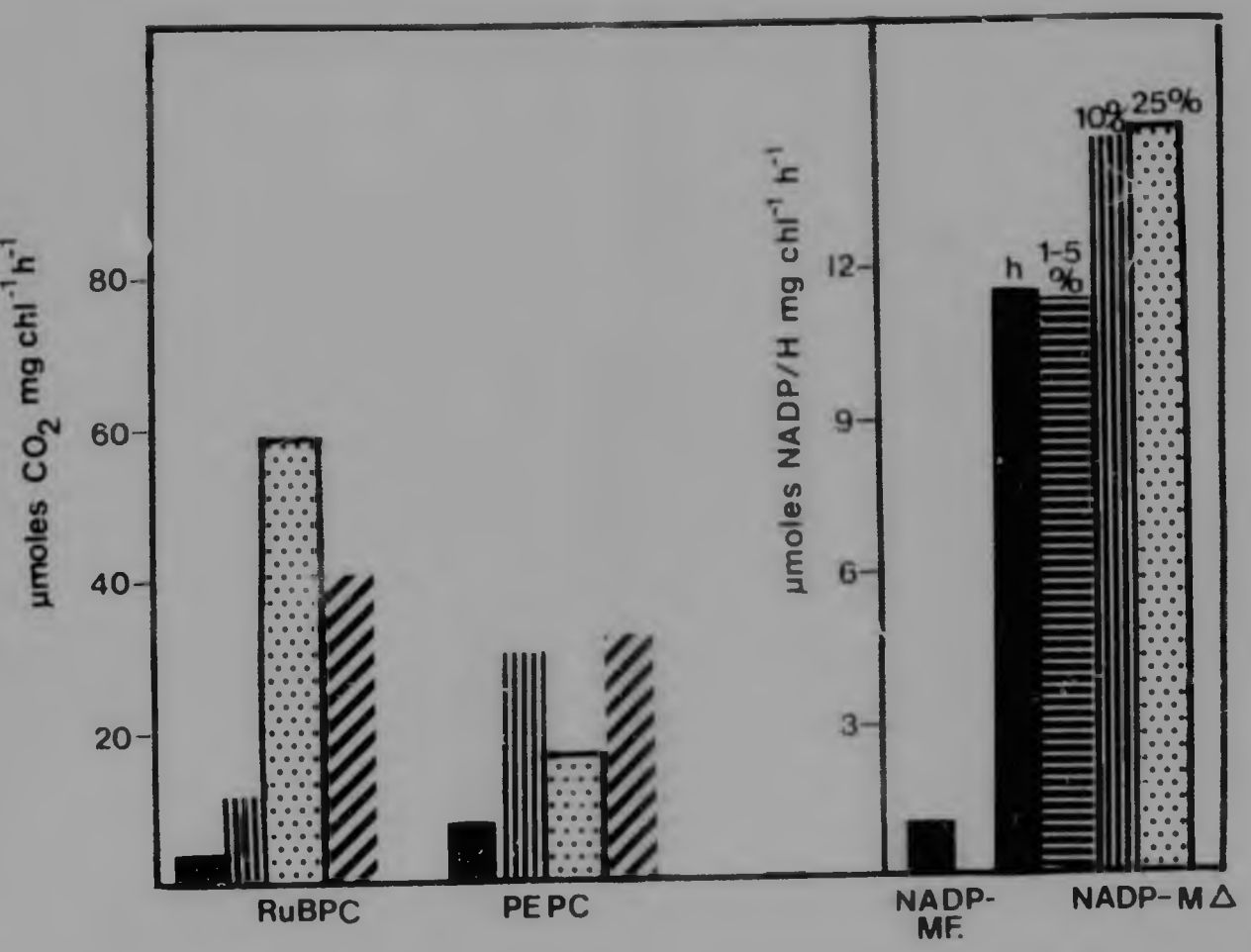


Fig.78 C_4 photosynthetic enzyme activities in healthy and tarspot-infected *P.maximum* leaves (1980/81)

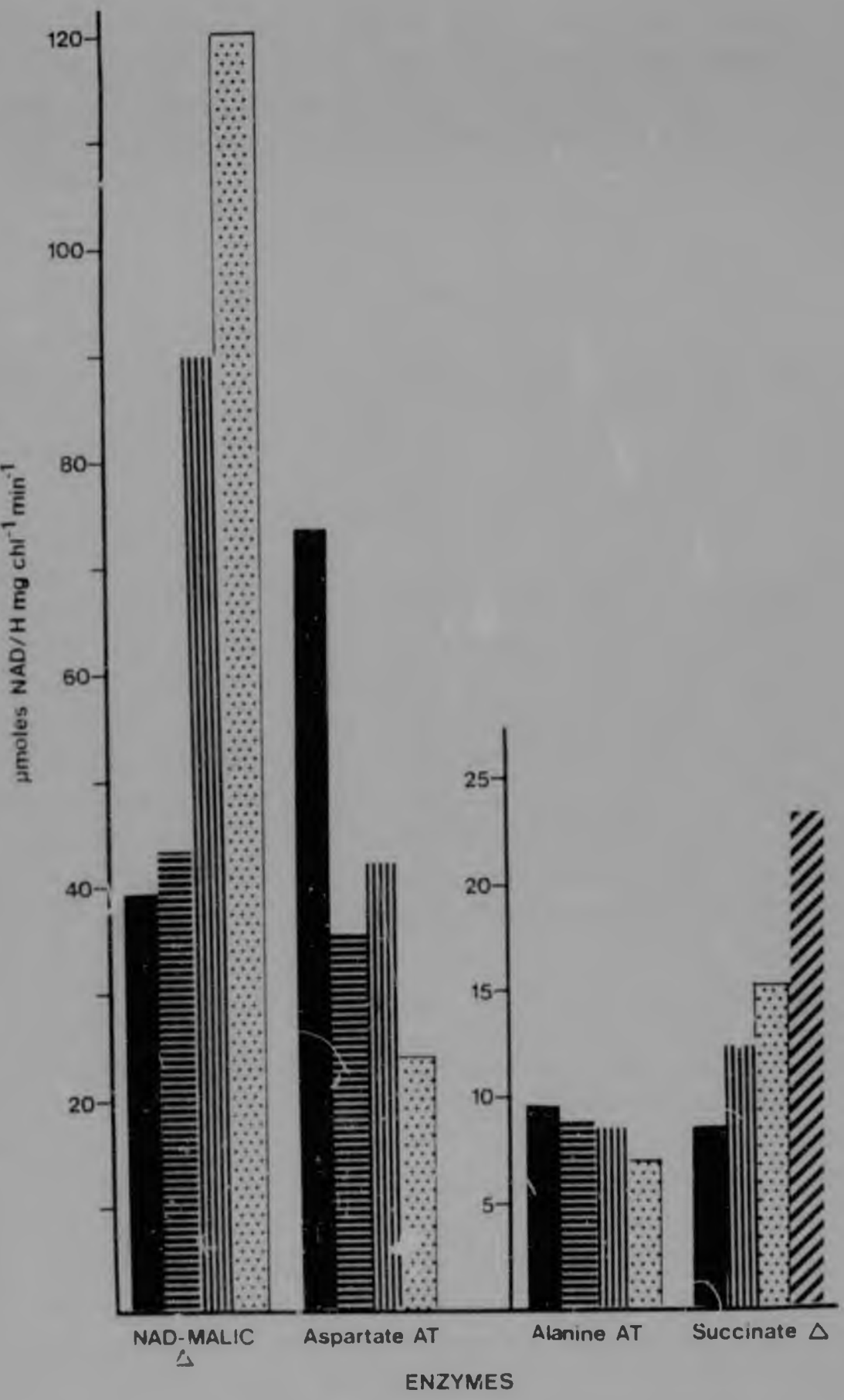


Fig.79 C_4 photosynthetic enzyme activities in healthy and tarspot-infected *P.maximum* leaves (1980/81), and the dark respiration enzymes NAD-malate dehydrogenase and succinate dehydrogenase

NAD-malate dehydrogenase both increased in activity in sporulating leaves (Figs. 80 and 81). In the case of NAD-malate dehydrogenase, the enzyme decreased in the post-sporulation stage but still exhibited a significantly greater stimulation than in healthy leaves (Table 16).

P. maximum

The results (Table 17) indicated a marked stimulation of NAD-malic dehydrogenase, but only a small increase in the enzyme rates of succinate dehydrogenase in 10-25% tarspot-infected leaves (Fig. 79). At 50% infection levels the increase in succinate dehydrogenase became significant.

4.1.5 Chlorophyll

B. africana

Chlorophyll content of non-necrotic and necrotic leaves is recorded in Table 18. Differences in chlorophyll content between necrotic (1-10%) and non-necrotic leaves were insignificant ($p = 0.05$) (Figs. 82 and 83). There is however a significant decrease in chlorophyll in leaves exhibiting 25% necrosis. The effects of necrosis are localized and when the lesion areas are small (1-10%) the effects on the remainder of the leaf tissue are negligible. In some cases the non-necrotic tissue may even compensate for the areas of necrosis. Halos of chlorosis around the necrotic lesions were observed infrequently.

D. eriantha

From the results obtained for chlorophyll content (Table 19) it appeared that the rust infection had no effect on chlorophyll in infected leaves at the early stages of flecking (Fig. 84). However as the disease progressed and sporulation commenced, chlorophyll levels began to decline in heavily infected leaves (>25%). During post-sporulation chlorophyll content declined rapidly until leaf senescence occurred (Fig. 84). There was also a positive correlation between intensities of infection and chlorophyll content. Leaves showing a high level of infection (50-75%) showed a more significant decrease in chlorophyll than leaves with lower degrees of disease (<25%).

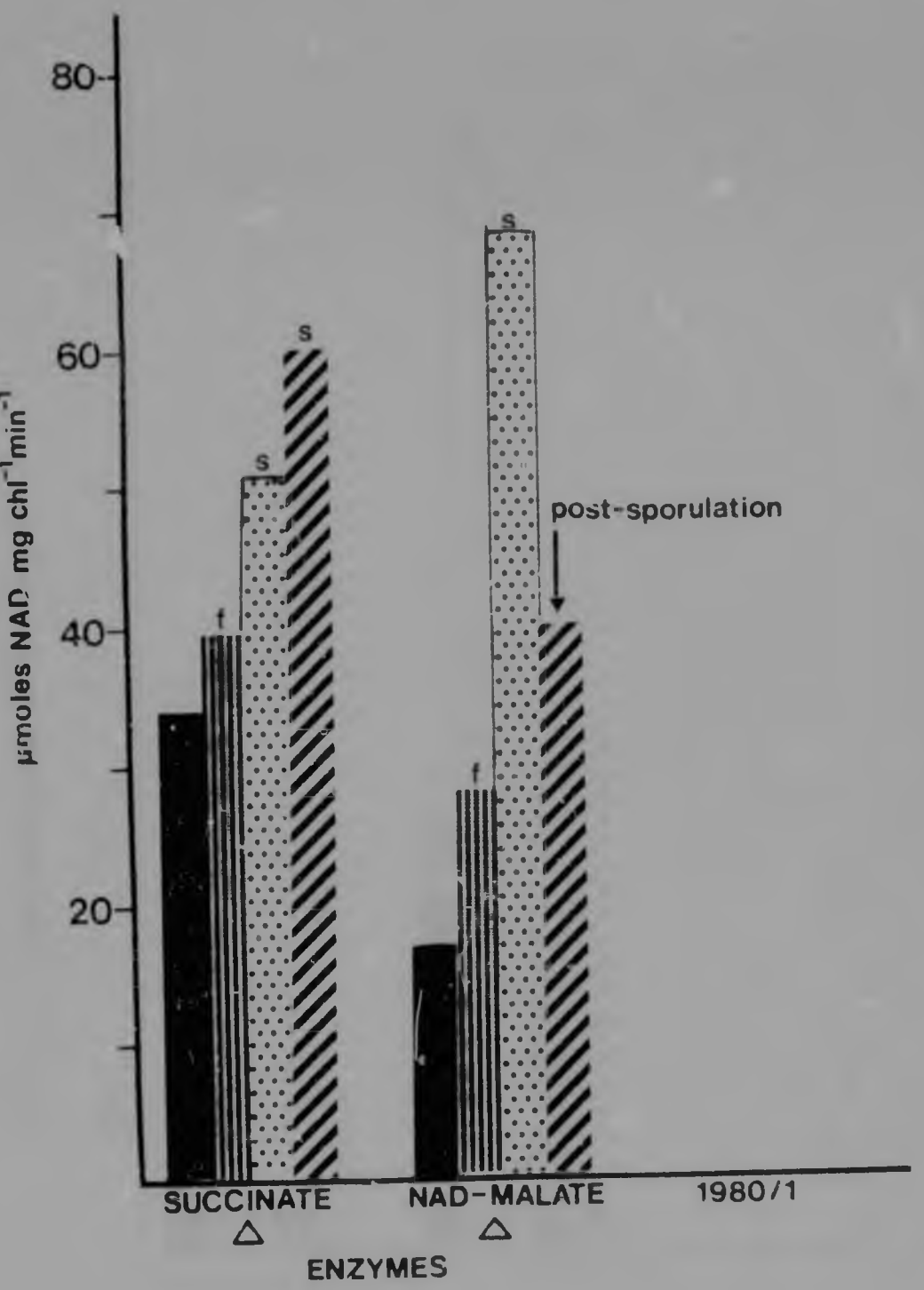


Fig.80 Dark respiration enzyme activities (Succinate dehydrogenase and NAD-malate dehydrogenase) in healthy and rust-infected *D. eriantha* leaves (1980/81)

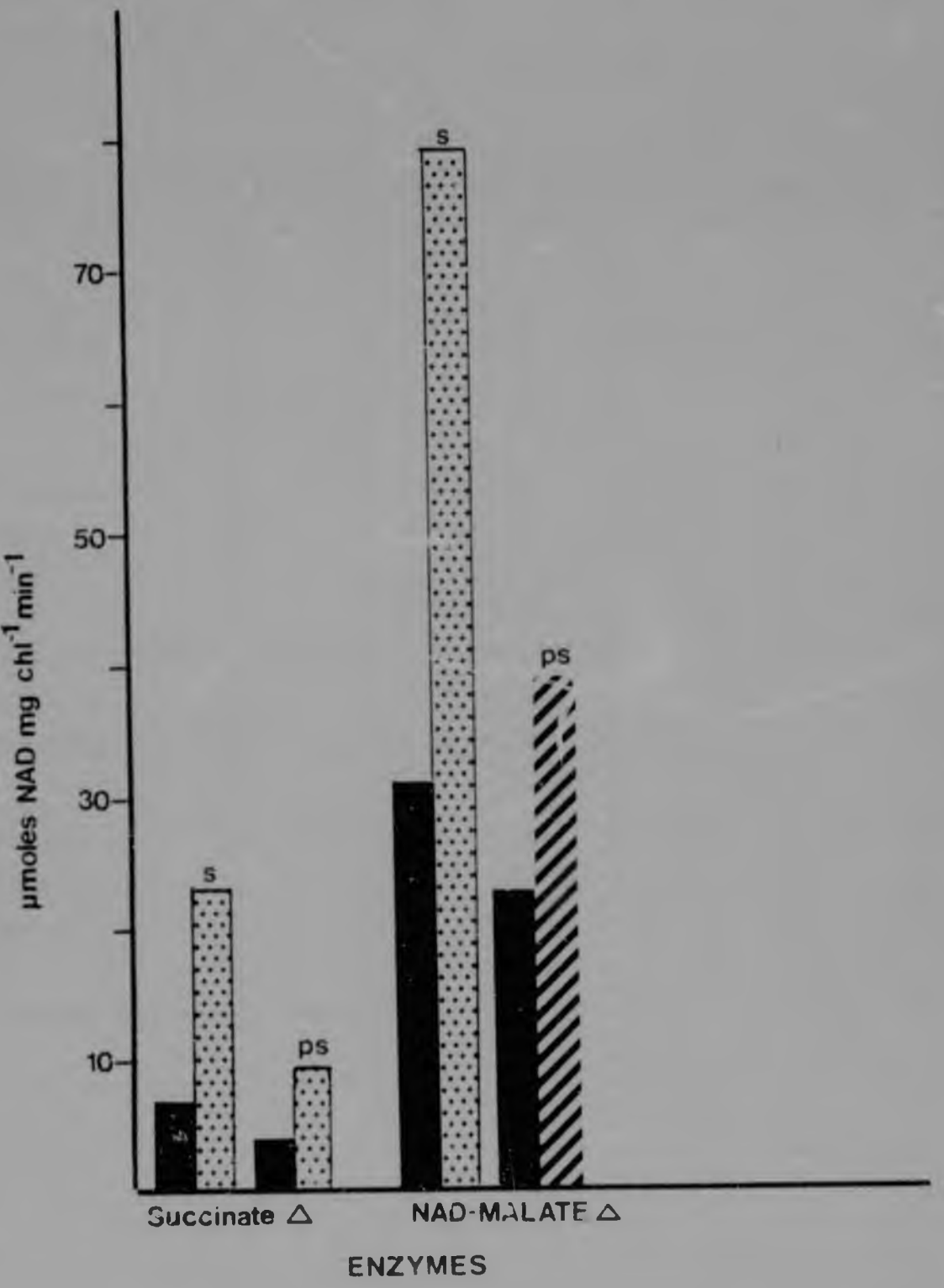


Fig.81 Dark respiration enzyme activities (Succinate dehydrogenase and NAD-malate dehydrogenase) in healthy and rust-infected *D.eriantha* leaves (1981/82)

Table 18 Chlorophyll content (mg cnl dm^{-2}) of *B. africana* leaves (1978/79; 1979/80 season)

MONTH	HEALTHY	NECROTIC	
1978			
OCTOBER	2.7 ± 0.20	1%	2.7 ± 0.06
NOVEMBER	4.4 ± 0.20	1%	4.8 ± 0.41
DECEMBER	4.6 ± 0.15	1%	4.5 ± 0.14
1979			
FEBRUARY	4.7 ± 0.08	5%	4.4 ± 0.13
MARCH	5.8 ± 0.22	5%	5.3 ± 0.07
APRIL	4.5 ± 0.19	10%	3.9 ± 0.21
	3.4 ± 0.17	10%	3.2 ± 0.19
NOVEMBER	3.4 ± 0.19	1%	3.2 ± 0.41
DECEMBER	4.4 ± 0.27	5%	3.9 ± 0.48
1980			
JANUARY	3.5 ± 0.09	1%	3.9 ± 0.07
FEBRUARY	3.2 ± 0.15	5%	3.3 ± 0.65
MARCH	5.3 ± 0.11	10%	4.7 ± 0.12
	4.3 ± 0.20	25%	3.1 ± 0.15

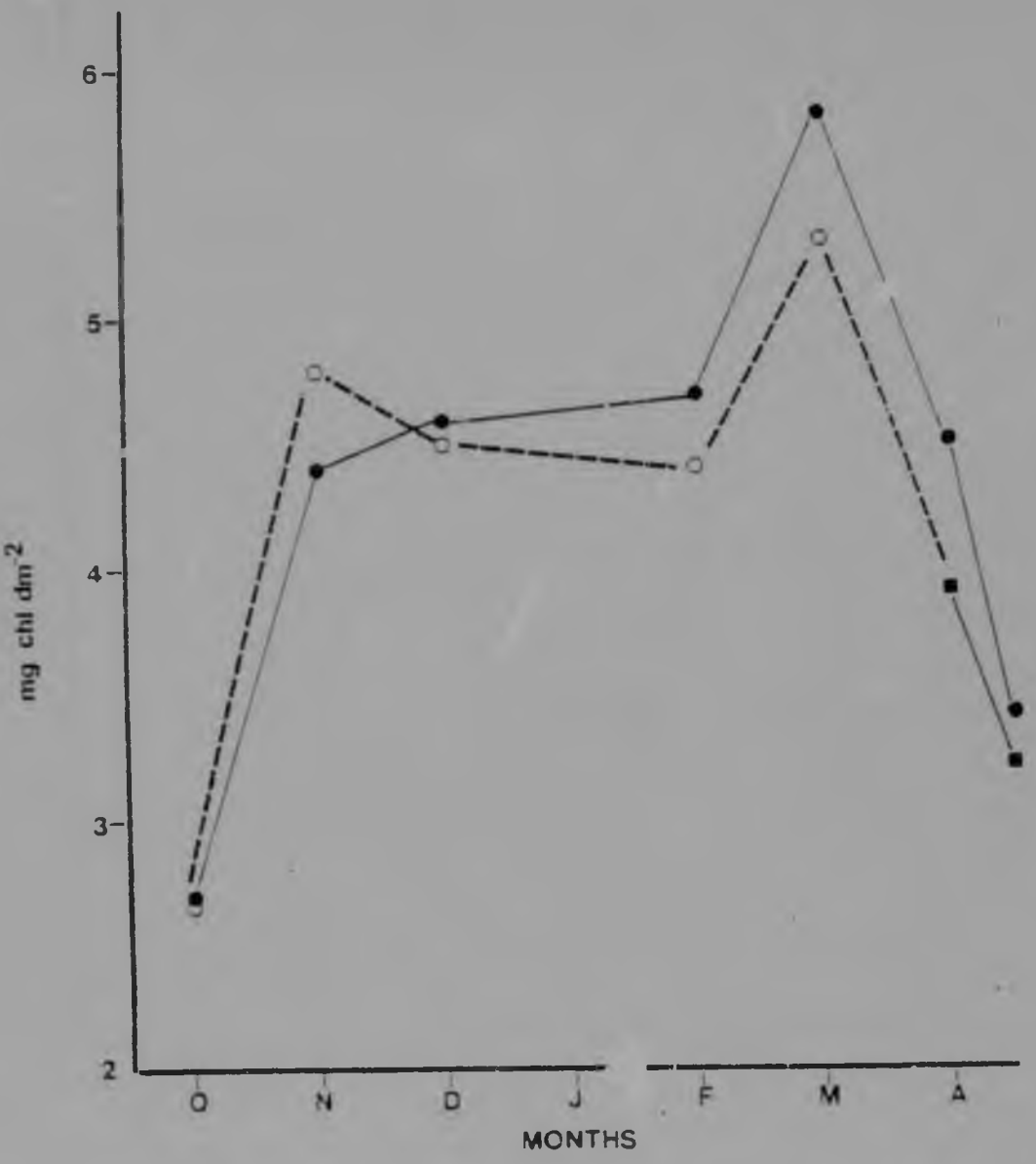


Fig.82 Chlorophyll content of necrotic and non-necrotic *B.africana* leaves (1978/79)

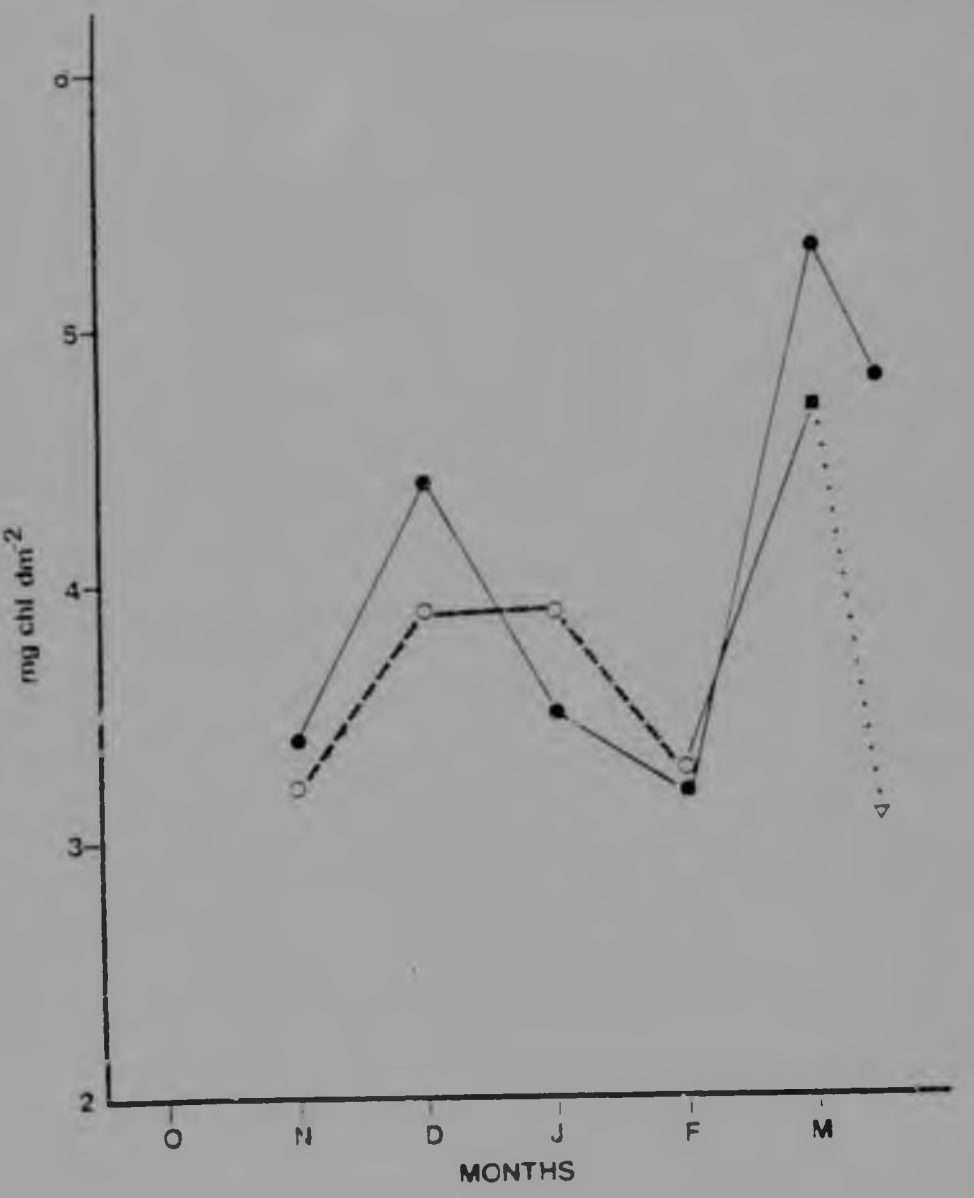


Fig.83 Chlorophyll content of necrotic and non-necrotic *B.africana* leaves (1979/80)

Table 19 Chlorophyll content (mg chl m^{-2}) of healthy and rust-infected *P. graminis* (1979/80; 1980/81 season), and chlorophyll a : b ratios (1979/80).

MONTH	HEALTHY	RUST-INFECTED		
1979 NOVEMBER	3.5 ± 0.3	1-5%	flecking	3.2 ± 0.1
DECEMBER	2.5 ± 0.3		flecking	
		1-5%		2.6 ± 0.20
		10%		2.9 ± 0.06
		25%	sporulating	1.1 ± 0.33
1980 JANUARY	2.2 ± 0.1		flecking	
		1-5%		2.7 ± 0.04
		10%		2.6 ± 0.10
			sporulating	
		25%		2.0 ± 0.10
		50-75%		1.6 ± 0.10
FEBRUARY	1.7 ± 0.2		sporulating	
		10%		1.1 ± 0.07
		25%		1.3 ± 0.06
		50-75%		1.0 ± 0.02
		50-75%	Post-sporulation	0.8 ± 0.07
MARCH	2.4 ± 0.3		sporulating	
		25%		1.3 ± 0.07
		50%		1.3 ± 0.1
		50-75%	Post-sporulation	1.2 ± 0.2
OCTOBER	2.8 ± 0.7	1-5%	flecking	2.2 ± 0.10
			sporulating	
		10%		1.3 ± 0.04
		25%		1.5 ± 0.03
		50-75%		0.9 ± 0.05
NOVEMBER	2.1 ± 0.06		flecking	
		1-5%		3.1 ± 0.2
		10%		2.8 ± 0.4
			sporulating	
		25%		1.9 ± 0.1
		50-75%		1.6 ± 0.05
DECEMBER	3.3 ± 0.4	10%	flecking	3.4 ± 0.11
			sporulating	
		25%		2.1 ± 0.14
		50-75%		1.8 ± 0.06
CHLOROPHYLL a : b RATIO			SPORULATING	
OCTOBER	3.3 ± 0.5	1-5%		2.8 ± 0.6
		25%		2.3 ± 0.4
		50-75%		1.9 ± 0.3
NOVEMBER	3.5 ± 0.6	1-5%		3.4 ± 0.3
		25%		2.4 ± 0.6
		50-75%		1.3 ± 0.1
DECEMBER	4.6 ± 0.3	1-5%		4.3 ± 0.5
		25%		3.5 ± 0.6
		50-75%		2.2 ± 0.2

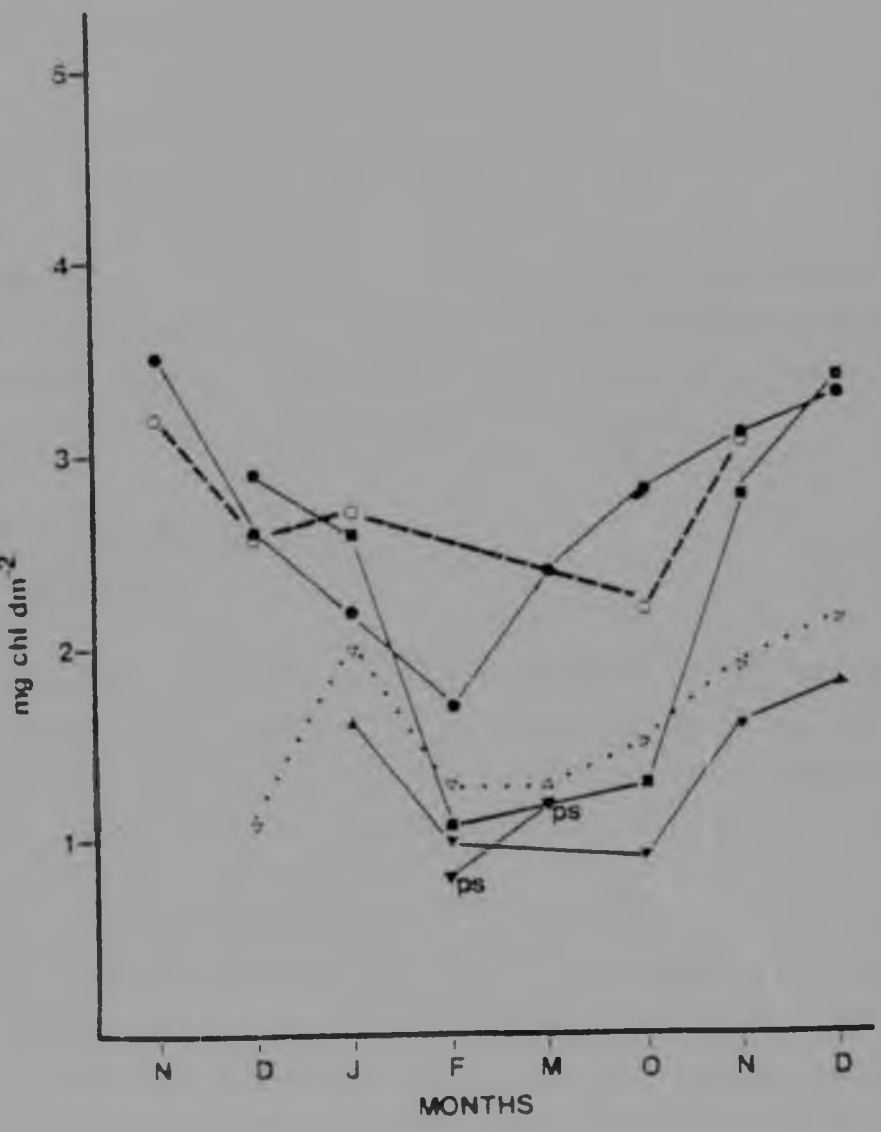


Fig.84 Chlorophyll content of healthy and rust-infected *D.eriantha* leaves (1979/80)

Significant differences in chlorophyll a : b ratios were observed between healthy and infected leaves (>25%). Chlorophyll a : b ratios declined in heavily infected leaves indicating that chlorophyll a declined to a greater extent than chlorophyll b (Fig. 85).

P. maximum

From Table 20, it can be observed that there is no significant difference between healthy leaves and tarspot-infected leaves showing a low level of infection (<25%). However at infection severities greater than 25% there was a significant decline in chlorophyll content in infected leaves (Fig. 86).

Chlorophyll a : b ratios did not change between healthy and 1-5% infected leaves, but ratios dropped in leaves exhibiting infection levels higher than 25% (Table 20). This indicates a greater decrease in chlorophyll a compared to chlorophyll b.

4.2 Nitrogen metabolism

4.2.1 Nitrates

D. eriantha

Nitrates (μmoles NO_3^- g dry wt^{-1}) were measured in healthy and rust-infected leaves (Table 21). Nitrates increased markedly once flecking was visible (Fig. 87). Nitrate levels continued to rise until sporulation, but declined rapidly during post-sporulation.

P. maximum

From the results presented in Table 21, there appeared to be a small stimulation of nitrates in tarspot-infected (10%) leaves. However T-test analysis proved the differences between healthy and infected leaves to be highly significant at the 50% infection level (Fig. 88) although increases in nitrates were far greater in rust-infected *D. eriantha* compared to *P. maximum* leaves.

4.2.2 Total nitrogen or crude protein

B. africana

Total nitrogen or crude protein (6.25 x total N) measurements are presented in Table 22. Percentage total nitrogen in necrotic (1-5%) and non-necrotic leaves were not significant (Fig. 89).

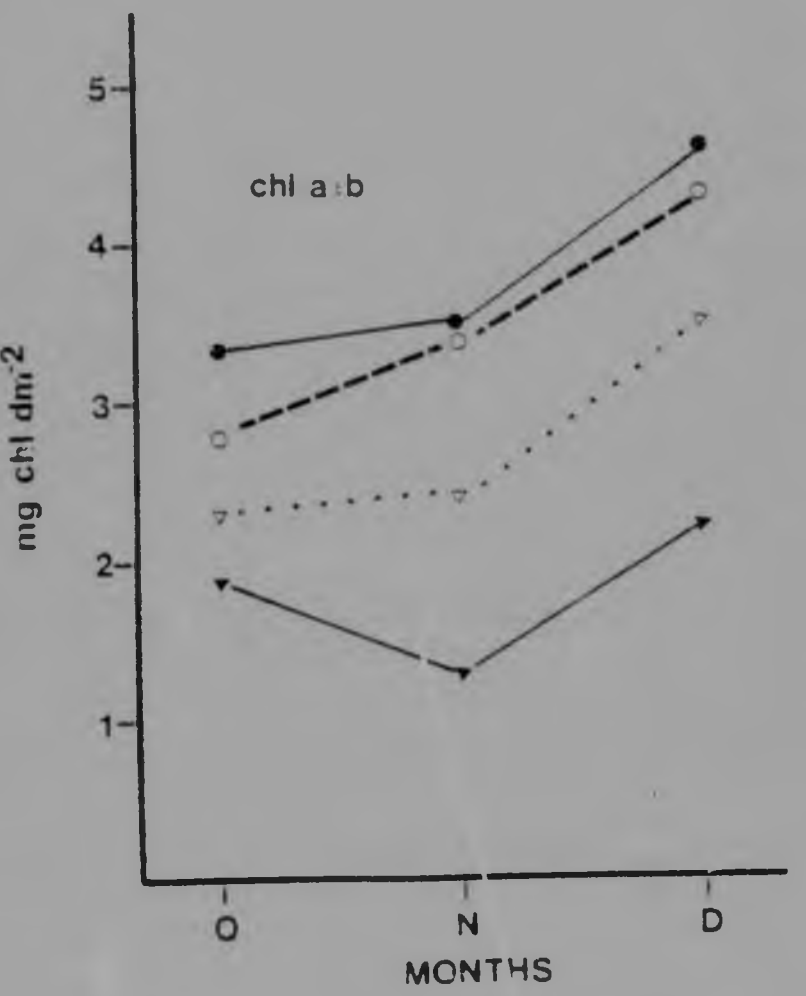


Fig.85 Chlorophyll a:b ratio in healthy and rust-infected *D.eriantha* leaves (1980/81)

Table 20 Chlorophyll content (mg chl dm^{-2}) of healthy and tarspot-infected *P. maximum* and chlorophyll a : b ratios (1979/80).

MONTH	HEALTHY	TARSPOT-INFECTED	
1980			
JANUARY	2.0 ± 0.15	1-5%	1.9 ± 0.02
		10%	1.7 ± 0.04
		25%	1.1 ± 0.06
		50%	0.9 ± 0.02
FEBRUARY	1.7 ± 0.1	1-5%	1.6 ± 0.10
		10%	1.5 ± 0.04
MARCH	2.1 ± 0.08	1-5%	1.5 ± 0.05
		25%	1.1 ± 0.03
		50%	0.9 ± 0.04
APRIL	1.8 ± 0.2	1-5%	1.4 ± 0.10
		10%	0.8 ± 0.10
		25%	0.4 ± 0.20
		50%	0.3 ± 0.15
DECEMBER	3.0 ± 0.16	1-5%	2.5 ± 0.40
		25%	2.4 ± 0.20
		50%	2.0 ± 0.11
CHLOROPHYLL a : b RATIO	3.2 ± 0.5	1-5%	3.3 ± 0.05
		25%	2.4 ± 0.10
		50%	2.4 ± 0.10

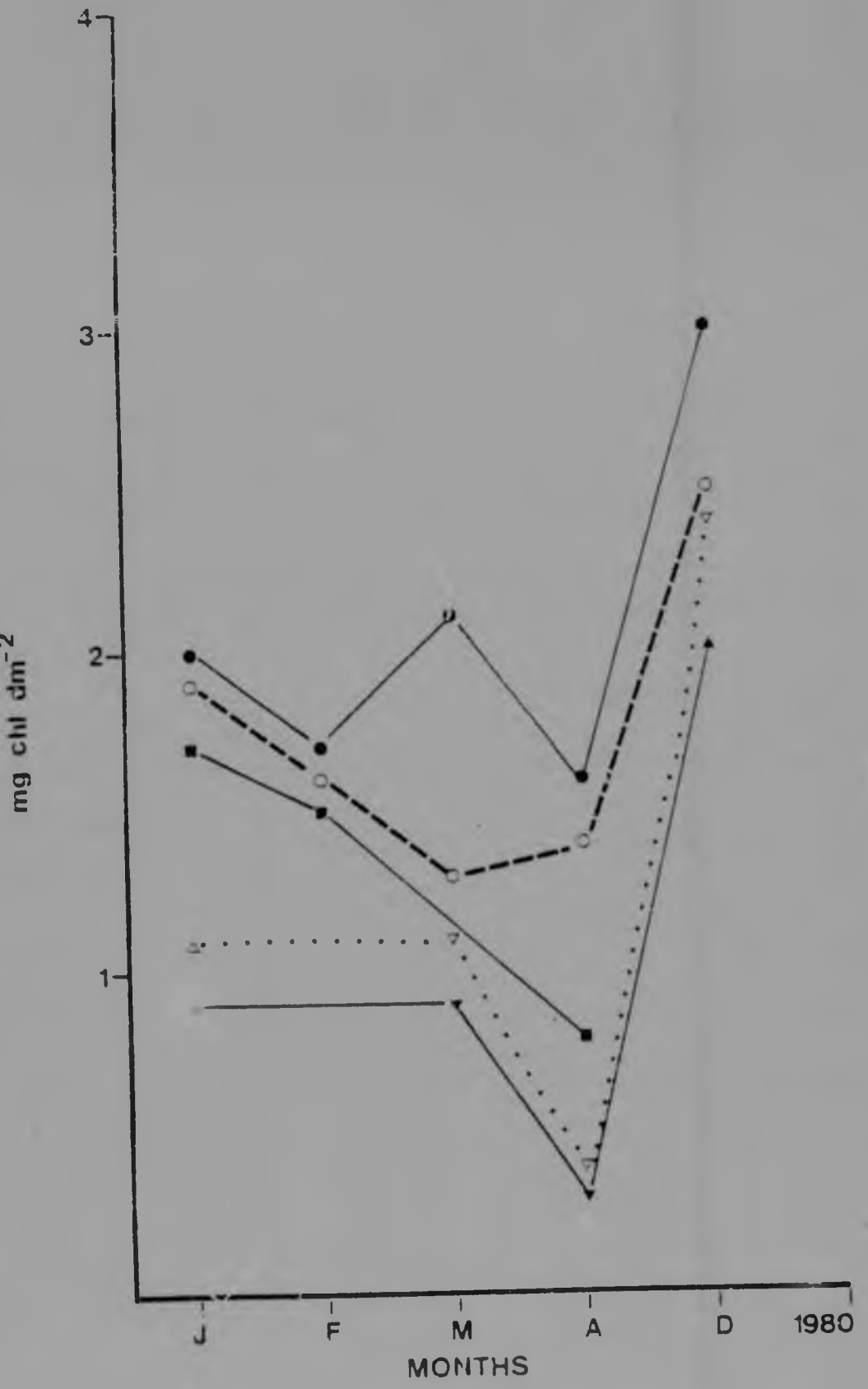


Fig.86 Chlorophyll content of healthy and tarspot-infected *P. maximum* leaves (1980)

Table 21 Nitrates (µmoles NO_3^- g dry wt.$^{-1}$) in healthy and infected leaves of *D. eriantha* and *P. maximum* (1981/82 season)

D. eriantha		
MONTH	HEALTHY	INFECTED
NOVEMBER 1981	25.7 ± 0.9	25% Flecking 41.7 ± 1.1
DECEMBER 1981	26.7 ± 1.6	25% Sporulating 35.2 ± 3.0 75% Post-sporulation 24.2 ± 2.2
JANUARY 1982	26.3 ± 0.7	25% Sporulating 48.8 ± 1.3 75% Post-sporulation 25.8 ± 0.8
P. maximum		
DECEMBER 1981	17.1 ± 2.3	10% 20.0 ± 1.9 50% 21.0 ± 1.4
JANUARY 1982	14.1 ± 1.4	10% 16.8 ± 1.1 50% 21.6 ± 1.2

Table 21 Nitrates (µmoles NO_3^- g dry wt.$^{-1}$) in healthy and infected leaves of *D. eriantha* and *P. maximum* (1981/82 season)

D. eriantha		
MONTH	HEALTHY	INFECTED
NOVEMBER 1981	25.7 ± 0.9	25% Flecking 41.7 ± 1.1
DECEMBER 1981	26.7 ± 1.6	25% Sporulating 35.2 ± 3.0 75% Post-sporulation 24.2 ± 2.2
JANUARY 1982	26.3 ± 0.7	25% Sporulating 48.8 ± 1.3 75% Post-sporulation 25.8 ± 0.8
P. maximum		
DECEMBER 1981	17.1 ± 2.3	10% 20.0 ± 1.9 50% 21.0 ± 1.4
JANUARY 1982	14.1 ± 1.4	10% 16.8 ± 1.1 50% 21.6 ± 1.2

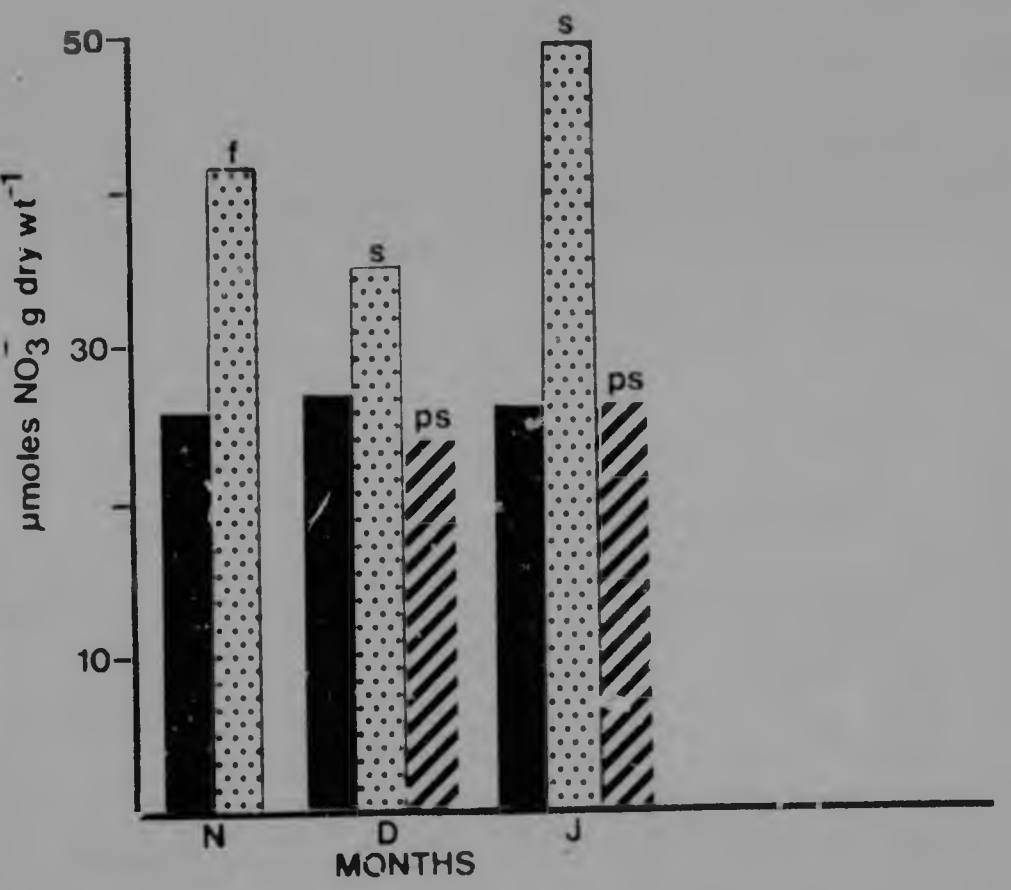


Fig.87 Nitrate measurements in healthy and rust-infected *D.eriantha* leaves (1981/82)

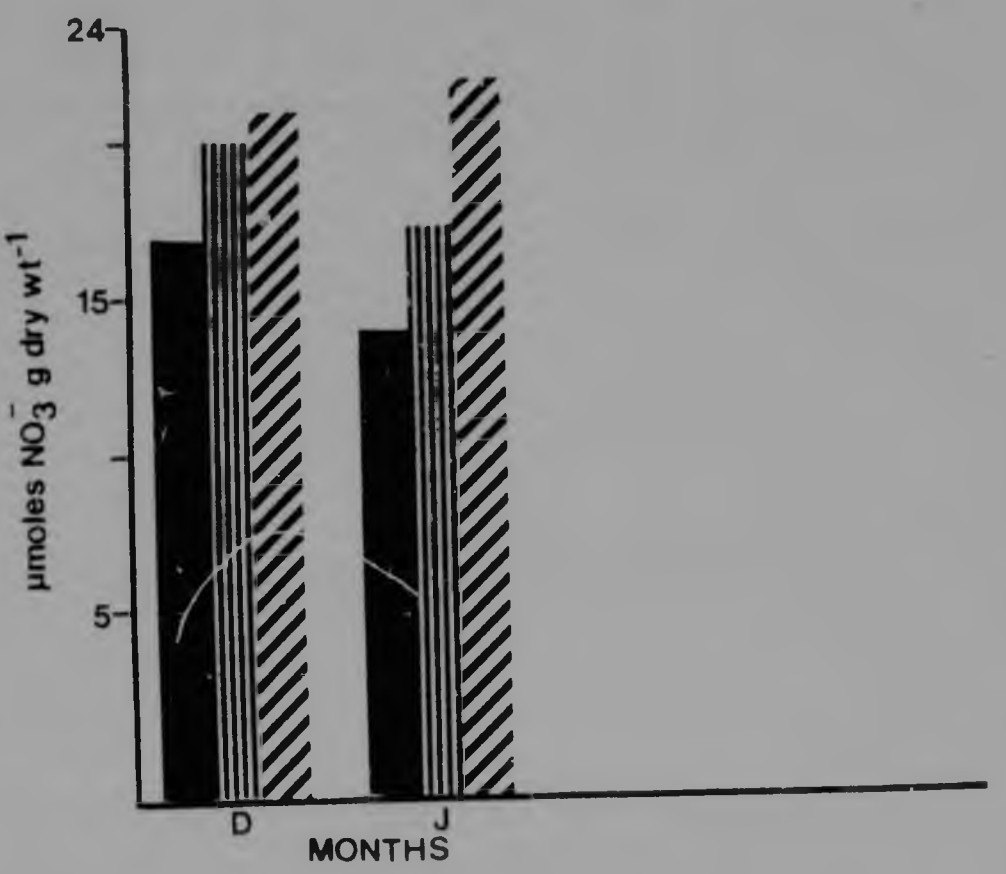


Fig.88 Nitrate measurements in healthy and tarspot-infected *P.maximum* leaves (1981/82)

Table 22 Percentage total nitrogen of healthy and necrotic *. africana* leaves (1979/80).

MONTH	HEALTHY (NON-NECROTIC)	NECROTIC
1979 NOVEMBER	2.7 ± 0.02 2.6 ± 0.04	1% 2.7 ± 0.04 1% 2.5 ± 0.04
DECEMBER	2.2 ± 0.02	1% 2.3 ± 0.01
1980 JANUARY New Flush	2.2 ± 0.02 2.8 ± 0.05	1% 2.1 ± 0.03 5% 2.5 ± 0.05
FEBRUARY	2.3 ± 0.02	5% 2.5 ± 0.04
MARCH	2.5 ± 0.03	5% 2.5 ± 0.04

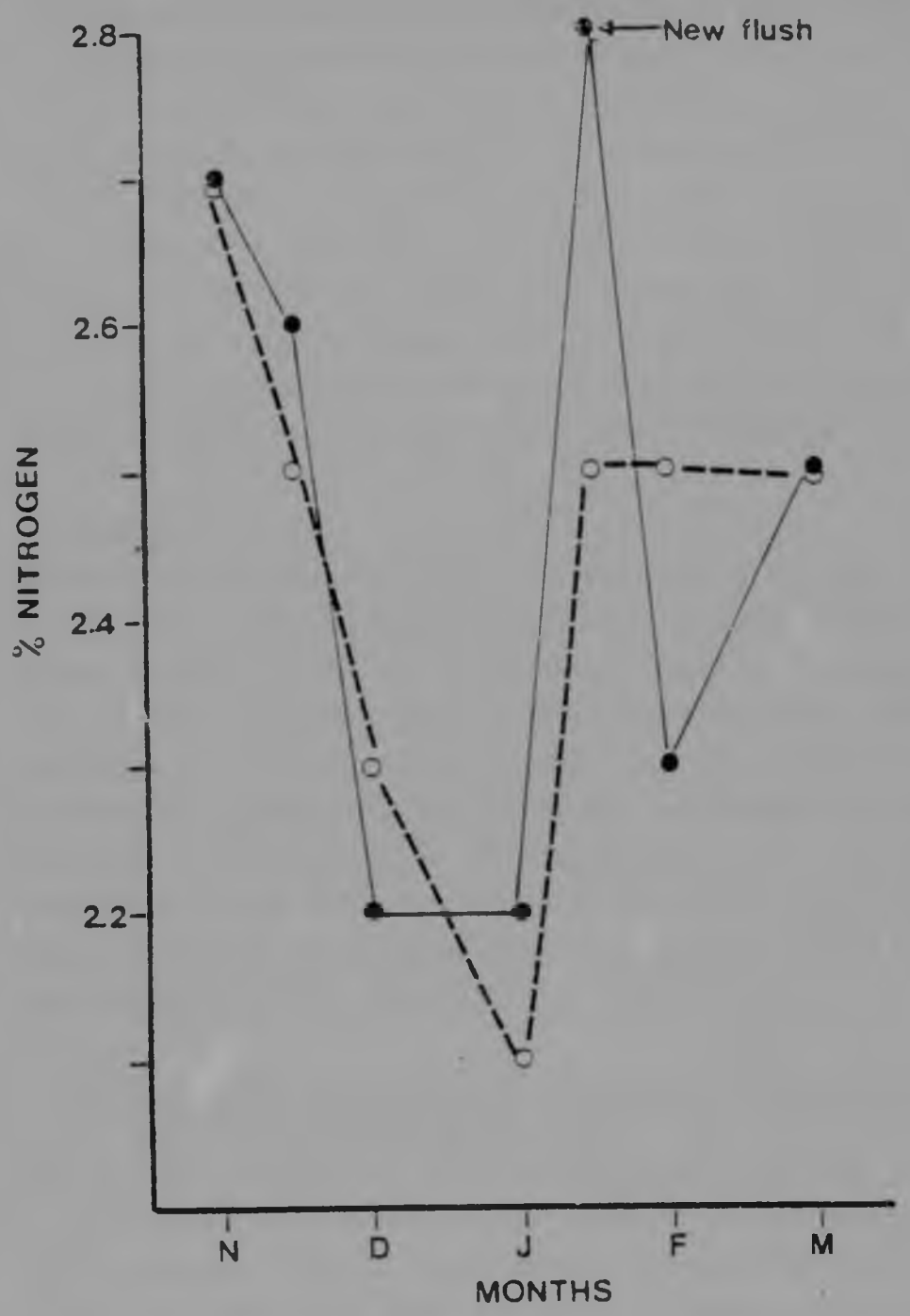


Fig.89 Total nitrogen content of necrotic and non-necrotic *B.africana* leaves (1979/80)

D. eriantha

From the results in Table 23, the difference between total nitrogen in healthy and sporulating leaves (1-25%) proved insignificant ($p = 0.005$). However in heavily infected leaves (>25%) total nitrogen levels decreased markedly (Fig. 90). Similar results were obtained for experiments carried out in the 1979/80 (Fig. 90) and 1980/81 (Fig. 91) season. In leaves exhibiting early flecking (1-5%) total nitrogen increased to a small extent in comparison to healthy leaves (Fig. 91). There was a positive correlation between total nitrogen content and degree of infection. The greater the severity of disease the greater the reduction in nitrogen content was observed (Table 23).

P. maximum

Similar results were obtained as in the case of *D. eriantha* (Table 24). Total nitrogen content only declined in heavily infected leaves (25%) and although decreases were noted in the less severely infected leaves (1-25%) these decreases were not significant ($p = 0.05$) (Figs. 92 and 93). The decline in total nitrogen in tarspot-infected leaves was not however as great as in the case of *D. eriantha* and there was a positive correlation between degree of infection and total nitrogen. Similar results were obtained for experiments carried out in the 1979/80 (Fig. 92) and 1980/81 (Fig. 93) seasons.

4.3 Estimation of the overall effect of pathogens on primary productivity of the grass layer

The national co-operative project at Nylsvley was interested in the overall effect of these two fungal diseases on the grasses *D. eriantha* and *P. maximum*. The following formula was devised to estimate the effect of a specific disease e.g. rust or tarspot on primary production of one grass species, but can be adopted for any other grass in the herbaceous layer :-

$$R = \frac{\sum_{i=1}^{n} C^n - \sum_{i=1}^{n} B^n}{\sum_{i=1}^{n} C^n} \times 100\%$$

Table 23 Percentage total nitrogen of healthy and rust-infected *D. eriantha* leaves (1979/80 and 1980/81 seasons)

MONTH	HEALTHY	RUST-INFECTED
1978 NOVEMBER	1.7 ± 0.06	1-5% Sporulating 1.6 ± 0.05
DECEMBER	1.5 ± 0.03	1-5% Sporulating 1.4 ± 0.05
1979 JANUARY	2.4 ± 0.01	1-5% Sporulating 2.2 ± 0.01
FEBRUARY	2.4 ± 0.02	Sporulating 10% 1.6 ± 0.06 25% 1.5 ± 0.03 50% 1.3 ± 0.03 75% 0.9 ± 0.04
MARCH	1.5 ± 0.01	10% 1.6 ± 0.07 25% 1.4 ± 0.07 50% 1.2 ± 0.03 75% 0.7 ± 0.05
NOVEMBER	2.3 ± 0.06	1-5% Flecking 3.0 ± 0.03 Sporulating 10% 1.8 ± 0.02 25% 1.6 ± 0.01 50% 1.4 ± 0.01
DECEMBER	2.3 ± 0.05	1-5% Flecking 2.8 ± 0.02
1980 JANUARY	1.6 ± 0.30	Sporulating 10% 1.3 ± 0.07 25% 1.1 ± 0.10
FEBRUARY	2.1 ± 0.10	10% 1.3 ± 0.08 75% 0.8 ± 0.03

Table 24 Percentage total nitrogen of healthy and tarspot-infected *P. maximum* leaves (1979/80 and 1980/81 seasons)

MONTH	HEALTHY	TARSPOT-INFECTED
1979 JANUARY	2.1 ± 0.01	1-5% 1.9 ± 0.03
FEBRUARY	2.4 ± 0.02	1-5% 2.1 ± 0.02 10% 1.8 ± 0.03 25% 1.6 ± 0.03 50% 1.2 ± 0.01
MARCH	2.4 ± 0.01	1-5% 2.2 ± 0.10 10% 1.7 ± 0.10 25% 1.6 ± 0.05 50% 1.3 ± 0.04
DECEMBER	3.1 ± 0.01	1% 3.0 ± 0.01
1980 JANUARY	2.4 ± 0.10	1-5% 2.2 ± 0.06 10% 2.1 ± 0.06 25% 1.9 ± 0.04
FEBRUARY	2.6 ± 0.20	1-5% 2.1 ± 0.05 10% 2.0 ± 0.06 25% 1.8 ± 0.04 50% 1.6 ± 0.04

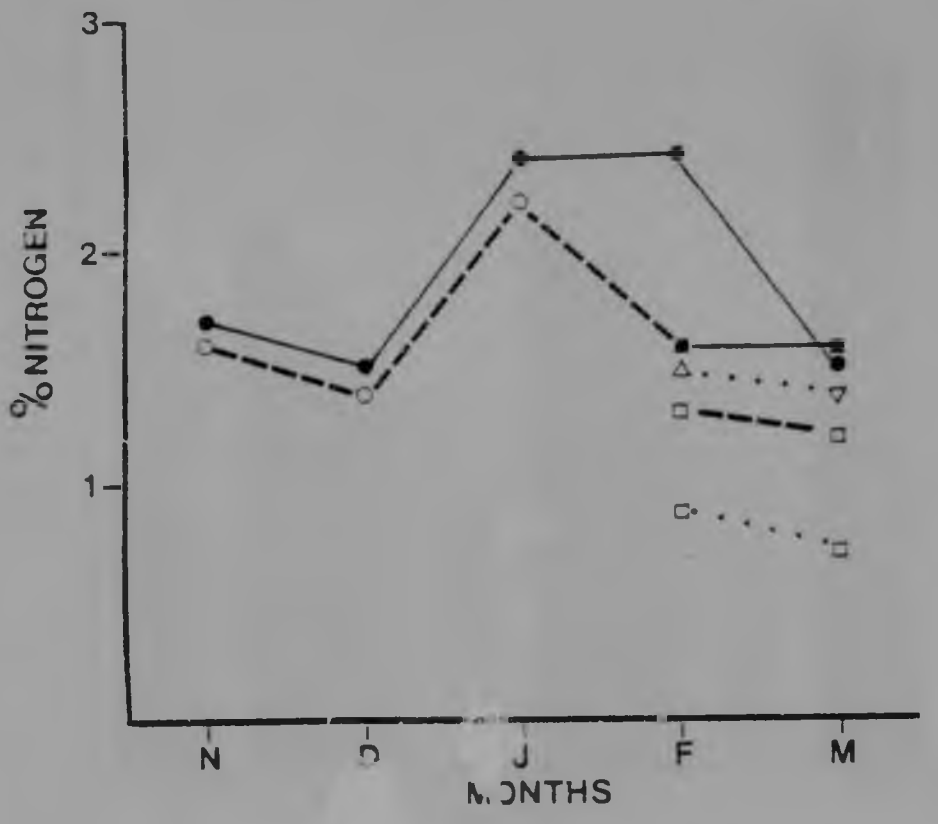


Fig.90 Total nitrogen content of healthy and rust-infected *D.eriantha* leaves (1979/80)

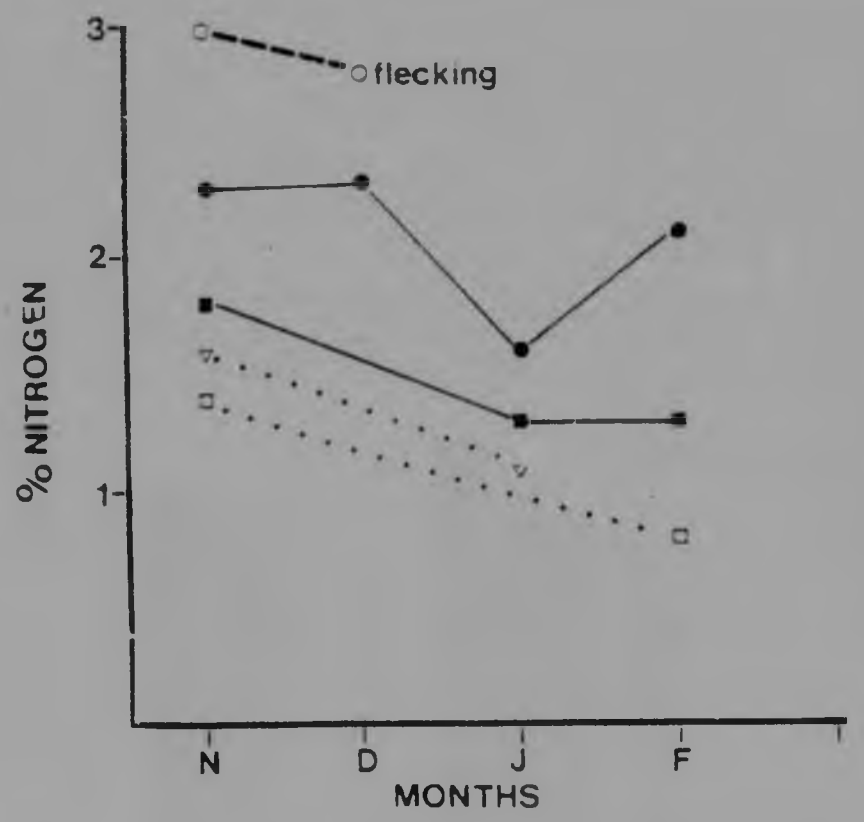


Fig.91 Total nitrogen content of healthy and rust-infected *D.eriantha* leaves (1980/81)

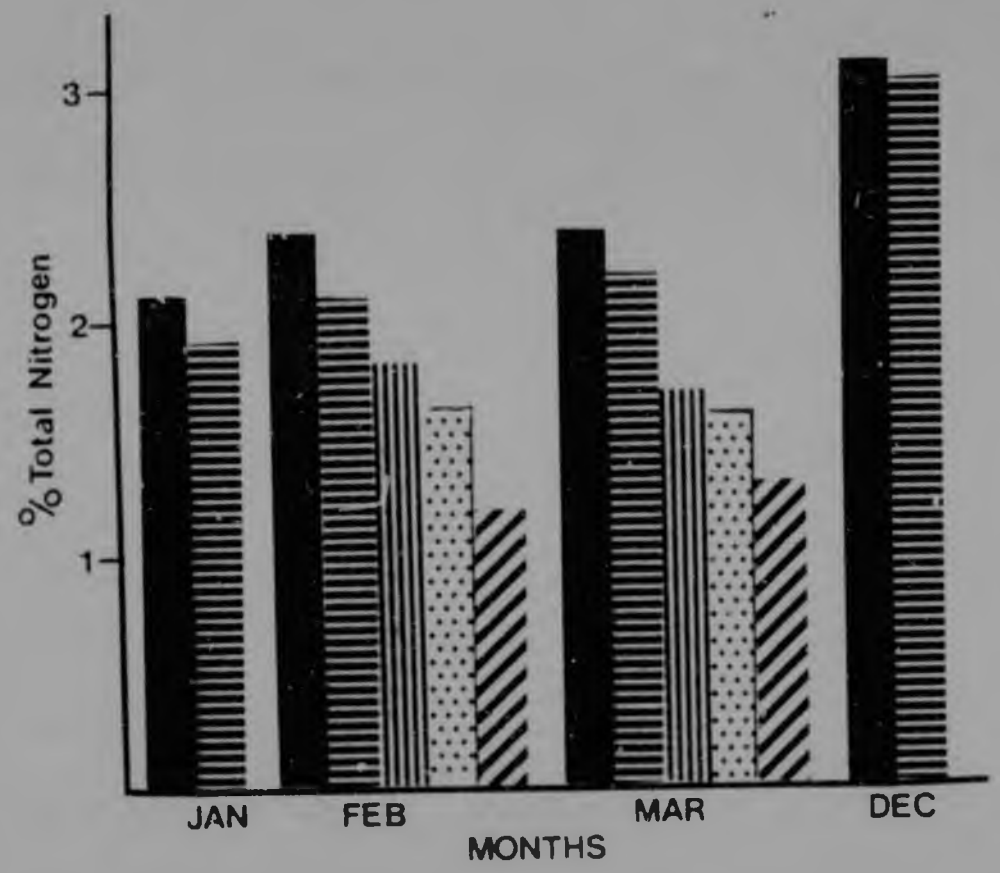


Fig.92 Total nitrogen content of healthy and tarspot-infected *P. maximum* leaves (1979/80)

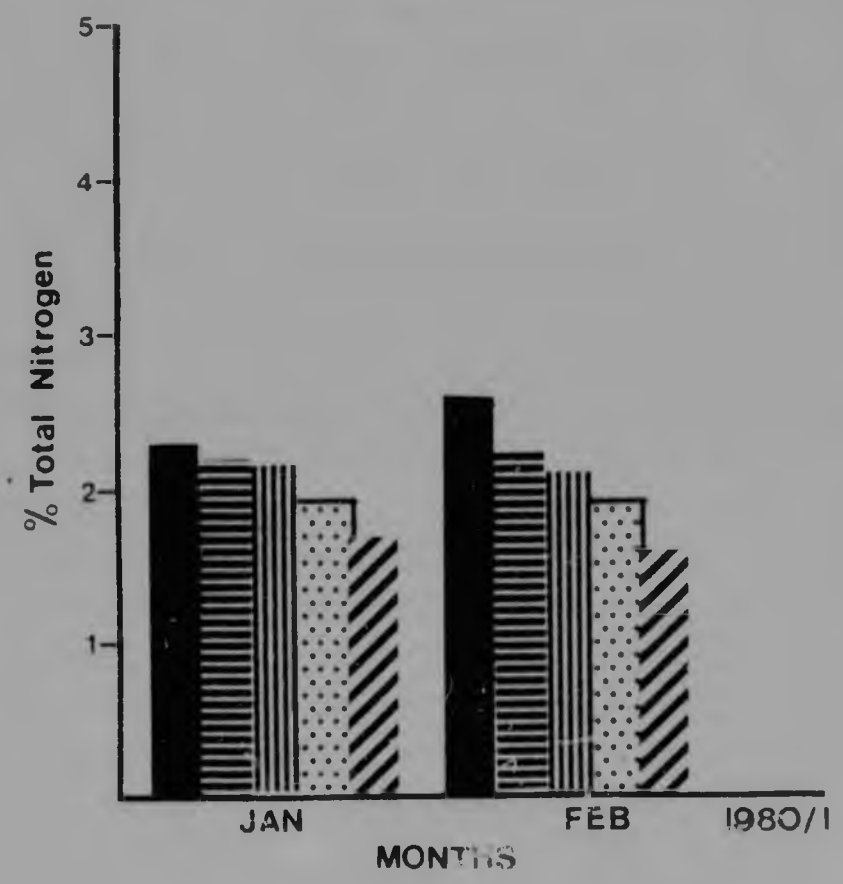


Fig.93 Total nitrogen content of healthy and tarspot-infected *P maximum* leaves (1980/81)

where $C = (B_i . (A_i . S_i . I_i .) + B_i$

and $A_i = \frac{PI_i}{PH_i}$

R = % reduction in primary productivity of one species

n = no. of months in the growing period

C = true CO_2 fixation/month if no infection was present

$\sum_{i=1}^{n} C$ = true <u>total</u> CO_2 fixation of one species

B_i = apparent average CO_2/month = mg CO_2 $dm^{-2} ha^{-2}$ for one species

PH_i = normal photosynthetic rates of healthy plants

PI_i = photosynthesis of infected leaves

A_i = reduction in photosynthesis

I_i = incidence of disease (%)

S_i = severity of disease (%)

Rationale

This formula was based on the view that at y% incidence, 100-y% of leaves would be photosynthesizing normally and only y% would have reduced photosynthetic rates. However as observed in the photosynthesis results presented in Section 5.4.1, severity of infection also influences photosynthetic activities. Since rust and tarspot fungi are pathogens producing local lesions, the effects are limited to the lesion areas and environs surrounding the lesions (x%) to a certain extent. Consequently the severity of disease also had to be taken into account, and at x% severity, approximately 100-x% leaf tissue photosynthesizes

normally. Therefore providing incidence and severity are known for each month during the growth period, and B_i is calculated for each month of the growing season, reductions in primary productivity (amount of CO_2 fixed) can be estimated.

4.4 Biomass

However above ground biomass or dry matter production also involves the efficiency of conversion of CO_2 into dry matter, and is influenced by many factors. According to D. Grossman (1981) net above ground production can be calculated as follows :-

$$NAAP = (RB + \sum_{n=1}^{k} (B_n - B_{n-1}) \times C_1 \times C_2 + IC (+PL)$$

where RB = residual biomass

K = no. of increments

C_1 = empirical constant to account for losses to litter

C_2 = empirical constant to account for losses to necromass

IC = insect consumption

PL = loss due to pathogens

Therefore providing NAAP is determined, the loss due to pathogens (PL) can be incorporated in the formula with 'other' losses providing the relationship between CO_2 fixed and dry matter production is established and the individual contribution of diseased grasses to total biomass is calculated.

Biomass figures of *D. eriantha* and *P. maximum* have been estimated, but not for the corresponding seasons when these studies were undertaken. In addition B_i figures were not available for the two growing seasons in which this research was accomplished, as had been originally planned for the project. Therefore no estimations were actually calculated, and the formulas presented above (5.4.3) may only be employed once the necessary data is obtained in future seasons at Nylsvley.

5.5 DISCUSSION AND CONCLUSIONS

General comments

Physiological changes were noted in *B. africana*, but only to a small extent. Only at high levels of necrosis (25-50%) do gross photosynthetic rates decline. Differences in chlorophyll and total nitrogen content between non-necrotic and necrotic leaves (1-10%) proved insignificant. Therefore it appears from this study that the effects of necrosis on these physiological properties are localized, and that leaf tissue adjacent to necrotic lesions is unaffected. When the percentage of leaf tissue rendered necrotic is low the physiological responses are negligible, and reductions in gross photosynthesis at high levels of necrosis are merely due to loss in green photosynthetic tissue.

D. eriantha and *P. maximum* both demonstrate physiological responses to infection and correspond in many instances to the changes due to obligate parasites reported by many workers. In both cases, responses were positively correlated to degree of infection. In heavily infected leaves (>25%) the differences became greatly significant. This is understandable since both rust on *D. eriantha* and tarspot on *P. maximum* are localized diseases forming distinct lesion areas sometimes surrounded by chlorotic halos. At early stages of infection or low severities of infection the physiological effects are more or less confined to the lesion and immediate surrounding leaf areas, and therefore the overall changes are not noticeable when measurements are made on entire leaves. At high levels of infection (>25%) the areas of infection are greater and therefore physiological responses become measurable. In addition the influence of disease extends to other parts of the leaf tissue and changes can take place in unaffected tissue.

In this study the changes in rust-infected *D. eriantha* leaves were always greater than in tarspot-infected *P. maximum*. This is probably due to the fact that *Phyllachora* species are less destructive obligate parasites than *Puccinia* species. The degree of specialization of rust fungi (4.4.2) was observed to be greater than tarspot (4.4.3) and this may partly be responsible for the less severe effects of tarspot on *P. maximum* than rust on *D. eriantha*.

As tarspot and rust fungi are obligate parasites they require nutrients from their hosts. Consequently host metabolic processes are in some instances initially stimulated eg. during the early flecking stages of rust development, but at later stages of infection a decline in photosynthetic and nitrogen metabolism occurs. This is understandable in view of the evidence that obligate parasites draw on metabolites from their hosts and therefore require their hosts to remain relatively intact until sporulation has occurred. The studies presented in this chapter seem to indicate a competition for carbon and nitrogen between the host and parasite and between infected and non-infected areas. In some instances host metabolism was stimulated such as in the presporulation stages of *P. digitariae* infection, but at the same time dark respiration rates began to increase at the onset of sporulation. It appears that there is a changing balance between synthetic and breakdown processes, depending on pathogen requirements and the stage of disease development. Energy is needed by the pathogen in order for sporulation to occur, but at the same time synthetic pathways requiring energy are occurring in order to provide metabolites for both host and pathogen.

Photosynthetic metabolism

D. eriantha

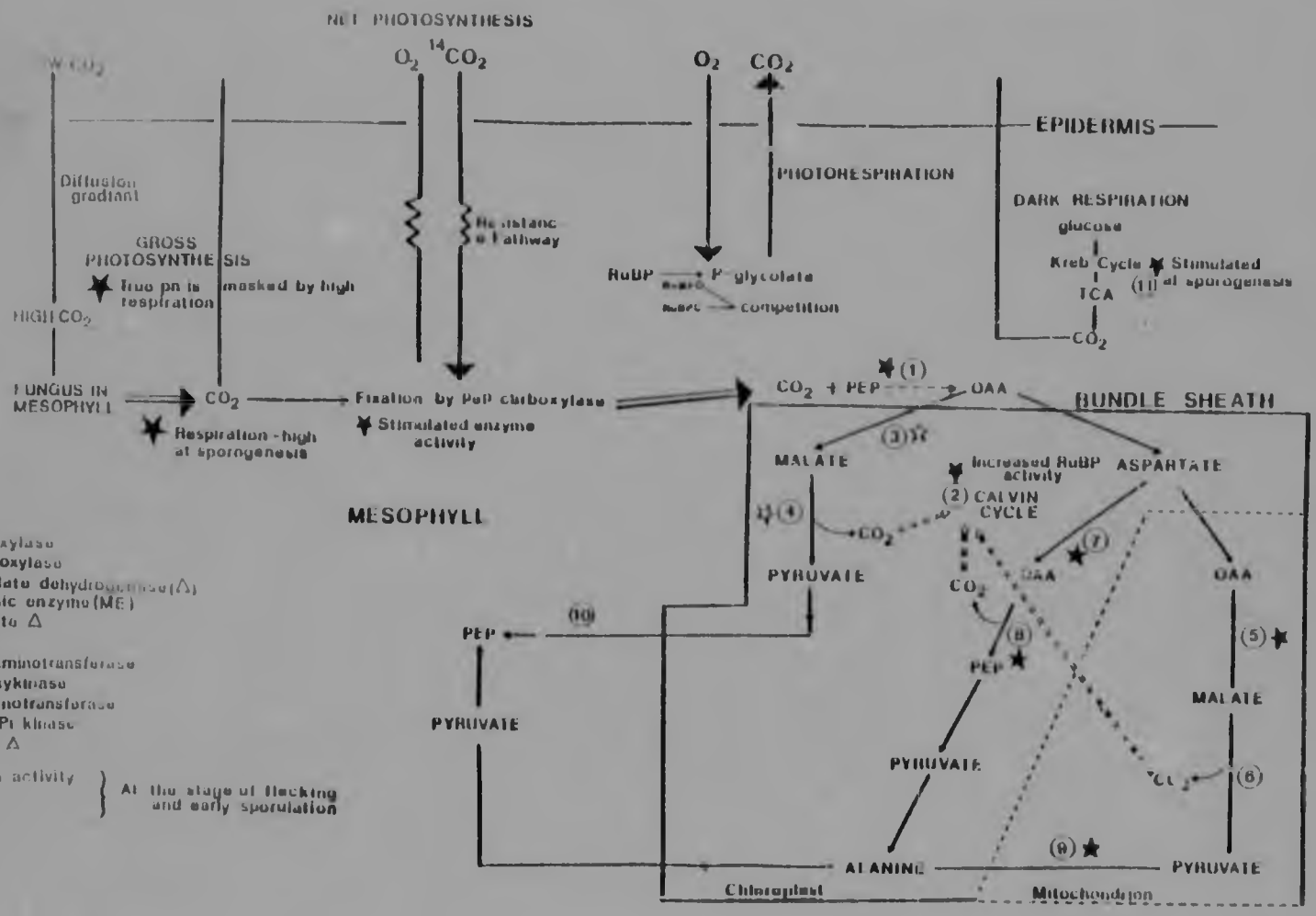
In this study the decrease in photosynthetic metabolism in the later stages of rust infection in *D. eriantha* appears to be attributed to chloroplast disruption (Fig. 38 A), a decline in chlorophyll levels (Figs. 84 and 85) and a decrease in C_4 photosynthetic enzyme activities (Fig. 74-77). The decline in these physiological processes may be a result of the deterioration of the host's metabolism after sporogenesis. The reduction in photosynthetic rates as sporulation occurs may be due to a feedback mechanism by photosynthate accumulation in rust-infected leaves. Certainly these results do indicate an accumulation of nitrogenous and photosynthetic metabolites in infected leaves at the onset of sporogenesis (5.4.2 and 6.4.2). Chlorophyll a : b ratios declined which indicates that chlorophyll a decreased to a greater extent than chlorophyll b. The reason for this is not clear, but chlorophyll

a is the more important pigment than chlorophyll b, being involved in Pigment System I, and therefore may be more severely affected However the greater reduction in chlorophyll a relative to chlorophyll be may merely be due to the fact that chlorophyll a occurs in greater amounts than chlorophyll b in the first place. Whatever the reason may be, the reduction of chlorophyll a is important with respect to its obligate role in photosynthesis, and is partially responible for the decline in photosynthesis during the post-sporulation period.

Gross and net photosynthetic rates were initially stimulated to a small extent during the early stages of yellow flecking in rust-infected *D. eriantha*. This is in agreement w th the findings of many workers eg. Doodson et al., 1975, who suggest this stimulation to result in the supply of metabolites to the pathogen. This would seem likely in view of the obligate nature of rust fungi. However the apparent decline in gross and net photosynthetic rates during late flecking and early sporulation contrasts the observed stimulation of the CO_2 fixation enzymes PEPC and RuBPC in rust-infected *D. eriantha* leaves prior to sporogenesis. Further evidence such as the increase in nitrate (5.4.2.1) and sugar content (6.4.2) in infected leaves tends to suggest that host metabolism is in fact stimulated prior to sporulation.

From the work accomplished in this study, the suggestions are put forward that true photosynthetic rates in infected leaves may be masked due to several reasons. A model for the host-pathogen system is illustrated in Fig. 94. First, high respiration rates, indicated by a stimulation in dark respiration and an increase in host succinate dehydrogenase and NAD-malic dehydrogenase activity (5.4.1.4) may have contributed to the apparent decline in net photosynthetic measurements. Mitochondrial counts (3.4.2) also indicate a greater number of swollen mitochondria in infected mesophyll and bundle sheath cells prior to sporulation than healthy cells. This suggests an increase in surface area of the mitochondrial membranes which may be associated with s mulation of dark respiration.

FIG 94 PHOTOSYNTHETIC MODEL OF THE HOST-PARASITE SYSTEM OF DIGITARIA ERIANTHA-PUCCINIA DIGITARIAE PRIOR TO AND AT THE TIME OF SPORULATION



These results are similar to those of Mitchell (1979) who found dark respiration increases at late flecking and sporulation of *Puccinia graminis* f. sp. *tritica* Eriks. and Henn. in wheat. He also however found no changes in photorespiration and states that, since the differences in combined photorespiration and dark respiration between healthy and infected leaves was less than 0.96 mg CO_2, the increase in respiration was not the cause for the decrease in photosynthesis. Mitchell (1979) therefore concludes that rust influences the carboxylation processes of the host itself. This will be discussed below.

The second indication of a masking effect can be sought in the evidence that RuBPC and PEPC activities are stimulated prior to sporulation. This indicates a high internal CO_2 concentration in the infected areas, yet gross photosynthetic rates appear to decrease in rust-infected *D. eriantha* leaves prior to sporogenesis. The higher internal CO_2 concentration may be explained by high fungal respiration in infected areas and stimulated host respiration. The increase could also be due to a stimulation of the oxidative pentose phosphate pathway (Daly et al., 1957) which in fact is not necessarily incompatible with the simultaneous increase in the absolute rate of turnover of the TCA cycle, although the percentage contribution of the latter would be lowered to a certain extent. However this study indicates increased TCA cycle enzymes and therefore it appears as if much of the CO_2 may come from the Kreb Cycle and not the PPP. An increase in the internal CO_2 concentration in diseased areas would result in a decline in CO_2 diffusion from the atmosphere due to an increase in the resistance or diffusion gradient. This may explain the apparent decline in gross photosynthesis.

Evidence for the existence of a high internal CO_2 concentration in infected areas of the leaf mesophyll is provided by the experiments (Fig. 71 B) where the CO_2 concentration was increased from 100 to 500 ppm to overcome the resistance effects. A greater stimulation of net photosynthetic activity was recorded in infected relative to healthy leaves. Therefore despite the apparent

decline in net photosynthesis prior to sporulation, there is in fact a stimulation of CO_2 fixation enzymes RuBPC and PEPC by the internal CO_2 generated.

Edwards (1970) has suggested that a stimulation in apparent photosynthesis under high CO_2 concentrations, in mildew-infected barley, could be that at high CO_2 glycollate metabolism is impaired in infected leaves thus giving an apparent stimulation of photosynthesis. He also suggests that the fu[illegible]auses partial closure of stomata which at high CO_2 would have [illegible]ttle effect on photosynthetic rates. However most mildew fungi grow in the epidermis or penetrate superficially and barley is a C_3 plant, lacking the C_4 photosynthetic pathway. Therefore it is feasible that mildew fungi cause stomatal closure and that photorespiration (which is higher in C_3 than C_4 plants) is reduced under high CO_2 . However rust fungi are not confined to the epidermal layers and spread throughout the leaf mesophyll. *D. eriantha* is a C_4 grass and is therefore capable of refixing CO_2 via its additional C_4 pathway (Fig. 51). Taking this into consideration, the stimulation of photosynthesis in rust-infected *D. eriantha* leaves prior to sporulation in this case would appear to be more a result of the high CO_2 diffusion gradient, due to increased respiration, being overcome at high external CO_2 concentrations.

A third interesting possibility exists, but is unlikely in view of the generally accepted fact that C_4 plants have very low photorespiratory rates (Chollet and Ogren, 1972; Laetsch, 1974). Nevertheless contrary to these accepted views high photorespiration has been demonstrated in C_4 plants under high nit[illegible]gen conditions (Amory, 1982). The enzymes RuBPC and RuBP oxygenase (RuBPO) compete for CO_2 and O_2 respectively at the same site in the mesophyll cell. RuBPC appears to be stimulated in the infected areas of *D. eriantha* leaves (5.4.1.3), but at the same time it is possible that a simultaneous decrease in CO_2 is taking place in the non-infected regions resulting in a stimulation of RuBPO to compensate for the infection sites. The stimulated RuBPO activity would result in CO_2 being evolved. This difference in

the RuBPC/RuBPO ratio between infected and healthy areas may, if it exists, partially account for the stimulation of the CO_2 fixation enzymes but apparent decrease in net photosynthesis prior to sporulation.

There are other facts to be taken into account however which render this suggestion unlikely. When the degree of rust infection increased in *D. eriantha* leaves, there was a corresponding increase in RuBPC and PEPC (Table 16). As areas of infection increase from 10 to 75%, the ratio of healthy to infected tissue declines. This means the effect of RuBPO would also be reduced and apparent photosynthetic rates would increase. This does not occur, and therefore the conclusion is reached that photorespiration has a negligible or no effect on photosynthetic measurements. However it may explain the positive correlation between degree of infection and RuBPC and PEPC carboxylation. When the ratio of infected to healthy leaf tissue increases, the internal CO_2 in those infected areas increases and the carboxylating enzymes are accordingly stimulated.

C_4 Enzymes

Enzyme activities were expressed on a per chlorophyll basis. Since chlorophyll content itself is not constant, changing in heavily infected leaves, it may appear at first as if alterations in enzyme activities are a function of chlorophyll, and not a true reflection of pathogen-induced alterations. However this is not the case, since the maximum change in chlorophyll content is of the order of 50% in heavily infected leaves, while alterations of 300-400% in enzyme activities were recorded in infected leaves which exhibited a decline in chlorophyll content. Therefore there appears to be no direct evidence for a positive correllation between enzyme

activity and chlorophyll, and despite the probability of reductions in chlorophyll content in infected leaves influencing enzyme activity to a small degree, there is no doubt that the alterations in enzyme activities are real.

Alanine and aspartate aminotransferase and PEP carboxykinase

Increases in aspartate aminotransferase, PEP carboxykinase and alanine aminotransferase in rust-infected leaves (Figs. 75 and 77) prior to sporulation and a loss in activity in NADP-malic enzyme and NADP-malic dehydrogenase rates (Figs. 74 and 76) indicates a shift from the malate forming pathway to the alanine forming pathway. This is extremely interesting since alanine is one of the amino acids most readily utilized by rust fungi (Scott, 1972).

RuBPC and PEPC

The increase in RuBPC and PEPC in rust-infected leaves in this study are in agreement with the findings of Malca et al., 1964 who demonstrate similar increases in maize leaves infected with *Helminthosporium carbonum* ullstup. However Malca and Zscheile (1963) reported a decrease in PEPC and Rowe and Reid (1979a) a decrease in RuBPC in susceptible barley infected with *H. teres*. Malca and Zschele (1963 also at the same time show an increase

in CO_2 fixation in resistant barley infected with *H. teres*. This is of great interest as the increase in PEPC and RuBPC in rust-infected *D. eriantha* may indicate a degree of host resistance to the rust fungus.

P. maximum

Gross and net photosynthetic rates declined in tarsport-infected *P. maximum*, but as was the case in *D. eriantha* the differences between healthy and infected leaves only became significant when disease levels were high (>25%). The effect of tarspot was not as dramatic as rust and this indicates that *P. paspalicola* is not as severe as *P. digitariae*, although both being obligate parasites they exhibit similar patterns.

The changes in C_4 photosynthetic enzyme activities were not as remarkable as in rust-infected *D. eriantha* leaves. NADP-malic enzyme activity which is normally low in healthy *P. maximum*, exhibited loss of activity in tarspot-infected leaves, whereas there was no change in NADP-malic dehydrogenase (Fig. 78). NADP-malate dehydrogenase is involved in the formation of malate from oxaloacetic acid (OAA) (Fig. 51,. Malate is then decarboxylated by NADP-malic enzyme and since NADP-malic enzyme activity was lost in tarspot-infected leaves, it is possible that malate is removed from the mesophyll and utilized by the fungi.

No change was observed in alanine aminotransferase, although aspartate aminotransferase activity decreased in infected *P. maximum* leaves (Fig. 79). Even though small PCK activities were obtained in *P. maximum*, this may have been a result of inadequate techniques, since *P. maximum* is a suspected PCK-type. Many attempts were made by Amory, 1982 (pers. comm.) to isolate PCK but to no avail. However since aspartate aminotransferase activity declined one would suspect PCK activity to decline too in tarspot-infected leaves. Increased RuBPC and PEPC were noted in infected leaves (10-25%). The effect of tarspot therefore appears to have a similar if not as severe pattern as rust-infected *D. eriantha*. The respiratory enzyme NAD-malic dehydrogenase was also stimulated in infected leaves. Fixation of CO_2 would appear to be stimulated

in CO_2 fixation in resistant barley infected with *H. teres*. This is of great interest as the increase in PEPC and RuBPC in rust-infected *D. eriantha* may indicate a degree of host resistance to the rust fungus.

P. maximum

Gross and net photosynthetic rates declined in tarsport-infected *P. maximum*, but as was the case in *D. eriantha* the differences between healthy and infected leaves only became significant when disease levels were high (>25%). The effect of tarspot was not as dramatic as rust and this indicates that *P. paspalicola* is not as severe as *P. digitariae*, although both being obligate parasites they exhibit similar patterns.

The changes in C_4 photosynthetic enzyme activities were not as remarkable as in rust-infected *D. eriantha* leaves. NADP-malic enzyme activity which is normally low in healthy *P. maximum*, exhibited loss of activity in tarspot-infected leaves, whereas there was no change in NADP-malic dehydrogenase (Fig. 78). NADP-malate dehydrogenase is involved in the formation of malate from oxaloacetic acid (OAA) (Fig. 51). Malate is then decarboxylated by NADP-malic enzyme and since NADP-malic enzyme activity was lost in tarspot-infected leaves, it is possible that malate is removed from the mesophyll and utilized by the fungi.

No change was observed in alanine aminotransferase, although aspartate aminotransferase activity decreased in infected *P. maximum* leaves (Fig. 79). Even though small PCK activities were obtained in *P. maximum*, this may have been a result of inadequate techniques, since *P. maximum* is a suspected PCK-type. Many attempts were made by Amory, 1982 (pers. comm.) to isolate PCK but to no avail. However since aspartate aminotransferase activity declined one would suspect PCK activity to decline too in tarspot-infected leaves. Increased RuBPC and PEPC were noted in infected leaves (10-25%). The effect of tarspot therefore appears to have a similar if not as severe pattern as rust-infected *D. eriantha*. The respiratory enzyme NAD-malic dehydrogenase was also stimulated in infected leaves. Fixation of CO_2 would appear to be stimulated

and the reason may be the same as discussed for *D. eriantha*. However the changes in the decarboxylating pathways in *D. eriantha* and *P. maximum* are different and the shift from the malate to the alanine forming pathway in *D. eriantha* was not observed in *P. maximum*.

Carbon and nitrogen metabolism

Cresswell et al. (1974) and Amory (1982) have shown than an increase in nitrates in leaf tissues results in an increase in RuBPC and PEPC activity in *Themeda* and *Eragrostis* species. Amory, 1982 (pers. comm.) has also indicated that nitrogen starvation leads to a decrease in aspartate and alanine aminotransferase activities. Increases in nitrates were noted in rust-infected *D. eriantha* and tarspot-infected *P. maximum* prior to sporulation (5.4.2.1) and this may be an additional cause for the increases in RuBPC, PEPC and alanine and aspartate aminotransferase.

Nitrogen metabolism

Nitrogen metabolism is important due to its association with photosynthetic metabolism and protein synthesis. A high level of nitrates in rust-infected leaves of *D. eriantha* during flecking and presporulation, and in *P. maximum* prior to ascospore sporogenesis, may be due to the mobilization of nitrogenous substances from healthy to infected tissues as was suggested by Jones (1963). Increased nitrate levels have also been demonstrated by Piening (1972) in rust-infected rye, who proved that high nitrates in leaves can be toxic to cattle.

Most of the total nitrogen measurements in this study were performed on *D. eriantha* leaves exhibiting sporulating pustules, (although a few measurements were carried out on leaves exhibiting early flecking) and on sporulating *P. maximum* leaves. The few analyses performed prior to sporulation indicated a slight increase in total nitrogen, but at the time of sporulation and during the post-sporulation period total nitrogen (and nitrate) levels dropped. Therefore it appears as if nitrates and total nitrogen are initially high in infected leaves but as sporulation proceeds, amino acids are utilized by the pathogens and levels decrease.

Shaw and Colctelo (1961) have found decreases in total nitrogen in rust-resistant wheat varieties (Khapli). This suggests that these grasses still exhibit a certain resistance to disease, which was also reflected in the increase in RuBPC and PEPC demonstrated previously.

Although changes in individual amino acids were not measured in this study, the shift from the malate to alanine forming pathway in rust-infected *D. eriantha* leaves suggests that this amino acid is increased. Large increases in alanine, serine and glutamine have been found by other workers in rust-infected leaves (Shaw and Colotelo, 1961). Increases in total nitrogen concentration have also been reported by Calonge (1967) in barley infected with *Puccinia hordei* Otth. Alanine is readily absorbed and utilized by rust fungi (Burrell and Lewis, 1977). The initial increases in total nitrogen may be due to stimulation of host metabolism as well as transolcation into and retention of soluble nitrogen in infection areas (Samborski and Shaw, 1956).

Raggi et al. (1974) are of the view that infection reduces the incorporation of amino acids into proteins, resulting in an accumulation of inorganic nitrogen. The results from the physiological experiments in this study indicate a stimulated host metabolism in the early stages of infection, and suggests that increases in total nitrogen are a result of this host stimulation, although the added effect of translocation of soluble nitrogen from healthy to infected areas is likely.

Decreases in total nitrogen as sporulation occurred may be a result of pathogen utilization and increased breakdown processes since energy is required for sporogenesis. The decline in total nitrogen and nitrates during the post-sporulation period is likely due to leaf senescence and retranslocation from the leaves to the storage organs.

The fluctuations in total nitrogen or crude protein and nitrates in infected leaves is best intepreted as changes between leaf

and pathogen compositions and between infected and non-infected areas at different stages of development of the disease, depending on pathogen requirements.

Foliar diseases such as rust and tarspot may reduce forage quality by inducing higher levels of undesirable constituents and reducing the amount of desirable constituents. Reductions in crude protein have been demonstrated in alfalfa leaflets infected with *Pleoma medicaginis* and orchard grass infected with *Stagonospora arenaria* (Mainer and Leath, 1978). They also demonstrated that crude protein was reduced in proportion to disease severity. Similar results were obtained in this study where the greatest reduction occurred in the more heavily infected leaves (Tables 23 and 24).

Primary production and biomass

From the formula devised to calculate reduction in primary production (5.4.3) and biomass (5.4.4) it would be possible to estimate the overall effect of plant pathogens on dry matter production, providing all parameters involved are measured. Even though the actual reductions were not calculated due to lack of certain data such as individual primary production figures, the conclusion is reached that the two fungal diseases at Nylsvley have in fact a negligible effect on overall biomass loss. This conclusion was reached taking into account :-

1. The intensity and severity early on in the growing season is relatively low compared to later on in the season after peak biomass has already been attained.
2. The contribution to the herbaceous layer biomass by *D. eriantha* and *P. maximum* is relatively small (<10%) (Ower-Smith, 1982).
3. Losses due to pathogens are negligible in comparison with insect and other losses presented by Grossman (1982).
4. Despite the effect of pathogens on individual leaves, parasites may in fact accelerate growth by a) accelerating leaf flushes after host leaves have senesced leading to further photosynthate production; b) gradual defoliation (not too intensive) can in fact stimulate new growth; c) pathogens can accelerate mineral cycling by returning nutrients to the soil.

Final remarks

The results in this chapter have confirmed the findings of some workers with respect to the changes in metabolism following infection. They also however have added new light on certain aspects of photosynthetic metabolism. The study of the C_4 photosynthetic pathway in *D. eriantha* and *P. maximum* has revealed the changes in enzyme activities, and in doing so has established that shifts in host metabolism are in fact responsible for the observed changes in photosynthetic measurements. The research also confirms the suspicions of Mitchell (1979) that rust influences the carboxylation processes itself. It was also interesting to compare the more widely studied rust parasite with the tarspot fungus. Both are obligate parasites and both have similar effects on their hosts, although the rust was more severe than tarspot. The unique nature of the Kranz anatomy and compartmentation of the C_4 photosynthetic pathways in *D. eriantha* compared to C_3 plants also allowed for new suggestions explaining photosynthetic changes. The results demonstrate that stimulation of dark respiration is partially responsible for the apparent decline in net photosynthesis. Results also however indicate that a high internal CO_2 concentration in infected areas may reduce the diffusion of CO_2 from the atmosphere through the mesophyll in those infected areas whilst at the same time stimulating RuBPC as the CO_2 is refixed internally. Thus apparent gross photosynthetic rates decline prior to sporulation, whereas in fact CO_2 fixation by RuPBC is initially stimulated.

What is also extremely clear from these studies is that the changes in host metabolism are fluctuating and depend on the stage of disease development and pathogen requirement. Prior to sporulation host metabolism is stimulated whilst during post-sporulation slowing down of metabolic processes occur as senescence commences. The host-parasite complex can therefore be regarded as a fluctuating balance in synthetic and breakdown processes between host and pathogen and infected and non-infected areas. This balance changes according to degree of infection, pathogen requirement and stage of development of the host and its parasite.

6. CHAPTER SIX CARBOHYDRATE METABOLISM

6.1 LITERATURE REVIEW

6.1.1 Nutrients and plant disease

Nutrient uptake by obligate parasites has been studied by several workers (Scott, 1972; Andrews, 1975; Bushnell and Gay, 1978; Mendgen, 1981). Infections which involve biotrophic fungi such as the rusts, require a different experimental approach to other facultative parasites because the mycelium grows in restricted areas within the leaf. The fungus derives most of its nutrients from the host in one form or the other, and in many cases alters aspects of the host metabolism such as photosynthesis and the direction of normal phoem transport (Lewis, 1978). Billett and Burnett (1977) observed that *Ustilago maydis*, the smut fungus, has an influence on the translocation of assimilates in smutted maize. Transport of $^{14}CO_2$ assimilates into infected areas was enhanced at the expense of other plant parts. The rust pustules act as foci for the accumulation of many metabolites. Increases in respiratory activity (Daly, 1976) in infected areas indicate that normal patterns of translocation of photosynthetic metabolites in host cells undergo alterations. The haustoria themselves have significant respiration rates (Dekhuijken, 1966). It seems as if substrates such as sugars are absorbed first into the extrahaustorial matrix and enter the haustorial cytoplasm in the second stage, thus accounting for a lag between initial transfer of labeled assimilates to the complex and respiration of these nutrients (Manners and Gay, 1977). In addition the mycelia convert a large proportion of assimilates into insoluble compounds and thus maintain the concentration gradient of soluble translocates. Extensive synthesis of fungal tissue occurs during infection, especially during sporogenesis and metabolities are required for this synthesis. Sugars such as sucrose, fructose, and glucose accumulate in the lesion area (Lewis, 1976). Although several investigators have reported a decrease in sugar content of infected leaves (Hodges and Robinson, 1977) others have presented conflicting evidence for the accumulation of several sugars, particularly during pre-sporulation and sporogenesis.

This has been demonstrated in both powdery mildew and rust infections (Gerwitz and Durbin, 1960; Wang, 1961; Bushnell and Allen, 1962; Lewis, 1973). Holligan et al. (1973) showed that as the pustules develop on *Tussilago farfara* leaves infected with *Puccinia poarum* there is a progressive accumulation of dry matter in diseased areas. Long et al. (1975) showed an increase in activity of an acid invertase located on the walls of both host and parasite in the sites of infection. They concluded that sucrose from the host is first hydrolysed and then absorbed by the parasite. Invertase also plays a key role in the provision of substrate for the accumulation of starch around pustules of biotrophic fungi on host species which store this polysaccharide. The movement of sucrose to infection sites occurs in both the light and the dark (Holligan et al., 1974). The accumulation of starch in the chloroplasts in leaf tissue surrounding pustules and fructans within the pustules has also been demonstrated (Wang, 1961). Sugar feeding to the pustules shows that even heavily infected tissue almost devoid of chlorophyll can synthesize sucrose (Long and Cooke, 1974).

It is thought that the haustorium has a major role in nutrient uptake from the host (Bushnell, 1972). Masri and Ellingboe (1965) and Mount and Ellingboe (1969) demonstrated that the successful establishment of the haustorium was a prerequisite for the transfer of ^{32}P and ^{35}S from the host to superficial fungal structures and for the development of functional secondary hyphae. Manners and Gay (1977) showed that products of photosynthesis by *Pisum sativum* enter mycelia and haustoria of *Erysiphe pisi*. However there has been much debate concerning the stage at which nutrients are transferred. Sargent et al. (1973) suggested that the fungus receives little or no nutrition before formation of the primary vesicle of *Bremia lactucae*, the downy mildew of lettuce. However Andrews (1975) presented evidence that glucose from the host is taken up by the pathogen even before penetration. The liberation of $^{14}CO_2$ by haustoria *in vitro* after feeding them with labelled substrates constitutes invaluable evidence that assimilates enter the haustorial complex and since entry can occur in the absence

of superficial mycelium, it appears as if nutrients traverse the host haustorium interface *in vivo*. The transfer of nutrients from host to pathogen is probably dependent upon the quantity and nature of nutrients in the host cytoplasm especially in the epidermal cells; the capacity of the sink (mycelium and spores) and the efficiency of transfer across the interface (Manners and Gay, 1977). There have been many reports of alterations in host physiology which affect nutrients at the source (Edwards, 1971;Hewitt and Ayres, 1976; Mayarosy et al., 1976).

6.1.2 Methodology

Many methods have been proposed to study the uptake of nutrients by the rust fungi. There has been no direct demonstration as yet, of uptake by the haustorium because of the difficulties in studying haustoria *in situ*. Attempts have been made to culture the rust fungi in axenic culture in the correct nutritional environment but these studies were limited (Fuchs and Gärtner, 1958, in Mendgen, 1981). Axenic culture methods have improved over the years, and further experiments have been carried out. Coffey and Shaw (1972) performed nutritional studies with axenic cultures of the flax rust *Melampsora lini*. Dekhuizen (1966) developed a technique for the isolation of purified fractions of haustorial structures from cucumber infected with powdery mildew and this was improved upon by Gil and Gay (1977). Autoradiographic methods have proved extremely useful in the study of nutrient uptake by pathogens. The majority of studies using labelled tracers have involved labelling of the host (Shaw, 1967). Shaw and Samborski (1956) were the first to use autoradiographic methods in studying facultative and obligate parasites. Since then much work has been done using labelled amino acids and nucleosides (Staples and Ledbetter, 1958;1960). Mendgen (1979) demonstrated the exchange of ^{3}H-lysine between *Uromyces phaseoli* and *Phaseolus vulgaris*. Ehrlich and Ehrlich (1970) labelled germinating uredospores of *Puccinia graminis* Pers. f. sp. tritici with ^{14}C by generating $^{14}CO_2$ and followed its subsequent incorporation into host tissues. Mendgen and Heitefuss (1975) also demonstrated nutrient transfer using tritium labelled uredospores of *Uromyces phaseoli*. Electron microscopical autoradiography employing

^{3}H-glucose has also been carried out, but problems exist with the leaching of the glucose into the fixative and dehydrating medium. Some glucose is metabolized however into insoluble storage products and it is possible to detect the label. Pfeiffer et al. (1966) (in Mendgen, 1981) fed wheat leaves with ^{14}C-glucose and analysed the uredospores of *Puccinia graminis* f. sp. tritici. They concluded that hexose is taken up and incorporated into fungal polysaccharides. A study of label distribution in the uredospores also indicated that glucose metabolites are to some extent incorporated into amino acids. Therefore it appears as if this is a useful technique, but there are problems involved, such as whether the label in the fungal structures is the original labelled metabolite that was offered to the plant. Autoradiographic studies are consequently most useful when the nutrients used are minimally metabolized on their way to the fungal structures and which can be immobilized by chemical fixation to avoid nonspecific diffusion (Mendgen, 1981).

Ion exchange chromatography has often served for the separation of monosaccharides (Larson and Samuelson, 1965; Kennedy and Fox, 1977). However the elution times are generally very long, and conventional ion exchange chromatography (cation or anion) techniques have gradually been improved to the point where one may speak of modern highperformance liquid chromatography (HPLC). To-day the most convenient method of sugar analysis is HPLC with refractive index (RI) detection and columns of silica bearing a chemically bonded amine function (Mopper and Degens, 1972). HPLC is based on forcing the liquid mobile phase through a ion exchange resin (stationary phase) under high pressure. There are several advantages of HPLC over other forms of liquid chromatography (Hamilton and Swell, 1977). Firstly the HPLC column can be used many times without regeneration. Secondly the resolution exceeds that of older methods and in addition the instrumentation of HPLC lends itself to automation and quantitation. Thirdly the analysis times are shorter and also the HPLC is efficient in separating unstable or insufficiently volatile organic compounds.

6.2 AIMS

Nutrient competition between host and pathogen is an important part of the discrete relationship and ultimately influences the many metabolic processes of the host. As mentioned previously massive respiratory activities in the infected areas occur at the time of sporulation and even in the pre-sporogenesis period. Therefore it seems likely that sugars accumulate in the infected and immediate adjacent areas to act as substrates for the pathogen. Also the uredospores and mycelium absorb nutrients for the conversion into storage products for future germination. It has been demonstrated (Andrews, 1975) that competition for glucose not only occurs at the time of sporogenesis but at an early infection stage when the substomatal vesicle and primary hyphae are produced. There is no direct evidence for the uptake of glucose by rust primary infection structures and most experiments in the past have involved labelling the pathogen with amino acids and nucleosides at later stages of infection. This study incorporates four objectives to add to our knowledge about rust-grass nutritional relationships in a natural environment :

1) To determine whether glucose accumulates in the areas of infection at an early stage of hyphal penetration.

2) To demonstrate the uptake of glucose by the rust primary infection structures even at the initial stage of infection (twenty one hours).

3) To study the uptake of ^{3}H-glucose by uredospores at the time of sporulation.

4) To determine the overall changes in sucrose, glucose and fructose content in leaves falling within several infection classes at pre-and post-sporulation periods. This is significant with respect to fodder crop quality since both *D. eriantha* and *P. maximum* are grazed heavily by the herbivores in the reserve.

6.3 MATERIALS AND METHODS

6.3.1 Autoradiography

3.1.1 Feeding leaves with D-(6-^{3}H) glucose before spore inoculation

Growth of plants and inoculation

D. eriantha seeds were planted in pots and supplied with a nutrient

solution (see Appendix). Plants were grown in a growth chamber (25°C day T°; 20°C night;12h photoperiod;humidity 60). Three-week old plants were used for spore inoculation.

Spore suspension preparation

Rust-infected leaves exhibiting mature pustules liberating spores, were collected from the reserve and dried for a few days. The leaves were then added to 10mℓ water with 2-3 drops of Tween-20 surfactant and the uredospores dislodged by vigorous agitation for 1h. The solution was centrifuged at 3000rpm for 15min and the sediment resuspended in distilled H_2O and used for spore inoculation.

Inoculation

Leaves were immersed in water and excised using a razor blade and the cut edge placed in 50µℓ solution of D-(6-^{3}H) glucose (1mCi/ml; specific activity 30Ci/mmol). Vials containing the young leaves were placed under 8000 lx illumination, the air circulated with a fan to ensure uniform photosynthesis and transpiration, and left until all the liquid had been taken up (3-4h). This was followed by a coldchase (1h) of a 5 solution of non-labelled glucose. The basal portion of the leaves immersed in the isotope was discarded and the leaves placed on a damp filter paper in a petri dish with water, thereby allowing for a highly saturated atmosphere for spore germination. The leaves were then inoculated with the suspension using a paint brush. The leaves were incubated in a growth chamber (90-95 humidity; 25°C), for 3;6;8;16; and 21 h and removed for light microscope (LM) autoradiography. Control plants were fed with non-radioactive glucose.

Preparation for light microscope autoradiography

Tissues were processed using similar methods to Andrews, 1975. Sections (1mm^2) were cut from the inoculated leaves and fixed at room T° in 4 glutaraldehyde containing 4 sucrose in 0.05M sodium cacodylate buffer, pH 7.1 (6h) and post-fixed in 2 osmium tetroxide for 2h. Tissues were dehydrated in a graded alcohol series and embedded in epoxy resin (Spurr, 1969). Sections (1µm)

were cut on a LKB ultramicrotome, placed on slides subbed in a subbing solution (0.5g gelatine and 0.05g chrome alum in 100mℓ distilled H_2O) and coated with Ilford L4 nuclear emulsion. The slides were exposed for 4 weeks at 4°C. Development was at 20°C in Kodak D-19B developer for 1; 3; and 7 min (7 min period proved to be the most successful) and fixation was for 8 min. Slides were dried and examined using both light and dark-field microscopy. Some of the sections from the same series used for autoradiography, were employed for differential staining.

3.1.2 Feeding leaves with labelled glucose after infection

Leaves exhibiting mature and developing pustules were collected from the nature reserve and immersed in labelled isotope as before (50µl of a D-6-^{3}H - glucose solution). Sections were cut of the pustule and adjacent areas at 3; 6; 8; and 16h for LM autoradiography as before. Control leaves were fed with non-labelled glucose.

6.3.2 SUGAR ANALYSIS

3.2.1 Extraction procedure

Preparation of materials

0.1M Acetate buffer, pH 4.65

13.6g of sodium acetate in 900mℓ distilled water. Adjust pH to 4.65 with acetic acid and make up to 1000mℓ.

Deionization of the resin

Bio-Rad AG 50 1-X8 'mixed resin' was used. Because the hydroxide form of the anion exchange component tends to absorb sugars the resin was converted to the bicarbonate form to minimize this effect. Conversion to the bicarbonate form was achieved by passing a continuous stream of CO_2 gas through a continuously stirred suspension (aqueous) of resin for a period of 8-10h.

Hydrolysis of sucrose

β-fructosidase from Boehringer-Mannheim was used. This was stored at 5°C until use. An aqueous suspension (2mg/mℓ) was prepared for hydrolysis.

Extraction procedure

Approximately 0.7-0.8g of dried grass leaf material (dried at 60° for 3 days) was placed with 0.4g calcium carbonate in a 50ml volumetric flask. Thirty mℓ of distilled H_2O was added to the flask and heated in a boiling water bath for 1h. After cooling to room T° the volume was made up to 50mℓ. The extract was shaken for a few minutes and left to settle. The extract was divided as follows :

a) 20mℓs extract was pipetted into a 50mℓ volumetric flask and 1mℓ saturated neutral lead acetate solution added and made up to volume. The flask was shaken and left to settle.

b) 20mℓs extract was pipetted into a 50mℓ volumetric flask. 25mℓ acetate buffer and 2mℓ β-fructosidase was added, the flask shaken and incubated at room T° (22-23°C) for 60min. One mℓ saturated neutral lead acetate solution was then added and the flask shaken after making up to volume. Ten mℓ of solution (prepared as per procedure a) or b) above) was decanted into a 25mℓ volumetric flask, 3g resin added, and shaken intermittently for 30 min. After the resin had settled 5mℓ supernatant was pipetted into a 10mℓ volumetric flask and made up to volume with 95% ethanol. The extract was then filtered through a millipore filter (0,4 μm) and the filtrate used directly for chromatography.

3.2.2 Sugar detection

The method used for analysis of sucrose, glucose and fructose was High Performance Liquid Chromatography (HPLC), with certain adaptations by A. Wight, Food Research Institute, CSIR (pers. comm.) (Fig. 95). The silica column (5μm particle size) was modified by adding a small amount of polyfunctional amine HPLC (Amine Modifier 1, 0.01-0.1%) to the solvent which impregnates the silica column (Aitzetmuller, 1978). A post-column reaction system based on the reduction of 3'3-(3'3 dimethoxy 1'1-biphenyl-4'4 diyl) bis 2'5-diphenyl 1-2 H- tetrazolium dichloride (tetrazolium blue) was used for detection purposes (Noel et al., 1979). The detection employed was a micromeritix uv III Monitor, Model 1203 with a 550nm absorbance filter. The flow rate of the reagent was 0.6mℓ/min and the pressure 200-250 bars. The reactor for the reduction of tetrazolium blue consisted of long coiled tubing. The reactor was connected to

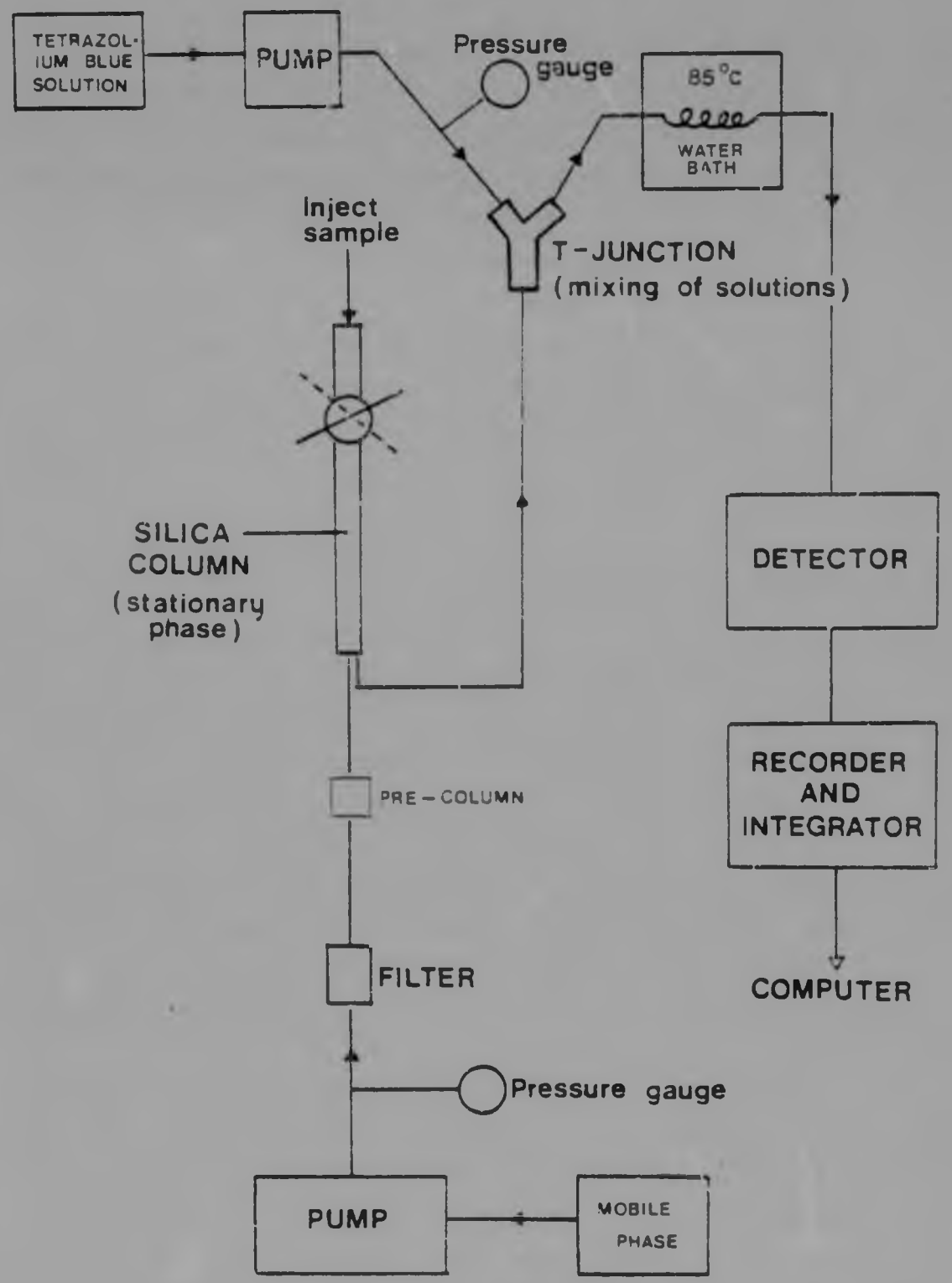


Fig.95 Diagram of the High Pressure Liquid Chromatography (HPLC) system employed to separate sugars

the outlet of the chromatographic column, to a pump, and to a detector through a three-way valve. The coil was immersed in a water bath at 85°C, (Fig. 95). Tetrazolium blue is reduced to monoformazan and this product absorbs at 530nm. The mobile phase used was acetonitrile water (3:1 acetonitrol water: distilled water + 0.01 % HFLC modifier) and the detection solution tetrazolium blue was made up in NaOH (0.1 % in 0.36M NaOH). A series of sugar standards (0.01- 1% glucose, fructose and sucrose) was also made up. To some of the grass samples 0.01g xylose and 0.01g maltose was added to act as internal standards to check sugar recoveries.

3.3 Staining procedures

In order to confirm that the structures were fungal, several staining procedures were carried out :-

1) Toluidine Blue - Safranin Procedure (Pomerleau, 1970) Spurr resin - embedded sections (0.5 - 1mm) were flooded with toluidine blue (1 percent in a 1 percent borax solution) and heated on a hot plate at 65°C until a few bubbles appeared. After washing in distilled water the slides were flooded with HCl (2.5 percent of IN HCl in a 50 percent solution of ethanol) for a few seconds and then decolorized by 2 percent of a normal solution of NaOH in a 50 percent solution of ethanol.

Following rinsing in distilled water, the sections were counterstained with 1 percent Safranin in a 1 percent borax solution for a few minutes, rinsed in distilled water and mounted in Permount. Sections often stained a violaceous brown colour with occasional red walls, with the fungal cytoplasm staining a mauve colour.

the outlet of the chromatographic column, to a pump, and to a detector through a three-way valve. The coil was immersed in a water bath at 85°C, (Fig. 95). Tetrazolium blue is reduced to monoformazan and this product absorbs at 530nm. The mobile phase used was acetonitrile water (3:1 acetonitrol water: distilled water + 0.01 % HPLC modifier) and the detection solution tetrazolium blue was made up in NaOH (0.1 % in 0.36M NaOH). A series of sugar standards (0.01- 1% glucose, fructose and sucrose) was also made up. To some of the grass samples 0.01g xylose and 0.01g maltose was added to act as internal standards to check sugar recoveries.

3.3 Staining procedures

In order to confirm that the structures were fungal, several staining procedures were carried out :-

1) Toluidine Blue - Safranin Procedure (Pomerleau, 1970)

Spurr resin - embedded sections (0.5 - 1mm) were flooded with toluidine blue (1 percent in a 1 percent borax solution) and heated on a hot plate at 65 C until a few bubbles appeared. After washing in distilled water the slides were flooded with HCl (2.5 percent of IN HCl in a 50 percent solution of ethanol) for a few seconds and then decolorized by 2 percent of a normal solution of NaOH in a 50 percent solution of ethanol.

Following rinsing in distilled water, the sections were counterstained with 1 percent Safranin in a 1 percent borax solution for a few minutes, rinsed in distilled water and mounted in Permount. Sections often stained a violaceous brown colour with occasional red walls, with the fungal cytoplasm staining a mauve colour.

Author Rey M E C
Name of thesis Epidemiological, Morphological and Physiological studies of selected plant diseases at Nylsvley 1982

PUBLISHER:
University of the Witwatersrand, Johannesburg
©2013

LEGAL NOTICES:

Copyright Notice: All materials on the University of the Witwatersrand, Johannesburg Library website are protected by South African copyright law and may not be distributed, transmitted, displayed, or otherwise published in any format, without the prior written permission of the copyright owner.

Disclaimer and Terms of Use: Provided that you maintain all copyright and other notices contained therein, you may download material (one machine readable copy and one print copy per page) for your personal and/or educational non-commercial use only.

The University of the Witwatersrand, Johannesburg, is not responsible for any errors or omissions and excludes any and all liability for any errors in or omissions from the information on the Library website.